

**MOLECULAR CHARACTERIZATION OF CYTOPLASMIC-
NUCLEAR MALE STERILITY (CMS) SOURCES AND
TALL/DWARF NEAR-ISOGENIC LINES IN PEARL MILLET**

By

Ashok Kumar Chhabra

**Thesis submitted to the CCS Haryana Agricultural University
in partial fulfillment of the requirements for the degree of:**

DOCTOR OF PHILOSOPHY

IN

PLANT BREEDING

**College of Agriculture
Hisar 125004, Haryana, India**

1995

To mum and dad
Santosh & Murari Lal Chhabra
with deep love and heart-felt thanks

CERTIFICATE I

This is to certify that this thesis entitled, "Molecular characterization of cytoplasmic-nuclear male sterility (CMS) sources and tall/dwarf near-isogenic lines in pearl millet" submitted for the degree of Doctor of Philosophy in the subject of Plant Breeding of the Chaudhary Charan Singh Haryana Agricultural University, is a bonafide research work carried out by Ashok Kumar Chhabra under my supervision and that no part of this thesis has been submitted for any other degree.

The assistance and help received during the course of investigation have been fully acknowledged.



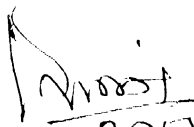
(I.S. Khairwal)
Major Adviser



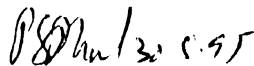
(K.N. Rai)
Co-Major Adviser

CERTIFICATE II

This is to certify that this thesis entitled, "Molecular characterization of cytoplasmic-nuclear male sterility (CMS) sources and tall/dwarf near-isogenic lines in pearl millet" submitted by Shri Ashok Kumar Chhabra to the Chaudhary Charan Singh Haryana Agricultural University in partial fulfillment of the requirements for the degree of Doctor of Philosophy in the subject of Plant Breeding has been approved by the Student's Advisory Committee after an oral examination on the same, in collaboration with an External Examiner.


3/6/95

MAJOR ADVISER

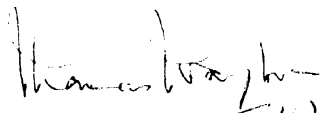


EXTERNAL EXAMINER

CO-MAJOR ADVISER 



HEAD OF THE DEPARTMENT


5/6/95

DEAN, POST-GRADUATE STUDIES

Acknowledgement

Research endeavor and attainment of parsimony in research are, undoubtedly, a team work. I put on record my compliments to all those who in one or the other way helped me in completing this piece of research.

This research project was spearheaded under the able guidance of Dr. I.S. Khairwal, Associate Professor, Department of Plant Breeding, CCS Haryana Agricultural University, Hisar. Dr. Khairwal's deep insight and understanding of research problem led me to develop conceptual framework on characterization of cytoplasmic-nuclear male sterility in time to the present day research needs. I feel highly indebted to him for the supervision and counselling provided to me all through the course of the study.

It is my immense pleasure to express my utmost gratitude to Dr. K.N. Rai, Senior Scientist (co-major adviser) and Dr. C.T. Hash, Principal Scientist, Pearl Millet Breeding. They took keen interest in guiding my work at ICRISAT and monitored the progress of research. Not only this, the motivation and encouragement available from them in giving newer dimensions to this research project proved quite valuable in carrying out quality research.

I am also thankful to other members of my advisory committee, Dr. (Mrs.) Santosh Dhillon, Associate Professor, Department of Biochemistry, Dr. D.P. Deswal, Scientist, and Dr. H.S. Nainawatee, Professor of Biochemistry, for constructive suggestions and guidance for completion of this research project.

I am highly thankful to Dr. T.P. Yadav, Professor and Head, Department of Plant Breeding and also the former Head, Dr. R.L. Kapoor for extending all possible help and support during the course of my study.

The research project in hand required multifarious approaches and for that reason the research work had to be undertaken at ICRISAT Asia Center in the Protein Laboratory (Cell Biology), Electron Microscope Unit, and Radio Isotope Laboratory. Dr. Y.L. Nene, Deputy Director General and Dr. J.P. Moss, Principal Scientist, Cell Biology were kind enough to allow me to work in their laboratories. The timely help and cooperation provided by Dr. N. Seetharama, Senior Scientist (Molecular Biology), Dr. A.K. Murthi, Senior Engineer (Electron Microscope Unit), and Dr. S. Sivaramakrishnan, Scientist (Radio Isotope Laboratory), are also thankfully acknowledged. Prof. R.L. Smith deserves special mention to permit me to reproduce restriction maps of the homologous probes used in the present study. My sincere and heart-felt thanks are for him.

The assistance rendered by Ms. Santosh Gurtu, Senior Research Associate (Cellular and Molecular Biology Division), K. Seetha, Senior Research Associate (Radio Isotope Laboratory) and Dr. S.K. Manohar, Research Associate (Electron Microscope Unit) helped me in completing my lab work efficiently and smoothly.

I am thankful to the CCS Haryana Agricultural University, Hisar for granting me leave for undertaking doctorate studies. I am grateful to Council of Scientific and Industrial Research (CSIR), Govt. of India for the award of Senior Research Fellowship from January 1992 to August 1993. I also acknowledge with grateful thanks the grant of Research Scholarship by ICRISAT from September 1993 onwards, which helped me to interact with scientists of international repute at the institute and learn a lot during the process of my research.

Dr. D.E. Byth, Associate Director General, Dr. B. Diwaker, Program Leader, Training and Fellowship Program (TAFP) and Dr. Y.L. Nene, Deputy Director General provided me moral support and made my stay at ICRISAT comfortable.

I express my sincere gratitude to Dr. S.M. Virmani, Principal Scientist, Agronomy for boosting my moral and giving me time for scientific discussions.

It was with the utmost blessings and good wishes of my parents and affection of my brothers Satish, Naresh and sister Rama that I could attain academic heights by undergoing doctorate studies.

The sufferings that my wife Seema and my dear baby Vasundhra had to undergo during the course of my study period has been a great sacrifice on their part. Vasundhra even while being in her formative years could not get due attention from me. I thank them from the deepest corner of my heart.

The love and affection given to me by my father-in-law, Dr. R.K. Sharma, Professor of Extension Education, CCSHAU, Hisar; mother-in-law, Mrs. Kaushalya Devi; brothers-in-law, Dr. Azad Kaushik, D.Sc. (Paris), Er. Anil Kaushik and Mr. Sunil Kaushik is worth mentioning here. Er. V.D. Sharma and Ms. Madhu Sharma always showered their good wishes on me and were even good enough to visit me both at ICRISAT and Hisar is indeed worth appreciating.

I thank Mr. G. Swaminathan, Research Associate (Statistics) and Mr. K.D.V. Prasad for the assistance and cooperation rendered in statistical analysis. I gratefully acknowledge the secretarial assistance rendered to me by Mr. S.B. Stanley, Senior Secretary (PMB) at the ICRISAT. He has been very nice to me by promptly completing any assignment given to him. He deserves my sincere thanks.



Ashok K Chhabra

HISAR

April 17, 1995

CONTENTS

<i>Chapter Number</i>		<i>Page Number</i>
I	INTRODUCTION	1-5
II	REVIEW OF LITERATURE	6-49
	2.1 Experiment No. 1 (MtDNA-RFLP Analysis)	6-20
	✓ 2.1.1 Cytoplasmic male sterility	7
	2.1.2 Mitochondrial genome rearrangements and the synthesis of variant polypeptides in relation to CMS	7-13
	2.1.3 Evidences emphasizing the need to widen the cytoplasmic diversity	13-14
	2.1.4 Applications of RFLP technique in pearl millet with particular reference to cytoplasmic diversity	14-20
	2.2 Experiment No.2 (Microsporogenesis)	20-31
	2.2.1 Chromosome number and morphology	21
	2.2.2 Meiosis and sterility induced by meiotic disturbances	21-22
	2.2.2.1 Desynapsis	22-23
	2.2.2.2 Segmental interchange	23
	2.2.2.3 Other meiotic abnormalities	23-24
	2.2.3 Discovery of cytoplasmic-genetic male sterility	24-26
	2.2.4 Cytoplasmic diversity	26-29
	2.2.5 Microsporogenesis in cytoplasmic-genetic male sterility	29-31
	2.3. Experiment No. 3 (Isozyme analysis)	31-49
	2.3.1 Disease resistance	33-37
	2.3.2 Phylogenetic affinities	37-40
	2.3.3 Genetic diversity and geographical distribution	40-42
	✓ 2.3.4 Cytoplasmic diversity/cytoplasmic male sterility	42-43
	2.3.5 Gene introgression and chromosome depletion	43-45
	2.3.6 Cultivars identification	45-46
	2.3.7 Tissue culture	46
	2.3.8 Ageing effect	46-47
	2.3.9 Assessment of gametophytic competition	47
	2.3.10 Other applications	48-49
III	MATERIALS AND METHODS	50-76
	3.1 Experiment No. 1 (MtDNA-RFLP Analysis)	50-62
	3.1.1 Plant material	50-52
	3.1.2 Seed multiplication	52
	3.1.3 Clones used	52-53
	3.1.3.1 Homologous mtDNA probes	53
	3.1.3.2 Heterologous mtDNA probes	53
	3.1.4 Mitochondrial DNA isolation	54-56
	3.1.5 Restriction enzyme digestion	56-57
	3.1.6 Electrophoresis	57
	3.1.7 Southern blot hybridization	57-62
	3.1.7.1 Preparation of southern blots	57-58
	3.1.7.2 Purification of inserts from plasmid DNA	58

3.1.7.3	Labelling of probes	58
3.1.7.4	Hybridization to labelled probe	59-62
3.1.7.4.1	Prehybridization	59
3.1.7.4.2	Hybridization	59
3.1.7.5	Washing of the blots	59
3.1.7.6	Autoradiography	60
3.1.8	Cluster analysis	60-61
3.1.9	Other comparisons	61-62
3.2	Experiment No.2 (Microsporogenesis)	62-70
3.2.1	Development of near-isonuclear lines	62-63
3.2.2	Meiosis	64-65
3.2.2.1	Material collection for meiotic analysis	64
3.2.2.2	Staining of chromosomes	64-65
3.2.3	Pollen sterility	65-67
3.2.3.1	Material collection for pollen sterility/fertility observations	65
3.2.3.2	Sample preparation and staining of pollen grains	65-66
3.2.3.3	Staining of pollen inside the nondehiscent anthers	66-67
3.2.4	Microsporogenesis	67-70
3.2.4.1	Collection and preparation of samples for histological studies	67-70
3.2.4.1.1	Sample collection	67-68
A.	Premeiotic	67
B.	Meiotic	67
C.	Postmeiotic	67-68
3.2.4.1.2	Sample Preparation	68-70
A.	Fixation	68
B.	Postfixation	68
C.	Dehydration	69
D.	Embedding	69
E.	Sectioning	69
F.	Mounting and staining	69-70
3.3	Experiment No. 3 (Isozyme analysis)	70-76
3.3.1	Plant material / Development of near-isogenic lines	70
3.3.2	Seed multiplication	71
3.3.3	Methods	71-76
3.3.3.1	Germination	71
3.3.3.2	Extraction	71-73
3.3.3.3	Sample preparation	73
3.3.3.4	Gel preparation	73-74
3.3.3.5	Sample loading	74
3.3.3.6	Electrophoretic run	74-75
3.3.3.7	Staining	75
3.3.3.8	Scoring of gels	75-76

IV RESULTS

77-200

4.1	Experiment No. 1 (MtDNA-RFLP Analysis)	77-104
4.1.1	MtDNA hybridization patterns	78-93
4.1.1.1	MtDNA hybridization with homologous clones	79-90
4.1.1.2	MtDNA hybridization with heterologous clones	91-93
4.1.2	Analysis of aggregate dendrograms	93-95
4.1.2.1	Homologous probes	93
4.1.2.2	Heterologous probes	93-95
4.1.3	MtDNA hybridization patterns from open-pollinated seeds	95
4.1.4	Total DNA hybridization patterns using mitochondrial probes	95-104
4.2	Experiment No.2 (Microsporogenesis)	105-165
4.2.1	Observations on male meiotic events	105-109
4.2.2	Anther development and microsporogenesis in 81B	109-122
4.2.3	Anther development and microsporogenesis in isonuclear A-lines	122-151

<i>Chapter Number</i>	<i>Page Number</i>
4.2.3.1 Premeiotic degeneration	122-124
4.2.3.1.1 Pb 406A ₃	122-124
4.2.3.2 Degeneration during meiosis	124-126
4.2.3.2.1 Pb 310A ₂ and Pb 311A ₂	124-125
4.2.3.2.2 81A _v (ICMA 88001)	126
4.2.3.3 Postmeiotic degeneration	127-151
4.2.3.3.1 81A ₁	127-128
4.2.3.3.2 Pb 310A ₂ and Pb 311A ₂	128
4.2.3.3.3 Pb 406A ₃	129
4.2.3.3.4 81A _m /81A ₁	129-130
4.2.3.3.5 ICMA 88001 (81A ₁)	130-151
4.2.4 Other developmental changes in anther components during microsporogenesis	152-165
4.2.4.1 Tapetum	152-153
4.2.4.2 Endothecium	153
4.2.4.3 Epidermis	153
4.2.4.4 Middle layer	154
4.2.4.5 Anther lobe diameter	154
4.2.5 Pollen fertility/sterility	154-165
4.3 Experiment No. 3 (Isozyme analysis)	166-200
4.3.1. General observations/effect of electrophoretic conditions and source of plant extract on isozyme spectrum	166-168
4.3.2. Alcohol dehydrogenase [ADH] EC 1.1.1.1.	168-169
4.3.3. Catalase [CAT] EC 1.11.1.6.	169
4.3.4. Esterase [EST] EC 3.1.1.	169-170
4.3.5. Glutamate dehydrogenase [GDH] EC 1.4.1.2.	170
4.3.6. Glutamate oxaloacetate transaminase [GOT] EC 2.6.1.1	170
4.3.7. Lactate dehydrogenase [LDH] EC 1.1.1.27.	170
4.3.8. Malate dehydrogenase [MDH] EC 1.1.1.37.	171
4.3.9. Malic enzyme [ME] EC 1.1.1.40.	171
4.3.10. 6-phosphogluconate dehydrogenase [6-PGD] EC 1.1.1.44.	171
4.3.11. Phosphoglucoisomerase [PGI] EC 5.4.2.2.	171-172
4.3.12. Shikimate dehydrogenase [SKDH] EC 1.1.1.25.	172
4.3.13. Superoxide dismutase [SOD] EC 1.15.1.1.	173
V DISCUSSION	201-252
5.1 Experiment No. 1 (MtDNA-RFLP Analysis)	201-223
5.1.1 MtDNA RFLP using pearl millet (homologous) clones	202-203
5.1.2 MtDNA RFLP using maize (heterologous) clones	203-205
5.1.3 Dendrogram analysis (aggregate)	205-223
5.2 Experiment No.2 (Microsporogenesis)	223-242
5.2.1 Pollen meiosis	224-227
5.2.2 Anther development and microsporogenesis	227-234
5.2.3 PMC/Microspore/pollen abortion	234-242
5.3 Experiment No. 3 (Isozyme analysis)	242-252
VI SUMMARY	253-256
LITERATURE CITED	i-xxiii
APPENDIX	i-xiv

LIST OF TABLES

Table No.	Particulars	Page No.
Table 1.	Peroxidase banding pattern in downy mildew affected plant parts of pearl millet	36
Table 2.	Description of male-sterile lines used in the present study	51
Table 3.	Combinations of restriction enzymes and probes used	53
Table 4.	Origin of tall/dwarf near-isogenic pairs of pearl millet	72
Table 5.	Constituents for gel preparation	74
Table 6.	Enzymes used and their abbreviations	75
Table 7.	Total number of bands, polymorphic bands and number of cytoplasmic groups obtained by various enzyme-probe combinations	78
Table 8.	Meiotic anomalies observed in Pb 406A ₃	107
Table 9.	Effect of source of plant extract and electrophoretic conditions on resolution of isozyme bands	167
Table 10.	Banding pattern of Alcohol dehydrogenase (18 h IS) in tall/dwarf near-isogenic pairs of pearl millet	176
Table 11.	Banding pattern of esterase (Seedlings) in tall/dwarf near-isogenic pairs of pearl millet	180
Table 12.	Esterase (18hIS) banding pattern in tall/dwarf near-isogenic lines of pearl millet	181
Table 13.	Banding pattern of gluconate dehydrogenase (18hIS) in tall/dwarf near-isogenic pairs of pearl millet	184
Table 14.	Banding pattern of glutamate oxaloacetate transaminase (seedling/dry seeds/18h IS) in tall/dwarf near-isogenic pairs of pearl millet	187
Table 15.	Banding pattern of malate dehydrogenase (dry seeds) in tall/dwarf near-isogenic pairs of pearl millet	187
Table 16.	Banding pattern of malic enzyme (seedling) in tall/dwarf near-isogenic lines of pearl millet	190
Table 17.	Banding pattern of phosphoglucoisomerase (seedlings/18h IS) in tall/dwarf near-isogenic pairs of pearl millet	193

Table No.	Particulars	Page No.
Table 18.	Banding pattern of phosphoglucosomerase (dry seeds) in tall/dwarf near-isogenic pairs of pearl millet	193
Table 19.	Banding pattern of shikimate dehydrogenase (18hIS/dry seeds) in tall/dwarf near-isogenic pairs of pearl millet	197
Table 20.	Banding pattern of superoxide dismutase (seedlings) in tall/dwarf near-isogenic pairs of pearl millet	200
Table 21.	Unique mtDNA fragment(s) of different cytoplasms	219
Table 22.	Differential mtDNA banding patterns ¹ of different cytoplasms	220
Table 23.	Effectiveness of various enzyme-probe combinations to distinguish different CMS sources in pearl millet	221
Table 24.	Similarity indices among pearl millet isonuclear cms lines based on mitochondrial DNA RFLP pattern	222
Table 25.	Range in pollen fertility (%) observed in pearl millet isonuclear male-sterile lines, and their maintainer 81B, during the hot dry and cool dry seasons of 1993-94	228
Table 26.	Frequency distribution of anthers with varying degrees of pollen fertility/sterility in isonuclear lines of pearl millet	229
Table 27.	Percent pollen fertility within line, within plant, and within spike of pearl millet isonuclear lines in hot dry (HD) and cool dry (CD) seasons of 1993-1994	230
Table 28.	Stage(s) of tapetum degeneration in isonuclear A-lines of pearl millet	231
Table 29.	Distribution of bands with respect to isozyme spectrum in tall/dwarf near-isogenic pairs of pearl millet	244
Table 30.	Isozyme spectrum of twelve enzyme systems in tall/dwarf near-isogenic pairs of pearl millet	249
Table 31.	Banding pattern of three most polymorphic tall/dwarf near-isogenic pairs of pearl millet	250
Table 32.	Similarity index values between seven tall/dwarf near-isogenic pairs based upon isozyme spectrum of twelve enzyme systems in pearl millet	251

LIST OF FIGURES

Figure No.	Particulars	Page No.
Figure 1.	Restriction map of pearl millet clones used in the present study	12
Figure 2.	Southern blot hybridization of mtDNA from different CMS lines and 81B of pearl millet digested with <i>Pst</i> I (top) and <i>Hind</i> III (bottom) and probed with pearl millet 4.7 kb gene clone	81
Figure 3.	Schematic representation of mtDNA hybridization patterns and dendrograms constructed on the basis of similarity indices among the various CMS lines in individual enzyme-probe combinations	82
Figure 4.	Southern blot hybridization of mtDNA from different CMS lines and 81B of pearl millet digested with <i>Hind</i> III and probed with pearl millet 10.9 kb gene clone	83
Figure 5.	Schematic representation of mtDNA hybridization patterns and dendrogram constructed on the basis of similarity indices among the various CMS lines in individual enzyme-probe combination	84
Figure 6.	Southern blot hybridization of mtDNA from different CMS lines and 81B of pearl millet digested with <i>Bam</i> HI and probed with pearl millet 4.7 kb gene clone	85
Figure 7.	Schematic representation of mtDNA hybridization patterns and dendrogram constructed on the basis of similarity indices among the various CMS lines in individual enzyme-probe combination	86
Figure 8.	Southern blot hybridization of mtDNA from different CMS lines and 81B of pearl millet digested with <i>Bam</i> HI and probed with pearl millet 13.6 kb gene clone	87
Figure 9.	Schematic representation of mtDNA hybridization patterns and dendrogram constructed on the basis of similarity indices among the various CMS lines in individual enzyme-probe combination	88
Figure 10.	Southern blot hybridization of mtDNA from different CMS lines and 81B of pearl millet digested with <i>Pst</i> I and probed with pearl millet 9.7 kb gene clone	89
Figure 11.	Schematic representation of mtDNA hybridization patterns and dendrogram constructed on the basis of similarity indices among the various CMS lines in individual enzyme-probe combination	90

Figure No.	Particulars	Page No.
Figure 12.	Southern blot hybridization of mtDNA from different CMS lines and 81B of pearl millet digested with <i>Bam</i> HI (top) and <i>Hind</i> III (bottom) and probed with maize <i>cox</i> I gene clone	97
Figure 13.	Schematic representation of mtDNA hybridization patterns and dendrograms constructed on the basis of similarity indices among the various CMS lines in individual enzyme-probe combinations	98
Figure 14.	Southern blot hybridization of mtDNA from different CMS lines and 81B of pearl millet digested with <i>Pst</i> I and probed with maize <i>cox</i> I gene clone	99
Figure 15.	Schematic representation of mtDNA hybridization patterns and dendrogram constructed on the basis of similarity indices among the various CMS lines in individual enzyme-probe combination	100
Figure 16.	Southern blot hybridization of mtDNA from different CMS lines and 81B of pearl millet digested with <i>Pst</i> I (top) and <i>Bam</i> HI (bottom) and probed with maize <i>atp</i> 6 gene clone	101
Figure 17.	Schematic representation of mtDNA hybridization patterns and dendrograms constructed on the basis of similarity indices among the various CMS lines in individual enzyme-probe combinations	102
Figure 18.	Southern blot hybridization of mtDNA from different CMS lines and 81B of pearl millet digested with <i>Hind</i> III and probed with <i>atp</i> 6 gene clone	103
Figure 19.	Schematic representation of mtDNA hybridization patterns and dendrograms constructed on the basis of similarity indices among the various CMS lines in individual enzyme-probe combinations	104
Figure 20.	Comparison of microsporogenesis and PMC/microspore/pollen degeneration in pearl millet isonuclear lines	110
Figure 21.	Meiosis in 81B, 81A ₁ , Pb 310A ₂ , Pb 311A ₂ , 81A _m , and 81A _v (ICMA 88001).	112-115
Figure 22.	Meiotic anomalies in Pb 406A ₃ .	117-120
Figure 23.	Transverse sections of fertile anthers (81B) representing microsporogenesis from young sporogenous stage to the anther dehiscence	132-134
Figure 24.	Microsporogenesis in pearl millet A ₁ cytoplasm CMS line 81A ₁ .	136-137

Figure No.	Particulars	Page No.
Figure 25.	Microsporogenesis in pearl millet A_2 cytoplasm CMS lines (Pb 310A ₂ and Pb 311A ₂).	139-140
Figure 26.	Summary of microsporogenesis in pearl millet A_3 cytoplasm male-sterile line Pb 406A ₃ = 81A ₃ .	143-147
Figure 27.	Microsporogenesis in pearl millet A_m cytoplasm CMS line 81A _m .	149
Figure 28.	Microsporogenesis in pearl millet <i>violaceum</i> cytoplasm CMS line 81A _v = ICMA 88001.	151
Figure 29.	Tapetum and endothecium thickness at different anther developmental stages in pearl millet iso-nuclear lines	155
Figure 30.	Epidermis and middle layer thickness at different anther developmental stages in pearl millet iso-nuclear lines	156
Figure 31.	Anther lobe diameter at different anther developmental stages in pearl millet iso-nuclear lines	157
Figure 32.	Frequency distribution of anthers of varying fertility status in pearl millet iso-nuclear lines	161
Figure 33.	Frequency distribution of anthers in percent pollen fertility classes in pearl millet iso-nuclear lines	162
Figure 34.	Staining of aborted and nonaborted pollen grains of male-sterile and fertile lines of pearl millet	164-165
Figure 35.	Isozyme spectrum of alcohol dehydrogenase using 18-hour imbibed seeds and five-day old etiolated seedlings in tall/dwarf near-isogenic lines of pearl millet	174
Figure 36.	Schematic zymogram of alcohol dehydrogenase in tall/dwarf near-isogenic lines of pearl millet	175
Figure 37.	Schematic zymogram of catalase in tall/dwarf near-isogenic lines of pearl millet	175
Figure 38.	Isozyme spectrum of esterase using 18-hour imbibed seeds (18h), five-day old etiolated seedlings (SL) and dry seeds (DS) in tall/dwarf near-isogenic lines of pearl millet	178
Figure 39.	Schematic zymogram of esterase in tall/dwarf near-isogenic lines of pearl millet	179
Figure 40.	Isozyme spectrum of glutamate dehydrogenase using 18-hour imbibed seeds (18h), five-day old etiolated seedlings (SL) and dry seeds (DS) in tall/dwarf near-isogenic lines of pearl millet	182

Figure No.	Particulars	Page No.
Figure 41.	Schematic zymogram of glutamate dehydrogenase in tall/dwarf near-isogenic lines of pearl millet	183
Figure 42.	Isozyme spectrum of glutamate oxaloacetate transaminase (using 18-hour imbibed seeds (18h), five-day old etiolated seedlings (SL) and dry seeds (DS)) and malate dehydrogenase using DS in tall/dwarf near-isogenic lines of pearl millet	185
Figure 43.	Schematic zymogram of glutamate oxaloacetate transaminase and malate dehydrogenase in tall/dwarf near-isogenic lines of pearl millet	186
Figure 44.	Isozyme spectrum of malic enzyme (using five-day old etiolated seedlings (SL) and 6-phosphoglutamate dehydrogenase using DS, SL and 18hIS in tall/dwarf near-isogenic lines of pearl millet	188
Figure 45.	Schematic zymogram of malic enzyme and 6 phosphogluconate dehydrogenase in tall/dwarf near-isogenic lines of pearl millet	189
Figure 46.	Isozyme spectrum of phosphoglucoisomerase using dry seeds (DS), five-day old etiolated seedlings (SL) and 18-hour imbibed seeds (18h) in tall/dwarf near-isogenic lines of pearl millet	191
Figure 47.	Schematic zymogram of phosphoglucoisomerase in tall/dwarf near-isogenic lines of pearl millet	192
Figure 48.	Isozyme spectrum of shikimate dehydrogenase using dry seeds (DS), five-day old etiolated seedlings (SL) and 18-hour imbibed seeds (18h) in tall/dwarf near-isogenic lines of pearl millet	195
Figure 49.	Schematic zymogram of shikimate dehydrogenase in tall/dwarf near-isogenic lines of pearl millet	196
Figure 50.	Isozyme spectrum of superoxide dismutase using five-day old etiolated seedlings (SL) in tall/dwarf near-isogenic lines of pearl millet	198
Figure 51.	Schematic zymogram of superoxide dismutase in tall/dwarf near-isogenic lines of pearl millet	199
Figure 52.	Dendrogram of cytoplasmic male sterile lines of pearl millet based on homologous (4.7 kb, 9.7 kb, 10.9 kb, 13.6 kb) and heterologous (<i>atp6</i> , <i>coxI</i>) clones hybridized to mtDNA digested with three restriction enzymes (<i>Bam</i> HI, <i>Hind</i> III and <i>Pst</i> I)	206
Figure 53.	Dendrogram of cytoplasmic male sterile lines of pearl millet based on homologous (4.7 kb, 9.7 kb, 10.9 kb,	

Figure No.	Particulars	Page No.
	13.6 kb) clones hybridized to mtDNA digested with three restriction enzymes (<i>Bam</i> HI, <i>Hind</i> III and <i>Pst</i> I)	207
Figure 54.	Dendrogram of cytoplasmic male sterile lines of pearl millet based on <i>atp6</i> gene clones hybridized to mtDNA digested with three restriction enzymes (<i>Bam</i> HI, <i>Hind</i> III and <i>Pst</i> I)	208
Figure 55.	Dendrogram of cytoplasmic male sterile lines of pearl millet based on maize <i>cox1</i> gene clones hybridized to mtDNA digested with three restriction enzymes (<i>Bam</i> HI, <i>Hind</i> III and <i>Pst</i> I)	209
Figure 56.	Dendrogram of cytoplasmic male sterile lines of pearl millet based on heterologous (<i>atp6</i> , <i>cox1</i>) clones hybridized to mtDNA digested with three restriction enzymes (<i>Bam</i> HI, <i>Hind</i> III and <i>Pst</i> I)	210
Figure 57.	Southern blot hybridization of the pearl millet 4.7 kb gene clone to (a) <i>Hind</i> III-, (b) <i>Bam</i> HI-, and (c) <i>Pst</i> I-digested mtDNA from open pollinated seed of CMS lines	214
Figure 58.	Southern blot hybridization of the maize <i>cox1</i> (1) gene clone to (A) <i>Hind</i> III-, (B) <i>Bam</i> HI-, and (C) <i>Pst</i> I-digested mtDNA from open pollinated seed of CMS lines; and Southern blot hybridization of the maize <i>atp6</i> (2) gene clone to (A) <i>Bam</i> HI- and (B) <i>Pst</i> I-digested mtDNA from open pollinated seed of CMS lines	216
Figure 59.	Southern blot hybridization of the pearl millet 4.7 kb gene clone to (a) <i>Hind</i> III-, (c) <i>Bam</i> HI-digested tDNA and maize <i>cox1</i> gene clone to (b) <i>Hind</i> III, (d) <i>Bam</i> HI-digested tDNA from CMS lines	217
Figure 60.	Comparison of grouping pattern of various dendrograms constructed based upon various enzyme-probe combinations	218
Figure 61.	Dendrogram of cluster analysis of the combined 3 Early Composites (EC), 3 Medium Composites (MC), and 1 Nigerian Composite (NC) tall/dwarf near-isogenic pairs of pearl millet	252

I INTRODUCTION

Pearl millet [*Pennisetum glaucum* (L.) R. Br.], is known by scientific name as *P. americanum* (L.) Leeke and *P. typhoides* [(Burm.) Stapf and Hubbard] and common name as bulrush or cattail millet. It is primarily grown for food but also for fodder, feed and fuel on about 26 million hectares in semi-arid tropics of the Africa and the Indian subcontinent. It is also grown on small scales as high quality forage crop in the United States, Australia, South America and southern Africa. It grows under severe drought, in soils that are too sandy, too acid, too dry and too infertile for sorghum or maize.

Pearl millet is cultivated on about 10 million hectares (Anonymous, 1993) in India. Rajasthan, Maharashtra, Gujarat, Uttar Pradesh and Haryana account for nearly 90% of the total acreage (Anonymous, 1993). It is the most important food crop of Rajasthan and Gujarat. It is essentially a dryland crop and is grown mostly during June-October under rainfed conditions (95% of it). It is also grown as a winter crop (November-February) or as a summer crop (March-June) under irrigated conditions, mostly for seed production.

Pearl millet yields were relatively stagnant until 1962 when the discovery of cytoplasmic male sterility (CMS) made the commercial exploitation of heterosis or hybrid vigor economically feasible in 1965 with the release of first pearl millet hybrid, HB 1. It was based on male-sterile line Tift 23A from Georgia. The series of hybrids that followed till to date were also based on single cytoplasmic source, i.e., the male-sterile Tift 23A (Khairwal *et al.*, 1990).

Due to adoption of these hybrids, the production of pearl millet increased dramatically from 3.75 million tons in 1965-66 to 8.72 million tons in 1992-93 (Anonymous, 1994). Most of the earlier and present day hybrids had their life-span for not more than three years. The primary cause was the breakdown of downy mildew (*Sclerospora graminicola*) resistance in female parent Tift 23A. Corrective research efforts led to the isolation of male-sterile lines from different sources (Burton and Athwal, 1967; Appadurai *et al.*, 1982; Aken'Ova, 1985). ICRISAT has made a major contribution to the research efforts by developing downy mildew resistant male-sterile lines, 81A, 842A, and 843A. A number of new male-sterile lines with variable cytoplasmic sources are now available (Gill *et al.*, 1986; Virk and Mangat, 1987, 1988, 1989; Virk *et al.*, 1989, 1990a,b,c).

The widespread use of the CMS in plant breeding programs, while being cost effective, is not without its drawbacks. Dependence on a single source of CMS in hybrid seed production has the inevitable consequence of conferring 'cytoplasmic genetic uniformity' on the hybrid. In 1970, cytoplasmic uniformity of the maize hybrids in the USA led to an epidemic caused by a fungal pathogen *Bipolaris maydis*, race T, formerly known as *Helminthosporium maydis* race T, which was particularly virulent on plants with T-cytoplasm used in the breeding program (Ullstrop, 1972; Pring and Lonsdale, 1985). Soon after, it was established that the maternally inherited disease susceptibility was due to the production of pathotoxin (T-toxin) by the fungus that

that specifically affected mitochondria from CMS-T maize. It is thus obviously important to increase cytoplasmic genetic diversity in crop plants by identifying or creating new sources of male sterility. With the available reports that sterile cytoplasm has probably no role to play in determining susceptibility to downy mildew (Anand Kumar *et al.*, 1983), and smut (Khairwal *et al.*, 1986) in pearl millet, however, Thakur *et al.* (1989) have reported the positive association of sterile cytoplasm with the ergot susceptibility. Therefore, the genetic diversification with Tift 23A cytoplasm may continue and to avoid unforeseen risks due to cytoplasmic uniformity alternate sources of CMS may be used.

So far, fertility restoration pattern in F_1 hybrids has been widely used in maize (Durick, 1965; Gracen and Grogan, 1974), sorghum (Schertz and Ritchey, 1978; Rao *et al.*, 1984) and pearl millet (Burton and Athwal, 1967; Appadurai *et al.*, 1982; Aken'Ova, 1985; Rai and Hash, 1990) for the classification of cytoplasmic sources of male sterility. In these studies effects of environment and parental nuclear genotype may cause considerable difficulties in the classification of different sources of cytoplasmic male sterility. The cytoplasmic differentiation is, however, facilitated if the same genome is introduced in to different cytoplasms to develop isonuclear lines. Virk and Brar (1993) utilizing polycytoplasmic isonuclear lines concluded the distinctness of cytoplasmic sources. However, the procedure involved in these studies also involves a lot of labor and time.

Traditionally, CMS sources of crop plants have been characterized using combination of morphological and agronomical traits and the techniques cited above. The biochemical or molecular markers, such as isozymes, restriction fragment length polymorphism (RFLP), reflect the CMS sources much more closely and therefore may provide a better image of CMS sources than that derived from fertility restoration pattern in F_1 hybrids. Cytoplasmic male sterility is manifested in a number of ways depending on the plant species which includes abnormal anther development, failure in anther dehiscence to pollen abortion at various stages during microsporogenesis. Thus, cytohistological studies may explain the effect of cytoplasmic sources on anther development and microsporogenesis with special reference to cause and the stage of degeneration of pollen mother cells/pollens leading to pollen sterility.

The identification and utilization of dwarfing genes in cereals enabled breeders to develop lodging resistant high yielding cultivars in rice and wheat. Burton and Fortson (1966) discovered d_2 dwarfing gene in pearl millet which reduces height by nearly 50% by shortening the internodes except the peduncle. Pearl millet improvement programs for forage and grain production are largely based on the utilization of d_2 dwarfing genes for the development of semi-dwarf male-sterile and restorer lines, their ultimate utilization in breeding commercial hybrids. The effect of d_2 dwarfing gene on several seedlings and morphological characters in some pairs of near-isogenic lines have been demonstrated (Rai and Hanna, 1990; Khairwal *et al.*, 1992). Tall

and dwarf pearl millet isolines need to be characterized at biochemical levels to assess the degree of isogenicity so that effect of d_2 gene on other traits may be examined without interference from other factors. This study was therefore carried out with the following objectives in mind:

1. to study mitochondrial DNA (mtDNA) RFLP pattern for classification of CMS sources
2. to study the anther morphology and microsporogenesis of isonuclear CMS lines and their maintainers
3. isozyme analysis of seven diverse pairs of tall/dwarf near-isogenic lines

II REVIEW OF LITERATURE

2.1 Experiment No. 1: Mitochondrial DNA RFLP analysis of pearl millet CMS lines

The objective of this review is to present critical synthesis of various techniques related to objectives outlined for the study (i.e. mitochondrial DNA RFLP analysis of cytoplasmic sources, microsporogenesis and anther development, and isozyme analysis of tall/dwarf near-isogenic pairs of pearl millet). While doing so we shall draw not only on the published research work on pearl millet, which is quite meager, but also on other crops relevant to pearl millet. The objective wise critical review is given below:

Literature on mitochondrial aspects (mtDNA-RFLP, mitochondrial structure, translation and genome organization) available in pearl millet, and other crops is briefly reviewed here to better understand the subject and its need and scope in pearl millet. The review is divided into four subheads:

1. Cytoplasmic male sterility.
2. Mitochondrial genome arrangements/mutations and the synthesis of variant polypeptides in relation to CMS
3. Evidences emphasizing the need to widen the cytoplasmic diversity
4. Applications of RFLP technique in pearl millet with particular reference to cytoplasmic diversity.

2.1.1 Cytoplasmic male sterility

Cytoplasmic male sterility (CMS) results in the failure of the mature plant to produce functional pollen, while not affecting female fertility. It provides a means of pollination control for commercial production of F₁ hybrid seeds. CMS is reported in a wide range of plant species (more than 140 species) including maize, sorghum, wheat, pearl millet, sugarbeet (Edwardson, 1970; Laser and Larsten, 1972), beans (Bassett and Shuh, 1982) and rapeseed (Erickson *et al.*, 1986). CMS was discovered in pearl millet during the mid-1950's both in India and the USA (Burton, 1958; Menon, 1959).

2.1.2 Mitochondrial genome rearrangements and the synthesis of variant polypeptides in relation to CMS

CMS is maternally inherited, indicating that the factors responsible are present on the organelle genome. This is the only cytoplasmically inherited trait extensively exploited by plant breeders. CMS, in most cases results from either an incompatibility between the nuclear genome of one race or species and the mitochondrial genome of another, or, specific mutations in the mitochondrial genome. Although chloroplasts also contain their own genome, this is highly conserved in higher plants (Herrman, 1970; Kirk, 1971). On the other hand, the mitochondrial genome of higher plants is astonishingly large and exhibits considerable size variation and genetic diversity even within a single family (Ward *et al.*, 1981). Even in closely related species, wide variations in complexity are evident. The mitochondrial genome of pearl millet

was calculated to be 407 kb, while that of other *Pennisetum* species ranged from 341 to 486 kb (Chowdhury and Smith, 1988). The first CMS-associated loci were identified in maize T-CMS and *Petunia* CMS lines, which provided models for locating mitochondrial loci associated with sterility in other species (Dewey *et al.*, 1986; Hanson *et al.*, 1989; Stamper *et al.*, 1987; Young and Hanson, 1987). In pearl millet, Smith *et al.* (1987) reported that endonuclease restriction fragment patterns of mitochondrial DNA (mtDNA) from a CMS line, its fertile revertants and a normal fertile cytoplasm showed polymorphism, whereas chloroplast DNA (cpDNA) from those lines did not show any variation. Most data on other crops also indicate that mtDNA restriction endonuclease patterns correlate with fertility/sterility, while no consistent variability is detected in cpDNA restriction patterns, in maize (Levings and Pring, 1976; Pring and Levings, 1978), wheat (Quetier and Vedel, 1977), faba bean (Boutry and Briquet, 1982), sorghum (Pring *et al.*, 1979, 1982; Conde *et al.*, 1982), sugar beet (Powling, 1982), and rapeseed (Erickson *et al.*, 1986). Extensive evidences suggest that CMS in most crop species is due to mutations in mtDNA (Srivastava, 1981; Hanson and Conde, 1985). The main evidence is based on the mtDNA structure, its restriction endonuclease fragment analysis, translation products, disease susceptibility and chemical effects.

Evolution of complex genomes of mitochondria appears to occur via reorganization of sequences rather than by point mutation. As a result of

intra- and/or inter-molecular recombination, several chimaeric genes have been produced or, in other cases such recombinations generated unique genes. These chimaeric genes are expressed as variant polypeptides, which in most cases are associated with the energy-transducing inner mitochondrial membrane, and appear to be causally related to the male-sterile phenotype. Examples include the *urf13* (within *Turf2H3* clone) gene in maize (Young and Hanson, 1987), *coxI* in sorghum (Bailey-Serres *et al.*, 1986), and *atp6* in radish (Makaroff *et al.*, 1989) and rice (Kadowaki *et al.*, 1990). Unique transcripts of the *Turf2H3* clone were analyzed by Dewey *et al.* (1986) and found to have chimaeric sequences containing portions of the *atp6* subunit, *rrn26* ribosomal genes of mitochondria and the tRNA arginine gene of chloroplast in addition to two large open reading frames, one of which (*urf13*) codes for a 13 kDa polypeptide present only in CMS-T cytoplasm. This phenotype is absent or truncated in male-fertile mutants (Wise *et al.*, 1987). This 13kDa polypeptide designated as T-urf13 is strongly associated with CMS in T-cytoplasm maize. It also binds T-toxin from *Bipolaris maydis* race T = *Helminthosporium maydis* race T (Levings, 1990), and causes susceptibility to this fungus (Dewey *et al.*, 1988). Barratt and Flavell (1975) showed that fertility restorer genes in maize have significant impact on the mitochondrial function. They isolated mitochondria from etiolated shoots of a range of maize genotypes with T-cytoplasm sensitive to pathotoxin isolated from *Helminthosporium maydis*, race T. The pathotoxin inhibits oxidation of α -ketoglutarate and malate and

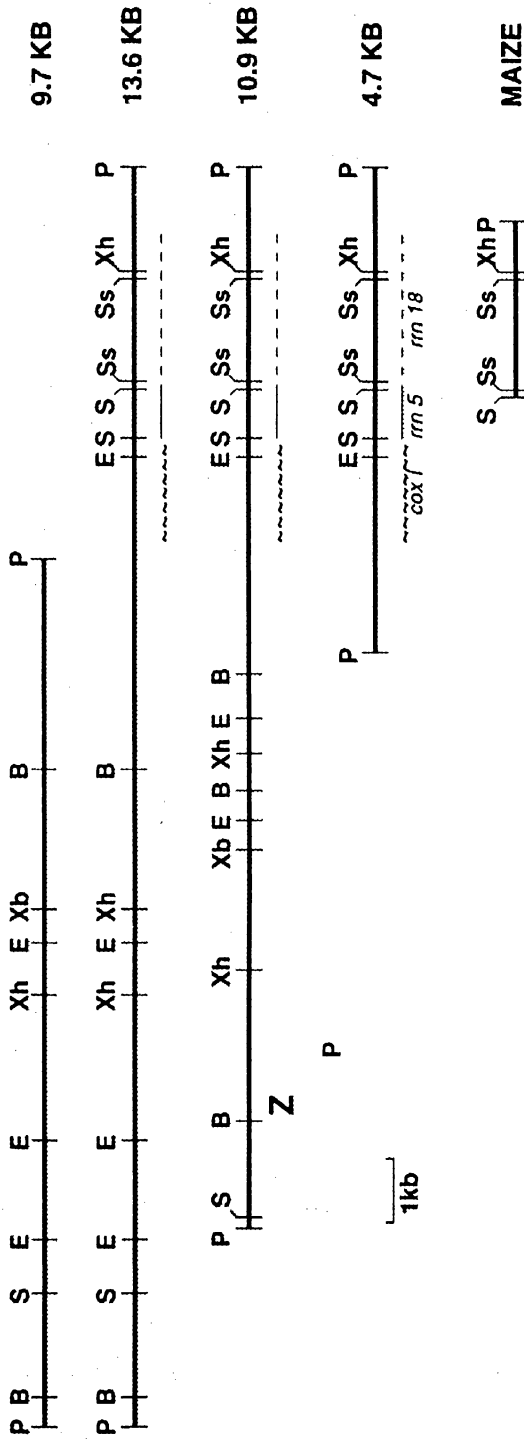
stimulates NADH oxidation. They compared the relative sensitivity to pathotoxin of nine different pairs of genotypes differing principally in the presence or absence of nuclear male fertility restorer alleles. In every case, the line carrying the restorer alleles was more resistant to the pathotoxin. They suggested that the restorer genes cause changes in mitochondria, that modify the functional aberration introduced by the cytoplasmically-inherited mutation causing sterility. In *Petunia*, the chimaeric gene *Pcf* associated with CMS is composed of sequences derived from *atp9*, *coxII* and an unidentified reading frame, and encodes for a fusion peptide produced only by male-sterile mitochondria (Young and Hanson, 1987). In *Sorghum bicolor*, rearrangements within the *coxI* gene in CMS 9E-cytoplasm resulted in variant polypeptides of higher molecular weight than the product of the gene in normal cytoplasm (Bailey-Serres *et al.*, 1986). A chimaeric *atp6* gene was present in the CMS B0-cytoplasm of rice in addition to the normal gene and was actively transcribed (Kadowaki *et al.*, 1990). Introduction of the fertility restoration gene altered its transcription but not that of the normal *atp6* gene.

Thus, genomic rearrangements of the mitochondrial genome can directly affect mitochondrial translation product which, resulting in failure or deficiency in mitochondrial functions leading to altered phenotypes like male sterility. Rearrangements in the mitochondrial genome also lead to reversion of sterility to fertility in pearl millet. Smith *et al.* (1987) compared mtDNAs of CMS-A₁, its fertile revertants, and the normal cytoplasm of the fertile

maintainer of CMS-A₁. Their results revealed the presence of a unique 4.7 kb *Pst*I fragment in the CMS line that was not detected in any of the revertant lines. A 13.6 kb fragment found in CMS and fertile lines was lost in seven of the eight revertants. In its place, a 9.7 kb fragment was detected in all the revertants. A 10.9 kb fragment was found in all cytoplasms and was not affected by reversion. The restriction maps (Fig. 1) of these fragments contained two sets of repeated sequences (homology). The 4.7kb, 10.9kb and 13.6-kb fragments had partial homology; and the 13.6kb and 9.7-kb fragments also showed partial homology. It was found that the repeated regions on 4.7kb, 10.9kb, and 13.6kb fragments contained the *rrn18*, *rrn5*, and *coxI* genes. The correlation observed between the reversion of CMS to fertility and the loss of fragments containing the *rrn18*, *rrn5*, and *coxI* genes indicated that those lost fragments and the genes contained in them could be responsible for the expression of CMS in pearl millet.

The chimaeric mitochondrial genes can be transcriptionally active and are expressed as novel or variant mitochondrial proteins that appear to be related to failure in mitochondrial function in the anther tapetum and microspores, leading to failure in the production of viable pollen. Smith and Chowdhury (1991) carried out transcriptional analysis of those mtDNA fragments involved in reversion. This was investigated in three ways: (i) by hybridizing Southern blots of the cloned mtDNA fragments to end-labelled total mtRNA probes (ii) by using the pearl millet clones as probes to hybridize Northern blots of

Figure 1. Restriction map of pearl millet clones used in the present study



Restriction maps of cloned pearl millet fragments rearranged by reversion. The restriction map of the maize *rrn18* gene shows similarity to the pearl millet *rrn* sequences. The location of the pearl millet *coxI*, *rrn6*, and *rrn18* genes are noted on the three clones; however, the sizes are only approximate. The region labelled Z contains an unidentified gene. B = BamHI, E = EcoRI, P = PstI, S = SmaI, Ss = SstII, Xb = XbaI, and Xh = XhoI

Source: Smith and Chowdhury (1991)
 Reproduced with the kind permission of Professor R.L. Smith

mtRNA from CMS, revertants, and fertile cytoplasm; and (3) by probing Northern blots with the pearl millet *coxI* gene probe. The hybridization analysis indicated that transcripts homologous to the *rrn18* and *coxI* genes were present in pearl millet total mtRNA. In both maize and *Petunia*, reversion from CMS to fertility was characterized by the loss of a mtDNA fragment. In pearl millet CMS-A₁ system reversion is always accompanied by the loss of the 4.7 kb *PstI* fragment. However, Smith and Chowdhury (1991) were not able to detect differential transcription patterns among the CMS and fertile revertants, as was done with both maize (Dewey *et al.*, 1987) and *Petunia* (Young and Hanson, 1987). Smith and Chowdhury (1991) suggested that the lack of detectable transcript differences between CMS and revertant cytoplasm does not exclude the possibility of involvement of genes on the cloned segments in CMS. They further interpreted that a mechanism may be operating in pearl millet that does not alter the size of transcript enough to be detected by blot hybridization. The sequencing of maize *coxI* gene would further confirm whether or not alterations occur in those genes are responsible for CMS phenotype.

2.1.3 Evidences emphasizing the need to widen the cytoplasmic diversity

Genetic uniformity of organelle genome in seed parents (CMS lines) of hybrids in any crop may lead to epidemics. This has been experienced in case of maize during 1970 in USA (due to Southern Leaf Blight) and in pearl millet due to

downy mildew caused by *Sclerospora graminicola* in the early 1970s in India as almost all the hybrids of maize possessed T-cytoplasm and that of pearl millet Tifton 23A (A₁) cytoplasm. Kumar *et al.* (1983) could establish the non-existence of relationship between Tift 23A cytoplasm and downy mildew susceptibility, yet it does not rule out the possibility of becoming it susceptible to any existing or unforeseen disease. The fungal pathogen which caused epidemic in maize was particularly virulent on plants with T-cytoplasm (Hooker *et al.*, 1970a,b). This pathogen causes a fungal disease *Bipolaris maydis* race T. It was soon established that the maternally inherited disease susceptibility was due to the production of pathotoxin (T-toxin) by this fungus that specifically affected mitochondria from CMS-T maize but not the fertile cytoplasm (Hooker *et al.*, 1970a,b; Turner and Martinson, 1972; Gracen *et al.*, 1972).

Besides these instances, the demonstration of cytoplasmic inheritance of disease reaction in tobacco (Durbin and Uchytel, 1977), insecticide susceptibility in maize (Humaydan and Scott, 1977), as well as herbicide resistance in cucumber (Duke *et al.*, 1984), further supports the need to increase cytoplasmic genome diversity in crop plants by identifying or creating new sources of male sterility.

2.1.4 Applications of RFLP technique in pearl millet with particular reference to cytoplasmic diversity

In recent years, developments in DNA cloning and the use of restriction

endonucleases have enabled the scientists to construct more quickly and efficiently the genetic maps by studying directly the segregation of DNA fragments. RFLP differences between plants are inherited in the same fashion as conventional genes, thus genetic maps of RFLPs can be constructed using conventional methods. Such RFLP maps indicate the location of specific restriction fragments of chromosomal DNA relative to one another. Hash (1991) emphasized the need of potential use of RFLPs in pearl millet breeding with particular reference to downy mildew resistance genes. Liu *et al.* (1992) constructed a RFLP-based genetic map in pearl millet using 180 probes from a *Pst*I genomic library. Later Liu *et al.* (1994) published first linkage map using 200 genomic DNA probes employing two crosses. The total length of this map, which comprised seven linkage groups, was 303 cM. On this map 181 loci were placed studying segregation (RFLP banding pattern) in F₂ population derived from a single F₁ plant. Their study on 19 diverse genotypes also revealed the polymorphic nature of *Pennisetum glaucum* as 85% of probes detected polymorphism using only two restriction enzymes.

In addition, total DNA (tDNA) RFLPs have been carried out in pearl millet to establish species relationships (Ramanan, 1992), to see the extent of gene introgression in crosses, e.g., the cultivated species, *Pennisetum americanum* has been crossed to *P. schweinfurthii*, *P. purpureum* (Napier grass), *P. orientale*, *P. setaceum*, *P. polystachion*, *P. macrourum*, and *P. squamulatum* to introduce genes for apomixis (Ozias-Akins, 1991). In a

further study Ozias-Akins *et al.* (1993) reported that transfer of apomixis to sexual cultivated pearl millet from the wild species (*P. squamulatum*) has resulted in an obligate apomictic backcross line with a low, but unknown, number of chromosomes from the wild species. They identified molecular markers (RFLPs and random amplified polymorphic DNAs) that unambiguously demonstrated the presence of *P. squamulatum* DNA in the BC₃ generation. ✓

Shenoy and Vasil (1992) investigated the extent of biochemical and molecular variation in 63 plants of *P. purpureum* K. Schum. regenerated from 3- to 24-week-old embryogenic callus cultures. They used isozyme and RFLP technique (mitochondrial, plastid and nuclear) to characterize these plants and found that their results agreed with the earlier reports of the genetic uniformity of plants derived from somatic embryos and suggested their use both for clonal propagation and for conducting genetic transformation experiments.

In conventional crosses (i.e., pollinating the female parent using pollen of the male parent) only nuclear genome from the male parent gets chances to recombine the nuclear genome of female parent while cytoplasmic genome of female parent is transferred to the progeny. In order to get more diversity, attempts have been made to make somatic hybrids. Ozias-Akins *et al.* (1988) studied somatic hybrid cell lines of *Pennisetum americanum* with *Panicum maximum* and *Saccharum officinarum* for the mtDNA restriction patterns.

Somatic hybrids in each case displayed unique mitochondrial restriction patterns indicating mitochondrial fusion and recombination. They were able to recover and clone fragments of the hybrids and used them to hybridize parental and somatic hybrid mtDNAs. They also found that in each somatic hybrid novel fragments were present at low copy number in one or both of the parental mtDNAs, and amplified 15 to 30 times in the hybrids.

Chowdhury and Smith (1988) employed mitochondrial restriction fragment and probe hybridization methods to study phylogenetic relationships of seven *Pennisetum* species, including five *P. americanum* ecotypes and a reference species from the distantly related genus *Panicum*. Except for an ecotype collected in Ethiopia, all pearl millet ecotypes were uniform. Zimbabwean and Ethiopian ecotypes showed variation from the others and from each other using probe hybridization method, while considerable restriction pattern polymorphism was noted among different species of *Pennisetum* and *Panicum*. The relationship observed between species by the hybridization method agreed more closely with the available cytological data than those indicated by the restriction pattern method thus indicating the superiority of hybridization method over the observations based on restriction profiles of mtDNA to study species relationships.

Besides these, mtDNA-RFLP has been carried out in CMS, male-fertile and restorer lines of pearl millet to detect cytoplasmic variation, and to search molecular markers differentiating various sterility sources. Five male-sterile

mutants from F-B₂ (fertile line, B₂) were compared with CMS lines of known sources (S-A_m, S-A₁, S-A₂, and S-A₃) along with their respective maintainers by their mtDNA restriction profile (Smith and Chowdhury, 1989). *Bam*HI restriction patterns differentiated the male-sterile cytoplasms S-A_m, S-A₁ and S-A₃ but grouped together S-A₂ and the male-sterile mutants. Not all the fertile maintainers could be distinguished but the CMS mutant S-M7 had a unique *Sma*I restriction pattern differentiating it from S-A₂ and the other four CMS mutants, thus verifying its (S-M7) and popand popmutant origin. Hybridization patterns using maize mitochondrial probes revealed similar classification as that of restriction patterns.

Rajeshwari *et al.* (1994) were able to distinguish between various pearl millet CMS sources using homologous (pearl millet) and heterologous (maize) probes. In addition to CMS lines grouped with A₁-cytoplasm (based on fertility restoration patterns), viz., 5141A and ICMA 1, ICMA 2, and PMC 30A also grouped with them when their mtDNAs were digested with *Pst*I, *Bam*HI, *Sma*I or *Xho*I and probed with 13.6-, 10.9-, 9.7-, or 4.7-kb pearl millet clones. Remaining CMS lines formed a distinct group having three subgroups. The maize *cox*I mtDNA clone also produced similar grouping patterns, whereas the *atp9* probe differentiated CMS line 81A₄ (= 81A_m) and the *cox*II gene probe did not detect any polymorphism among the CMS lines studied. The maize *atp6* gene proved to be the best in the way it could reveal four distinct cytoplasmic groups and four subgroups within the main group. These four groups were: (1)

CMS lines belonging to A₁-cytoplasm, (2) 81A₄, (3) 81A_v (=ICMA 88001), and (4) seven CMS lines forming a separate cluster having subgroups. They further interpreted that the different intensities of *atp6* gene in hybridized blots suggest the presence of more than one copy of the gene in different stoichiometries. They also indicated that the rearrangements involving the *coxI* and/or *rrn18-rrn5* genes (mapped within the pearl millet clones) might have resulted in the S-A₁ type of sterility and also discussed the possibility of the involvement of rearrangements involving *atp6* gene in the creation of other CMS sources in pearl millet.

A new source of CMS derived from the Early Genepool, EGP 261 (Rai and Hash, 1993), was used to develop a male-sterile line ICMA 90111. Its mtDNA RFLP patterns were compared with the other known cytoplasmic sources (Sujata *et al.*, 1994). Based upon hybridization patterns using various homologous and heterologous (maize and wheat) probes hybridized to restriction digests from several restriction endonucleases indicated the uniqueness/distinctness of ICMA 90111 from all other existing sources. The unique hybridization pattern obtained with *coxI* and many enzyme combinations suggested that the *coxI* gene might have undergone some rearrangements in ICMA 90111, thus indicating the possible use of *coxI* for its (ICMA 90111) identification. The maize *atp6* gene also displayed ICMA 90111 as a separate group. They further indicated the significance of using wheat *coxIII* gene probe as it could divide the CMS lines into four classes-81A₁,

Pb 406A₃, 81A_m, and ICMA 90111.

All these studies on mtDNA restriction analysis and/or probe hybridization analysis signify their importance in CMS-sources classification in pearl millet. Combined sequence- and translation products- analysis of the rearranged/mutated fragments of mitochondrial genome may precisely characterize the CMS genes.

2.2 Experiment No. 2: Anther development and microsporogenesis in pearl millet iso-nuclear lines

Cytoplasmic nuclear male sterility commonly known as cytoplasmic male sterility (CMS) is used extensively in the production of commercial pearl millet hybrids. Although several sources of CMS are available in pearl millet, most of them are not stable enough for commercial use. Till to date, a few studies have been conducted in male-sterile pearl millet to know the exact mechanism leading to pollen abortion.

The literature on cytoplasmic male sterility in pearl millet has been adequately discussed in a fairly recent review (Anand Kumar and Andrews, 1984). Literature reviewed in the present report will be limited to chromosomal factors related to male sterility and to reports dealing specifically with microsporogenesis and pollen abortion in pearl millet.

2.2.1 Chromosome number and morphology

Pearl millet is a favorable organism for genetic research. Its chromosome number, $2n = 14$, was determined more than 60 years ago by Rau (1929). Avdulov (1931) studied the chromosomes of pearl millet, and noticed a small nucleolar bivalent associated with the nucleolus. Later on, various authors (Pantulu, 1958; Venkateswarlu and Pantulu, 1968; Lobana and Gill, 1973; Krishnaswamy and Raman, 1953; Burton and Powell, 1968; Virmani and Gill, 1972; Tyagi, 1975) studied chromosome morphology in detail and characterized them as median, submedian etc. and also suggested the karyotype.

2.2.2 Meiosis and sterility induced by meiotic disturbances

Meiosis in diploid cultivated pearl millet species is normal, forming 7 bivalents (7II). Diakinesis shows one pair of nucleolar chromosomes (associated with the nucleolus) forming a bivalent, and maximum terminalization, so that bivalents are found desynapsed; migration to the poles is equal and regular. Second meiotic division is also regular and the pollen is highly fertile (Rangaswamy, 1935; Krishnaswamy, 1962).

Various kinds of male sterility have been reported in pearl millet e.g., genetic male sterility, genetic cytoplasmic male sterility, structural male sterility and chemically induced male sterility. Our greatest interest is in that ~~that~~ controls pollen sterility, i.e. nuclear, cytoplasmic factors, or the interaction of particular cytoplasmic and genetic factors. Apart from the cytogenetic type,

there are several types that behave in a Mendelian manner and are apparently chromosomal in origin. These often result from the failure of synapsis, segmental interchanges, fragmentation of chromosomes, and agglutination of chromatin resulting in abnormal meiosis.

2.2.2.1. Desynapsis

The first record of desynapsis in pearl millet was reported by Krishnaswamy *et al.* (1949) on plants from X-ray-treated seeds. A sterile plant examined at meiosis revealed the failure of synapsis in most of the homologues. One of the offspring, X-161, produced proliferating panicles with 98.5% sterility. This sterility was traced to desynapsis, and further study of meiosis produced evidence of conjugation at pachytene in one or two pairs, but by early diplotene, chromosome separation was complete, and the stages that followed exhibited random segregation, resulting in sterility.

Pollen meiosis studied in a plant of pearl millet genotype T.55 showed rapid terminalization of chiasmata and a tendency of chromosome pairs to fall apart in early diplotene, the few remaining bivalents had completely terminalized chiasmata (Patil and Vohra, 1962). Complete desynapsis occurred in many cells. Many other abnormalities were also observed that included poor spindle development, nonorientation of some univalents, clumping of chromosomes on the equatorial plates, and unequal distribution of the chromosomes in the tetrads. The seeds produced were of different sizes, and

probably had different chromosome numbers.

Jauhar (1969) found a desynaptic plant in the cultivar T.55. It had regular pairing only up to the diplotene stage, with varying numbers of univalents observed thereafter at diakinesis and metaphase. Minocha *et al.* (1968) also found several highly desynaptic plants in the Punjab genetic stock BT 91. Based on the meiotic studies they concluded that pollen sterility was higher in the desynaptic plants. Dhesi *et al.* (1973) observed desynaptic plants in BG 32 and found that it had irregular meiosis which resulted in unequal distribution of chromosomes at anaphase I. Such an abnormality was associated with pollen sterility.

2.2.2.2 Segmental interchange

Occasional sterile plants that occur in normal selfed lines or following irradiation from ultraviolet or X-rays appear to result from translocation or simple interchange between two chromosome pairs (Krishnaswamy and Ayyangar 1941, 1942). These interchanges often are manifested meiotically by a ring or chain of four chromosomes.

2.2.2.3 Other meiotic abnormalities

Krishnaswamy (1962) described other meiotic anomalies associated with male sterility, including stickiness of chromosomes, agglutination of chromatin, and others. In some irradiated progenies, inversions leading to bridge formation

and fragmentation were implicated. Most of these plants were completely or partially sterile.

In another male-sterile material that arose spontaneously in inbred line Vg 272, the anthers were phenotypically normal but nondehiscent (Rao and Koduru, 1978b). Except for slightly clumped bivalency, male meiosis was normal up to microspore formation. Microspores degenerated at the uninucleate stage just before the onset of the first mitotic division. Up to this stage, tapetal development was also normal. Pollen degeneration and tapetal breakdown occurred simultaneously. At anthesis, anthers had empty pollen grains and an acellular cytoplasm without nuclei.

In inbred line Vg 272, the *ms* gene causes microspore degeneration before first mitosis in the earlier generations. In later-segregating generations, the action of the *ms* gene is preponed and the gene inhibits archespore differentiation and function and no PMC's are formed. This change in the time of *ms* gene action is assigned by the authors to cytoplasmic mutation from C-2 to C-1, as in later generations a back mutation occurred. Thus, variation in the mode of *ms* gene action is due to cytoplasm and not to gene mutation. The *ms* gene action is highly influenced by modifier genes and environmental factor.

2.2.3 Discovery of cytoplasmic-genetic male sterility

The first report of male sterility in crop plants was made by Bateson and

Gairdner (1921) in flax. Since then male sterile plants have been reported in many other crop plants. Rhoades (1931, 1933, 1950) found a case of cytoplasmic male sterility in corn and reported that this type of sterility was not controlled by nuclear genes, but was transmitted from generation to generation through the egg cell. Similar forms of male sterility have subsequently been discovered in a number of other crop plants of economic importance, including pearl millet.

As early as 1940, Kadam *et al.* observed various forms of male sterility while working on local millet from Nasik. These were: complete steriles, partial steriles and headless plant types having no floret at all. The stigma appeared normal and exerted out of the floret in some of the partial sterile plants. Their anthers were shrunken and deformed and no seeds were set on these plants. But whether female fertility was normal or impaired was not ascertained.

A male-sterile mutant having shrivelled anthers and scanty nonviable pollen was isolated using x-irradiations (Krishnaswamy and Ayyangar, 1942). While female fertility of this mutant was normal, male sterility was complete and was conditioned by a recessive *ms* gene.

Kajjari and Patil (1956) reported male sterility in pearl millet but they couldn't confirm it to be a case of cytoplasmic male sterility. In fact, they reported the occurrence of spikes producing shrivelled anthers without pollen in crossbred progenies. On bagging some of these spikes, no seed was obtained

in those left unpollinated, those that were pollinated with pollen from normal spikes set seed fully. They realized the possibility of getting 100% hybrid seed but didn't establish that the observed male sterility could be of cytoplasmic type. Later, the discovery of CMS reported by Burton (1958), and its excellent maintainers (Burton, 1965), made it feasible to use CMS in seed multiplication of hybrids. The first CMS line Tift 23A was developed by repeated back crossing with Tift 23B (maintainer) and was released in 1965 (Burton 1965, 1969). By introducing dwarf gene (d_2) into these genotypes Tift 23DA and Tift 23DB were developed in which shoot height reduced to one half (Burton and Fortson, 1966; Burton, 1969).

2.2.4 Cytoplasmic diversity

The discovery of male-sterile line Tift 23A₁ and its exploitation in producing high-yielding hybrids and later, their failure to last long due to downy mildew (*Sclerospora graminicola*) epidemics led to intensified research on genetic and cytoplasmic diversification of male-sterile lines. Later on, two more CMS sources, A₂ (L 66A₂) and A₃ (L 67A₃), were identified by Burton and Athwal (1967), and a possible different source A₆, was obtained by Menon (1959) and Appadurai *et al.* (1982), but their use in commercial hybrid breeding remained negligible. Also two different cytoplasms, A_v (Marchais and Pernes, 1985) and A_m (Hanna, 1989) have been identified from *Pennisetum glaucum* spp. *monodii* = *violaceum* (based on different Senegolese accessions of the same wild relative

of pearl millet). Aken'Ova (1985) reported a different cytoplasm in the male-sterile Ex-Bornu [A_4 initially referred to as Gero cytoplasm; Aken'Ova and Chheda (1981)] from Nigeria.

The large scale and continuous use of a single cytoplasmic source runs the risk of rendering hybrid seed industry vulnerable to existing or unforeseen diseases due to a narrow cytoplasmic base parallel to that of sorghum (Schertz and Ritchey, 1978) and maize (Hooker, 1972). Hence it is essential to diversify the cytoplasmic base of male-sterile lines in any crop where these are extensively used in hybrid seed production. A large number of new pearl millet male-sterile lines are now available with cytoplasmic sources other than A_1 (Gill *et al.*, 1986; Virk and Mangat, 1987, 1988, 1989; Virk *et al.*, 1989, 1990a,b,c).

Cytoplasmic differentiation in pearl millet has been judged by the fertility restoration behavior/pattern of an inbred line on different male-sterile sources (Burton and Athwal, 1967). This method is not unambiguous in differentiating cytoplasmic sources. The cytoplasmic differentiation is, however, facilitated if the same genome is introduced into different cytoplasms to develop isonuclear lines (Virk and Brar, 1993). Such a material would be unique for studying (i) the influence of nuclear cytoplasmic interactions on agronomic traits, and (ii) the distinctness of different cytoplasms using biochemical/molecular techniques. Virk and Brar (1993) used four near-isonuclear versions of male-sterile lines 81A and two of Pb 402A to examine the effects of different

cytoplasm on agronomic traits and to assess the distinctness of various sources of cytoplasmic male sterility. The cytoplasmic differences were studied for several agronomic traits using mean values and general combining effects (gca) of male-sterile lines, and specific combining ability effects of hybrids with five inbred male testers. They observed significant differences among near isonuclear lines for a few traits and for gca. A differential behavior of cytoplasm, both in combination with a common pollinator and across pollinators, was observed for several traits. They concluded that the A_1 , A_2 , and A_3 cytoplasm were distinct and that their effect on phenotypic expression of nuclear genes is quite pronounced. They recommended the diversification of male sterility sources in the breeding of pearl millet hybrids. Since CMS is usually inherited maternally and evidence suggests the existence of no relationship between Tift 23A cytoplasm and downy mildew (Anand Kumar *et al.*, 1983), smut (Khairwal *et al.*, 1986), the cytoplasmic diversification within the Tift 23A cytoplasm may continue. However to avoid any devastating disease from cytoplasmic uniformity, alternative sources or systems of cytoplasmic male sterility should be utilized. Various sources of cytoplasm currently available should be characterized for the nature and magnitude of cytoplasmic diversity through the application of biochemical and molecular techniques. At the same time, the search should continue for alternative sources of cytoplasm in accessions and in segregating populations derived from crosses of genetically diverse materials.

To date, a few published reports are available dealing with ontogeny leading to pollen abortion in pearl millet.

2.2.5 Microsporogenesis in cytoplasmic-genetic male sterility

A few reports on cytohistological studies on male-sterile (CMS) lines of pearl millet are available. None of these explain the influence of the cytoplasm system on anther development and microsporogenesis with special reference to the cause and the stage of degeneration of pollen mother cells/microspores/pollen.

Microsporogenesis has been investigated in a few male-sterile materials. In one, microsporogenesis breakdown mainly occurs during tetrad formation (Burton, 1958). In other material, meiosis proceeds normally but microspores degenerate immediately after their release (Singh and Sharma, 1963). The tapetum in both the cases remained persistent near anther maturity.

Balarami Reddy and Reddi (1974) conducted cytohistological studies with male-sterile lines Tift 23A, 628A and their maintainer lines and revealed that meiosis was normal and degeneration of microspores occurred in the sterile lines after separation from the tetrads. There were no differences in the thickness of anther epidermis in male-sterile and maintainer lines. Differences existed in endothecium and tapetum. A-lines had thin endothecium initially but increased in thickness as pollen matured, while it was reverse in the B-lines. Tapetum attained its maximum thickness at meiosis (no particular

stage mentioned) in all the lines and degenerated completely towards the anther dehiscence except in Tift 23A where tapetum remained persistent and vacuolated. Male sterility was associated with thicker endothecium. Male sterility was also associated with tapetal persistence in Tift 23A but not in 628A. The differential behaviour of tapetum development in two CMS lines with A_1 cytoplasm indicates the role of nuclear genome in male sterility. Increased application of nitrogen resulted in increasing the thickness of endothecium and pollen sterility in maintainer lines indicating role of non-genetic factors in these traits. They also observed the differences in the development of epidermis, endothecium and tapetum in the pollen shedders of Tift 23A compared to the pure Tift 23A and Tift 23B. Epidermis of the pollen shedders was thicker compared to pure Tift 23A or Tift 23B. In respect of endothecium it was intermediate to Tift 23A and Tift 23B. But the tapetal cells degenerated completely as in Tift 23B.

Sharma (1978) based on his studies on cytoplasmic male-sterile line (CMS-23) and its fertile counterpart (Inbred-23) concluded that microsporogenesis in CMS and fertile lines of pearl millet differ only on the behavior of the tapetal cells; other developmental stages are quite similar. In the post-meiotic stages the tapetal cells took a light stain and persisted even after the formation of pollen grains in sterile anthers. In fertile line the tapetal cells attain their maximum size before the onset of meiosis. The vacuolation in these cells starts when the spore mother cells enter the cell division stage. The tapetal

cells took a deep stain at pollen mother cell stage and degenerated gradually during the pollen formation. The persistent nature of lightly stained tapetal cells seems to be responsible for the development of nonviable pollen grains.

2.3 Experiment No. 3: Isozyme analysis of tall/dwarf near-isogenic lines

The term isoenzyme was coined by Markert and Moller (1959) to describe different molecular forms (i.e having different molecular weights) of an enzyme with the same substrate specificity. Hunter and Markert (1957) proposed the term "zymogram" to refer to the strips in which the enzyme location is demonstrated. Detection of isozyme using electrophoresis techniques has been extensively used for the characterization and identification of species, inbred lines, isogenic lines, and crosses in plant breeding studies.

In pearl millet, enzyme diversity has mainly been studied in relation to disease resistance/susceptibility, as genetic markers for the construction of linkage maps, to assess taxonomic/phylogenetic affinities within the species, and to know the genetic variability in relation to geographical distribution and evolution.

One of the objectives of millet breeding since 1968 has been to reduce the quantity of stover by reducing plant height while maintaining the robustness of the traditional local varieties in west Africa and India. Several major genes causing substantial reduction in plant height (i.e. genes controlling the height of the first internodes) have been reported in pearl millet (Burton and Fortson,

1966; Gupta *et al.*, 1984; Appa Rao *et al.*, 1986). Of these, the d_2 dwarfing gene has been more widely used than others for the development of hybrid parents (Lambert, 1983). The International Crops Research Institute for the Semi-Arid Tropics (ICRISAT) continue to work on this type of dwarfing plants. Twelve pairs of tall and dwarf near-isogenic lines developed at ICRISAT in the diverse genetic background of three composites were evaluated for grain yield and yield components (Rai and Rao, 1991). The d_2 gene or the genes linked to it, on an average, reduced plant height by 42%, grain yield by 14%, and head girth by 8%, but increased head length and number of tillers per plant by about 5-6%. Days to 50% flowering and seed weight were least affected by the d_2 gene (Rai and Rao, 1991). Although the preliminary tests showed the absence of pleiotropic effects of d_2 gene on fertility (Thakare and Murty, 1972), yet it is not well understood whether the changes in plant characters other than height are due to pleiotropic effects of the d_2 gene, due to linkage between the d_2 gene and other loci, or due to lack of isogenicity. Tall and dwarf pairs look morphologically similar except for height, but other field observations on various morphological traits indicate differences within pairs (Appendix I). However, since quantitative traits are affected by the environment, further investigation is necessary to confirm the degree of isogenicity within these pairs using molecular markers which are least affected by the environment and reflect the true image of genotype, hence they can be used to look at the degree of similarity within the pair of these tall/dwarf near-isogenic lines.

Alcohol dehydrogenase (ADH) was the first enzyme system whose genetics has been worked out in pearl millet (Banuett-Bourillon and Hague, 1979; Banuett-Bourillon, 1982a,b). Another enzyme system subjected to a detailed study is that of esterase (Sandmeier *et al.*, 1981; Tostain and Riandey, 1984; Subba Rao *et al.*, 1989) and MDH was studied by Tostain and Riandey (1985) and Lavergne *et al.* (1986). The inheritance pattern of some other enzymes 6-phosphoglutamate dehydrogenase (6-PGD), catalase (CAT), glutamate oxaloacetate transaminase (GOT), peroxidase (POX), phosphoglucomutase (PGM), phosphatase (Phos) and phosphoglucoisomerase (PGI) have been studied by Trigui *et al.* (1986).

These enzyme systems have been used in pearl millet for various purposes as reviewed hereunder.

2.3.1 Disease resistance

Esterase and/or peroxidase enzymes have been studied in relation to resistance/susceptibility to ergot (*Claviceps fusiformis*), downy mildew (*Sclerospora graminicola*) by various workers (Gupta *et al.*, 1980; Chahal *et al.*, 1986, 1988; Kumar *et al.*, 1987; Shekhawat *et al.*, 1984). Gupta *et al.* (1980) used 8 downy mildew susceptible and resistant varieties (HB-3, 23A, 23B, J-104, PHB-14, L 111A, L IIIB and PIB-228) for studies on esterase (EST) and peroxidase (POX) during early growth stages (seedling stage). Variable intensity and number of bands were observed for both the enzymes in resistant

and susceptible varieties. The number of peroxidase isozyme bands of high molecular weight (i.e., bands with low electrophoretic mobilities), were more in resistant varieties than in the susceptible ones; a reverse pattern was observed for esterases. Satija *et al.* (1983) compared the amount of phenol and polyphenoloxidase (PPO) isozyme activity in 12 genotypes having differential degree of resistance to downy mildew. Observations recorded at two growth stages (30 days and 50 days) particularly crucial for disease development revealed maximum amount of phenols at 30-days growth stage in the immune genotype L5 and minimum in susceptible genotypes, L10 and in A7. The ranking was also similar at 50-days growth stage but with much higher content. PPO activity had a linear relationship with resistance. The immune genotype (L5) was characterized by presence of an anodal band (A1) at 30-days stage whereas no single band characterized at 50-days stage although, the bands possessed differential intensity. Thukral *et al.* (1983) determined genetic and/or biochemical variation for POX and PPO enzymes among pearl millet lines possessing differential degree of resistance to downy mildew. They observed significant differences among lines for the pattern as well as intensity of bands. Even with within line variation it was possible to differentiate the resistant lines from the and susceptible ones on the basis of certain bands, however, no single band perfectly discriminated all the resistant genotypes from the susceptible ones. They suggested that the pattern and intensity of peroxidase and polyphenoloxidase isozymes could be fairly correlated with

resistance to downy mildew in pearl millet. Subsequently, Kumar *et al.* (1987) studied five genotypes having differential resistance to downy mildew and associated the degree of resistance with the presence or absence of a cathodal band (C2) and an anodal band (A4). Shekhawat *et al.* (1979) reported highest peroxidase activity in the suppressed ear-heads followed by green-ear initial stage, diseased half of half-deformed ear-heads, completely proliferated ear-heads and diseased leaves over their healthy counterparts. In another study Shekhawat *et al.* (1984) found that the number of peroxidase isozymes followed the same line (Table 1). It is evident that POX banding pattern was similar in healthy panicle and healthy half deformed panicle; and between panicle at initial stage of disease and diseased half panicle. However few bands appear only after the infection has started, thus indicating that the POX is not the cause of resistance but is the effect of susceptibility. Several other studies have also revealed that peroxidases are the effects rather than the cause of resistance (Seevers *et al.*, 1971). The cause and effect relationship, however, can be studied only by analyzing the material (resistant and susceptible genotypes) grown under disease free as well as diseased conditions. Most of the studies discussed above do not clearly mention the disease conditions of the experimental plot.

Later on, Chahal *et al.* (1988) also studied the peroxidase isozyme pattern in five downy mildew resistant, five susceptible inbred lines and downy mildew-free plants (from downy mildew sick plots) of susceptible lines of pearl

millet. For isozyme analysis, samples comprising of top internodes from 30-days old plants were collected. POX isozyme pattern revealed six anodal (A1-A6) and 11 cathodal (C1-C11) bands. Band C9 was specifically present in resistant plants of resistant lines and disease free plants of otherwise susceptible lines. The presence of the unique band suggested its possible involvement in disease resistance mechanism. These results were in accordance with the observations of Thukral *et al.* (1983) on pearl millet downy mildew, where the presence of an extra cathodal band in resistant plants has been reported. The involvement of two other isozymes (C5 and C6) was also indicated in the resistance mechanism.

Chahal *et al.* (1986) analyzed five each of the ergot susceptible and resistant pearl millet lines (field conditions not mentioned) for their peroxidase isozyme patterns and observed considerable differences in the number and intensity of peroxidase isozymes between the resistant and susceptible genotypes. The enzyme patterns in all the resistant lines were similar, except ICMPE-8 which showed only two cathodal isozymes, C3 and C5, and its mean

Table 1 Peroxidase banding pattern in downy mildew affected plant parts of pearl millet

Band	HL	DL	HE	½D	IS	½E	CP	SH
A13	+	+	+	+	+	+	+	+
A12	+	+	+	+	+	+	+	+
A11	-	-	-	-	+	+	-	+
A10	+	+	-	-	-	-	-	+
A9	-	-	-	-	+	+	+	+
A8	-	-	-	-	-	-	-	+
A7	-	-	-	-	+	+	-	+
A6	-	+	-	-	-	-	-	-
A5	-	+	-	-	-	-	-	-
A4	-	+	+	+	+	+	+	+
A3	+	+	+	+	+	+	+	+
A2	+	+	+	+	+	+	+	+
A1	-	-	-	-	+	+	+	+

HL = Healthy leaves, DL = Diseased leaves, HE = Healthy ear-head, ½D = Healthy half of deformed ear-head, IS = Green-ear initial stage, ½E = Diseased half ear-head, CP = Completely proliferated ear-head, SH = Suppressed ear-head

Prepared from Shekhawat et al. (1984)

ergot severity was also relatively high (15.5% as compared to 0.8 to 1.9% in resistant and 31.5 to 52.5% in susceptible genotypes). Based on their and earlier results, Gupta *et al.* (1980) suggested that peroxidase, if not the only factor, is one of the major factors related to disease resistance. Though, it is difficult to draw a definite conclusion based on different patterns of peroxidase isozymes in these limited number of resistant and susceptible genotypes, further studies involving large number of lines are required to generalize these conclusions.

The above studies indicate that POX isozyme pattern may be utilized as selection criterion for screening downy mildew resistant plants in pearl millet because of the presence of cathodal band(s) in both, the resistant and the disease free susceptible plants.

2.3.2 Phylogenetic affinities

Probably, the first report related to interspecific relationships using proteins, esterase enzyme pattern and phenolic compounds in pearl millet is that of Sujatha (1984). Observations recorded on the distribution pattern of 15 phenolics, 23 proteins and 19 esterases using paper chromatography and PAGE revealed that 12 species grouped into 5 clusters with 7 species in one cluster, 2 in another cluster, and 1 each in three clusters (Rao *et al.*, 1984). Saideswara Rao *et al.* (1986) studied esterase variability in five *Pennisetum* species. Subba Rao *et al.* (1988) reported that closer affinities existed among

the species belonging to $x=9$ type and that *P. mezianum* ($x=8$) was closer to species of $x=9$ series than to those with $x=7$. Subsequently, a more detailed study was carried out (Hussain *et al.*, 1990) in 12 species with putative base numbers of $x=7$, 8 and 9 using 4 enzyme systems (acid phosphatase, amylase, peroxidase, and glutamic oxalo transaminase). Their zymogram patterns appeared to be in agreement with available cytological data (Hanna and Dujardin, 1982; Minocha and Singh, 1971; Patil and Singh, 1964; Raman 1965). For example, the similarities (11-25%) in acid phosphatase, amylase and GOT patterns between *P. glaucum* and *P. purpureum* were consistent with the genome homologies reflected by the extent of chromosome pairing between the genomes of these species representing the $x=7$, 8 and 9 basic types. *P. setaceum*, *P. clandestinum*, *P. villosum* and *P. squamulatum* ($x=9$) showed affinities with species of the $x=7$ and $x=8$ types, supporting their allopoloid nature. Most of the species examined showed distinct species-specific patterns. The phylogenetic relationships among the *Pennisetum* species of three taxonomic gene pools have been analyzed by Lagudah and Hanna (1989). Variation in leaf esterases, 6-PGD, SKDH, leucine aminopeptidase (AMP=cytosolaminopeptidase), phosphoglucomutase (PGM) and malate dehydrogenase (MDH) have been observed. In the primary gene pool, polymorphism for EST, AMP and SKDH was very high, as compared to the near-monomorphism for 6-PGD. Two loci controlling leaf esterases, *Est1* and *Est2*, were identified in the primary gene pool. Cultivated and the wild pearl

millet species differed for the allelic frequency distribution of *Est1* locus and the prevalent alleles (in primary genepool) of *Est1* were absent in *P. purpureum* (secondary genepool). A monomorphic band of the α -EST-specific *Est2* locus was identified in most of the secondary genepool accessions, *P. squamulatum* and an accession of *P. pedicellatum*. Most of the tertiary genepool species differed in the SKDH and EST patterns. They also observed that species of the Brevivalvula section are closely related on the basis of the 6-PGD and α -EST pattern, but the same are highly divergent on the basis of AMP, thus emphasizing that the choice of an enzyme system may lead to variable interpretations and phylogenetic relationships.

In addition to ascertain interspecific relationships, species-specific isozyme patterns were also observed for most of the enzymes, which may be useful in the identification of the individual species as well as for their identification in the hybrid genomes.

Chemotaxonomic studies have been carried out to detect species relationship of the genus *Pennisetum* using peroxidase, esterase and acid phosphatase (ACP) (Kaushal and Sidhu, 1993). Based on similarity index values calculated from the isozyme bands, 3 phylogenetic groups were identified comprising (1) *P. glaucum*, *P. glaucum* subsp. *violaceum* and *P. purpureum*, (2) *P. squamulatum* and (3) *P. orientale* and *P. setaceum*. They also observed that EST isozyme patterns were most effective in differentiating between different *Pennisetum* species since each species exhibited at least one

unique band.

2.3.3 Genetic diversity and geographical distribution

Based on conventional botanical studies, Porteres (1962) identified four centers of diversity for pearl millet in Africa, while Harlan (1971) and Brunken *et al.* (1977) suggested the existence of independent domestication centers. Tostain *et al.* (1987), Tostain and Marchais (1989) and Tostain (1992) made extensive studies of enzyme diversity in cultivated and wild pearl millet from Africa and India. Tostain *et al.* (1987) studied eight enzyme systems in 74 cultivated samples (37 samples each of early and late group) and 8 wild millets from West Africa and observed that cultivars of pearl millet formed three distinct groups (wild types, early and late maturing cultivars), which enabled them to put forward hypothesis on the evolution of pearl millet. The highest enzyme diversity was shown by the early maturing group, whereas the late group showed the lowest. Tostain *et al.* (1987) hypothesized that the West African late cultivars were derived from a common cultivated early complex, which must have been distributed across the Sudanian zone. This complex might have been modified later by the limited gene flow with local early maturing cultivars. Tostain and Marchais (1989) extended the survey of enzyme polymorphism by including 199 populations (including 74 populations studied earlier) from other regions of Africa and from India. These were studied for eight enzyme systems which included: ADH, β -EST, CAT, PGI, PGM, 6-PGD,

GOT and MDH. Based on the results obtained, they proposed an evolutionary hypothesis which stated, multiple domestications in the Sahel, creation of early-maturing cultivars and their migration eastward to India plus a southward migration to Sudanian zone, and creation of late-maturing cultivars and their migration simultaneously westward, eastward, and southward to southern Africa. The Harlan's (1971) the non-center outline fitted very well with Tostain and Marchais (1989) enzyme data, and the evolutionary outline proposed above for pearl millet showed a remarkable parallelism with those proposed for *Sorghum* and finger millet, *Eleusine coracana* (Purseglove, 1976).

Besides, Tostain (1992) studied isoenzyme polymorphism for 8 enzyme systems in 188 accessions of wild millet, *P. glaucum* L. subsp. *monodii* [SYN *P. violaceum* (Lam) L. Rich.], representative of the species' geographic distribution in Africa. Variation in isoenzyme banding pattern corresponded to geographical zonation in five groups: (1) Western Group (Senegal, Mauritania, western Mali), (2) Central Group (eastern Mali and Niger), (3) Air Group (Air Mountains of Niger), (4) West Chad Group, and (5) Darfur Group (encompassing eastern Chad and western Sudan). Overall Nei's diversity was equal in wild and cultivated millets but their locus by locus diversity was different. Wild millet, particularly populations growing far from the cultivated crop (allopatric wild accessions), shows most diversity from the cultivated millets for the alleles *Got A*, *Pgd A* and *Cat A*, whereas cultivated millets are the most diverse from each other for *Pgm A* and *Pgi A*. Based on enzyme

allele distribution, Tostain further interpreted that the allopatric wild millet populations were more divergent from cultivated populations than sympatric wild millets and the cultivated millets from western Mali were closest to wild millets.

2.3.4 Cytoplasmic diversity/cytoplasmic male sterility

Mangat and Virk (1992) analyzed seven male-sterile lines (81A₁, Pb 310A₂, Pb 311A₂, ICMA88001, Pb 406A₃, Pb 402A₁ and Pb 402A₃) and their maintainers for peroxidase, acid phosphatase and esterase isozymes. The banding patterns were different between and within cytoplasmic sources. Even the male-sterile and -fertile versions of the same cytoplasm also showed differences indicating that the cytoplasmic differences can be ascertained by isozyme analysis. Virk *et al.* (1993) included five near-isonuclear versions of 81A₁ and two of Pb 402A₃ CMS lines and their corresponding maintainer lines, 81B and Pb 402B and recorded 14 agronomic, 2 disease-resistance traits, and 3 enzyme systems (PO, ACP and EST) of unbursting anthers and leaves. They observed significant differences for several agronomic traits among the lines, and also found variable peroxidase banding patterns which up to some extent could reveal differences between cytoplasmic sources. However, differences for isozymes of acid phosphatase and esterase were not clearcut. They could differentiate different cytoplasmic sources by looking at the number and/or intensity of band(s) but could not find unique band(s) which could characterize a particular cytoplasmic source.

Though Virk *et al.* (1993) reported the inability of esterases to differentiate cytoplasmic sources, Thakur and Murty (1993) could discriminate and identify different cytoplasms on the basis of esterase isozymes. They used leaf samples of three iso-nuclear lines containing the A₁, A₂ and A₃ cytoplasms (having nuclear genome of L110) and their maintainers [L 110(A₁)B, L 110(A₂)B and L 110(A₃)B]. Leaf samples were analyzed at 4, 6 and 8 weeks stage after sowing and observed different isozyme patterns among the lines at all three growth stages but the discrimination and identification of cytoplasms was easiest at 6-week stage by individual or group of isozyme bands.

2.3.5 Gene introgression and chromosome depletion

In addition to morphological observations (phenotypic markers), enzyme- and DNA-based markers have been used to examine the extent of gene introgression and to identify and select the hybrids. In a study on the transfer of genes governing apomictic mode of reproduction from *P. squamulatum* to pearl millet, Ozias-Akins *et al.* (1993) followed molecular markers (RFLP and RAPD) assisted selection, and confirmed the presence of *P. squamulatum* DNA in BC₃ population. By further analysis of advanced backcross populations, they could depict the co-inheritance of apomictic mode of reproduction and two of the molecular markers. In a study including *P. glaucum*, *P. squamulatum*, their F₁, F₂ and BC₁ hybrids, five enzyme systems and chromosome numbers were used to characterize them. The parental taxa easily separated from the

hybrids whose morphological characters extensively overlapped. However, F_1 s possessed characteristics of both parents to varying degrees while BC_1 s with *P. glaucum* as female parent showed closer resemblance to pearl millet than BC_1 s obtained from crosses in which pearl millet was the male parent. The enzyme study revealed that AMP and β -EST were better genetic markers for the two parental taxa and their hybrids than 6-PGD, PGM and SKDH. However, combining all five systems produced better separation of taxa than using any of the systems singly.

Marchais (1994) studied spontaneous introgression of wild genome into cultivated and vice-versa using morphometric and isozyme analysis of adjacent cultivated and spontaneous populations of pearl millet (*P. glaucum*) in Niger. The analysis revealed a unique continuous distribution of phenotypes ranging from a typical cultivated phenotype to one of a cultivated x wild hybrid. Based on the analysis, the natural population was subdivided into a major wild group and a hybrid (wild x cultivated) group. Cultivated millets displayed an equilibrium state between recombined domesticated and wild genes. The natural population, despite a high rate of immigration via pollen gene flow from cultivated plants, retained its genetic structure by some unknown method of isolation.

Hybridizing tetraploid pearl millet with *P. squamulatum* yields a partially fertile, but unstable, hybrid which loses its chromosomes through its quasi-sexual progeny. Busri and Chapman (1992) studied reproductive and isozyme

variation in an unstable *Pennisetum* hybrid (induced tetraploid pearl millet, $2n = 4x = 28 \times P. squamulatum$, $2n = 6x = 54$) progeny. From embryosac analysis and isozyme (PGI, 6-PGD, and GOT) studies of 30 F_2 (22 selfed, 8 open-pollinated) plants, they concluded that the possibility of chromosome depletion may be linked with the variation of isozyme band patterns which need to be further examined.

2.3.6 Cultivars identification

There are a number of different cultivars available including synthetic, composite, open-pollinated and hybrids. Discrimination between cultivars or lines by seed morphology is extremely difficult. Use of electrophoresis for such discrimination is important for the efficient operation of the seed certification schemes. The use of isoelectric focussing (IEF) (Varier *et al.*, 1992) for distinguishing between and identifying cultivars and lines (HHB 67, H-77/833-2, 843A, HHB 50, H-90/4-5, and 81A₁) of pearl millet has been investigated (Varier and Cooke, 1992). The analysis of water-soluble seed esterases was found to be potentially useful which showed clear differences between the eight cultivars studies and good replication of protein patterns (but complex banding pattern) from within each cultivar. This was the first reported demonstration of the use of IEF for discrimination between pearl millet cultivars/lines. It has been shown (Varier *et al.*, 1992) that the expression of pearl millet esterases is unaffected by both, the site and season (year) of seed production in

composite varieties.

2.3.7 Tissue culture

Tissue culture methods are now widely used for the clonal propagation of plants. However, the presence of considerable genetic variation in the cultures as well as in the plants derived from them is a matter of serious concern in clonal propagation and genetic transformation. Shenoy and Vasil (1992) investigated the extent of biochemical and molecular variation in 63 plants of *P. purpureum* regenerated from 3- to 24-week-old embryogenic callus cultivars. The calli were derived from cultured basal segments of young leaves and immature inflorescences obtained from a single field-grown donor plant. Enzyme analysis (14 isozyme systems) and DNA (mitochondrial, plastid and nuclear DNA RFLP) studies revealed no variation in a representative sample of regenerated plants, thus confirming earlier reports of genetic uniformity of plants derived from somatic embryos and highlighting their value both for clonal propagation and genetic transformation.

2.3.8 Ageing effect

Loss in viability due to ageing during seed storage is reported to result in loss of nucleic acid and protein synthetic capacity (Robert *et al.*, 1973; Ghosh and Choudhury, 1984). This could result in differences in banding patterns of proteins/enzymes between seed lots of the same variety having different levels

of viability or vigor. Esterase banding pattern has been studied to examine the effect of ageing [under ambient and high humidity (75% RH)-high temperature (35°C) conditions] on this enzyme in pearl millet (Varier and Dadlani, 1992). They found that the banding pattern of esterase isozymes changed both under natural and accelerated ageing conditions. Lower mobility bands present in freshly harvested seeds were not detectable after ageing; instead, some additional bands having higher mobility were detected. They suggested that additional bands which appeared after ageing might have resulted from the breakdown of lower mobility bands (high molecular weight proteins) or may have been synthesized in response to the shock caused by accelerated ageing.

2.3.9 Assessment of gametophytic competition

Sarr *et al.* (1988) investigated gametophytic competition by means of pollen mixture technique. Five millet genotypes (Ligui, Massye, 23d₂B, Chinese and Thiotande') with well defined characteristics and characterized for isozymes (EST, ADH) pattern were used. The genetics of these enzymatic markers was already known (Sandmeier *et al.*, 1981; Trigui *et al.*, 1986). The relative competitive ability of pollen was assessed by isozyme electrophoresis of progeny plants. Autopollen competed better than various types of allopollen in case of Ligui genotype.

2.3.10 Other applications

In addition to the uses of isozymes described above, there are few reports about other applications of isozymes in pearl millet. Isozymes of β -amylase were studied during germination (Sheorain and Wagle, 1981) and it was found that the number of bands increased up to 48 h of germination and then decreased. Protogyny in relation to peroxidase and esterase variation was reported by Gupta *et al.* (1980). The isozyme patterns were studied at the stages of complete ear emergence, first style emergence and first anther emergence of the ear-head. The objective was to identify biochemical markers for screening of short duration of protogyny lines that would lead to check of loss due to tip sterility, disease infection and poor seed set. The results indicated that the peroxidase activity decreased from the stage of ear emergence to the time of anthesis, while the activity of esterase showed just the reverse trend, in genotypes with short duration of protogyny. The intensity of bands of peroxidase at style emergence and its decline at anther emergence was more important while the availability of esterase at anther emergence was most determining factor in determining the shorter duration of protogyny. Sandmeier (1993) used ADH (locus *A1A1*) as an marker to determine selfing rates in pearl millet, and found that selfing rates of nine test plants (homozygous for ADH locus *A1A1*) varied from 2.2 to 21.7%. Selfing rates were not significantly different within spikes of the same plant, except for one individual.

The genetic linkage relations between the d_2 dwarfing gene and seven enzymatic marker genes (*Adh A*, *Est A*, *Mdh D*, *Pec A*, *Pgi A*, *Pgm A*, and *Skdh A*) were evaluated in three crosses between semi-dwarf and normal inbred lines of pearl millet (Tostain, 1985). All the eight genes segregated in Mendelian fashion and various linkages were observed between *Pgi A* and *Pgm A* [4 ± 4 centimorgans (cM)], between *Skdh A* and *Adh A* (11 ± 7 cM), between D_2 and *Skdh A* (9 ± 5 cM) and between D_2 and *Adh A* (17 ± 8 cM). The order of linkages is: *Adh A* - 11 cM - *Skdh A* - 9 cM - D_2 . He suggested that the linkage between d_2 gene and *Skdh-A* could be used in the separation of D_2D_2 and D_2d_2 at the seedling stage.

III MATERIALS AND METHODS

3.1 Experiment No. 1: Mitochondrial DNA RFLP analysis of pearl millet CMS lines

3.1.1 Plant material

Nineteen male-sterile lines (A-lines) of pearl millet were used in this study included 6 near-isonuclear A-lines with known/classified cytoplasmic sources; and 13 unclassified sources (Table 2). The later consisted of 9 CMS lines from Large-Seeded Genepool (LSGP) and, 2 each from Early Genepool (EGP) and Population Varieties. The line 81A₁ is based on the A₁ cytoplasm (Burton, 1965), bred at ICRISAT (Anand Kumar *et al.*, 1984). Pb 310A₂, Pb 311A₂, and Pb 406A₃, were bred at PAU, Ludhiana (for references see Table 2) from L 66A₂ and L 67A₃ CMS sources of Burton and Athwal (1967). The 81A_v was bred at ICRISAT from *P. glaucum* subsp. *violaceum* (Lam.) L. Rich. (Marchais and Pernes, 1985) and 81A_m, was bred at ICRISAT from the *P. glaucum* subsp. *monodii* (= *violaceum*) (Maire) Brunken (Hanna, 1989).

Male-sterile lines from LGSP were developed from male-sterile S0 plants. Large-Seeded gene pool was developed by random mating about 1,000 pearl millet accessions that are having 1000 grain mass of more than 9.0 g and flower in less than 80 days. Early Genepool was constituted by random mating 1143 accessions having less than 50 days flowering. EC87/89-7 was

Table 2. Description of male-sterile lines used in the present study.

Cytoplasm	Description	Reference	Symbol used in figures
<i>Classified cytoplasm</i>			
81A ₁	A ₁ cytoplasm from Tift 23A ₁	Anand Kumar <i>et al.</i> , 1984	A ₁
Pb 310A ₂	A ₂ cytoplasm of L 66A (present in Pb 305A ₂) carrying 81B genome	Virk and Mangat (1987) Virk <i>et al.</i> (1990a)	0A ₂
Pb 311A ₂	A ₂ cytoplasm of L 66A (present in Pb 307A ₂) carrying 81B genome	Virk and Mangat (1987) Virk <i>et al.</i> (1990a)	1A ₂
Pb 406A ₃	A ₃ cytoplasm of L 67A (present in Pb 405A ₃) carrying 81B genome	Virk and Mangat (1988, 1989) Virk <i>et al.</i> (1990a)	A ₃
81A _v	<i>violaceum</i> cytoplasm from <i>P. glaucum</i> subsp. <i>violaceum</i> carrying 81B genome	ICRISAT	A _v
81A _m (=81A ₄)	<i>monodii</i> cytoplasm from <i>P. glaucum</i> subsp. <i>monodii</i> (= <i>violaceum</i>) with 81B genome	Hanna (1989)	A _m
<i>Unclassified cytoplasm</i>			
(1) Large Seeded Genepool¹			
LSGP 6	Plant number 6 from LSGP	ICRISAT	L6
LSGP 14	Plant number 14 from LSGP	ICRISAT	L14
LSGP 17	Plant number 17 from LSGP	ICRISAT	L17
LSGP 22	Plant number 22 from LSGP	ICRISAT	L22
LSGP 28	Plant number 28 from LSGP	ICRISAT	L28
LSGP 36	Plant number 36 from LSGP	ICRISAT	L36
LSGP 43	Plant number 43 from LSGP	ICRISAT	L43
LSGP 55	Plant number 55 from LSGP	ICRISAT	L55
LSGP 66	Plant number 66 from LSGP	ICRISAT	L66
(2) Early Genepool₂			
EGP 15	Plant number 15 from EGP	ICRISAT	E2
EGP 33	Plant number 33 from EGP	ICRISAT	E1
(3) Population Varieties			
LRE 29-2	Landrace from Rajasthan	ICRISAT	P1
EC87/89-7	Developed by merging various composites ³	ICRISAT	P2

¹ Large Seeded Genepool developed by random mating about 1,000 accessions that are having 1000 grain mass of more than 9.0 g. and flowering in less than 80 days; ² Early Genepool developed by random mating 1143 accessions having less than 50 days flowering; ³ EC87: Developed by merging two promising early composites (EC II and BSEC), which differed in maturity, seed size and tillering; EC89: Developed by merging BSEC, TCPI and EC-C6.

constituted by merging various composites. EC87 was developed by merging two promising early composites (EC II and Bold-Seeded Early Composite, BSEC) which differed in maturity, seed size and tillering. The EC89 was developed by merging BSEC and EC-C6.

3.1.2 Seed multiplication

Two types of seed lots were produced, open-pollinated and seed produced by backcrossing male-sterile lines (having 81B genome) with 81B.

Open-pollinated seed lot came from the harvest of bulk seeds from the open-pollinated panicles of each line. For getting backcrossed seed (referred to as sib seed), true to the type panicles were bagged at boot stage and pollinated with 81B pollen at the time of stigma emergence. Panicles from each line were harvested separately and bulked. Off-types and pollen shedders were not used for seed production.

3.1.3 Clones used

Four DNA clones from pearl millet (homologous) and two from maize (heterologous) were used to probe mitochondrial DNA (mtDNA) restriction fragments obtained by digestion with three restriction enzymes to get 12 enzyme-probe combinations (Table 3).

Table 3. Combinations of restriction enzymes and probes used.

Restriction enzyme	Homologous probes				Heterologous probes	
	4.7 kb	9.7 kb	10.9 kb	13.6 kb	<i>atp 6</i>	<i>cox I</i>
<i>Bam</i> HI	Yes	--	--	Yes	Yes	Yes
<i>Hind</i> III	Yes	--	Yes	--	Yes	Yes
<i>Pst</i> I	Yes	Yes	--	--	Yes	Yes

3.1.3.1 Homologous mtDNA probes

Four *Pst*I-digested mtDNA fragments were gifted by Professor Smith, University of Florida, USA. These fragments were cloned in pUC18 plasmid and transformed into *Escherichia coli* strain JM83. Hybridization studies have shown that these fragments are related and show multiple homologies, the 4.7 kb fragment had partial homology with a 10.9 kb and a 13.6 kb fragment and the 9.7 kb fragment was partially homologous to the 13.6 kb fragment (Smith *et al.*, 1987).

3.1.3.2 Heterologous mtDNA probes

Maize clones containing known mitochondrial genes (*atp6* and *coxI*) were used as probes. The F₁-F₀ ATPase submit 6, *atp6* (Dewey *et al.*, 1985) was gifted by C.S. Levings III, Genetics Department, North Carolina State University, Raleigh, NC, USA, as purified plasmid DNA with this insert. Clones of cytochrome *c* oxidase submit I, *coxI* (Isaac *et al.*, 1985) was gifted by C.J. Leaver, Department of Botany, University of Oxford, Oxford.

3.1.4 Mitochondrial DNA isolation

Basic steps involved in any mtDNA isolation procedure include:

Dark-grown, young seedlings (etiolated) or soft, non-green, internode stem tissues are generally used to isolate mtDNA as they yield better DNA with better digestibility with restriction enzymes because of lower concentrations of phenolics and other adhering compounds as compared to green tissues. Further, grinding of the plant material in a Waring blender with 10 volumes of a high ionic strength saline extraction buffer is done. The extraction buffer should contain EDTA, BSA (bovine serum albumin) and a sulfhydryl reagent like 2-mercaptoethanol (2 ME = β ME). It is followed by differential centrifugation to isolate mitochondria from nuclei, plastids and cell debris, DNase treatment to remove extra-mitochondrial DNA (mtDNA is not damaged because highest proportion of mitochondria are intact), lysis of mitochondria with sodium dodecyl sulfate (SDS) and proteinase K, precipitation of SDS-protein-carbohydrate complexes with potassium acetate, ammonium acetate-isopropanol precipitation, phenol and phenolchloroform extractions, and second ammonium acetate-isopropanol precipitation of mtDNA.

Several procedures for mtDNA isolation have been reported in literature (Kemble *et al.*, 1980; Hanson *et al.*, 1986; Leaver *et al.*, 1983; Smith *et al.*, 1987). Ramanan (1992) compared procedures outlined by above workers. The results obtained from the protocol given by Smith *et al.* (1987) were most satisfactory. Therefore, the procedure given by Smith *et al.* (1987) was adopted

in the present study.

According to this protocol, mtDNA was isolated from dark-grown, 6-day-old seedlings (sterilized seeds sown in sterile vermiculite at 30°C in the germinator). Seedlings were homogenized in a Waring blender and extracted with 10 volumes of buffer A (30-60 g of plant tissue using 300-600 ml of buffer A) containing 1 M NaCl, 50 mM Tris-HCl pH 8.0, 5 mM EDTA, 0.1% BSA and 0.7% β -MCE, and then filtered through four layers of cheese cloth and one layer of Miracloth (Calbiochem Biochemicals). The supernatant obtained by centrifuging that filtrate at 1000 x *g* was centrifuged again at 16000 x *g* to pellet the mitochondria. Pellets were taken up in 250 ml of buffer G containing 0.15 M NaCl and 50 mM Tris-HCl pH 7.5, centrifuged at 1600 X *g* for 15 min, and then resuspended in buffer G (10 ml/35 g tissue) containing 10 mM MgCl₂ and digested with DNase (50 μ g/ml) (Sigma Chemical Co., Type II, at approx. 1425 Kunitz units/mg) for 45 min at room temperature (25°C) to remove extramitochondrial DNA. Before carrying the lysis of mitochondria, DNase was removed by underlaying the samples with 20 ml shelf buffer (600 mM sucrose, 20 mM EDTA pH 8.0 and 10 mM Tris-HCl pH 7.5) and centrifuged at 15000 x *g* for 20 min. The mitochondrial pellets were washed with saline wash buffer (1 M NaCl, 50 mM Tris-HCl pH 8.0, 20 mM EDTA pH 8.0) by resuspending the pellets and then centrifuging at 15000 x *g* for 10 min. The washed pellet was taken up in 6 ml NN buffer (50 mM Tris-HCl pH 8.0 and 20 mM EDTA pH 8.0) and mitochondria were lysed by adding proteinase

K (100 $\mu\text{g/ml}$) and 10% SDS (0.5% w/v) and incubated at 37°C for 40 min. Equal volume of 2x extraction buffer (0.15 M Tris-HCl pH 8.0, 0.008 M EDTA pH 8.0, 0.1 M NaCl, 1.5% SDS) was added to the lysed mitochondria and incubated at 65°C for 20 min, then kept at room temperature for 5 min. One-third volume of cold 5 M potassium acetate was added to the lysate and incubated on ice for 30 min. Following centrifugation at 15000 X g in a Sorvall SS-34 rotor for 20 min, nucleic acids (mtDNA + RNA) were then precipitated from the supernatant by addition of 0.5 volume of chilled isopropanol after adjusting to 0.34 M ammonium acetate. After the overnight (O/N) incubation at -20°C, nucleic acid was pelleted by centrifugation at 15000 X g in a Sorvall SS-34 rotor for 25 min. The pellet was washed twice with 70% ethanol, air dried for 45-60 min and dissolved in 700 μl of $T_{50}E_{10}$ buffer (50 mM Tris-HCl pH 8.0 and 10 mM EDTA pH 8.0). This procedure was followed by phenol extraction (once), twice with phenol-chloroform extraction (1:1) and twice with chloroform extraction, and reprecipitation with isopropanol, 70% ethanol wash (twice) and brief vacuum/air drying. The nucleic acid (containing mtDNA) was finally resuspended in $T_{10}E_1$ (10 mM Tris-HCl and 1 mM EDTA pH 8.0) and stored at -20°C for further use. Various buffers and other chemicals used for mtDNA analysis are given in Appendix II.

3.1.5 Restriction enzyme digestion

About 5 μg of mtDNA in $T_{10}E_1$ buffer was used for restriction endonuclease

digestion with *Bam*HI, *Hind*III and *Pst*I following endonuclease supplier's instructions. The digestion was carried out in the presence of RNaseI (15 µg/ml) in a total volume of 30 µl. The reaction was terminated by the addition of 5 µl loading buffer (25% sucrose, 0.1% bromophenol-blue and 20 mM EDTA) in each 30 µl sample.

3.1.6 Electrophoresis

Fragments of mtDNA obtained after enzyme digestion were separated by electrophoresis for ≈16 h in 0.8% agarose horizontal slab gels (BIO-RAD DNA SUB CELL™) 5 mm thick using 15 teeth comb at 2 v/cm in TBE (89 mM Tris-HCl, 89 mM Boric acid and 2 mM EDTA, pH 8.3) or TAE (0.04 M Tris-acetate, 0.001 M EDTA, pH 7.8) buffer. The gels were prepared in the same buffer which was used for electrophoresis. *Hind*III-digested Lambda DNA (λ DNA) was used as molecular size marker. The gels were stained in 0.5 µg/ml ethidium bromide for 15 min, destained for 30 min in distilled water, viewed on a UV-transilluminator and photographed to see the quality of digestion.

3.1.7 Southern blot hybridization

3.1.7.1 Preparation of southern blots

DNA fragments obtained after digestion were transferred from agarose gel onto Nucleic Acid Nylon Transfer Membrane (Hybond-N+, Amersham) using the Vacugene blotting apparatus (LKB Vacu Gene XL, Pharmacia) following

manufacturer's instructions (Appendix III).

3.1.7.2 Purification of inserts from plasmid DNA

DNA inserts of maize and pearl millet mtDNA specific gene probes were isolated according to Maniatis et al. (1982) (Appendix IV).

3.1.7.3 Labelling of probes

Random-primed method of Feinberg and Vogelstein (1983) was used for radiolabelling of DNA. Purified insert DNA was denatured by heating at 95°C for 10 min, immediately cooled on ice for 5 min and labeled using ³²P-deoxycytidine 5' triphosphate (dCTP) using the Promega labelling kit (following the supplier's instructions). The probe was labelled in a 50 µl reaction mixture containing ≈25-50 ng of denatured probe DNA, 1x labelling buffer, 2 µl equimolar concentrations of dATP, dGTP and dTTP, 2 µl (10 mg/ml) acetylated BSA, 5 µl of 50 uCi ³²P-dCTP, 1 µl Klenow enzyme. The reaction mixture was incubated at room temperature (≈25°C) for one hour. The reaction was terminated by adding 5 µl of 20 mM EDTA. To the labelled probe, 450 µl of T₅₀E₁₀ was added. The labelled probe was again denatured by heating at 95°C for 5 min and subsequent snap cooling on ice for 5 min to use in the hybridization step.

3.1.7.4 Hybridization to labelled probe

3.1.7.4.1 Prehybridization

Southern blots were washed with sterile distilled water (SDW) followed by 3x SSC (preheated to 65°C) and prehybridization was carried out in hybridization solution (7% SDS phosphate solution) containing 7% SDS, 1% BSA and 500 mM Na₂HPO₄, pH 7.2 and 20 µg/ml of sheared, denatured salmon sperm DNA. Care was taken to remove all the air bubbles trapped between the blot and the bottle. Prehybridization was carried out at 65°C in hybridization oven (HYBAID) for 3 h.

3.1.7.4.2 Hybridization

Labelled probe was added to the prehybridization mixture and incubated at 65°C in the hybridization oven for at least 16 h (O/N). Care was taken to remove air bubbles present in between the blot and the hybridization bottle.

3.1.7.5 Washing of the blots

Following hybridization, the membranes were washed following two changes of 150 ml each of ³²P-Wash solution (3x SSC containing 0.1% SDS). Each washing was carried out for 15 min at 65°C in the hybridization bottles using hybridization oven. Third washing was done with 400 ml of ³²P-Wash solution for 30-45 min at 65°C in hybridization oven. The membrane was air-dried by blotting in between two layers of Kim wipes and enclosed in Saran wrap.

3.1.7.6 Autoradiography

Autoradiography was conducted at -70°C by exposing the membrane to Indu X-ray films using KODAK intensifying screens in a cassette for various exposure times. The X-ray films were developed with KODAK developer for 2 min, followed by a stop bath (1% acetic acid solution) treatment for 1 min, fixed with KODAK fixer for 2 min, washed in running tap water and air-dried. The autoradiograms were photographed using KODAK 100 ASA colored films.

3.1.8 Cluster analysis

Restriction fragment sizes of sample DNA were calculated by plotting on X-axis the distance travelled by λ DNA fragments against their molecular weights on Y-axis. The curve so obtained was used to calculate the molecular weight of DNA fragments obtained from the samples being tested. Similarity index matrices were calculated based on proportion of common fragments between two lanes (Nei, 1987) by using

$$F = \frac{2 M_{xy}}{M_x + M_y}$$

where F is the similarity index (also represented as SI in the text), M_x is the number of bands in accession x , M_y is the number of bands in accession y , and M_{xy} is the number of bands common to both x and y . $F \times 100$ gives the percent similarity ($\%S$) between the two accessions, thus $F = 1.0$ would mean that the patterns in the two accessions are identical. The data are presented in the

form of matrices of order $n \times n$ where 'n' is the number of accessions. The cluster analysis was done based on the expression of similarity of objects and respective groups by the agglomeration method of hierarchical clustering techniques which proceed by a series of successive fusions of the 'n' objects into clusters, using computer program "GENSTAT Release 4.03".

3.1.9 Other comparisons

Both open-pollinated (OP) and sib seed of isonuclear lines were used for the RFLP analysis to examine whether or not any differences exist between the two seed lots. Since the production of OP seed requires less efforts than the production of sib seeds, the objective was to examine the feasibility of using OP seed to meet the seed requirements which sometimes puts constraints to conduct such experiments. In addition, three isonuclear male-sterile lines (81A₁, 81A_m and PB 406A₃) and 81B were used to analyze their total DNA (tDNA) RFLP patterns using three restriction enzymes in combination with pearl millet 4.7 kb and maize *coxI* probe to compare the results from mt- and t-DNA. The objective was to find out the possibility of using tDNA to determine the heterogeneity among various cytoplasms as tDNA isolation is quicker, demands less seed, yields more DNA and is cost effective as compared to mtDNA.

Total DNA was isolated using the method of Dellaporta *et al.*, 1983 (Appendix V). Restriction enzyme digestion reactions were set up as per

supplier's instructions with $\approx 15 \mu\text{g}$ DNA in a final volume of $30 \mu\text{l}$. Southern blotting, prehybridization, labelling of probe and hybridization procedures were similar to those as described for mtDNA.

3.2 Experiment No. 2: Anther development and microsporogenesis in pearl millet iso-nuclear lines

Seeds of six near-isonuclear male-sterile lines belonging to five different cytoplasmic sources and their maintainer counterpart (81B) were obtained from ICRISAT Asia Center (IAC), Patancheru, India. Earlier, these have been maintained by backcrossing with 81B. The six isonuclear A-lines based on the nuclear genome of 81B, included in this study were : 81A₁ with Tift 23A₁ cytoplasm, ICMA 88001 = 81A_v with *violaceum* cytoplasm (Marchais and Pernes, 1985), 81A_m = 81A₄ with *monodii* = *violaceum* cytoplasm (Hanna, 1989), Pb 310A₂ and Pb 311A₂ (A₂ cytoplasm), and Pb 406A₃ (A₃ cytoplasm).

3.2.1 Development of near-isonuclear lines

The male-sterile line 81A₁ (= ICMA 1) was developed at the International Crops Research Institute for the Semi-Arid Tropics (ICRISAT), Hyderabad (Anand Kumar *et al.*, 1984), and has been extensively utilized in hybrid breeding programs in India because of its good combining ability. ICMA 1 = 81A₁) and ICMB1 (= 81B) were developed by irradiating dry seeds of Tift 23DB

(a maintainer line highly susceptible to downy mildew) with 30kR of gamma rays from a $^{60}\text{C}_0$ source. M_0 generation plants were selfed and grown head-to-row in a downy mildew disease nursery. Dwarf, vigorous, and disease free plants were both selfed and crossed with Tift 23DA (A_1 system male sterile line). For those Tift 23B selections that completely maintained sterility on Tift 23A, the process of selection and backcrossing into A_1 cytoplasm was repeated twice a year for six generations in the downy mildew disease nursery at ICRISAT Center. The ICMA 1 and ICMB 1 pair was identified on the basis of phenotypic similarity, vigor, seed-set and downy mildew resistance, and preliminary combining ability tests (ICRISAT, 1985).

The 81B genome was substituted into the A_2 and A_3 cytoplasm at Punjab Agricultural University, Ludhiana by backcrossing of the 81B line onto the Pb 305 A_2 , Pb 307 A_2 and Pb 405 A_3 male-sterile lines in A_2 and A_3 cytoplasm (Burton and Athwal, 1967) which resulted in Pb 310 A_2 (= 81 A_2), Pb 311 A_2 (= 81 A_2) and Pb 406 A_3 (= 81 A_3) near-isonuclear male-sterile lines, respectively (Virk and Mangat 1987, 1988, 1989; Virk *et al.*, 1990a, c). The material was grown in the polyhouse in the cool dry season (CDS) and the hot dry season (HDS) of 1993/94 at ICRISAT Asia Center (IAC). Observations on meiosis, anther development, microsporogenesis and pollen sterility were recorded in each season.

3.2.2 Meiosis

3.2.2.1 Material collection for meiotic analysis

For meiotic studies, 4-5 spikes obtained from 5 plants of each line were used in each season. Spikes were collected when they were still about 1-2 cm inside the flag leaf. They were collected and fixed between 05:30 and 06:40 h (HDS) and 07:00 and 08:00 h (CDS) in a freshly prepared Carnoy's fluid (6 absolute alcohol : 3 glacial acetic acid : 1 chloroform) in which a few drops of ferric chloride (mordant) were added @ 1 ml of saturated aqueous solution of ferric chloride to 200 ml of Carnoy's fluid. For more efficient fixation, the material was transferred to fresh fixative after 1-2 h and stored at 4°C.

Meiotic stages occur more or less in a sequence along the rachis in a spike, this facilitated in identifying a particular position along the rachis where the PMCs contained in a floret show tetrad formation. Florets below that point along the rachis were used to analyze other meiotic stages.

3.2.2.2 Staining of chromosomes

An anther from a floret of appropriate size was squashed in a drop of 2% acetocarmine. The anther was gently crushed with a blunt end of a polished needle so that all PMCs were released in a drop of stain. A coverslip was then carefully placed over the drop and the slide was slightly warmed on a mild flame and tapped. Excess stain was removed from under the coverslip with a few drops of 45% acetic acid which helped in bringing about a better contrast

between stained chromosomes and the cytoplasm.

3.2.3 Pollen sterility

3.2.3.1 Material collection for pollen sterility/fertility observations

Pollen sterility/fertility observations were recorded on 5 plants of each line in both seasons. For each plant two spikes were used with 10 spikelets per spike, 3 florets per spikelet and 3 anthers per floret, leading to 180 anthers per plant and 900 anthers per line. Anthers were collected just before dehiscence.

3.2.3.2 Sample preparation and staining of pollen grains

Pollen fertility was studied by squashing mature anthers (before dehiscence) in a drop of Alexander stain (Alexander 1969, 1980), covered with a cover slip, warmed gently over a flame, and examined under the microscope. Fully formed and dark red stained pollen grains were scored as fertile (nonaborted), whereas, deformed, stained green were counted as sterile (aborted).

The chemical composition and method of preparation of Alexander's stain is given below:

Preparation of Alexander's stain:

The stain was prepared by adding the following constituents in the order given below, and stored in a dark colored bottle:

95% alcohol	10 ml
malachite green	10 mg (1 ml of 1% solution in 95% alcohol)
distilled water	50 ml
glycerol	25 ml
phenol	5 g
chloral hydrate	5 g

acid fuchsin	50 mg (5 ml of 1% solution in water)
orange G	5 mg (0.5 ml of 1% solution in water)
glacial acetic acid	1-4 ml

The amount of glacial acetic acid added to the mixture depends on the thickness of the pollen walls, 2 ml of glacial acetic acid was added for pollen grains and 4 ml for nondehiscent anthers.

3.2.3.3 Staining of pollen inside the nondehiscent anthers

Intact nondehiscent anthers were also examined to find the sterility/fertility status of anthers to estimate the amount of nonaborted and aborted pollen within the anthers. The Alexander's stain was acidified by mixing 100 ml of the stain mixture with 4 ml of glacial acetic acid. Anthers were collected just before or immediately after anthesis. Non-dehiscent anthers were fixed for 24h in Östergren and Heneen's (1962) fixative (methanol, 60 ml; chloroform, 30 ml; distilled water, 20 ml; picric acid, 1 g; and HgCl₂, 1 g). Thereafter, these anthers were transferred through 70, 50 and 30% alcohol, allowing 30 minutes for each change, to gradually hydrate the anthers, and finally rinsed in water. Excess water was removed by slightly pressing the anthers between blotting papers. Mounts were then prepared using enough stain to cover the anthers, and kept at 60°C for 24h. Excess stain was removed with blotting paper and slides were examined under a light microscope.

The above procedure was modified with a view to examine more anthers in less time. In this context, anthers were collected just at dehiscence and dipped in acidified stain followed by vacuum infiltration. Stain was taken in small airtight glass bottles (1 ml) and anthers were placed in it and kept at 60°C for 48h. Before examining under the microscope, excess stain was

removed by pressing anthers between blotting papers. These anthers were then placed on clean glass slide and viewed under a light microscope. For permanent mounting of anthers, a drop of permount was placed over the specimen, covered with cover slip and slightly pressed. This procedure was found to be satisfactory for estimating the amount of nonaborted and aborted pollen within the anthers of pearl millet (modified from Alexander 1969, 1980).

3.2.4 Microsporogenesis

3.2.4.1 Collection and preparation of samples for histological studies

3.2.4.1.1 Sample collection

Florets/spikelets for histological studies were collected at various stages of anther development. These stages are defined as follows :

A. Premeiotic

- Stage 1.* Sporogenous tissue stage
- Stage 2.* Callose starts appearing at the center of locule

B. Meiotic

- Stage 3.* Callose separation starts along the walls of PMCs (early Prophase I)
- Stage 4.* Callose separation prominent (late Prophase I)
- Stage 5.* Callose movement half way towards tapetum (Metaphase I)
- Stage 6.* Callose near tapetum (early Anaphase I)
- Stage 7.* Wide cytoplasmic channels/connections present between PMCs (late Anaphase I)
- Stage 8.* Stretching between cytoplasmic channels exists (early Telophase I)
- Stage 9.* Cytoplasmic channels do not exist (late Telophase I)
- Stage 10.* Dyad formation
- Stage 11.* Tetrad formation

C. Postmeiotic

- Stage 12.* Young microspores (i.e. microspores recently released from tetrads)

Stage 13. Microspores embedded in the tapetum (developing microspores)

Stage 14. Traces of the tapetum seen

Stage 15. Mature pollen/absence of tapetum

Stage 16. Anther dehiscence starts

These stages were defined based on anther development in 81B (male-fertile control). Corresponding developmental stages were studied in male-sterile lines and compared with 81B, used as a male-fertile control. For each stage 50 to 60 florets were examined in each line.

3.2.4.1.2 Sample Preparation

All fixation steps were carried out carefully under a fume hood.

A. Fixation

Florets were collected and fixed in 3% glutaraldehyde in 0.1M phosphate buffer (pH 7.2). These were gently vacuum infiltrated at low pressure for 10 - 15 minutes until the florets sink. For better infiltration these were kept on a gyratory shaker overnight and then washed four times in 0.1M Sodium phosphate buffer (pH 7.2) over a period of 2 h.

B. Postfixation

Postfixation was carried out in 2% aqueous osmium tetroxide for 4 h. The postfixed samples turned black and brittle. Samples were then washed carefully thrice with distilled water till all excess fixative was removed.

C. Dehydration

Dehydration was carried out using a graded series of acetone; 30 to 45 min. each in 30%, 50%, 70%, 90% and two times in 100% acetone. The samples were then infiltrated with 1:1 mixture of Spurr epoxy resin and 100% acetone for about one hour followed by pure Spurr resin (Spurr, 1969) for another one hour and then dipped in fresh Spurr resin for over night.

D. Embedding

Finally, the samples were placed in resin poured into flat silicon rubber molds. The resin was polymerized to form blocks by placing the molds in an oven at 70°C for 24 to 48 hours.

E. Sectioning

Transverse sections of entire florets/spikelet were cut at a thickness of 5-8 μm with a glass knife using an Ultracut Reichert Jung Ultra-microtome, mounted on glass slides and stained.

F. Mounting and staining

Sections were spread on a drop of double distilled water placed on a glass slide and warmed gently to evaporate the drop so that the sections stuck firmly to the glass slide.

These sections were initially stained with LADD Multiple stain (LADD

70955) for 2 minutes by placing a drop of stain on the sections and briefly warming it, and the excess stain was removed by thorough washing with water. A drop of 0.5% Malachite green was then placed on the specimen, slightly warmed for about 3 minutes and washed thoroughly with water and gently dried. A cover slip was then mounted using a drop of Permount (Fisher). The resulting slides showed a yellowish red background of cell walls, and cytoplasm; dark violet callose and chromosomes; dark blue to violet nuclei; dark red starch grains; and red-violet exines. Samples were then examined under a light microscope (Olympus BH2 System) and photographed.

3.3 Experiment No. 3: Isozyme analysis of tall/dwarf near-isogenic lines

3.3.1 Plant material / Development of near-isogenic lines

The tall and dwarf near-isogenic lines (T/D NILs) were developed at ICRISAT Asia Center, Patancheru, A.P., India in the diverse genetic background of three composites: Early Composite (EC), Medium Composite (MC), and Nigerian Composite (NC).

A d_2 dwarfing gene from GAM 73 (a synthetic bred in Senegal) was introduced into EC, MC and NC by three backcrosses. Selfing of heterozygous tall plants in BC_3F_3 progenies and continuing this system up to BC_3F_8 generation led to the development of near-isogenic tall and dwarf inbred lines. Out of these total 12 pairs, seven pairs, 3 each from EC and MC and one from NC were selected to use in the present investigation (Table 4).

3.3.2 Seed multiplication

Seed of seven tall/dwarf near-isogenic lines (T/D NILs) was produced by selfing. Plants typical to the isolines were selected and selfed. Care was taken to remove a few off-type plants whenever they occurred. Selfed seeds from individual plants were bulked and used for isozyme studies. The seeds were produced during 1993 rainy season at CCS Haryana Agricultural University, Hisar and at ICRISAT Asia Center, Patancheru, India during summer 1993. The seed was stored at 4°C for further use.

3.3.3 Methods

3.3.3.1 Germination

Seeds were surface sterilized with 0.1% HgCl₂ for 10 minutes followed by 3-4 washing with distilled water to remove the traces of HgCl₂ and were sown in the plastic boxes between two filter papers. These were kept at 37°C in the germinator (i.e. in dark). Five days old etiolated seedlings (7-9 cm) were harvested (except roots) for getting the crude extracts to be used for isozyme studies. Imbibition of seeds was done by putting the surface sterilized seeds on water-soaked filter papers in sterilized glass petriplates at room temperature for 18 hours (18hIS).

3.3.3.2 Extraction

Crude extracts for electrophoresis were prepared either from etiolated

Table 4. Origin of tall/dwarf¹ near-isogenic pairs of pearl millet².

Near-siogenic pair no.	Designation	Origin	
		Recurrent composite	F ₉ progeny from
1*	EC 1	Early Composite (EC)	BC ₃ F ₃ -33
2*	EC 2		BC ₃ F ₃ -199
3*	EC 3		BC ₃ F ₃ -159
4	EC 4		BC ₃ F ₃ -203
5	MC 5	Medium Composite (MC)	BC ₃ F ₄ -4-3
6*	MC 6		BC ₃ F ₄ -4-4
7	MC 7		BC ₃ F ₄ -4-7
8	MC 8		BC ₃ F ₃ -31
9*	MC 9		BC ₃ F ₅ -121-6-2
10*	MC 10		BC ₃ F ₅ -121-6-3
11	MC 11		BC ₃ F ₃ -191
12*	NC 12	Nigerian Composite (NC)	BC ₃ F ₃ -143

1. GAM 73 was used as the d₂ dwarfing gene donor population.

2. Modified from Rai (1990)

* Tall/dwarf near-isogenic pairs used for isozyme studies.

seedlings (SL) or 18 hours imbibed seeds (18hIS) or dry seeds (DS). A sample of 50-100 mg of tissue, including coleoptile, plumule, and mesocotyle were homogenized in grinding buffer solution (@ 1 ml buffer per 1 g of tissue) with a prechilled mortar and pestle (Appendix VI). Thereafter, samples were transferred in prechilled 1.5 ml polyethylene microcentrifugation tubes (kept on ice). These were centrifuged at 12,000 rpm for 20-25 minutes and supernatant was collected in 0.5 ml microcentrifugation tubes. Samples were either used immediately or stored at -70°C for later use.

3.3.3.3 Sample preparation

One hundred microliters of the extract was mixed with two drops of glycerol and one drop of bromophenol blue (tracking dye) and the sample was thoroughly mixed on vortex and centrifuged for two minutes at 8,000 rpm. Afterwards, it was loaded on the gel.

3.3.3.4 Gel preparation

Different concentrations of acrylamide (6-12%) were prepared depending on the enzyme to be studied to get acceptable resolution. In some cases 4% stacking gel was also used. The constituents for gel preparation are given in Table 5. The constituents (1 to 4 in Table 5) were thoroughly mixed, degassed to remove air bubbles from the solution and TEMED was added just before casting the gel on the gel mold. A comb of 15 teeth was put on top of the gel to form wells

for sample loading. Gel thickness was kept 1.5 mm by placing the appropriate spacers between two glass plates.

Table 5. Constituents for gel preparation

Constituents	Gel % (for 50 ml)				
	Stack		Running		
	(4%)	(6%)	(8%)	(10%)	(12%)
1. H ₂ O	6.8 ml	26.5 ml	23.2 ml	20.0 ml	16.4 ml
2. 30% Acrylamide mix ^a	1.7 ml	10.0 ml	13.4 ml	16.6 ml	20.0 ml
3. 1.5M Tris (pH 8.8)	1.25 ml	12.5 ml	12.5 ml	12.5 ml	12.5 ml
4. 10% APS ^b	0.1 ml	0.5 ml	0.5 ml	0.5 ml	0.5 ml
5. TEMED ^c	0.01 ml	0.04 ml	0.03 ml	0.02 ml	0.02 ml

a. 28.2% acrylamide and 0.8% N,N'-methylene-bis-acrylamide.

b. Ammonium persulfate.

c. N,N,N',N'-Tetramethylethylenediamine.

3.3.3.5 Sample loading

After polymerization of the gel, the comb was removed and samples (100µl/sample) were loaded directly into the wells with the help of fine pipette. Wells were washed with the electrode/upper tank buffer before sample loading. Few drops of buffer were added on the top of the sample to avoid mixing of the samples with the reservoir buffer and cross contamination of the samples.

3.3.3.6 Electrophoretic run

Electrophoresis was conducted using Biorad vertical electrophoretic system. Gels were run at 20-60 mA depending on the enzyme under study until tracking dye migrated to the bottom of the gel. The gels were run at 4°C using cooling system (RCB 300, Refrigerated Circulating Bath) to avoid thermal

Table 6 Enzymes used and their abbreviations

denaturation of enzyme. The gels were removed carefully from the mold and stained for specific enzyme activity. Various buffers used have been listed in Appendix VII.

Enzyme	Abbreviation
Alcohol dehydrogenase	ADH
Catalase	CAT
Esterase	EST
Glutamate dehydrogenase	GDH
Glutamate oxaloacetate transaminase	GOT
Lactate dehydrogenase	LDH
Malate dehydrogenase	MDH
Malic enzyme	ME
6-Phosphoglutarate dehydrogenase	6-PGD
Phosphoglucoisomerase	PGI
Shikimate dehydrogenase	SKDH

3.3.3.7 Staining

Staining was done to locate the relative position of the multiple forms

of enzyme with a common catalytic activity after getting resolved by means of electrophoresis. The gel was removed from the mold and immersed into staining solution as per specific requirements of a particular enzyme system. Twelve enzyme systems studied are listed in Table 6 and the staining recipes and procedure for each enzyme are given in Appendix VIII.

3.3.3.8 Scoring of gels

Isozyme gels were visually scored by putting the gel on a light box. Bands with very dark to very light intensities were scored and used to construct the zymograms. R_f (= R_m = Relative mobility) value of each band was calculated using the following formula:

Distance of band from the well

$$R_f = \frac{\text{Distance of band from the well}}{\text{Distance between the well and the loading dye (bromophenol blue)}}$$

Very light bands could be visualized on the light box but were not easily detectable in the photographs. Similarity index matrices and cluster analysis were done as already described for mtDNA RFLP analysis.

IV RESULTS

4.1 Experiment No. 1: Mitochondrial DNA RFLP analysis of pearl millet CMS lines

The mtDNA isolated as per the method given by Smith *et al.* (1987) yielded satisfactory but variable amounts of mtDNA from the different genotypes. The mtDNA was digestible using *Bam*HI, *Hind*III and *Pst*I and continuous smear of UV absorbing material was seen along the entire lane. Individual digested fragments could not be visualized after staining with ethidium bromide and observing on U.V. transilluminator, but on hybridization with most of the probes, bands with acceptable clarity were observed.

Table 7 shows total number of bands, polymorphic bands and number of groups obtained using various enzyme-probe combinations. Twelve enzyme-probe combinations yielded 66 bands. Of these, 40 bands were polymorphic (60.6% of bands). Number of bands per enzyme-probe combination ranged from 3 (*Pst*I-9.7 kb, *Bam*HI-4.7 kb, and *Hind*III-*atp6* combinations) to 10 in *Pst*I-*coxI* combination. All combinations showed one or more polymorphic band(s), lowest proportion of polymorphic bands (one out of six bands) being exhibited by *Hind*III-10.9 kb and highest proportion (all the five bands) in *Bam*HI-*atp6* combination. Individually, these combinations differentiated all the CMS lines into maximum of 2 to 9 groups.

Table 7. Total number of bands, polymorphic bands and number of cytoplasmic groups obtained by various enzyme-probe combinations.

Enzyme-probe combination	Total number of bands	Number of polymorphic bands	¹ Maximum number of groups	
<i>Homologous probes</i>				
<i>Bam</i> HI-4.7 kb	3	1	2	
<i>Bam</i> HI-13.6 kb	6	3	3	
<i>Hind</i> III-4.7 kb	4	1	2	
<i>Hind</i> III-10.9 kb	6	1	2	
<i>Pst</i> I-4.7 kb	7	5	6	
<i>Pst</i> I-9.7 kb	3	2	3	
Total : 6	29	13 (44.8%)	7	
<i>Heterologous probes:</i>				
<i>Bam</i> HI- <i>atp6</i>	5	5	4	
<i>Bam</i> HI- <i>coxI</i>	8	6	4	
<i>Hind</i> III- <i>atp6</i>	3	2	3	
<i>Hind</i> III- <i>coxI</i>	7	4	6	
<i>Pst</i> I- <i>atp6</i>	4	3	4	
<i>Pst</i> I- <i>coxI</i>	10	7	8	
Total : 6	37	27 (73%)	13	
Grand total:	12	66	40 (60.6%)	10

1. Number of groups obtained following cluster analysis using similarity indices based on presence/absence of bands

4.1.1 MtDNA hybridization patterns

Heterologous probes proved to be more polymorphic (73%) than homologous probes (=45%) and also produced more number of bands (37). Combined analysis of all 12 enzyme-probe combinations revealed 61% polymorphic bands.

4.1.1.1 MtDNA hybridization with homologous clones

Hybridization patterns of mtDNA digested with *Hind*III and hybridized to 4.7 kb or 10.9 kb pearl millet clones distinguished cytoplasms consisting of CMS lines 81A₁, 81A_v, 7 lines from LSGP, two lines each of EGP and PV (Group I) from the remaining CMS lines Pb 310A₂, Pb 311A₂, Pb 406A₃, 81A_m, LSGP 14 and LSGP 55 forming Group II (Figs. 2, 3a, 4 and 5). *Hind*III-digested mtDNA probed with 10.9 kb produced two additional bands of 5.2 kb and 9.2 kb as compared to probed with 4.7 kb clone. In addition, 2.9 kb fragment observed in *Hind*III-4.7 kb was replaced by a 2.7 kb fragment in *Hind*III-10.9 kb combination. But in both the combinations, 3.9 kb fragment was the only polymorphic fragment, that characterized the CMS lines of Group I.

MtDNA digested with *Bam*HI and probed with 4.7 kb and 13.6 kb clones produced almost similar grouping pattern except LSGP 66 which had two extra faint bands (1.8 kb and 1.2 kb) in *Bam*HI-13.6 kb combination (Figs. 6 to 9). Two additional bands of 6.5 kb and 6.0 kb size were too faint in LSGP 66, which otherwise were of strong intensity in all other CMS lines of Group II (Figs. 8 and 9). These two bands were relatively of low intensities in *Bam*HI-4.7 kb combination, but the other two bands of low molecular weight (1.8kb, and 1.6 kb) could not be detected in *Bam*HI-4.7kb combination (Fig. 6). The 7.4 kb band present in all the lines with *Bam*HI-13.6 kb combination, was absent in *Bam*HI-4.7 kb combination, and did not contribute to polymorphism.

*Pst*I-digested mtDNA probed with 9.7 kb clone did not produce good quality

blots (Fig. 10), but with 4.7 kb produced acceptable resolution of bands (Fig. 2). This combination produced six clusters (Fig. 3b), Group I contained 81A₁ and four CMS lines from unknown sources, Group IV contained 81A_v and four CMS lines from unknown sources, Groups II, III and VI consisted of only unclassified CMS lines and Group V had 81A_m, CMS lines with A₂, A₃ and LSGP 14 cytoplasms. If we consider grouping at F = 0.85, two major groups are formed (Fig. 3b), A₁-, (81A₁, LSGP 22, EGP 1, EGP 2 and PV 2) and the non-A₁-groups (remaining CMS lines). The A₁-group CMS lines were characterized by the presence of a 16.9 kb fragment which was absent in the non-A₁ group CMS lines. Additionally, a 5.8 kb fragment was also present in the A₁-group CMS lines except in LSGP 66 of the non-A₁ group which also contained this fragment. LSGP 55 and LSGP 66, though present in the non-A₁-group, but were quite different from the other the non-A₁ CMS lines.

In all the enzyme-probe combinations discussed above, 81B was identical to Pb 310A₂, Pb 311A₂, Pb 406A₃ and 81A_m lines except in *Pst*I-9.7 kb combination. 81A_v was also included in this group.

Considering all the enzyme-probe combinations (with homologous probes) the 5 CMS lines, 81A₁, EGP 1, EGP 2, PV 2, and LSGP 22 were identical and formed one group; while Pb 310A₂, Pb 311A₂, Pb 406A₃, 81A_m, and LSGP 14 resembled each other thus forming another group.

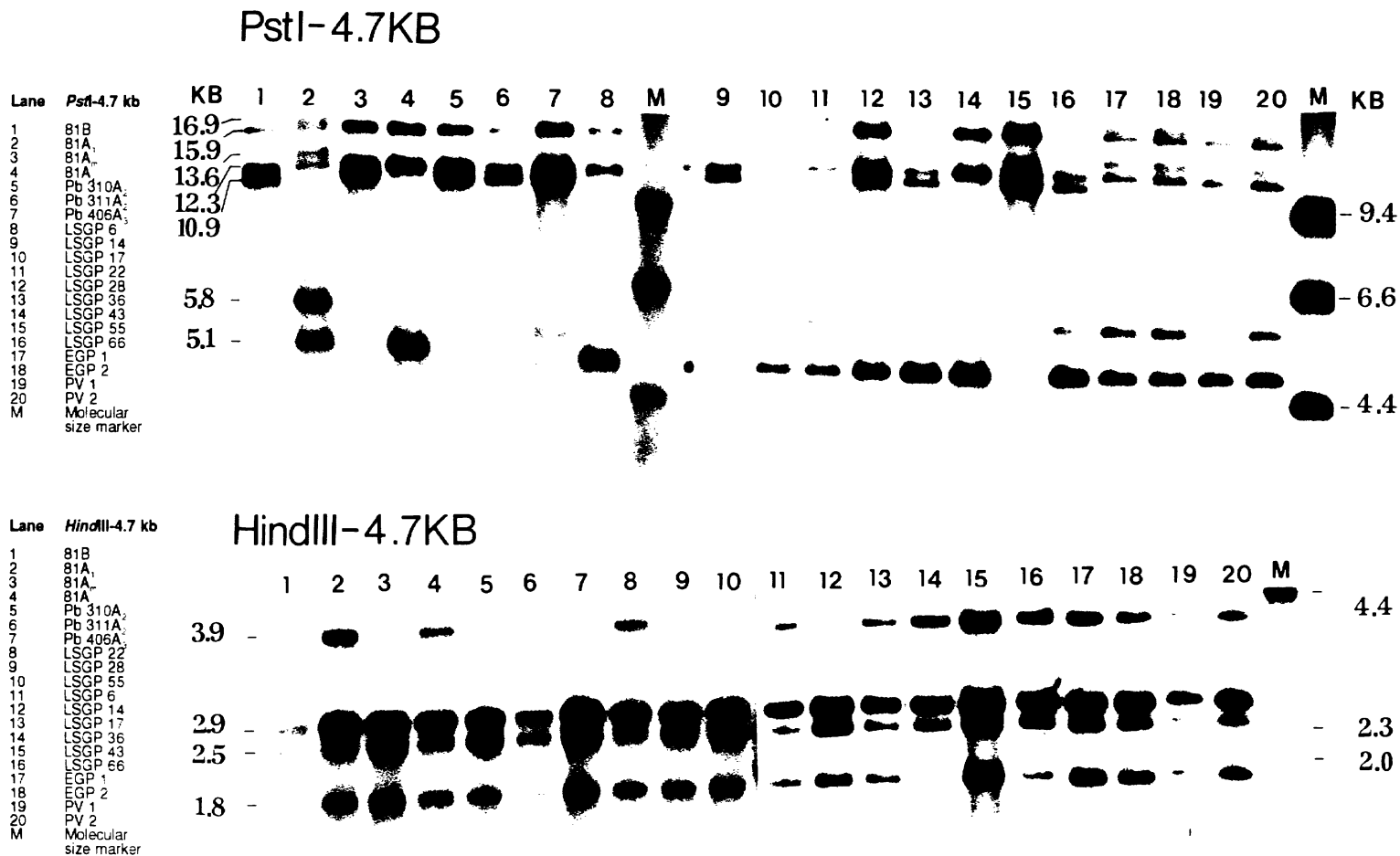
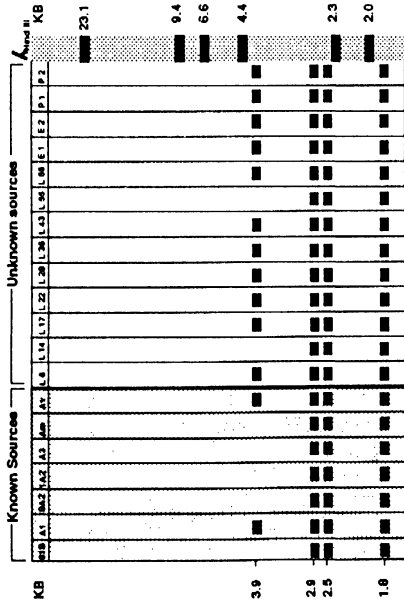


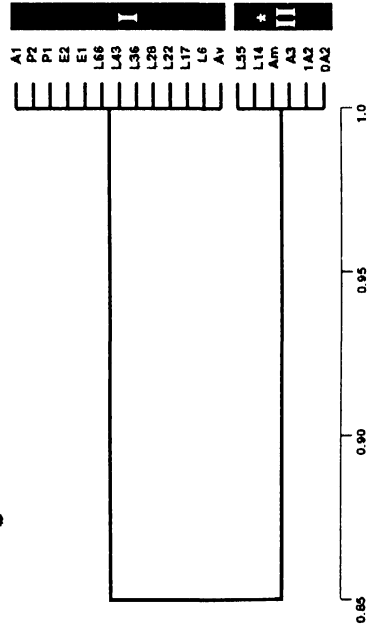
Figure 2. Southern blot hybridization of mtDNA from different CMS lines and 81B of pearl millet digested with *PstI* (top) and *HindIII* (bottom) and probed with pearl millet 4.7 kb gene clone

Figure 3. Schematic representation of mtDNA hybridization patterns and dendrograms constructed on the basis of similarity indices among various CMS lines in individual enzyme-probe combinations

(a) HindIII-4.7KB



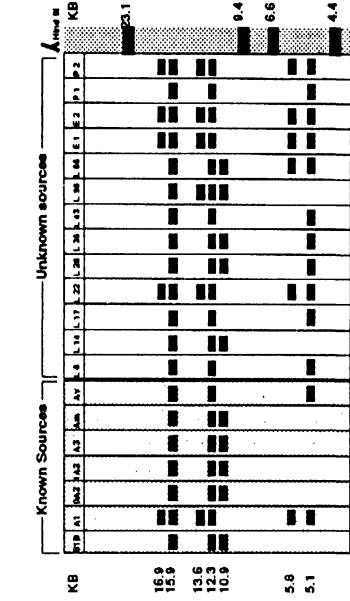
Dendrogram



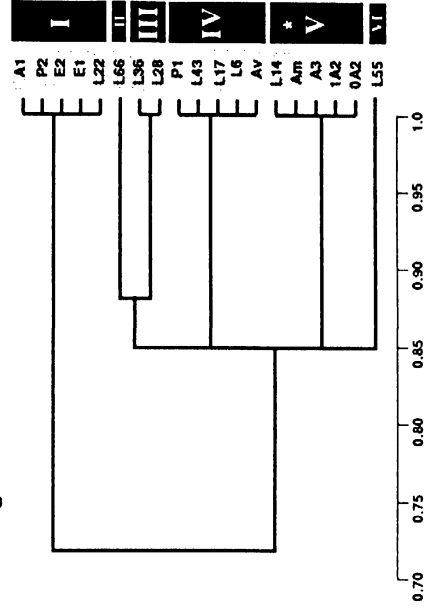
Similarity Index

* indicates the group of CMS lines having identical mtDNA banding pattern to 81B

(b) PstI-4.7KB

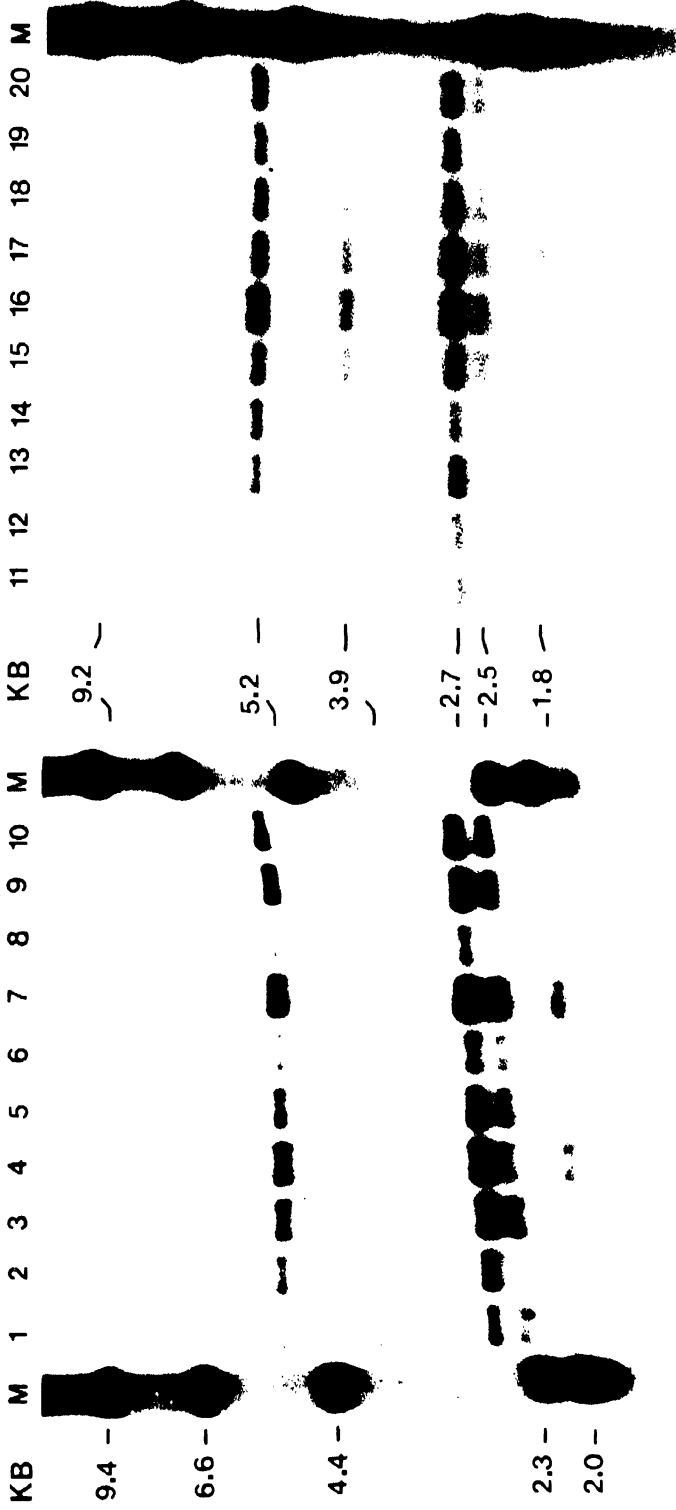


Dendrogram



Similarity Index

HindIII-10.9KB

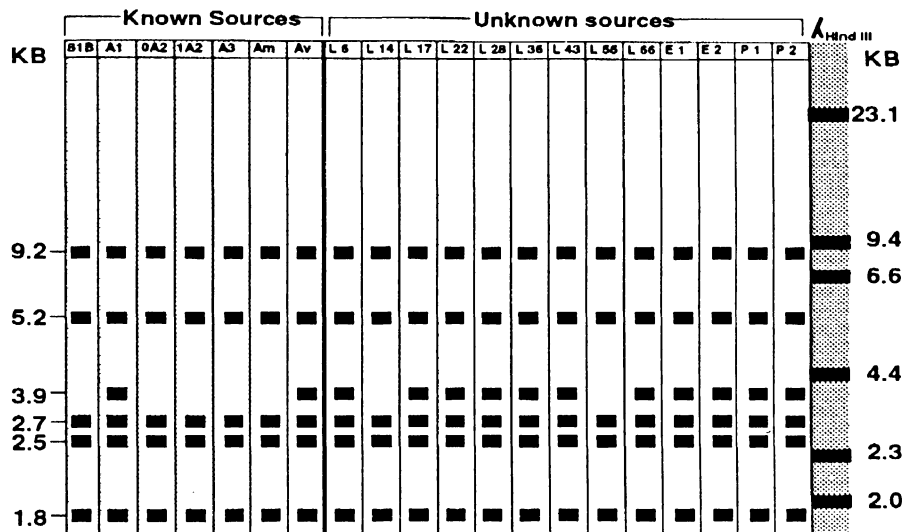


Southern blot hybridization of mtDNA from different CMS lines and 81B of pearl millet digested with *Hind*III and probed with pEarl10.9 kb gene clone

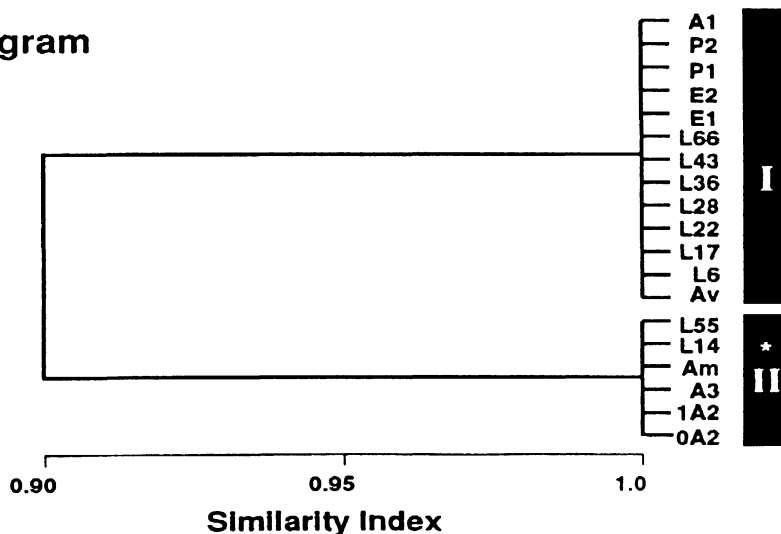
*Hind*III-10.9 kb: Lane 1: 81B, Lane 2: 81A₁, Lane 3: 81A_m, Lane 4: 81A₂, Lane 5: Pb 310A₂, Lane 6: Pb 311A₂, Lane 7: Pb 406A₃, Lane 8: LSGP 14, Lane 9: LSGP 6, Lane 10: LSGP 55, Lane 11: LSGP 17, Lane 12: LSGP 22, Lane 13: LSGP 28, Lane 14: LSGP 36, Lane 15: LSGP 43, Lane 16: LSGP 66, Lane 17: EGP 1, Lane 18: EGP 2, Lane 19: PV 1, Lane 20: PV 2, M: Molecular size marker (λDNA digested with *Hind*III)

Figure 5. Schematic representation of mtDNA hybridization banding patterns and dendrogram constructed on the basis of similarity indices among various CMS lines in individual enzyme-probe combination

HindIII-10.9KB



Dendrogram



* indicates the group of CMS lines having identical mtDNA banding pattern to 81B

BamHI-4.7KB

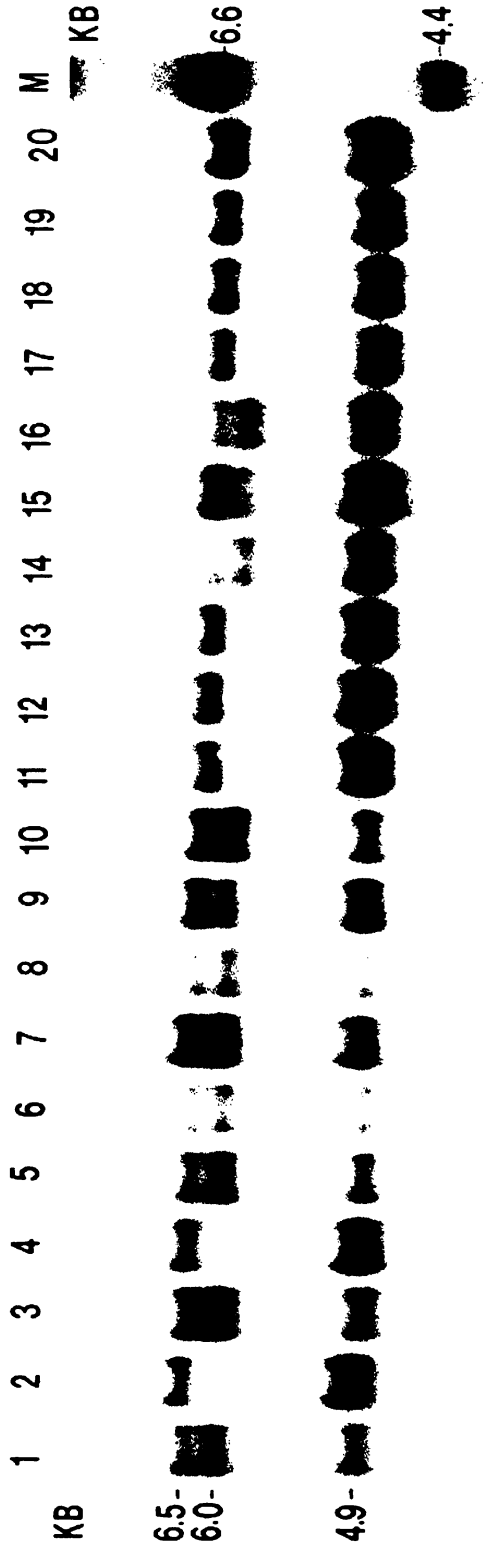
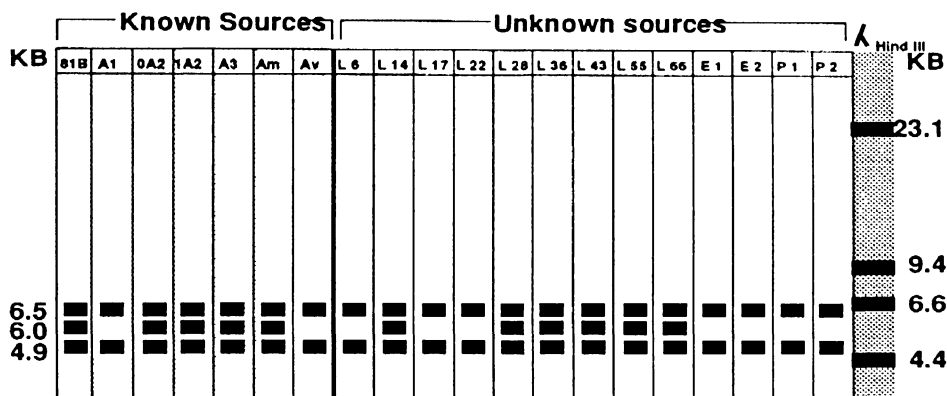


Figure 6. Southern blot hybridization of mtDNA from different CMS lines and 81B of pearl millet digested with BamHI and probed with pearl millet 4.7 kb gene clone

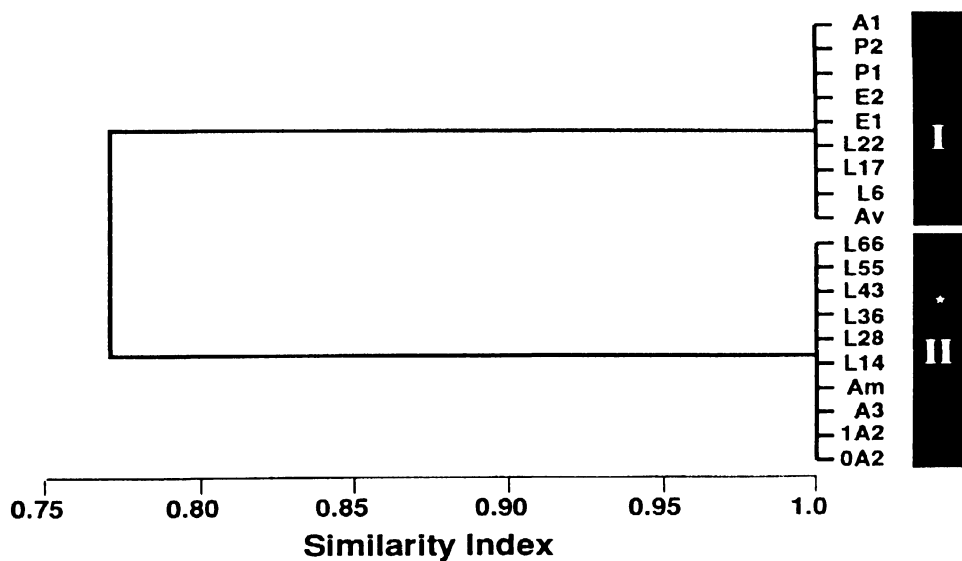
BamHI-4.7 kb: Lane 1: 81B, Lane 2: 81A₁, Lane 3: 81A₂, Lane 4: 81A₃, Lane 5: Pb 310A₂, Lane 6: Pb 311A₂, Lane 7: Pb 406A₃, Lane 8: LSGP 14, Lane 9: LSGP 28, Lane 10: LSGP 55, Lane 11: LSGP 6, Lane 12: LSGP 17, Lane 13: LSGP 22, Lane 14: LSGP 66, Lane 15: LSGP 43, Lane 16: LSGP 38, Lane 17: EGP 1, Lane 18: EGP 2, Lane 19: PV 1, Lane 20: PV 2, M: Molecular size marker (λ-DNA digested with HindIII)

Figure 7. Schematic representation of mtDNA hybridization patterns and dendrogram constructed on the basis of similarity indices among various CMS lines in individual enzyme-probe combination

BamHI-4.7KB



Dendrogram



* Indicates the group of CMS lines having identical mtDNA banding pattern to 81B

BamHI-13.6KB

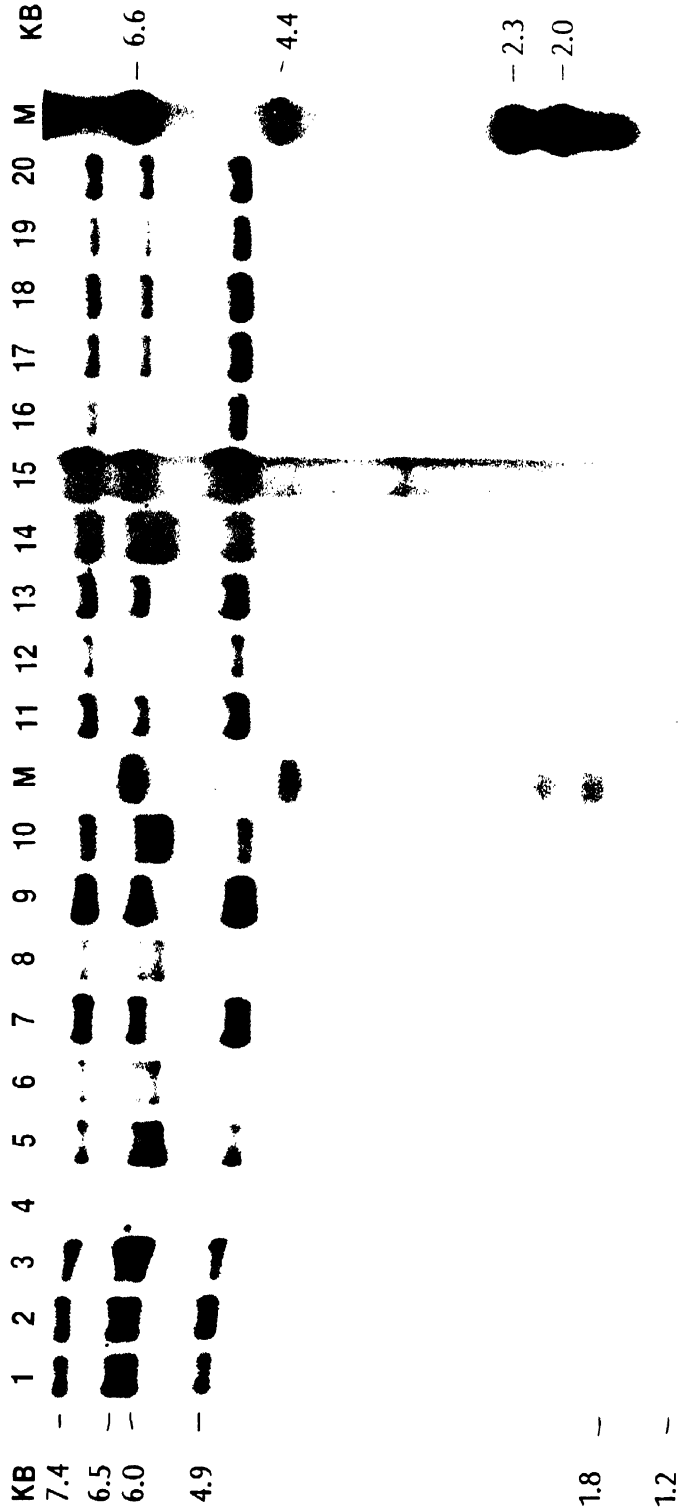
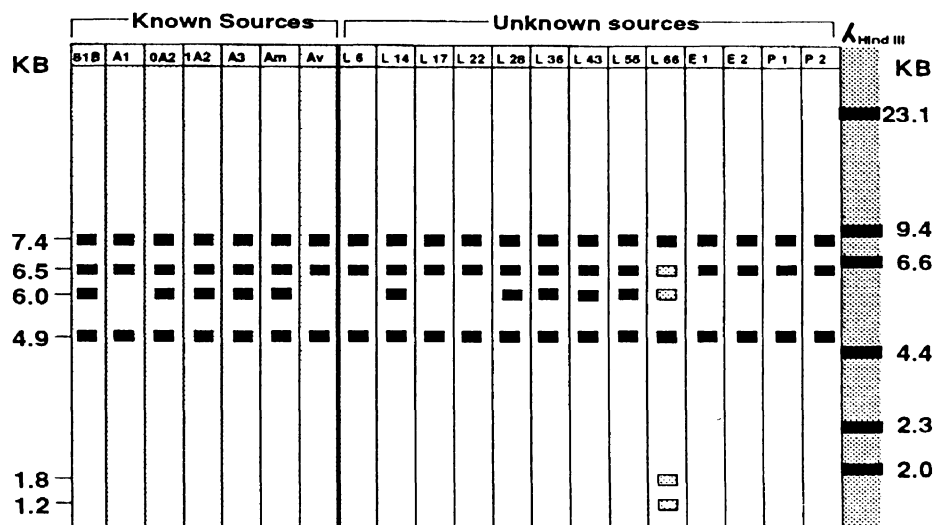


Figure 8. Southern blot hybridization of mtDNA from different CMS lines and 81B of pearl millet digested with *Bam*HI and probed with pearl millet 13.6 kb gene clone

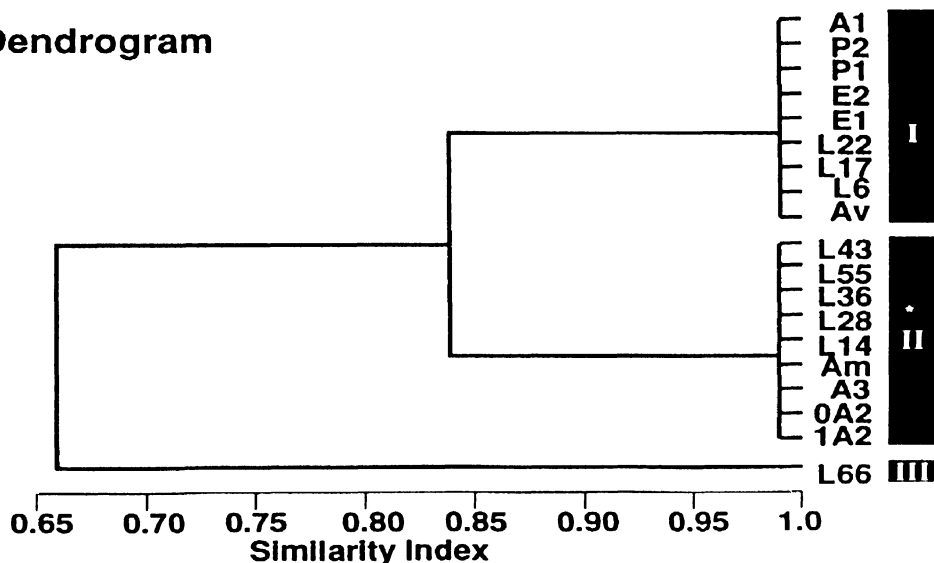
BamHI-13.6 kb: Lane 1: 81B, Lane 2: LSGP 28, Lane 3: Pb 310A₂, Lane 4: Pb 311A₂, Lane 5: Pb 406A₃, Lane 6: 81A_m, Lane 7: 81A₁, Lane 8: LSGP 14, Lane 9: 81A₁, Lane 10: LSGP 55, Lane 11: LSGP 6, Lane 12: LSGP 17, Lane 13: LSGP 22, Lane 14: LSGP 36, Lane 15: LSGP 43, Lane 16: LSGP 66, Lane 17: EGP 1, Lane 18: EGP 2, Lane 19: PV 1, Lane 20: PV 2, M: Molecular size marker (λDNA digested with *Hind*III).

Figure 9. Schematic representation of mtDNA hybridization patterns and dendrogram constructed on the basis of similarity indices among various CMS lines in individual enzyme-probe combination

BamHI-13.6KB



Dendrogram



* indicates the group of CMS lines having identical mtDNA banding pattern to 81B

PstI-9.7KB

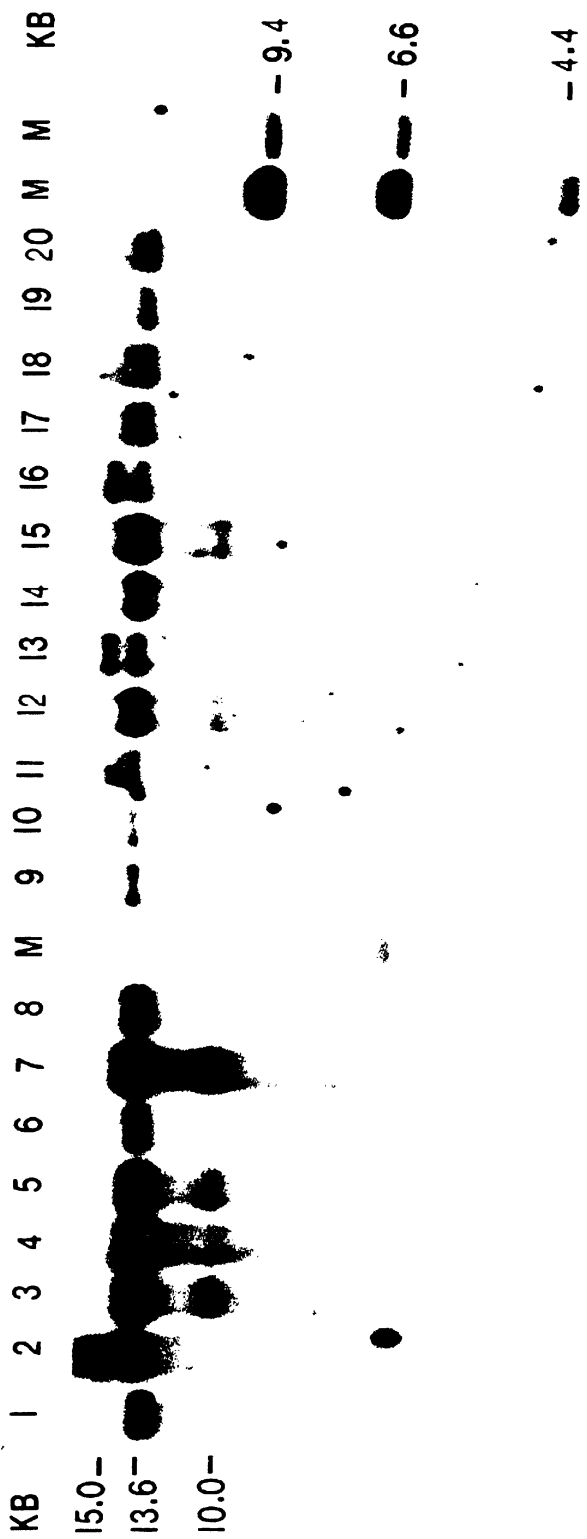


Figure 10. Southern blot hybridization of mtDNA from different CMS lines and 81B of pearl millet digested with *PstI* and probed with pearl millet 9.7 kb gene clone *PstI*-9.7 Kb: Lane 1: 81B, Lane 2: 81A₁, Lane 3: 81A_m, Lane 4: 81A₂, Lane 5: Pb 310A₂, Lane 6: Pb 311A₂, Lane 7: Pb 406A₃, Lane 8: LSGP 14, Lane 9: LSGP 6, Lane 10: LSGP 17, Lane 11: LSGP 22, Lane 12: LSGP 28, Lane 13: LSGP 66, Lane 14: LSGP 43, Lane 15: LSGP 55, Lane 16: LSGP 36, Lane 17: EGP 1, Lane 18: EGP 2, Lane 19: PV 1, Lane 20: PV 2, M: Molecular size marker (λ DNA digested with *HindIII*).

4.1.1.2 MtDNA hybridization with heterologous clones

Heterologous probes, maize *coxI* and *atp6* proved to be most effective, especially when used to hybridize *Bam*HI- and *Pst*I-digested mtDNA fragments (Table 7). These combinations distinguished all CMS sources but could not differentiate between A₂- and A₃-cytoplasms.

The maize *coxI* gene probe distinguished CMS line 81A_m from the remaining cytoplasms by hybridizing to 7.4 kb and 2.5 kb *Bam*HI fragments (Figs. 12 and 13a) that were not present in other CMS lines. Besides these, a 22.4 kb fragment was absent in 81A_m, which, otherwise was present in all other CMS lines. This enzyme-probe combination also distinguished 81A_v by the presence of a unique 24.0 kb fragment that was absent in all other lines. 81A₁ also had different restriction profile but many other CMS lines of LSGP, EGP and PV were also identical to 81A₁. Similarly, Pb 406A₃, A₂-lines formed a different group along with a few CMS lines of the LSGPs. On the other hand, *Hind*III-*coxI* combination revealed six groups but could not differentiate between A₂-, A₃- and A_m-CMS lines (Fig. 13b). LSGP 28 and LSGP 55 were characterized by the presence of a 3.3 kb fragment that was absent in all other lines and LSGP 14 was characterized by the absence of a 3.9 kb fragment which was substituted by either a 1.3 kb or 3.3 kb fragment in other CMS lines. Remaining CMS lines from unknown cytoplasmic sources clustered either with 81A₁ or 81A_v.

The maize *coxI* gene hybridized with *Pst*I digests revealed maximum number

of groups (8) differentiating all the known cytoplasmic sources except A_2 from A_3 and also distinguished CMS lines within LSGP and PV (Figs. 14 and 15). PV 2 was included in Group I with $81A_1$ and PV 1 was present in a different group with LSGP 6, LSGP 17 and LSGP 43. LSGP 28 and LSGP 36 formed a separate group whereas, LSGP 55 and LSGP 66 remained independent from all the clusters. *Bam*HI- and *Pst*I-digested mtDNA hybridized to *coxI* gene were the only combinations which could distinguish $81B$ (male fertile line) from all other lines.

Characteristic banding patterns were observed for $81A_m$ and $81A_v$ using maize *atp6* gene hybridized to *Pst*I- and *Bam*HI-digested mtDNA. A 4.5 kb fragment, present in all the lines, was missing in $81A_m$ (*Pst*I-*atp6*) and, an 18.5 kb fragment, missing in all the lines, was present in $81A_v$ (Figs. 16 and 17a). On the other hand, 7.3 kb and 2.4 kb *Bam*HI fragments that hybridized to *atp6* in $81A_m$, were absent in all other lines. Similarly, a 24.0 kb *Bam*HI fragment hybridized to *atp6* in $81A_v$ and was absent in all other lines (Figs. 16 and 17b). *Hind*III-*atp6* combination could not provide much information except that a 3.2 kb fragment showed its presence in few of the LSGPs which, otherwise, was found missing in all the CMS lines of known cytoplasmic sources. Pb 406 A_3 , $81A_m$ and A_2 -lines could not be differentiated and $81A_1$ and $81A_v$ showed identical banding pattern, also shared by few CMS lines of known cytoplasmic sources (Figs. 18 and 19). Based on homologous and heterologous probes hybridized to mtDNA digested with three restriction enzymes, all the

CMS lines were classified in to 10 groups (Fig. 52).

4.1.2 Analysis of aggregate dendrograms

4.1.2.1 Homologous probes

Seven groups were evident in the dendrogram obtained using all the six enzyme-probe combinations (Fig. 53). These combinations could not discriminate A_2 , A_3 and A_m cytoplasmic sources among themselves but differentiated LSGP 66 from all others at $F = 0.93$. Three male-sterile lines from LSGP (LSGP 28, LSGP 36, LSGP 43) formed a separate cluster at $F = 0.98$. Cytoplasmic male-sterile lines in groups I, II and VI were identical ($F = 1.0$).

4.1.2.2 Heterologous probes

The dendrogram based on the similarity indices generated from hybridization patterns of mtDNA digested with *Bam*HI, *Pst*I or *Hind*III and probed with the maize *atp6* clone revealed 7 groups (Fig. 54). The CMS lines 81A₁, EGP 1, EGP 2, LSGP 6, LSGP 17, LSGP 22, PV 1, and PV 2 formed a distinct cluster (Group I). Pb 406A₃, A₂-CMS lines and various LSGPs clustered together to form a major group at $F=0.90$, within which many sub-groups were evident. Cytoplasmic male-sterile line 81A_m and 81A_v were distinct from each other as well as from all other CMS lines (Fig. 54).

The dendrogram constructed based on similarity indices calculated from

banding patterns of mtDNA obtained by 12 enzyme-probe combinations revealed a maximum of 10 groups (Fig. 52). Five CMS lines, 81A_m, 81A_v, LSGP 43, LSGP 55 and LSGP 66 were distinct from each other as well as from all other CMS lines. Two LSGPs (LSGP 6, and LSGP 17) and PV 1 were identical (F=1.0) and formed a separate group, whereas, other two CMS lines, LSGP 28 and LSGP 36 formed a separate group. Another cluster (Group IX) contained three CMS lines, viz., Pb 406A₃, Pb 310A₂ and Pb 311A₂. The 81A₁, EGP 1, EGP 2, PV 2 and LSGP 22 were close to each other and form single cluster at F = 0.99.

The dendrogram constructed on the basis of similarity indices among various CMS lines following hybridizations of *Pst*I-, *Bam*HI-, and *Hind*III-digested mtDNA with maize *coxI* clone revealed two distinct groups, A_m- and the non-A_m groups at F = 0.88 significance limit (Fig. 55). The non-A_m group was further divided into many sub-groups (Groups I to IX). The 81A_m was the most distinct CMS line which joined the remaining 18 CMS lines at F = 0.82. Within the non-A_m group, LSGP 43, LSGP 55 and 81A_v differed from each other as well as from other CMS lines forming different sub-groups (Fig. 55). However a number of sub-groups further increased when combined analysis of heterologous probes was carried out (Fig. 56). 81A_m was the most distinct from other CMS lines at F = 0.75. At F = 0.88 two major groups A_m- and the non-A_m appeared. In the non-A_m group 12 sub-groups are evident (Group I to XII) and 81A₁ and EGP 2; EGP 1 and PV2; LSGP 17 and PV1; and Pb 310A₂, Pb 311A₂

and Pb 406A₃ were identical.

4.1.3 MtDNA hybridization patterns from open-pollinated seeds

The mtDNA RFLP analysis described above was carried out using 6-day old etiolated seedlings from open-pollinated seed (OP) of unknown cytoplasmic sources and from the sib seed of known cytoplasmic sources. Although the procedure for mtDNA isolation of Smith *et al.* (1987) assures the exclusion of nuclear DNA by DNase treatment followed by isolation of mitochondria by differential centrifugation, yet to confirm the results obtained using the different kinds of seed lots, OP seed of near-isonuclear CMS lines (known cytoplasmic sources) was also used for mtDNA RFLP analysis using the same restriction enzymes (*Bam*HI, *Hind*III, and *Pst*I) and probes (4.7 kb and *cox*I). Results of hybridization patterns with homologous (Fig. 57) and heterologous (Fig. 58) probes revealed restriction hybridization patterns identical with that of mtDNA RFLP analysis using sib seed. This clearly indicates that either of these two kinds of seeds may be used for mtDNA analysis, but from breeding point of view, it is comparatively much easier and cost effective to produce OP seed than to produce sib seed.

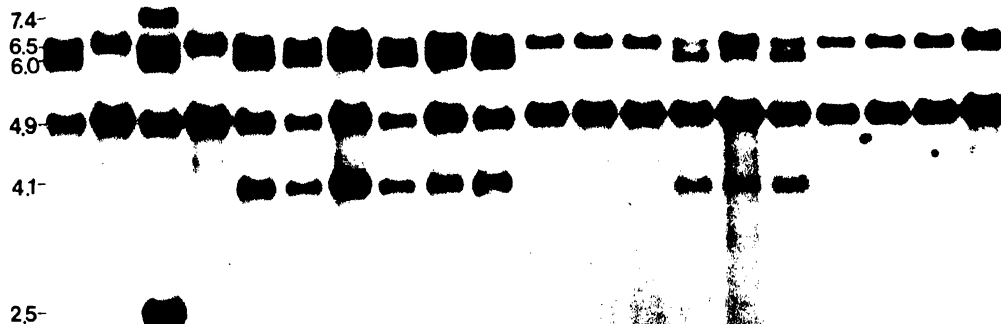
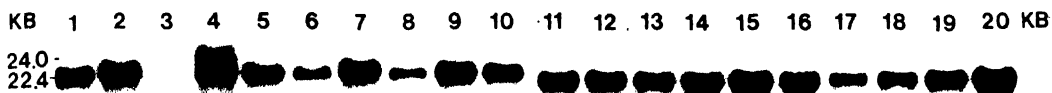
4.1.4 Total DNA hybridization patterns using mitochondrial probes

MtDNA isolation procedures requires 50-60 g seedlings to start with, while total DNA (tDNA) procedure (Dellaporta *et al.*, 1983) require only 5 g of

seedlings. Whether tDNA can be used to detect restriction hybridization patterns similar to mtDNA hybridization patterns (since the probes are mitochondrial specific) was the prime objective of this part of the study. As already mentioned in the materials and methods, tDNA from three isonuclear CMS lines (81A₁, Pb 406A₃, and 81A_m) and male-fertile line 81B was isolated, digested with *Hind*III and *Bam*HI and hybridized with pearl millet 4.7 kb and maize *coxI* gene clones (Fig. 59).

The tDNA hybridization patterns of *Bam*HI-*coxI* were identical to those from mtDNA (Figs. 12 and 59). Whereas, the resolution of bands was reduced in case of *Hind*III-*coxI* and *Hind*III-4.7 kb combinations (Figs. 2 and 12). A few of the neighboring bands were so close to each other that they appeared to merge resulting in thick and hazy bands. For example, 2.5 kb and 2.7 kb bands (*Hind*III-*coxI* and *Hind*III-4.7 kb) merged. This might be because restriction enzyme digested total DNA has large number of bands and need longer run as compared to mtDNA for separation of each fragment. On the other hand, in *Bam*HI-4.7 kb combination, additional 3.3 kb fragment appeared in all the lines (when total DNA was used) which otherwise was absent in this combination by using mtDNA indicating that nuclear genome also has some homology with this mitochondrial fragment. This did not alter the classification of cytoplasmic sources as the additional band appeared in all the lines.

BamHI-coxI



HindIII-coxI

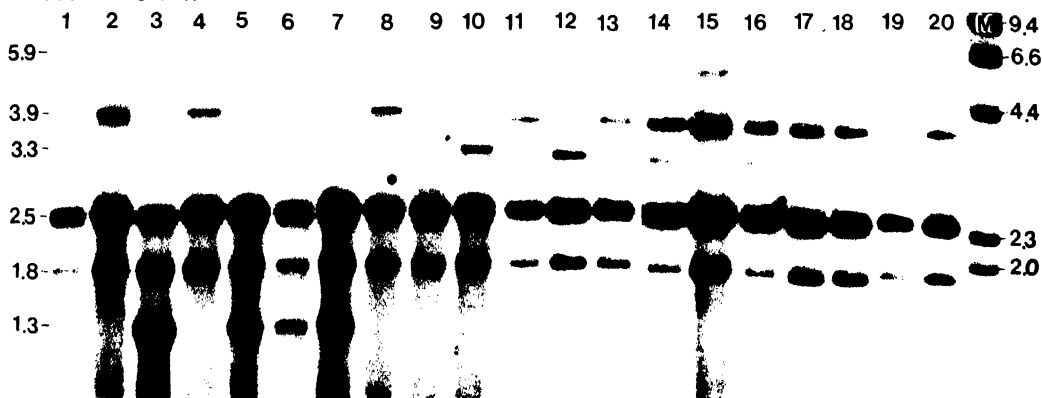
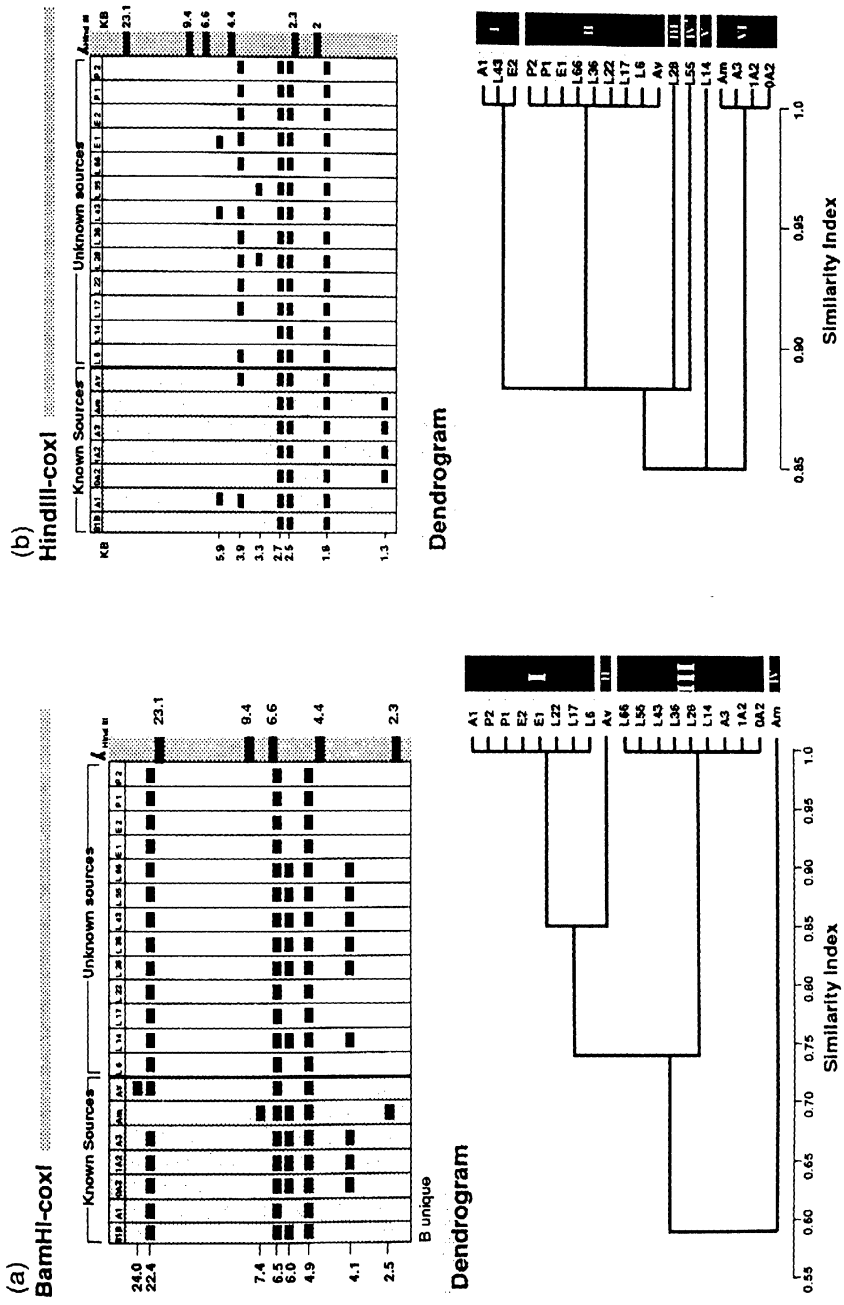


Figure 12. Southern blot hybridization of mtDNA from different CMS lines and 81B of pearl millet digested with *Bam*HI (top) and *Hind*III (bottom) and probed with maize *cox*I gene clone

*Bam*HI-coxI: Lane 1: 81B, Lane 2: 81A₁, Lane 3: 81A_m, Lane 4: 81A₂, Lane 5: Pb 310A₂, Lane 6: Pb 311A₂, Lane 7: Pb 406A₂, Lane 8: LSGP 14, Lane 9: LSGP 28, Lane 10: LSGP 55, Lane 11: LSGP 6, Lane 12: LSGP 17, Lane 13: LSGP 22, Lane 14: LSGP 36, Lane 15: LSGP 43, Lane 16: LSGP 66, Lane 17: EGP 1, Lane 18: EGP 2, Lane 19: PV 1, Lane 20: PV 2, M: Molecular size marker (λDNA digested with *Hind*III).

*Hind*III-coxI: Lane 1: 81B, Lane 2: 81A₁, Lane 3: 81A_m, Lane 4: 81A₂, Lane 5: Pb 310A₂, Lane 6: Pb 311A₂, Lane 7: Pb 406A₂, Lane 8: LSGP 22, Lane 9: LSGP 28, Lane 10: LSGP 55, Lane 11: LSGP 6, Lane 12: LSGP 14, Lane 13: LSGP 17, Lane 14: LSGP 36, Lane 15: LSGP 43, Lane 16: LSGP 66, Lane 17: EGP 1, Lane 18: EGP 2, Lane 19: PV 1, Lane 20: PV 2, M: Molecular size marker (λDNA digested with *Hind*III).

Figure 13. Schematic representation of mtDNA hybridization patterns and dendrogram constructed on the basis of similarity indices among various CMS lines in individual enzyme-probe combinations



* indicates the group of CMS lines having identical mtDNA banding pattern to 81B

PstI-coxI

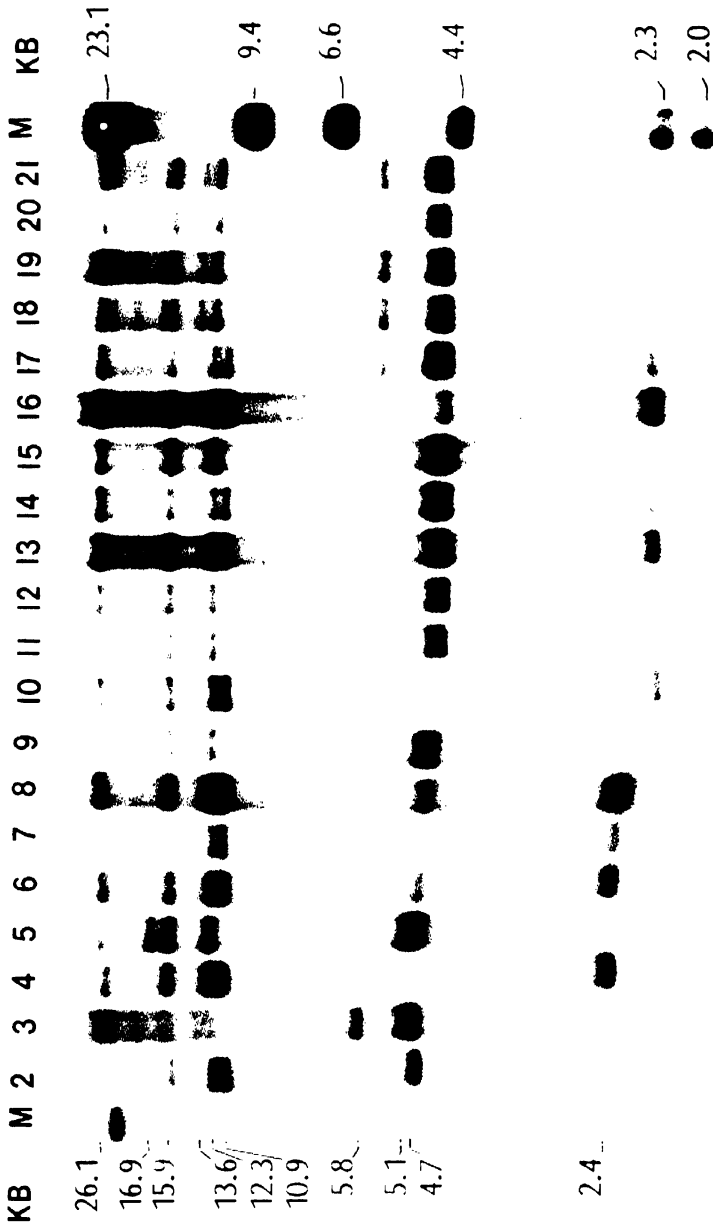
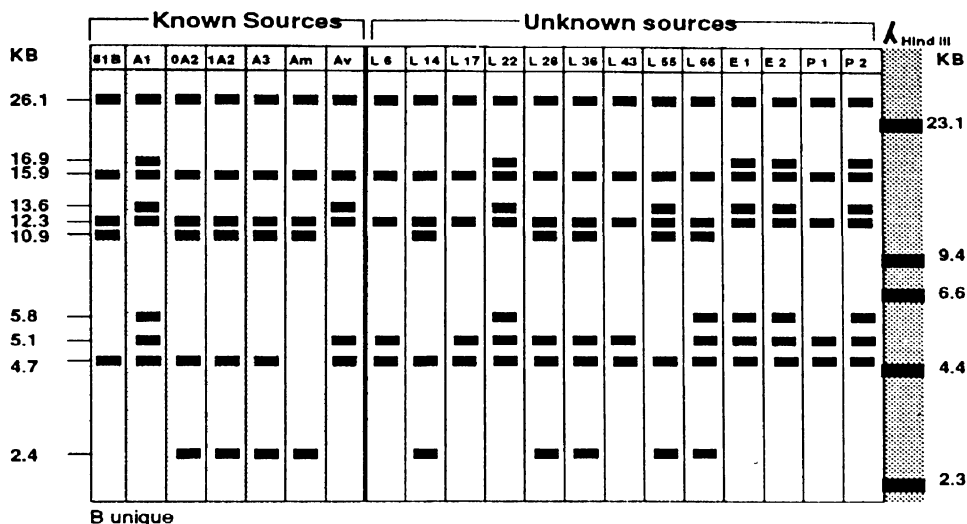


Figure 14. Southern blot hybridization of mtDNA from different CMS lines and 81B of pearl millet digested with *PstI* and probed with maize *coxI* gene clone

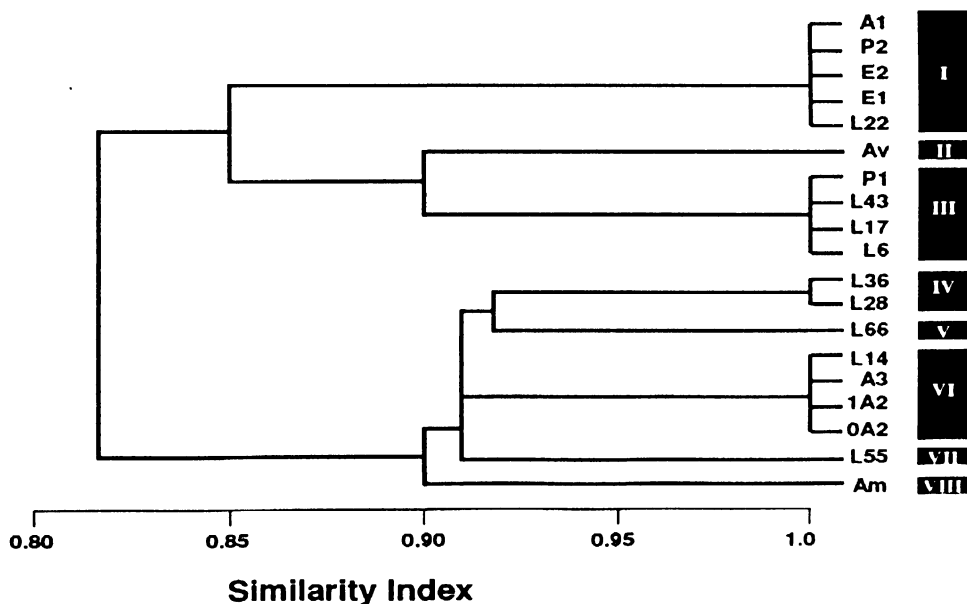
***PstI-coxI*:** Lane 2: 81B, Lane 3: 81A₁, Lane 4: 81A₂, Lane 5: 81A₃, Lane 6: Pb 310A₂, Lane 7: Pb 311A₂, Lane 8: Pb 406A₂, Lane 9: LSGP 6, Lane 10: LSGP 14, Lane 11: LSGP 17, Lane 12: LSGP 22, Lane 13: LSGP 28, Lane 14: LSGP 36, Lane 15: LSGP 43, Lane 16: LSGP 55, Lane 17: LSGP 66, Lane 18: EGP 1, Lane 19: EGP 2, Lane 20: PV 1, Lane 21: PV 2, M: Molecular size marker (λDNA digested with *HindIII*).

Figure 15. Schematic representation of mtDNA hybridization patterns and dendrogram constructed on the basis of similarity indices among various CMS lines in individual enzyme-probe combination

PstI-coxI



Dendrogram



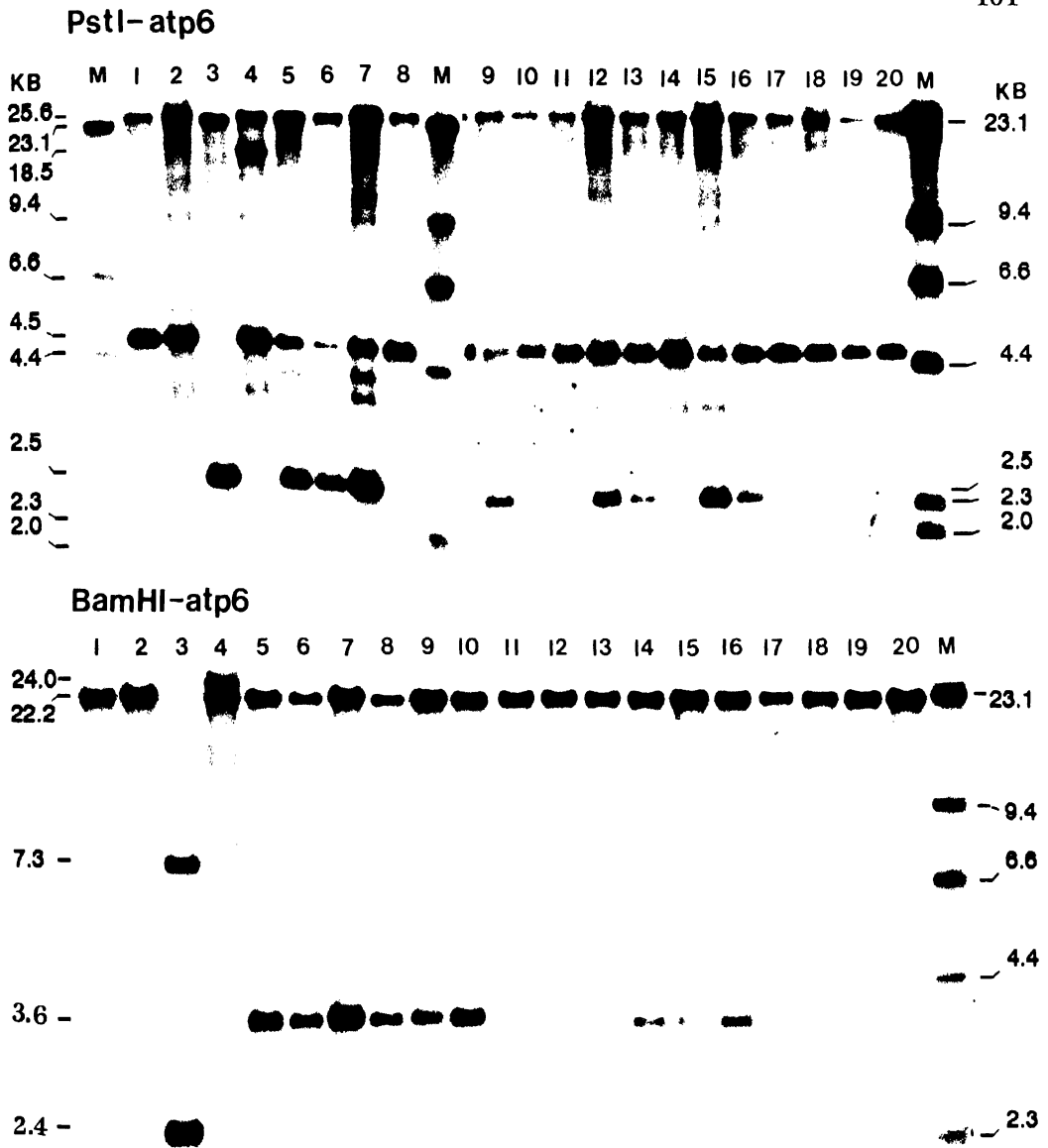


Figure 16. Southern blot hybridization of mtDNA from different CMS lines and 81B of pearl millet digested with *Pst*I (top) and *Bam*HI (bottom) and probed with maize *atp6* gene clone

*Pst*I-*atp6*: Lane 1: 81B, Lane 2: 81A₁, Lane 3: 81A_m, Lane 4: 81A_v, Lane 5: Pb 310A₂, Lane 6: Pb 311A₂, Lane 7: Pb 406A₂, Lane 8: LSGP 6, Lane 9: LSGP 14, Lane 10: LSGP 17, Lane 11: LSGP 22, Lane 12: LSGP 28, Lane 13: LSGP 36, Lane 14: LSGP 43, Lane 15: LSGP 55, Lane 16: LSGP 66, Lane 17: EGP 1, Lane 18: EGP 2, Lane 19: PV 1, Lane 20: PV 2, M: Molecular size marker (λ DNA digested with *Hind*III).

*Bam*HI-*atp6*: Lane 1: 81B, Lane 2: 81A₁, Lane 3: 81A_m, Lane 4: 81A_v, Lane 5: Pb 310A₂, Lane 6: Pb 311A₂, Lane 7: Pb 406A₂, Lane 8: LSGP 14, Lane 9: LSGP 28, Lane 10: LSGP 55, Lane 11: LSGP 6, Lane 12: LSGP 17, Lane 13: LSGP 22, Lane 14: LSGP 36, Lane 15: LSGP 43, Lane 16: LSGP 66, Lane 17: EGP 1, Lane 18: EGP 2, Lane 19: PV 1, Lane 20: PV 2, M: Molecular size marker (λ DNA digested with *Hind*III).

HindIII-atp6

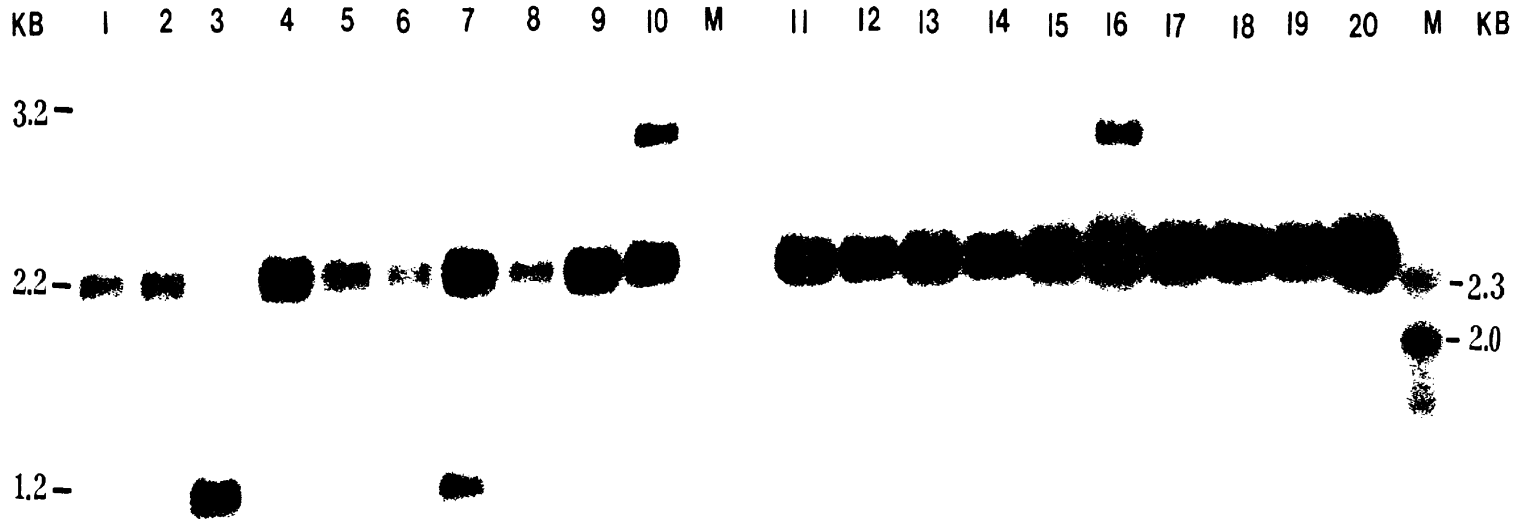
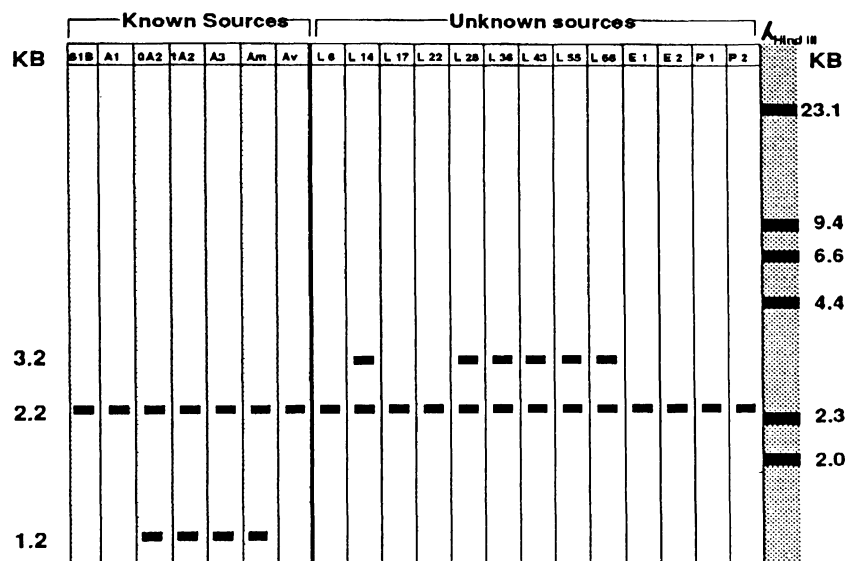


Figure 18. Southern blot hybridization of mtDNA from different CMS lines and 81B of pearl millet digested with *HindIII* and probed with *atp6* gene clone

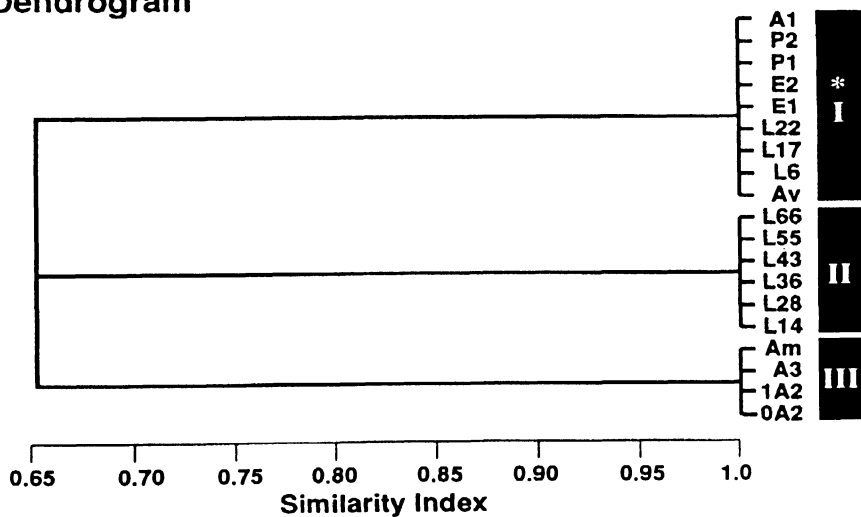
HindIII-atp6: Lane 1: 81B, Lane 2: 81A₁, Lane 3: 81A_m, Lane 4: 81A_v, Lane 5: Pb 310A₂, Lane 6: Pb 311A₂, Lane 7: Pb 406A₃, Lane 8: LSGP 14, Lane 9: LSGP 28, Lane 10: LSGP 55, Lane 11: LSGP 6, Lane 12: LSGP 17, Lane 13: LSGP 22, Lane 14: LSGP 36, Lane 15: LSGP 43, Lane 16: LSGP 66, Lane 17: EGP 1, Lane 18: EGP 2, Lane 19: PV 1, Lane 20: PV 2, M: Molecular size marker (λ DNA digested with *HindIII*).

Figure 19. Schematic representation of mtDNA hybridization patterns and dendrogram constructed on the basis of similarity indices among various CMS lines in individual enzyme-probe combination

HindIII-*atp6*



Dendrogram



* indicates the group of CMS lines having identical mtDNA banding pattern to 81B

4.2 Experiment No. 2: Anther development and microsporogenesis in pearl millet iso-nuclear lines

Six isonuclear A-lines and 81B were examined for the influence of cytoplasmic-nuclear male sterility systems on anther development, microsporogenesis and pollen fertility. Broadly, the process of pollen/anther development can be divided into three phases; premeiotic (stages 1-2 in Fig. 20), meiotic (stages 3-11 in Fig. 20) and postmeiotic (stages 12-16 in Fig. 20).

4.2.1 Observations on male meiotic events

Meiosis was regular in all isonuclear A-lines and 81B, (Figs. 21A-P) except Pb 406A₃, where a low frequency of pollen mother cells (PMCs) showed anomalous meiosis (Figs. 22A-U). There was no synchrony in the meiotic development of uninucleate PMCs within the anther of A-lines in contrast to the almost synchronous development in normal fertile anthers of 81B.

Isonuclear lines with regular meiosis showed normal chromatin attachment to the nucleolus (nucleolus organizer) during prophase I, i.e. leptotene, zygotene, pachytene, diplotene and diakinesis (Figs. 21A-D). Homologous chromosomes paired normally (Fig. 21B), formed chiasmata (Fig. 21C) and 7 ring bivalents (Fig. 21E). The seven bivalents (7_{II}) were arranged normally on the equatorial plate (Fig. 21F) at metaphase I and anaphase I segregation started normally (Fig. 21G) leading to equal division of the 14 chromosomes at two poles (Fig. 21I) and formation of normal dyads at the end

of telophase I (Fig. 21J). Meiosis II (prophase II, metaphase II, anaphase II, telophase II and cytokinesis) proceeded normally figure (Figs. 21K-P). Equational division of chromosomes occurred at anaphase II and meiosis was completed leading to the formation of the microspores. Except in Pb 403A₃, meiosis in PMCs was completed in all florets by the time the spike emerged completely from the boot. In Pb 406A₃, however, PMCs at various stages of meiosis were seen even in completely emerged spikes with protruding stigmas. In further contrast to male-fertile 81B and the other isonuclear A-lines studied, there was no synchronous development among the three anthers of a floret, or even within an anther in Pb 406A₃. Thus meiosis in Pb 406A₃ was both delayed and asynchronous.

Various types of meiotic anomalies were detected in Pb 406A₃ from leptotene through pollen grain formation (Figs. 22A-U). Anomalies along with their frequency of occurrence are given in Table 8. At leptotene, 1.67% of 4554 PMCs examined had two kinds of abnormalities: a nucleolus was absent in 0.55% of PMCs and in 1.12% of PMCs chromatin was not attached to the nucleolus (nucleolus organizer was absent) (Fig. 22A). However, such a situation was not observed in advanced stages of meiosis indicating such PMCs died at an early stage (sporogenous tissue stage). Of 978 PMCs studied at pachytene, presence of a small fragment (accessory chromosome) was detected in 1.12% (Fig. 22B).

A few PMCs in Pb 406A₃ had regular pairing up to pachytene stage,

Table 8. Meiotic anomalies observed in Pb 406A₃

Stage of cells/PMCs ¹	Total no. of PMCs	Normal PMCs	Abnormal PMCs ²	Percent of abnormal PMCs
Leptotene	4554	4478 (98.33%)	76 Nucleolus absent (Fig. 22A): Chromatin detached from nucleolus (nucleolus organizer absent (Fig. 22A):	1.67% 0.55%
Pachytene	978	967 (98.88%)	Accessory chromosome (Fig. 22B) :	1.12%
Diplotene	1478	1409 (95.33%)	69 Some univalents (Fig. 22C) : 4 _n ring + 3 _n rod (Fig. 22E) :	4.67% 2.84% 271.83%
Metaphase I	3973	3855 (97.00%)	118 Disorganized cluster of chromosomes (Fig. 22R) : 5 _n (Fig. 22F) : 6 _n (Fig. 22L) :	3.00% 0.58% 1.43% 0.97%
Anaphase I	3281	3107 (94.7%)	174 8 + 6, (Fig. 22G) : 7 + 6 + lagging chromosome further dividing (Fig. 22H & 22M) : 12 + 2, (Fig. 22I) : 12, (Fig. 22J) : 9 + 5, (Fig. 22K & 22P) : 10 + 4, (Fig. 22Q) : 5 ₁ (Fig. 22N) :	5.29% 0.88%
Dyad	2465	2461	4 8 + 6, (Fig. 22S) :	0.16%
Tetrad	2897	2871 (99.1%)	26 3 intact nuclei + one dividing nucleus (syncyte) (Fig. 22T) : Pentanucleate :	0.9% 0.62% 0.28%

¹ 1 Pollen mother cells; ² Bivalents (ii) and univalents (i)

with varying number of univalents observed, thereafter, at diplotene and diakinesis. Two or more univalents (2.84% of PMCs) or 4 ring and 3 rod bivalents (1.83% of PMCs) were observed at diplotene and diakinesis (Figs. 22C-E) instead of normal 7 bivalents. Rapid terminalization of chiasmata was commonly observed and there was a tendency for chromosomes to separate in early diplotene with the few remaining bivalents having completely terminalized chiasmata.

Chromosome orientation and segregation were also disturbed in Pb 406A₃. At metaphase I, 3.0% of PMCs studied showed three kinds of anomalies. Instead of the normal 7_{II}, 5_{II} (1.43% of PMCs), 6_{II} (0.97% of PMCs) and disorganized clusters of bivalents scattered throughout the cell (0.58% of PMCs) were observed (Figs. 22F, 22L, and 22R). Large number of anomalies were also detected at anaphase I. All the anomalies considered together account for 5.29% of PMCs of Pb 406A₃ examined (Table 8). All these anomalous PMCs showed unequal chromosomal disjunction. Observed combinations included: 6_I + 7_I with a lagging chromosome undergoing division to produce two miniature fragments in 1-4.6% of PMCs, 8_I + 6_I in 0.88% of PMCs (Fig. 22G), 12_I + 2_I in 0.55% of PMCs (Fig. 22I), 9_I + 5_I in 1.25% of PMCs (Figs. 22K, and 22P) and 10_I + 4_I in 0.82% of PMCs (Fig. 22Q). PMCs with 12_I in 0.27% of PMCs (Fig. 22J) and with 5_I in 0.06% of PMCs (Fig. 22N) were also seen. Although at dyad stage it is normally difficult to count chromosomes, in 4 of the 2465 dyads observed it was possible to do this. Each of these four

dyads had 8_1 and 6_1 in their two daughter nuclei (Fig. 22S), confirming the unequal chromosomal disjunction at anaphase I.

Two kinds of anomalies were also detected at the tetrad stage; (i) presence of more than four nuclei in a cell and failure of cytokinesis (0.28% of PMCs), and (ii) plasmodial sporocytes. In young anthers, archesporial cells and PMCs at leptotene were uninucleate and appeared normal. However older anthers contained very small proportion (0.62% of PMCs) of syncytes. There were 2-6 nuclei per syncyte (Fig. 22U). Fusion between PMCs might have initiated at early prophase I but was not detected at an early stage. Meiosis was delayed to an extent that plasmodial syncytes reached metaphase I when normal PMCs had already completed the second meiotic division. In one interesting example, of four nuclei present in one syncyte, only one underwent division (Fig. 22T). In the dividing nucleus chromosomes are oriented at the metaphase plate whereas other nuclei remain undivided indicating the meiotic arrest at prophase I. Consequences of such syncytes were seen at pollen grain formation in the form of multinucleate pollen grains (Fig. 22V). Multinucleate pollen containing up to 9 nuclei were observed (Figs. 22V-X) that were usually bigger than normal pollen grains.

4.2.2 Anther development and microsporogenesis in 81B

Histological studies at successive developmental stages revealed that anther development and microsporogenesis followed a normal course in male-fertile

Figure 20. Comparison of microsporogenesis and PMC/microspore/pollen degeneration in pearl millet isonuclear lines

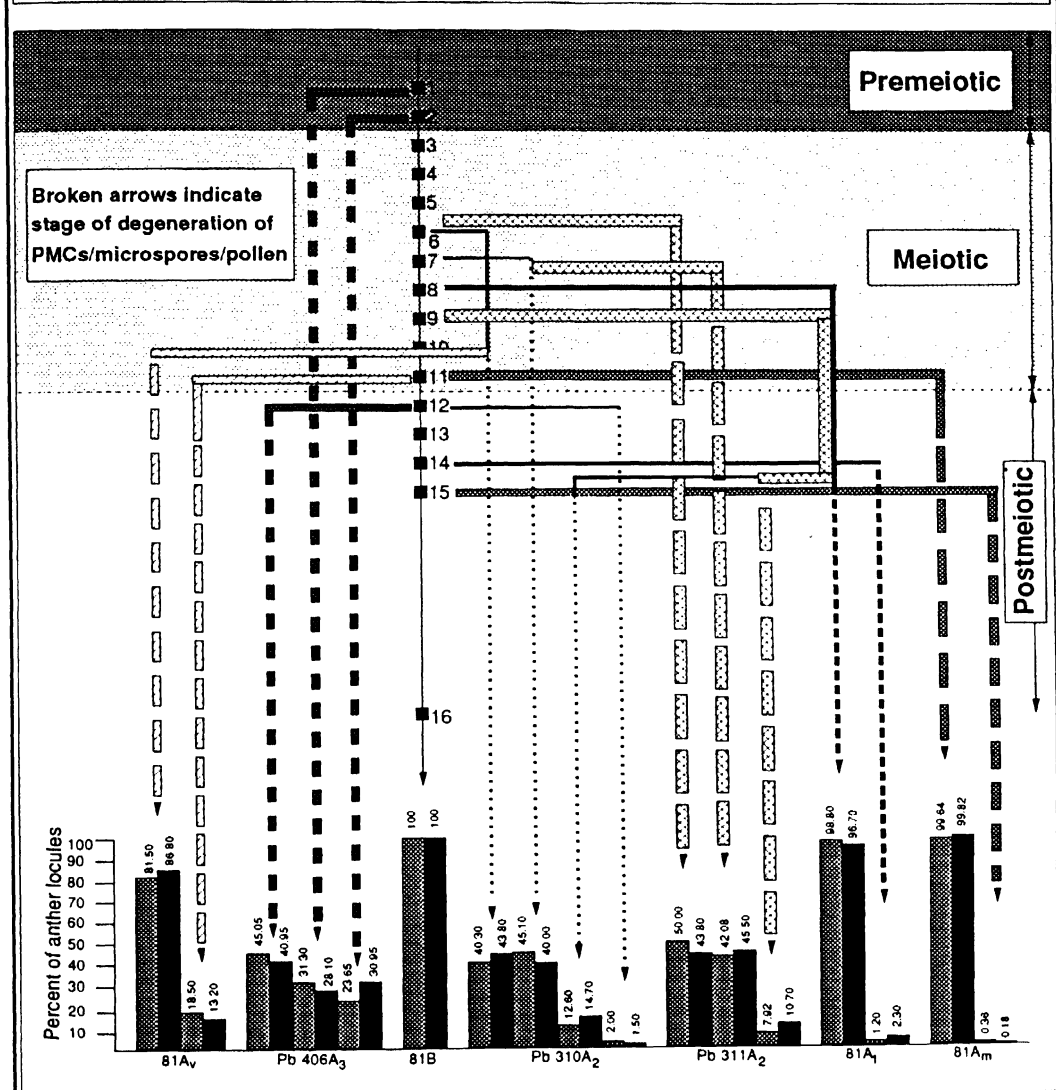


Figure 21 (A-P). Meiosis in 81B, 81A₁, Pb 310A₂, Pb 311A₂, 81A_m, and 81A₁ (ICMA 88001).

- A. Leptotene cells with long thread-like chromosomes having bead-like structures (chromomeres) along the entire length of the chromosome. Note the attachment of one chromosome i.e. nucleolus organizer (no) to nucleolus (nu) in each cell. (Photographed in 81B).
- B. Zygotene cell showing complete and perfect pairing between homologues (synapsis). (Photographed in 81B).
- C. Pachytene cell showing chiasmata formation along the entire length of chromosomes in all 7 bivalents (7_{II}). (Photographed in 81A_m).
- D. Late diplotene showing 7_{II}. (Photographed in 81B).
- E. Early diakinesis with 7_{II}. Note 6 bivalents with terminalized chiasmata and the nucleolar bivalent. (Photographed in 81A₁).
- F. Metaphase I with 7_{II} oriented at metaphase plate. (Photographed in 81B).
- G. Metaphase I with 7_{II}, one bivalent is already separated (initiation of anaphase I). (Photographed in Pb 310A₂).
- H. Anaphase I cell showing 14 chromosomes. (Photographed in Pb 310A₂).
- I. Telophase I with normal disjunction (7_i:7_i separation) evidencing completion of anaphase I. (Photographed in 81B).
- J. Formation of normal dyad after telophase I. (Photographed in 81B).
- K. Prophase II with two nucleoli and a nucleolar organizer chromosome in each cell. (Photographed in 81A_m).
- L. Cell at metaphase II. Note that one of the two nuclei is still in resting phase and the other is at metaphase. (Photographed in 81A₁).
- M. Cell with metaphase II/telophase II i.e. one nucleus is at metaphase and in the second normal 7_i:7_i separation of chromosomes is already completed. (Photographed in 81B).
- N. Cells with three nuclei observed at the tetrad stage. Possibly, the fourth nuclei is hidden on the other side due to the different view of the tetrad. (Photographed in 81B).
- O. Normal tetrad with four nuclei.
- P. Mature, well formed and round pollen grains (pg) of male-fertile line (81B) having a single germ pore (p) and thick exine.



A



D



C



E



F



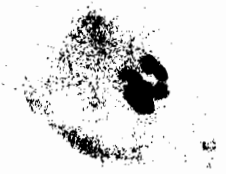
G



H

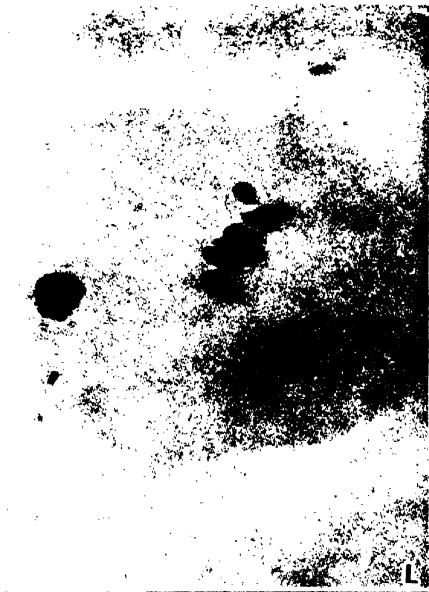


I



K

contd..



L



M



N



O

contd . .

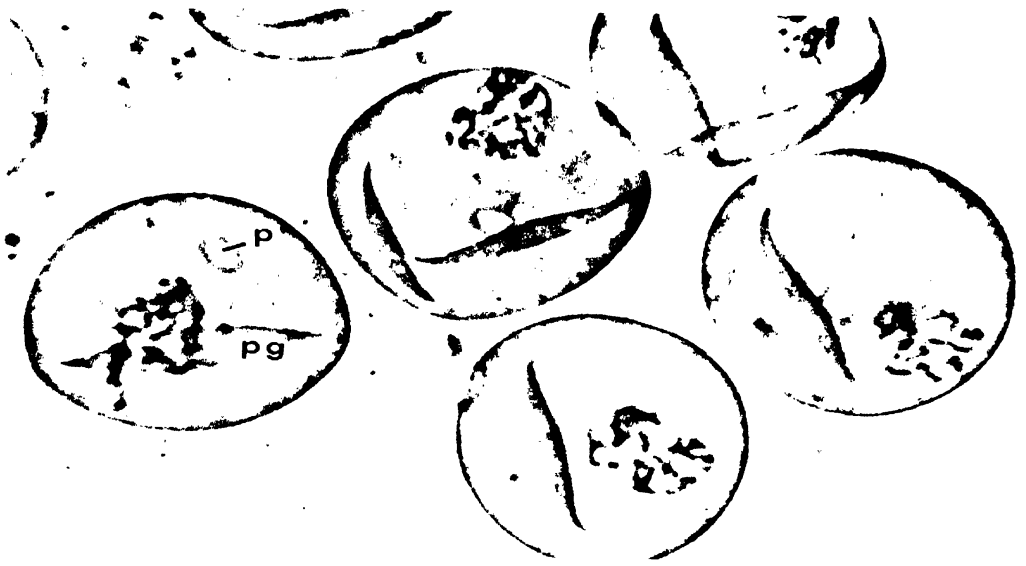


Figure 22 (A-X). Meiotic anomalies in Pb 406A₃.

- A. Normal leptotene cell (top left), with two others showing absence of nucleolus (lower cell) and detached chromatin from nucleolus (arrow).
- B. Miniature fragment/accessory chromosome (arrow) at the pachytene stage.
- C. Late diplotene cell with 5 ring bivalents, 1 rod (r) bivalent and 2 univalents.
- D. Late diplotene with 6_{II} (ring) and 2_I.
- E. Late diplotene with 4_{II} (ring) and 3_{II} (rod).
- F. 5_{II} at metaphase I instead of normal 7_{II}.
- G. Unequal (6_I + 8_I) chromosomal disjunction at anaphase I leading to a dyad (Fig. 23S) having unequal number of chromosomes.
- H. Anaphase I with a lagging chromosome undergoing division (arrow) to produce three miniature fragments.
- I. Unequal (2_I + 12_I) chromosomal disjunction at anaphase I.
- J. 12_I at anaphase I indicating loss of chromosomes during early meiotic stages.
- K. Unequal (5_I + 9_I) chromosomal disjunction at anaphase I with a lagging chromosome undergoing division.
- L. 6_{II} at metaphase I suggesting loss of a bivalent during early meiotic stages.
- M. Unequal (6_I + 7_I) chromosomal disjunction at anaphase I with a lagging chromosome undergoing division (arrow).
- N. Cells having unusual number of chromosomes with 13_I (upper cell) and 5_I (lower cell).
- O. Looks like unequal chromosome disjunction at anaphase I, but may be a view of the cell from an odd angle.
- P. Unequal (5_I + 9_I) chromosomal disjunction at anaphase I.
- Q. Unequal (4_I + 10_I) chromosomal anaphase I disjunction.
- R. Disorganized metaphase orientation with many clusters of paired chromosomes.
- S. Dyad with unequal (6_I + 8_I) chromosomes resulting from abnormal chromosomal disjunction as shown in Fig. 23G.
- T. Syncyte observed at the tetrad stage showing meiotic arrest at prophase I in three of the four nuclei.
- U. Multinucleate (penta- and hexa-nucleate) cells (syncytes) due to fusion of PMCs at prophase I.
- V-X. Multinucleate pollen grains (mpg) containing 5-9 nuclei.



A



B



C



D



E

Meiosis in A_3 (Pb 406A₃)

contd . .



F



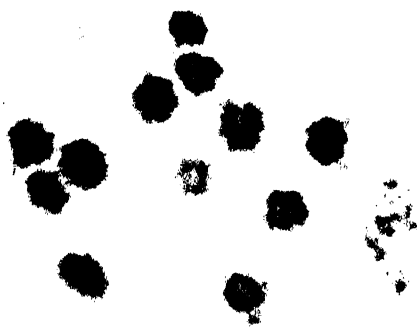
G



H



I

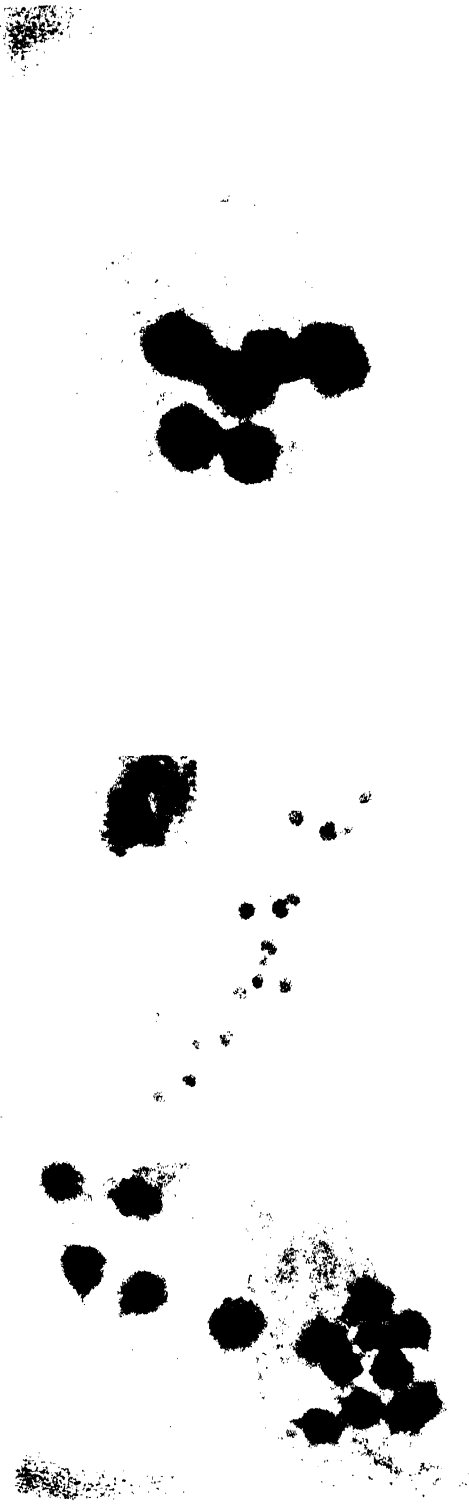


J



K

contd..

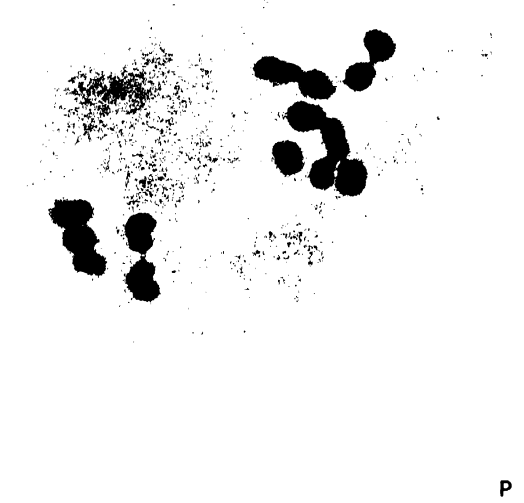


L



M

N



O

P
contd..



Q



F



S

T



mpg

U

V



mpg



mpg



W



line 81B. All the anthers studied followed the same developmental pattern (Fig. 20). The entire process of anther development was divided into 16 stages (explained in Materials and Methods, Section 2.3.4.1.1) to facilitate comparisons among the isonuclear lines. The sequence of anther development in 81B, from the sporogenous tissue stage (premeiotic) to pollen maturation (postmeiotic), is shown in Figs. 23A-R.

Prior to initiation of meiosis, young anthers contain sporogenous tissue surrounded by tapetum, followed by a middle layer, an endothecium and the epidermis (Fig. 23A). Callose deposition starts at the center of locule only after this stage (Fig. 23B), and becomes conspicuous at the onset of meiosis. A few of the tapetal cells become binucleate at prophase I (Fig. 23C). Tapetum thickness continues to increase and the central callose splits along the sporocyte walls (Fig. 23D). Following this, the sporocytes migrate towards the inner tapetal wall carrying callose tips on their inner face (Fig. 23E). This event occurs concurrently in all the locules of an anther (Fig. 23F). Some sporocytes become completely surrounded by callose (Fig. 23G). At late anaphase I, sporocytes become flattened and elongated. They are interconnected by wide cytoplasmic channels (Fig. 23I). At later stage, these cytoplasmic channels tend to break. Stretching of cytoplasmic channels is seen between the two adjacent sporocytes (Fig. 23J), and subsequently, cytoplasmic continuities between sporocytes disappear at telophase I (Fig. 23K). Minute callose tips attached to sporocytes are seen even at the dyad stage and the

middle layer of the anther is hardly detectable (Fig. 23L). Callose breakdown occurs after the tetrad stage when young microspores are liberated (Fig. 23M). Microspores are oriented in a ring along the densely stained tapetum (Fig. 23N) and embedded in it (Fig. 23O). Empty-looking pollen grains are slowly filled up with starch granules and the tapetum degenerates (Figs. 23O-Q). At this stage thickness of epidermis and endothecium is reduced. Well filled pollen grains with starch granules and fully developed exine and intine are seen at the anther maturity (Figs. 23Q-R).

4.2.3 Anther development and microsporogenesis in isonuclear A-lines

4.2.3.1 Premeiotic degeneration

All the CMS lines except Pb 406A₃ did not show premeiotic degeneration of the sporocytes. Microsporogenesis was normal before the initiation of meiosis and was similar to 81B.

4.2.3.1.1 Pb 406A₃

Degeneration of PMCs/sporocytes before the initiation of meiosis was observed only in Pb 406A₃. Various types of anomalies were associated with anther development in Pb 406A₃. About 28% of Pb 406A₃ locules examined showed degeneration of developing PMCs at the sporogenous tissue stage during the cool dry season (CDS) and 31.3% during the hot dry season (HDS) (Figs. 20, and 26A-J). Degeneration resulted due to anomalies in the tapetum or in

developing PMCs themselves. Various kinds of tapetal hypertrophy were observed at the very early stage of anther development (Figs. 26A-D, and 26F). The inner walls of tapetal cells appeared to dissolve/disorganize and their cytoplasmic contents intermingle to form a periplasmodium. This attained a balloon shape and almost covered the sporogenous tissues. As a result, the anther locule collapsed very soon leading to the death of developing PMCs (Fig. 26G). Such an anther typically had thick epidermis, middle layer, endothecium, and very small compressed locular cavity containing remains/debris of degenerated PMCs (Fig. 26G). The second kind of anomaly involved at this stage was related to the developing PMCs themselves. In a transverse section of a normal anther there are usually 8-11 sporogenous cells (Figs. 23A-C). But in Pb 406A₃, some anther locules had atypical giant PMCs (Figs. 26H, and 26I) or PMCs were unusually dark stained (Figs. 26H, and 26J). Locules containing giant cells had only 4-6 empty (without cytoplasmic material) sporogenous cells. Such PMCs were not observed at later stages of anther development, suggesting their death at an early stage. At stage 2 of anther development, when callose started appearing near center of the locule, degeneration occurred in $\approx 31\%$ of locules in the CDS and in about 24% of locules in the HDS. This degeneration also involved tapetal hypertrophy of different types (Figs. 26K, and 26L). Tapetal cells enlarge unusually and mask the developing PMCs. Such locules could not be traced out at later stages of anther development suggesting their death at this premeiotic stage of anther

development.

Only two of ≈ 3000 Pb 406A₃ anthers examined had atypical trilobed structure instead of normal four lobes. Two of the four lobes fused together and formed a 3-lobed structure. Such anthers were observed only during premeiotic period. Morphologically, all the four wall layers of the anther were normal except that the fused portion had none of the anther wall layers. The anther lobe diameter of the fused lobes was almost double than the normal ones. Such anthers were not found at later stages of anther development suggesting their degeneration at an early stage (premeiotic).

4.2.3.2 Degeneration during meiosis

A large proportion of anther locules in most of the isonuclear A-lines exhibited degeneration of developing PMCs during the meiotic and postmeiotic periods. Microspore degeneration during meiosis was observed in Pb 310A₂, Pb 311A₂ and 81A_v.

4.2.3.2.1 Pb 310A₂ and Pb 311A₂

Pb 310A₂ followed four- and Pb 311A₂ three- anther developmental paths. Two of the four anther developmental paths followed by Pb 310A₂ showed degeneration of microsporocytes during meiosis (Fig. 20). Path 1 was noticed in 40-44% of Pb 310A₂ locules that followed 81B till early anaphase I . Thereafter, it followed a different developmental pattern (Fig. 25).

Disintegration of the cytoplasmic mass starts at anaphase I (Fig. 25A). Callose remains attached to the sporocytes. The frequency of sporocytes with disintegrated cytoplasm abruptly increases at the dyad stage and callose breakdown also starts (Fig. 25B). Nuclei are densely stained and the degenerated cytoplasm also takes more stain as compared to the normal cytoplasm. Consequently, microspore degeneration occurs at the dyad stage.

Path 2, which occurred in 40-45% of locules, was similar to 81B up to late anaphase I. Degeneration started immediately after this stage (stage 7). It resulted due to degeneration of the cytoplasmic mass and sporocyte walls (Fig. 25C). Callose breakdown occurs in the form of fibrous strands which are scattered throughout the locule (Fig. 25C). Almost at the same time, interconnecting tapetal cell walls start dissociating and cytoplasmic fluid along with nuclei of tapetal cells gets mixed up and floats together (Fig. 25C). At this stage tapetum becomes highly vacuolated. Subsequently, in some anther locules either sporocytes and the tapetum degeneration occurs simultaneously or the tapetum degeneration is followed by the sporocytes degeneration (Fig. 25E).

Two of the three anther developmental paths observed in Pb 311A₂ showed microspore degeneration during meiosis as that of Pb 310A₂ but their frequency of occurrence were different (Fig. 20). Path 1 was recorded in 44-50% of locules and path 2 in 42-45% of locules.

4.2.3.2.2 81A_v (ICMA 88001)

Pollen abortion in 81A_v resulted from one of the following phenomenon: Firstly, anther development was similar to Pb 310A₂ up to the dyad stage (Fig. 20), later on, degeneration occurred in different ways (c.f. Figs. 25 and 28). In 81-87% of the 81A_v locules, degeneration occurred at the dyad stage during CDS and HDS. In remaining locules degeneration took place after the release of microspores from the tetrads (Fig. 20).

First type of degeneration involved callose breakdown at the dyad stage (Figs. 28A, and 28B). Broken callose tips from sporocytes remain intact and are seen along with the cytoplasmic mass and the nuclei released from sporocytes after the breakdown of their walls (Fig. 28A). Later on, debris of callose, nuclei, cytoplasmic mass and disintegrated walls of sporocytes gathers in center of the locule (Fig. 28B). Big vacuoles were not observed in the tapetum.

The second type of degeneration occurred in 13-18% of anther locules in the CDS and the HDS. The callose remains attached to the sporocytes and sporocytes migrate towards interior of the locule. At the same time sporocytes' walls start breaking resulting in release of the cytoplasmic fluid (Fig. 28D). Big vacuoles were present in the tapetum in the second type of degeneration which were absent in the first type of microspore degeneration (Fig. 28D). Occurrence of all these events leads to degeneration of PMCs.

4.2.3.3 Postmeiotic degeneration

Variable frequency of microspores showed postmeiotic degeneration in all the isonuclear A-lines involved in this study.

4.2.3.3.1 81A₁

Two types of anther developmental paths were observed in 81A₁, one of them occurred in about 97% (CDS) to 99% (HDS) of the 81A₁ locules examined. In this case, anther development was similar to that of 81B up to the early telophase I stage (when stretching between the cytoplasmic channels is seen). Subsequently, callose breakdown occurs in the form of fibrous strands. These strands spread throughout the locular cavity (Fig. 24A). Tapetum becomes thick and highly vacuolated at the late dyad stage (Fig. 24B). Dyads and young microspores remain adhered to the tapetum as in 81B, but, later on, contrary to 81B, microspores form a ring and migrate towards interior of the locule (Fig. 24C). Fibrous strands of callose accumulate in the center of locule (Fig. 24D). Tapetum thickness and vacuolation continue to increase. The anther middle layer which was hardly detectable at the dyad and the tetrad stages, reappeared and became prominent. Some microspores become binucleate by this stage (Fig. 24E). In advanced stages of anther development, cytoplasmic contraction and tapetal hypertrophy occurs and microspores start shrivelling/wilting (Fig. 24F). Ultimately, microspores degenerate completely and form cluster in center of the locule, the tapetum is still persistent (Fig.

24G). A few locules are seen empty having thick, vacuolated tapetum (Fig. 24H).

Second type of degeneration was observed only in 1.2% (HDS) to 2.3% (CDS) of locules. In this case, the anther development was similar to 81B up to the stage when traces of tapetum are seen in 81B locules (Fig. 23O), thereafter, pollen grains start collapsing. Such anthers do not dehisce and contain remnants of degenerated tapetum and pollen grains (Fig. 24K).

4.2.3.3.2 Pb 310A₂ and Pb 311A₂

Two of the four paths followed by Pb 310A₂ showed postmeiotic degeneration of microspores either at young microspore stage in 1.5 - 2.0% of locules (Path 1) or near pollen maturity in 13 - 15% of locules (Path 2). In path 1, anther development was similar to 81B till liberation of the microspores from the tetrads. Thereafter, tapetal cytoplasm becomes typically fibrous and microspore degeneration occurs at the uninucleate stage (Fig. 25F). Whereas, path 2 was similar to 81B up to late telophase I, then joined the path of 81A₁ (Fig. 20). Degeneration occurred in the same way as was observed in 81A₁ (Figs. 24A-G) i.e. callose breakdown at telophase I followed by loss of contact between microspores and tapetum resulted in microspore degeneration. Pb 311A₂ also followed path 2 and differed only for the frequency of occurrence of these events (8-11% of locules).

4.2.3.3.3 Pb 406A₃

Anther/pollen development in 41-45% of Pb 406A₃ locules proceeds normally up to the release of microspores from the tetrads (same as in 81B). Thereafter, degeneration results due to the formation of intratapetal syncytium (syn. plasmodial tapetum). This tapetal condition involves the dissociation of interconnecting tapetal cell walls and merging of cytoplasmic fluid and nuclei from different cells. The tapetal cell walls facing the sporocytes remains intact and bulges out to cover the interior of the locule and surrounds the microspores. These syncytes may be quite extensive, filling half or more of the cross section of a locule and extending vertically throughout the length of the anther locule. Consequently, the arrested microspores are compressed into a small central area and start degenerating (Figs. 26N-Q, 26W, and 26X). Ultimately, locules are completely filled with periplasmodium (Fig. 26R) and microspores die (Fig. 26T).

A few anthers were observed having darkly stained and persistent tapetum and compressed empty microspores at maturity (Fig. 26S). Some anther locules (<1%) had no tapetum and contained partially to completely fertile pollen grains at maturity (Figs. 26U, and 26V).

4.2.3.3.4 81A_m/81A₄

Majority of 81A_m locules showed identical anther developmental pattern as it occurred in 99.6% (HDS) to 99.8% (CDS) of total locules examined. The other

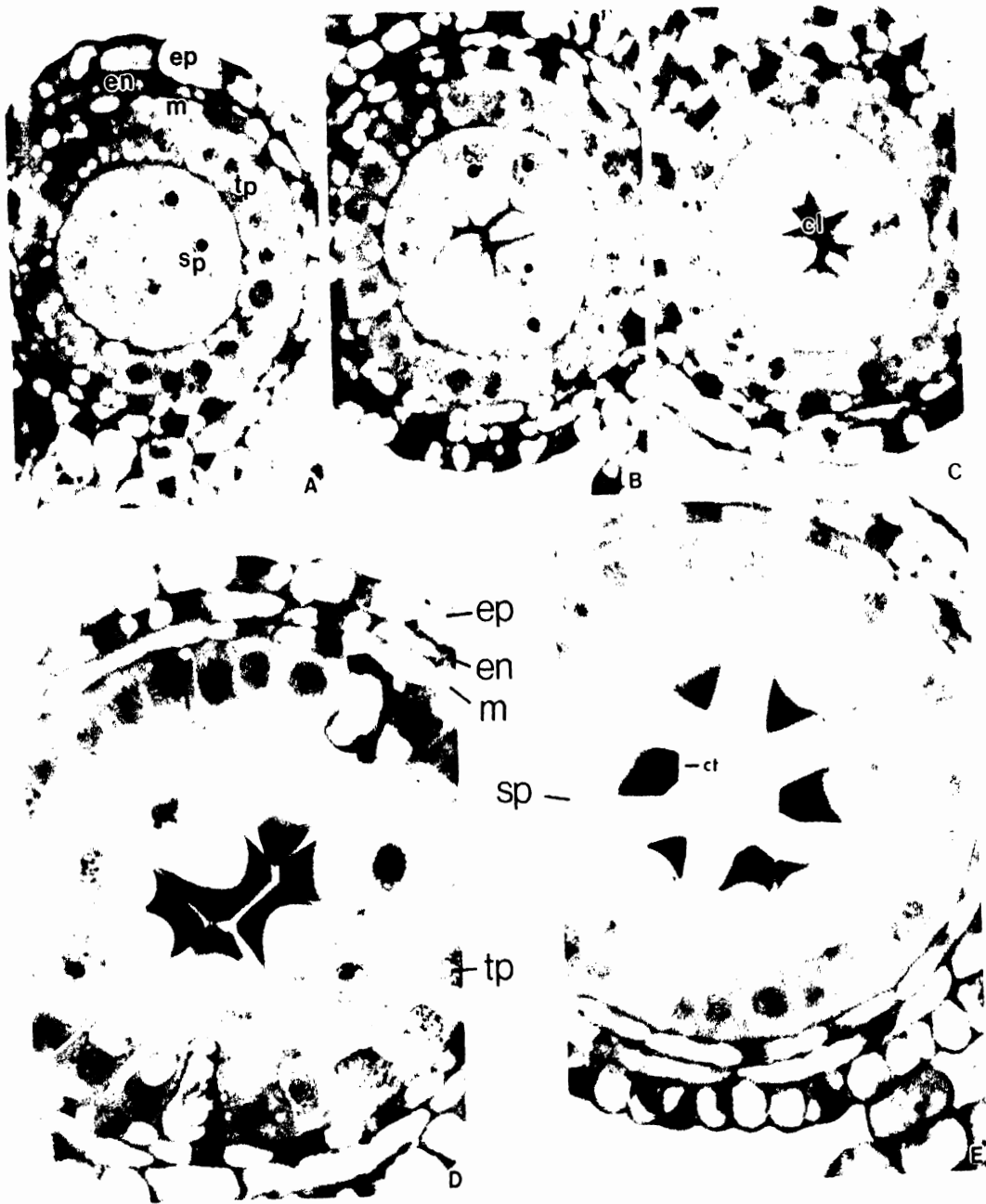
path occurred very rarely (0.36% of locules in the CDS and 0.18% of locules in the HDS). Up to the tetrad stage it (former) was similar to 81B (Fig. 20). Thereafter, it followed a different path (Figs. 27A-G). Initially, young microspores are scattered inside the locular cavity, later, they become oriented in a circle along the inner tapetal wall (Fig. 27B). At later stages microspores embed in the tapetum and both of them (microspores and the tapetum) start degenerating simultaneously (Figs. 27C-E). Ultimately, degeneration occurs and the association between the tapetum and microspores is lost. At this stage, only microspore walls (collapsed microspores) and disintegrated tapetum are present in the locular cavity (Fig. 27F). Sporadically, locules containing healthy pollen were also observed along with traces of the tapetum (Fig. 27G). The other developmental path can not be distinguished from 81B till formation of the mature pollen grains. Pollen degeneration occurs suddenly and anther contains traces of the tapetum and degenerated pollen grains as shown in Fig. 24K.

4.2.3.3.5 ICMA 88001 (81A_v)

Anther development was normal and same as that of 81B up to tetrad formation. About 13% (CDS) to 18% (HDS) of locules followed this path. Tapetum was persistent at maturity, and highly vacuolated (Fig. 28E) with very lightly stained cytoplasm and darkly stained nuclei. Most of the microspores are uninucleate, shrunken and have contracted cytoplasm at anther maturity.

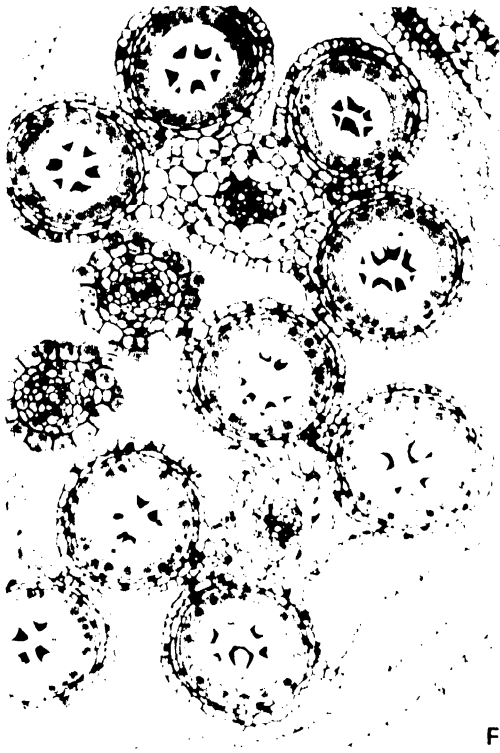
Figure 23 (A-R). Transverse sections of fertile anthers (81B) representing microsporogenesis from young sporogenous stage to the anther dehiscence

- A. Young anther locule before callose deposition comprising sporogenous tissue (sp), tapetum (tp), middle layer (m), endothecium (en), and epidermis (ep).
- B. Callose started appearing at center of locule, tapetal cells are still uninucleate.
- C. Microsporocytes in early meiotic prophase with well developed callose (cl) at center of locule. Some tapetal cells are binucleate.
- D. Central callose mass splitting along the sporocyte walls. Note the continuous thickening of tapetum and enlargement of tapetal nuclei.
- E. Separation and migration of sporocytes towards tapetum. Note that each sporocyte carries a tip of callose (ct) on its inner face. These tips represent segments of the central callose that have separated along planes of the sporocyte walls.
- F. Anthers of a floret showing synchrony in separation and migration of callose towards tapetum in all the locules.
- G. Anther locule at the same developmental stage as Figs. 23E and 23F showing one free sporocyte (sp) inside the locule surrounded by thick callose walls.
- H. Anther locule showing microsporocytes at anaphase I. Callose tips are still attached to them.
- I. Sporocytes become flattened and elongated. They are interconnected by wide cytoplasmic channels (cc).
- J. Cytoplasmic channels (cc) tend to break and stretching is seen between two adjacent sporocytes.
- K. No cytoplasmic continuities persist (arrow) between the sporocytes that are at telophase I.
- L. Part of anther locule showing dyads (d). Small callose tips attached to dyads can be seen. The middle layer of the anther is hardly detectable.
- M. Young microspores (mic) immediately after liberation from tetrads; broken strands of callose are present.
- N. Anthers with developing uninucleate microspores (mic) laying in a ring along the densely stained tapetum.
- O. Anther showing apparent attachment of developing pollen grains and the degenerating tapetum (dt).
- P. Anther showing developing pollen grains and remains of degenerated tapetum. Note that the thickness of epidermis and endothecium is reduced.
- Q. Mature pollen grains (pg) with many starch granules (sg), fully developed exine and intine. Tapetum is no longer visible.
- R. Mature and dehisced anther.

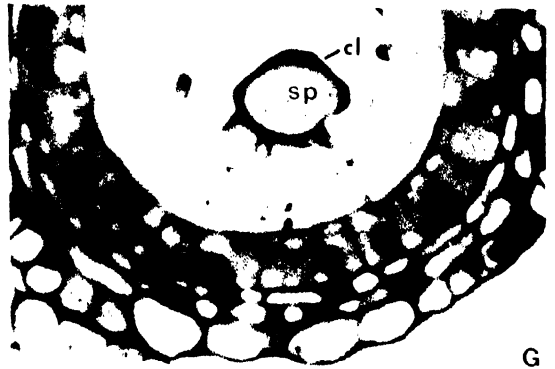


Microsporogenesis in 81B

contd ..



F



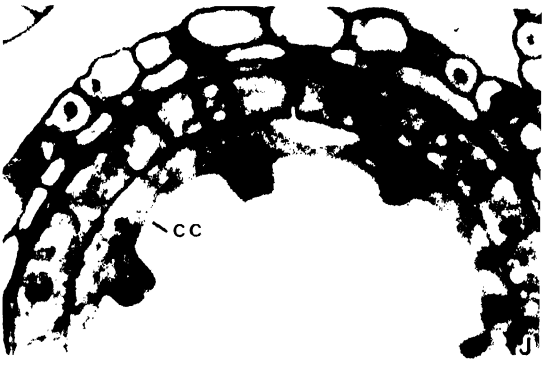
G



H



cc



cc

J



K

contd .

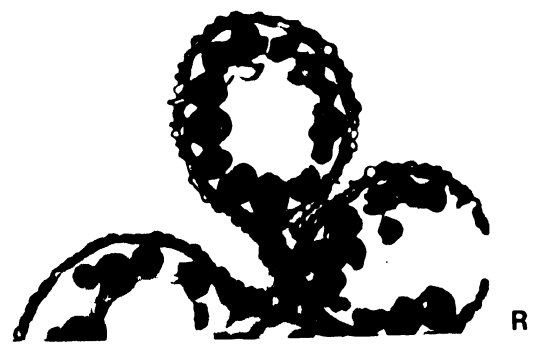
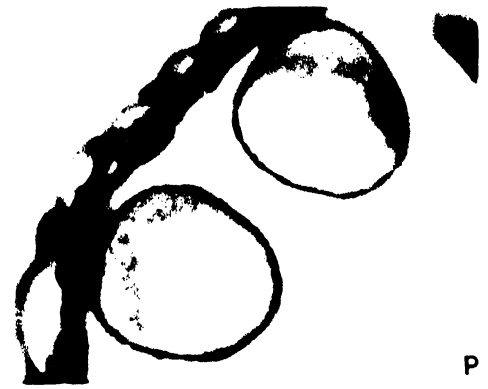
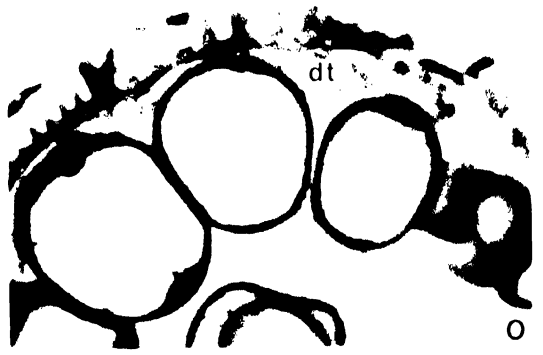
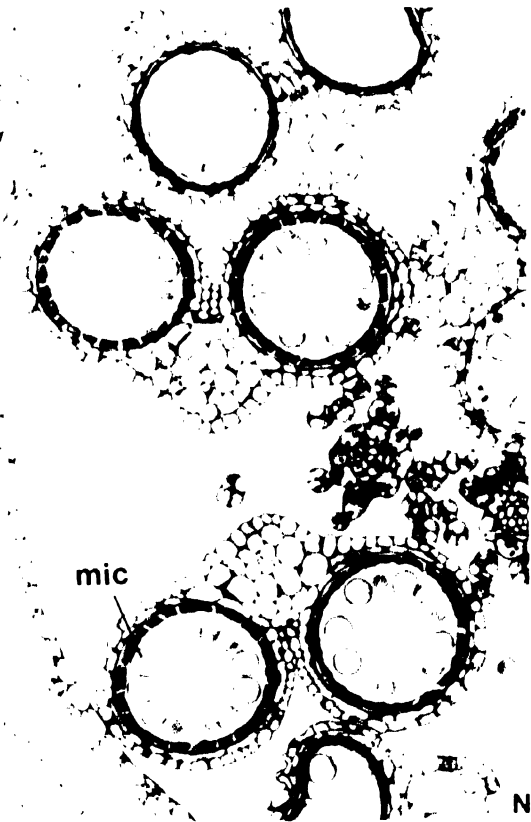
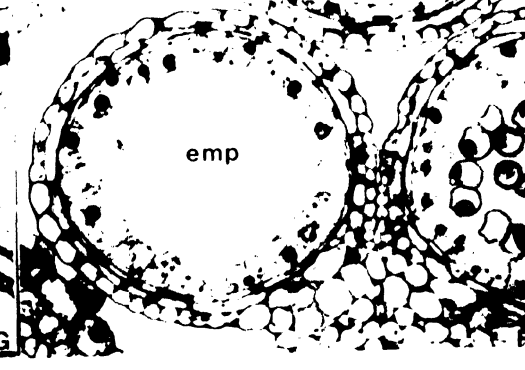
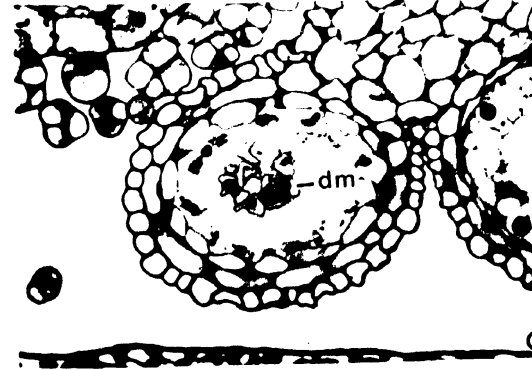
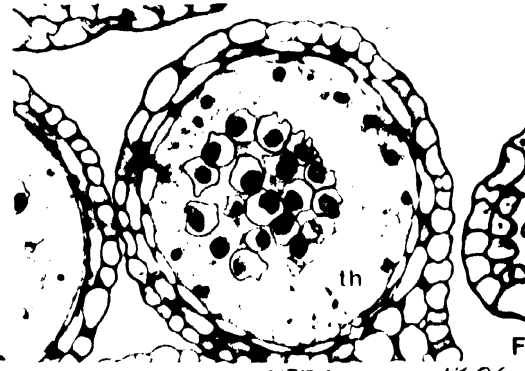
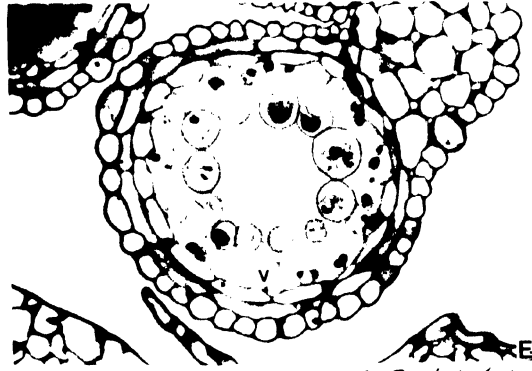
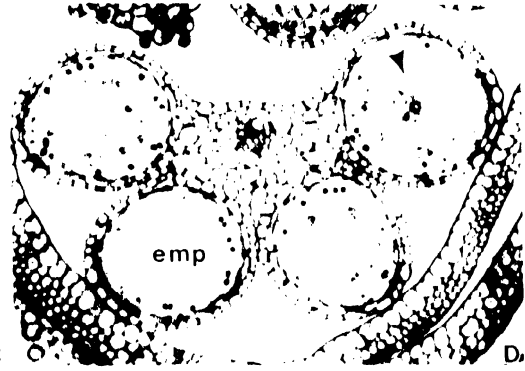
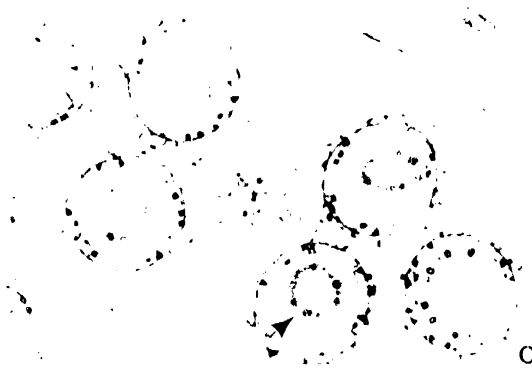
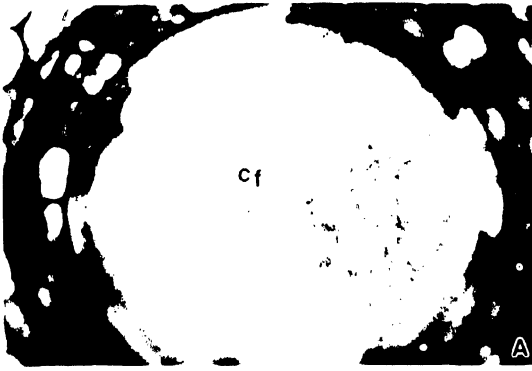


Figure 24 (A-K). Microsporogenesis in pearl millet A₁ cytoplasm cms line 81A₁.

Note: Anther development is similar (normal) up to Fig. 23J (81B). After that following anther developmental stages were observed in 81A₁.

- A. Callose breakdown occurs and forms fibrous strands (cf) which spreads throughout the locular cavity.
- B. Late dyad / early tetrad stage; tapetum is thick and highly vacuolated. Dyads are present in contact with the anther tapetum.
- C. The attachment/association of young microspores with the tapetum is temporary contrary to the fertile counterpart (Figs. 23N-Q). Microspores form a ring (arrow) and migrate towards the interior of the locule.
- D. Fibrous strands of callose are also accumulated in center of the locule (arrow). Empty locule (emp) is also seen.
- E. Tapetum thickness and vacuolation (v) increases. Middle layer which was hardly detectable at dyad/tetrad stage reappears and become prominent. Most of the microspores are binucleate by this stage.
- F. Advanced stage as compared to previous one showing degenerating microspores attaining irregular shape containing contracted cytoplasmic mass. Note the occurrence of tapetal hypertrophy (th) at certain places.
- G. Anther locule showing completely degenerated microspores clustered in center of the locule. Tapetum is still present.
- H. Locule at the same stage as Fig. 24F, but without microspores (emp).
- I-J. Advanced stage as compared to Fig. 24F. Tapetal hypertrophy leads to formation of intratapetal syncytium (ITS) which floats inside the locule surrounding the developing uni- to bi-nucleate microspores. Such situation was observed quite infrequently in 81A₁ cms line.
- K. Completely mature nondehiscent anther of 81A₁. Remnants of degenerated tapetum and collapsed pollen are visible.



Microsporogenesis in 81A,

contd ..

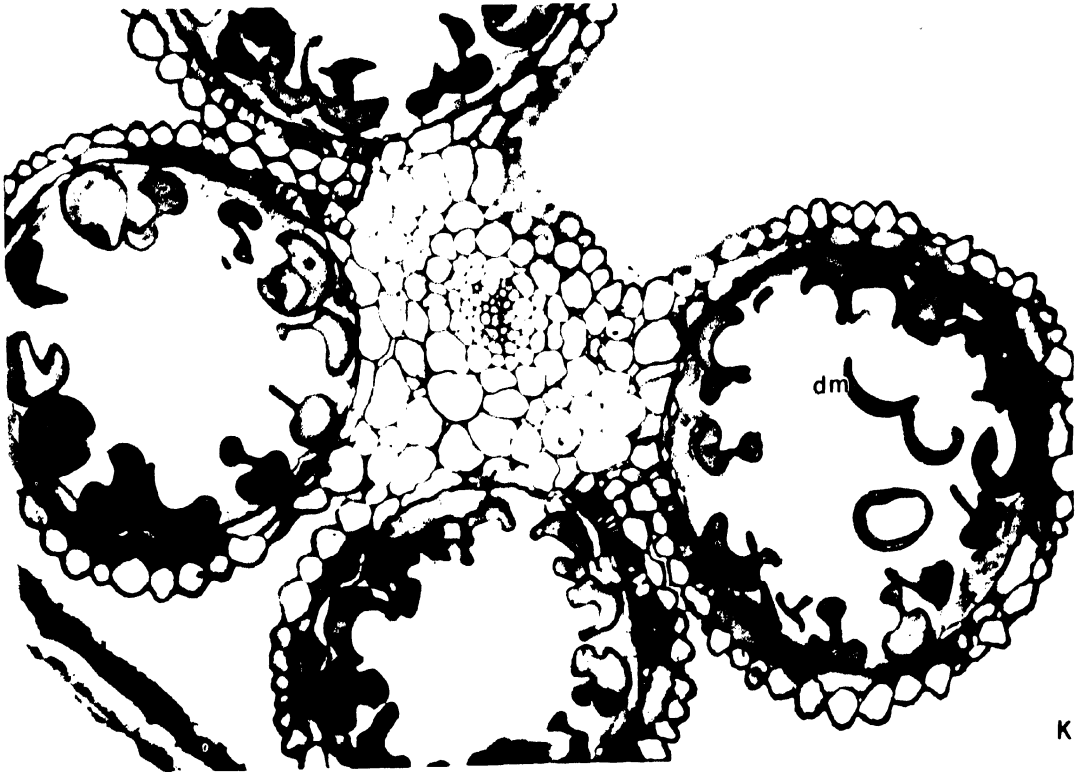
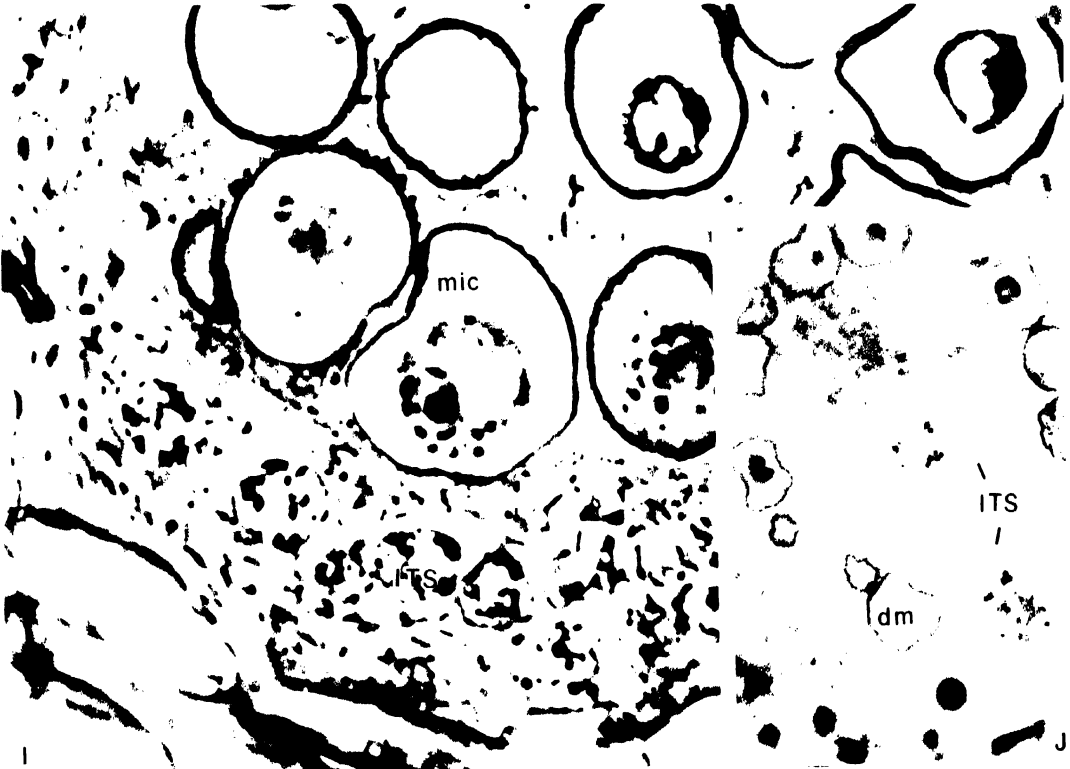


Figure 25 (A-E). Microsporogenesis in pearl millet A_2 cytoplasm cms lines (Pb 310 A_2 and Pb 311 A_2).

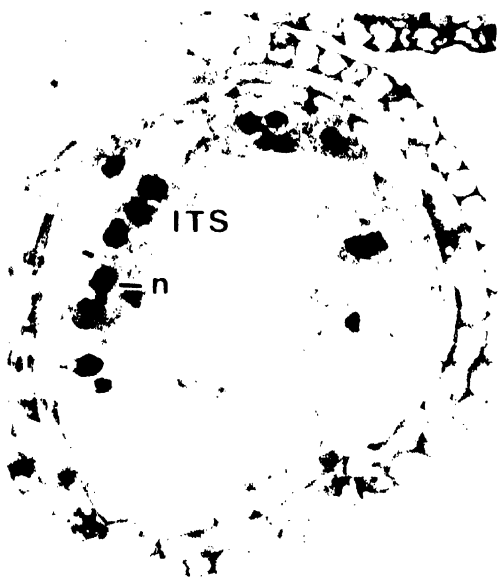
Note: Anther developmental stages before this are same as shown in Figs. 23(A-H). Thereafter, either the following path was followed or the path followed by 81A₁ (Fig. 24) was followed.

- A. The cytoplasm of the microspores at anaphase I stage starts disintegrating (arrow). Callose is present attached to the microspores.
- B. The same as in Fig. 25A but at an advanced stage (dyad). The frequency of microsporocytes increases having degenerated cytoplasmic mass. Callose breakdown starts.
- C. Anther developmental stage comparable to Fig. 25A but callose breaks at an early stage to form fibrous strands (cf) dispersed inside the locule. At the same time interconnecting walls of tapetal cells start dissociating and cytoplasmic fluid along with nuclei floats together (ITS). Note the thickening and vacuolation of the tapetum.
- D. Two locules of an anther, the upper one showing the contraction of the cytoplasmic mass in all microsporocytes and the lower one at more advanced stage compared to Fig. 25C.
- E. Anther showing disintegration of tapetum and microsporocytes, consequently, either the cytoplasmic fluid floats freely inside the locule (arrow) or the tapetal cells enlarge due to breakdown of inner tapetal cell walls. Tapetum becomes vacuolated and microsporocytes degenerate completely leaving their cytoplasmic mass inside the locule (other three locules).
- F. Anther locule showing persistent tapetum and degenerating uninucleate microspores (dm). Note that the tapetum is typically fibrous.
- G. Tapetal degeneration (ITS) at the dyad stage. All the three anther wall layers except tapetum are quite prominent.
- H. Locules inside a floret at the same stage as shown in Fig. 25F.



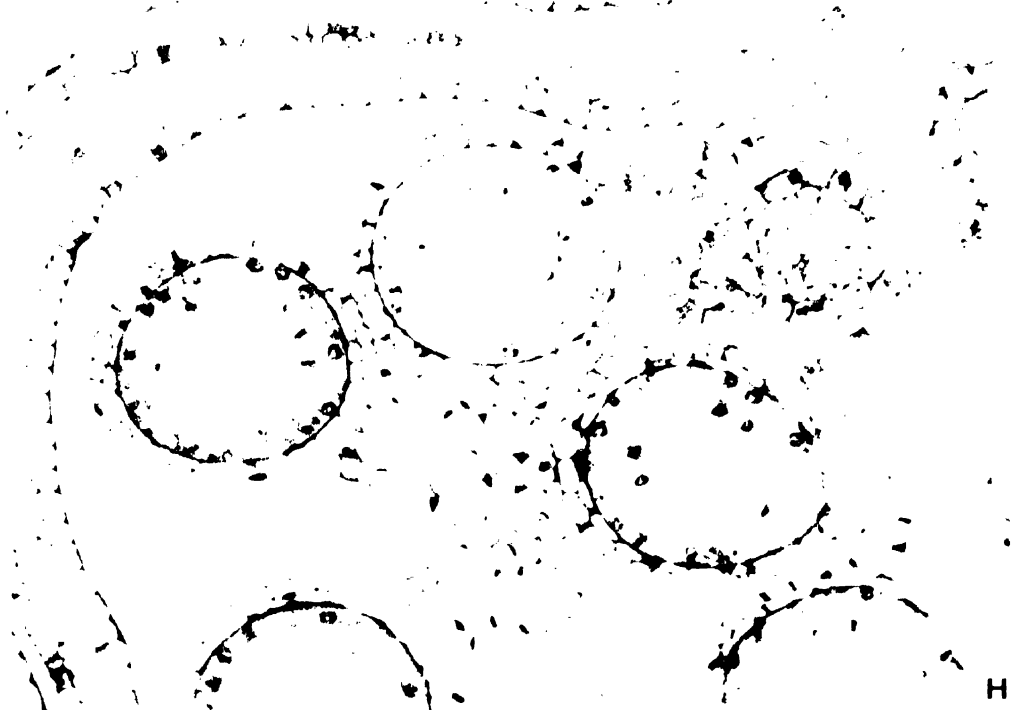
Microsporogenesis in Pb 310A₂ and Pb 311A₂

contd..



F

G



H

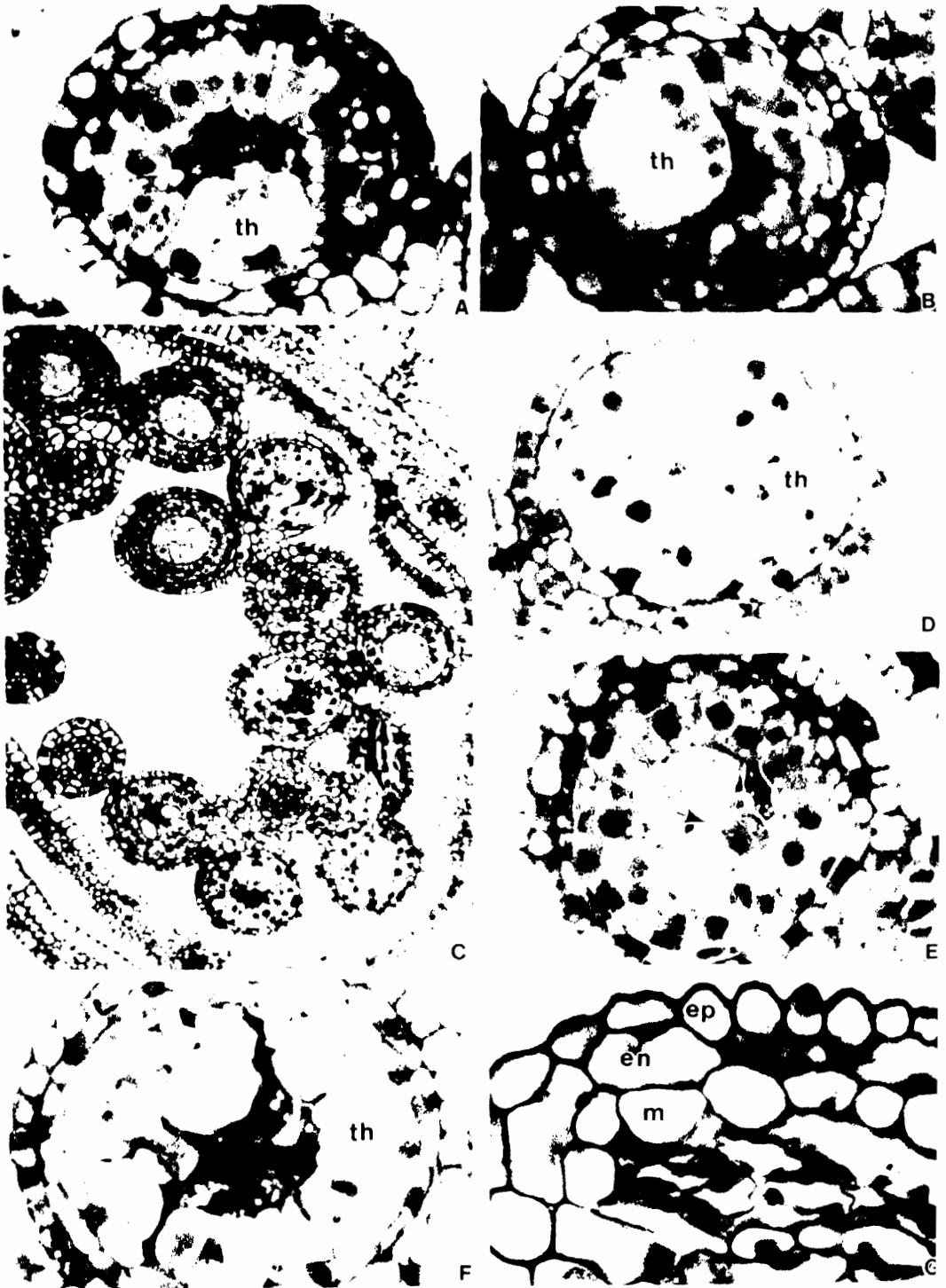
Figure 26 (A-X). Summary of microsporogenesis in pearl millet A_3 cytoplasm male-sterile line Pb 406 A_3 = 81 A_3 .

Figure 26 (A-J). Transverse sections of Pb 406 A_3 anther locules exhibiting various tapetal irregularities compared to normal tapetal development in male-fertile line 81B (Fig. 23A).

- A. Enlargement of few tapetal cells (th) covering the sporogenous tissue. Note that the microsporocytes are darkly stained.
- B. Balloon type tapetal hypertrophy (th) covering large area of locule. Floating tapetal nuclei can be seen.
- C. Floret showing anthers with some normally developing locules as that of Fig. 23A, and other locules associated with various anomalies shown in Figs. 24A, 24D, 24E, 24F, and 24G.
- D. Unusual tapetum development (th) comprising highly vacuolated tapetal cells.
- E. Some of the tapetal cells are binucleate. White area (arrow) surrounding microsporocytes is seen, which otherwise is not seen in normally developing locules.
- F. Same as in Fig. 26A except that tapetal cells are highly vacuolated.
- G. Collapsed locule with microsporocytes compressed between exceptionally thick anther wall layers.
- H. Anthers within a floret showing normally developing locules (anther on right) and anomalies in two of the four locules of second anther (left) shown in Figs. 26I and 26J.
- I. Anther locule showing unstained giant microspores (gm).
- J. Anther locule having exceptionally darkly stained microspores.
- K. Anthers inside a floret depicting various types of anomalies associated with tapetum development at the stage shown in Fig. 26L.
- L. Normally developed locule (left) and locule with abnormal tapetum (th) and microsporocytes showing imperfect differentiation of related tissues.
- M. Trichambered (3 locules) anther. Note that all four anther wall layers have normally developed in all three locules.

Figure 26 (N-R). Irregularities involving intratapetal syncytium (ITS)/plasmodial tapetum.

- N. Well developed uninucleate microspores. Tapetum is densely stained and interconnecting walls of tapetal cells start disintegrating and cytoplasmic fluid starts mixing up.
- O. More advanced stage than Fig. 26N. Inner tapetal wall (ITS) floats to the interior of locule and all tapetal nuclei (n) float in a common cytoplasmic fluid. Microspores (dm) start degenerating.
- P. Advanced stage of the locule as compared to Fig. 26Q showing degeneration of microspores whose remains can be seen. The locule is completely filled with the cytoplasmic mass, nuclei (arrow) and debris of microspores.
- Q. Anther showing free cytoplasmic mass of tapetal cells; nuclei and uninucleate microspores are embedded in it.
- R. Anther with all the four locules in same condition as in Fig. 26Q.
- S. Mature nondehiscent anther showing persistent, darkly stained tapetum and aborted pollen grains. Note that the locules have compressed.
- T. Anther showing two locules, the upper one is same as Fig. 26Q but the lower one shows normally developed uninucleate microspores of different sizes. Traces of tapetum are present.
- U-V. Mature anthers observed in cms line Pb 406A₃ with completely degenerated tapetum and fully developed pollen grains (pg).
- W. Anther locule at young microspore stage having plasmodial tapetum as shown in Fig. 26O.
- X. Anther having different kind of tapetal hypertrophy (ITS); all the tapetal cells simultaneously enlarge pushing the microspores (dm) towards center of the locule.



Microsporogenesis in Pb406A₃

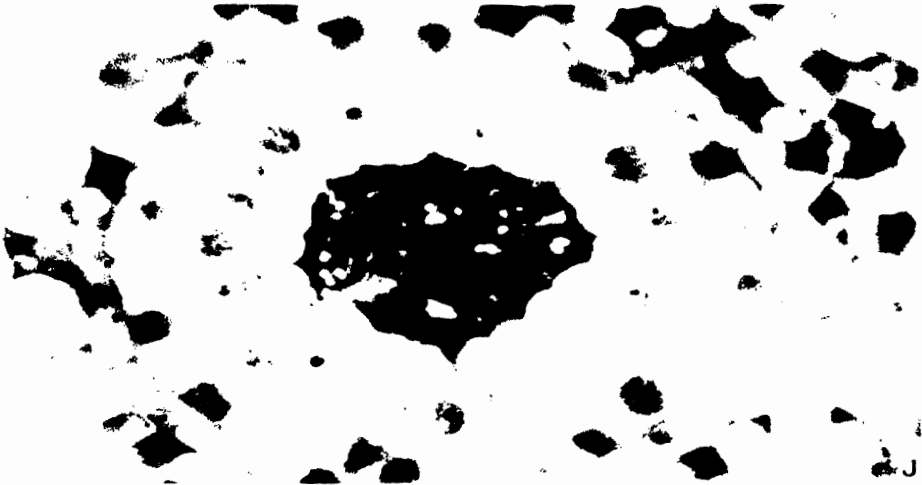
contd.



H

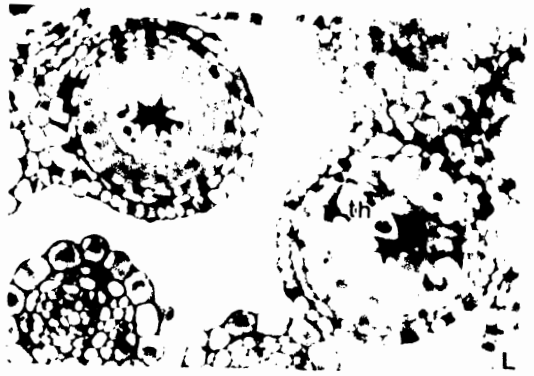
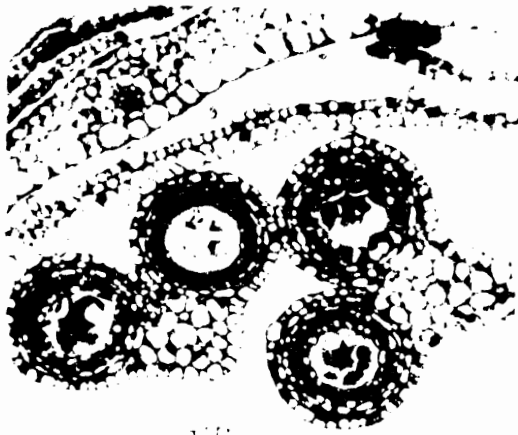


I

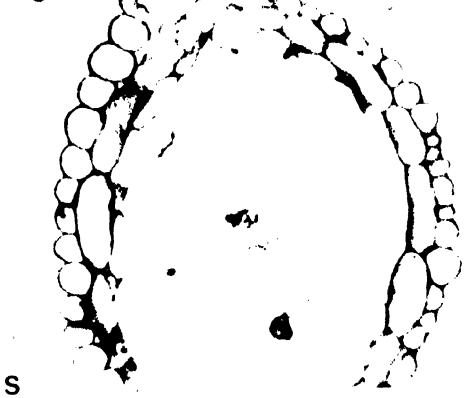
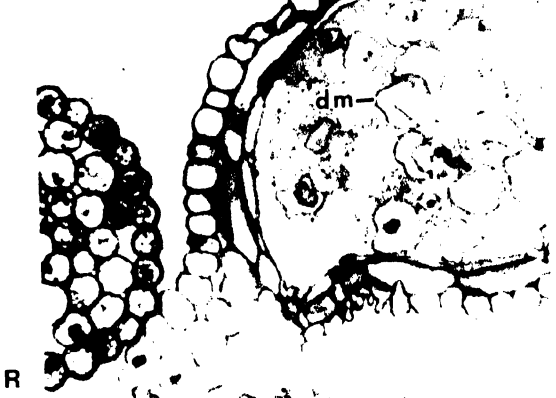
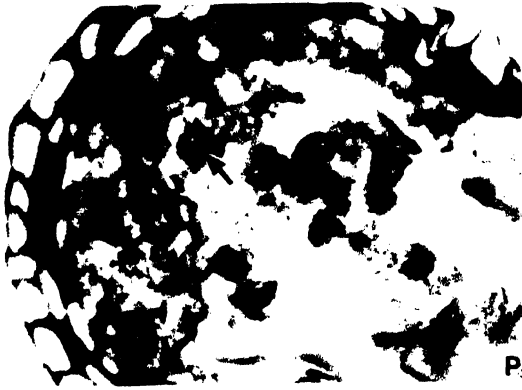


J

contd...



O
contd ...



T
contd..

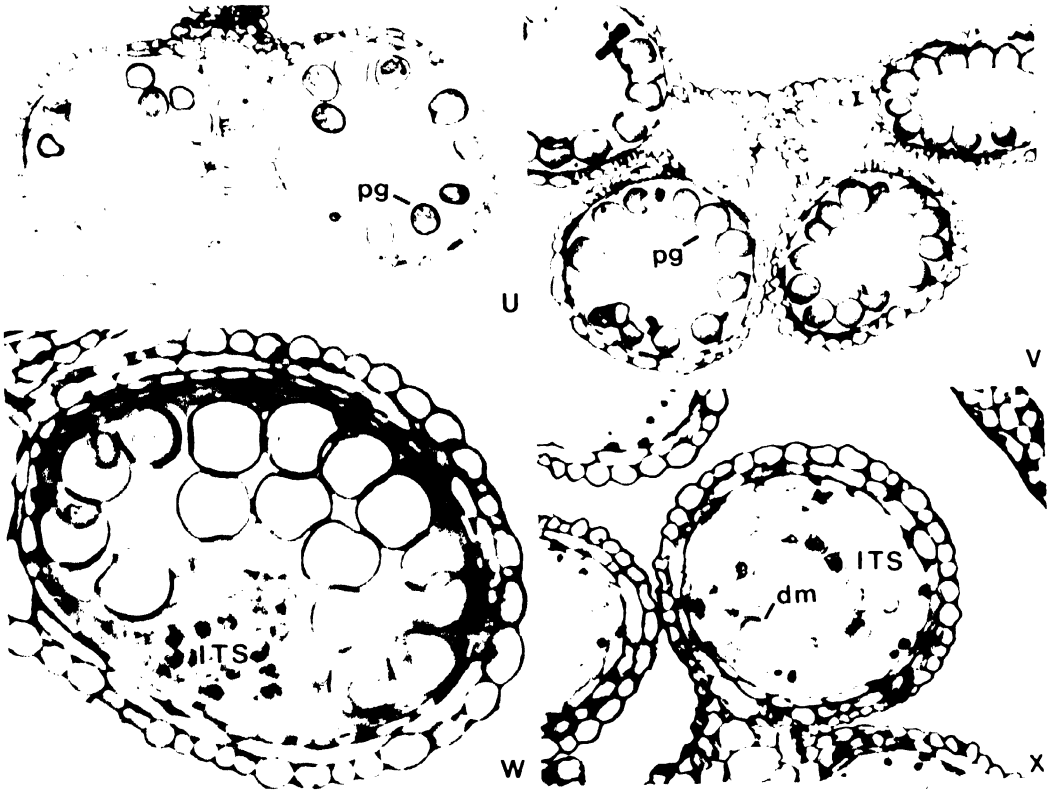
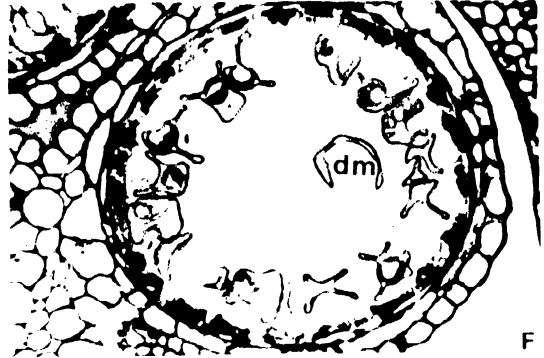
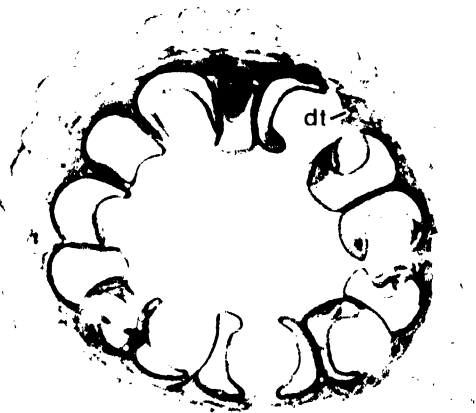
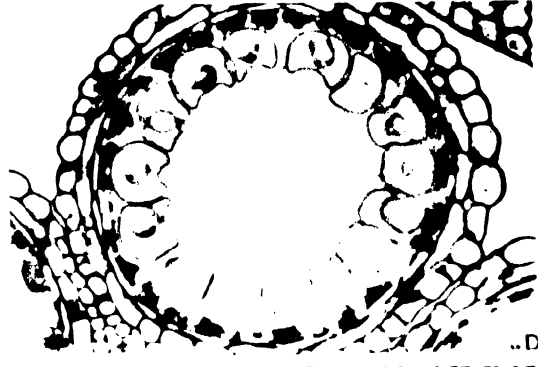
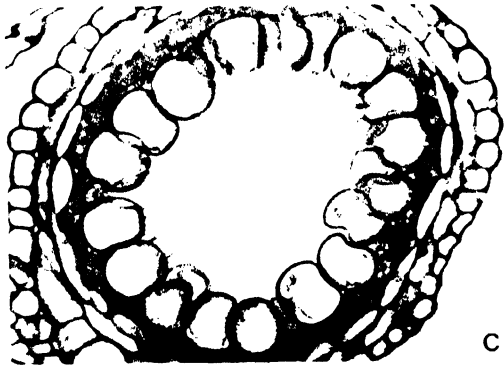
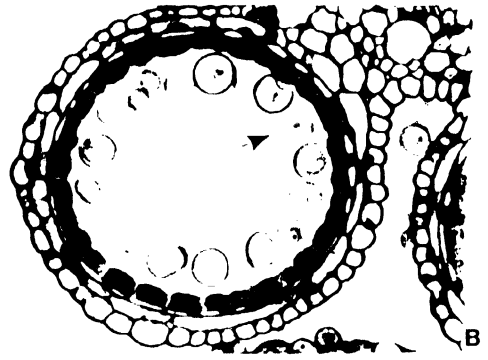
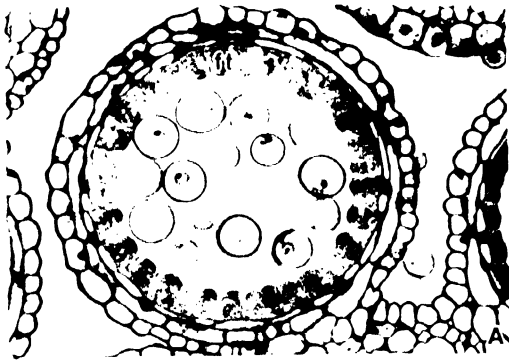


Figure 27 (A-G). Microsporogenesis in pearl millet A_m cytoplasm cms line 81 A_m .

Note: Microsporogenesis in 81 A_m is similar to that of Figs. 23A-M. Thereafter, following anther developmental stages were observed.

- A. Young microspores are scattered inside the locule. Note that the tapetum is typically fibrous and not vacuolated.
- B. Microspores migrate towards tapetum and are arranged along the inner tapetal wall. Tapetum is densely stained and individual tapetal cells can be seen.
- C. Tapetum and microspores start degenerating simultaneously. Degenerating microspores are embedded in the tapetum.
- D. Tapetum degeneration starts.
- E. Same as Fig. 27D but at an advanced stage. Traces of degenerated tapetum (dt) are seen.
- F. Contact between completely degenerated microspores (dm) and the tapetum is lost. The tapetum is reduced to an irregular mass.
- G. Very rarely, locules containing healthy pollen were seen along with the traces of the tapetum.



Microsporogenesis in 81A_m

Figure 28 (A-E). Microsporogenesis in pearl millet *violaceum* cytoplasm cms line 81A_m = ICMA 88001.

Note: The process of microsporogenesis is same up to Fig. 25B, thereafter, following stages were observed.

- A. Microsporocytes do not remain in contact with tapetum, callose breakdown occurs and the broken tips (ct) remain intact. Sporocytes' walls break and cytoplasmic mass comes out. Debris of sporocytes (dm) can be seen.
- B. Same as Fig. 28A but at an advanced stage. Note the persistent tapetum.
- C. Anther locules at same stage as in Fig. 28B. In some locules detachment of tapetum (arrow) from middle layer was observed.
- D. Callose tips remain attached to microsporocytes (same stage as shown in Fig. 28A). Microsporocytes migrate towards interior of locule, and simultaneously, sporocytes' walls break and cytoplasmic fluid comes out. Such an event was observed very rarely.
- E. Mature anther locule comprising intact and highly vacuolated tapetum (vt) enclosing densely stained nuclei. Degenerated pollen grains are uninucleate (when 81A_m-path is followed).



Microsporogenesis in 81A.

4.2.4 Other developmental changes in anther components during microsporogenesis

4.2.4.1 Tapetum

The tapetum attained its maximum thickness at the tetrad stage in most isonuclear lines. There were slight differences in its developmental pattern in the cool dry and hot dry seasons (Fig. 29).

In 81B, tapetum thickness was maximum at the tetrad stage. Thereafter, it reduced drastically and nearly disappeared at anther dehiscence (Figs. 23Q, and 23R).

In 81A₁, tapetum thickness started decreasing after the tetrad stage in the cool dry season or at young microspore stage in the hot dry season but the tapetum was still conspicuous at pollen maturity (Fig. 29a). The tapetal cells were vacuolated and remained intact at maturity (Fig. 24G). A similar developmental pattern was observed in 81A_m during early stages, but the tapetum thickness of 81A_m was relatively lower than 81A₁ at anther maturity (Fig. 27F). Further, tapetal cells of 81A_m were not vacuolated and lost their identity so only their remains were seen at anther maturity. Tapetum thickness continued to increase after the tetrad stage in male-sterile lines having the A₂ and A₃ cytoplasm. Maximum thickness was attained either at the young microspore stage or pollen formation (i.e. tapetum persisted till anther maturity), but tapetal cells lost their identity because of ITS formation.

Extreme case of ITS was observed in Pb 406A₃ as the tapetal material completely dispersed in the locular cavity (Figs. 26P-R). On the other hand, the situation was not so bad in A₂-lines since the tapetum retained its shape up to some extent.

4.2.4.2 Endothecium

It was well developed in all seven isonuclear lines at early stages of anther development (2.10c, and 2.10d). In 81B endothecium attained its maximum thickness at the dyad stage then decreased in thickness as microspores matured facilitating anther dehiscence (Fig. 23R).

In A₁- and A_m-lines endothecium thickness increased rapidly as anthers matured. The increase in endothecium thickness might have contributed to the nondehiscence of anthers in these A-lines.

4.2.4.3 Epidermis

The thickness and its growth pattern remained more or less the same in all the seven isonuclear lines (Figs. 30a, and 30b). Thickness continued to increase gradually up to young microspore or pollen maturation stage among all lines in both the seasons. In Pb 406A₃ and Pb 311A₂ endothecium thickness declined after the dyad/tetrad stage. Their (Pb 406A₃ and Pb 311A₂) pollen fertility was also higher (discussed in section) than other A-lines in which the endothecium thickness was thicker.

4.2.4.4 Middle layer

The anther middle layer did not follow any consistent developmental pattern (Figs. 30c and 30d). In male fertile line 81B it was well developed during premeiotic period and either retained same thickness (CDS) or increased a little bit at anaphase I stage (HDS). Thereafter, it started disappearing and became almost undetectable at the tetrad stage. In the HDS, it almost vanished at anther maturity but reappeared in the CDS (Figs. 30c and 30d). It was interesting to note that in all isonuclear lines its thickness first decreased near tetrad stage, thereafter, it started increasing again. In four of the six A-lines (81A₁, Pb 310A₂, Pb 311A₂ and Pb 406A₃), it attained maximum thickness at anaphase I.

4.2.4.5 Anther lobe diameter

81B possessed wider anther lobes than its A-lines at all growth stages in both seasons (Figs. 31a and 31b). The developing fertile microspores must exert considerable pressure on the anther walls resulting in expansion of the anther lobe and thereby increasing its diameter. In A-lines most of the anther lobes were compressed at maturity.

4.2.5 Pollen fertility/sterility

Observations on pollen fertility/sterility (subsequently referred as fertility) are summarized in Tables 25 and 27 and Figs. 32, 33 and 34. Anthers were

Figure 29. Tapetum and endothecium thickness at different anther developmental stages in pearl millet isonuclear lines

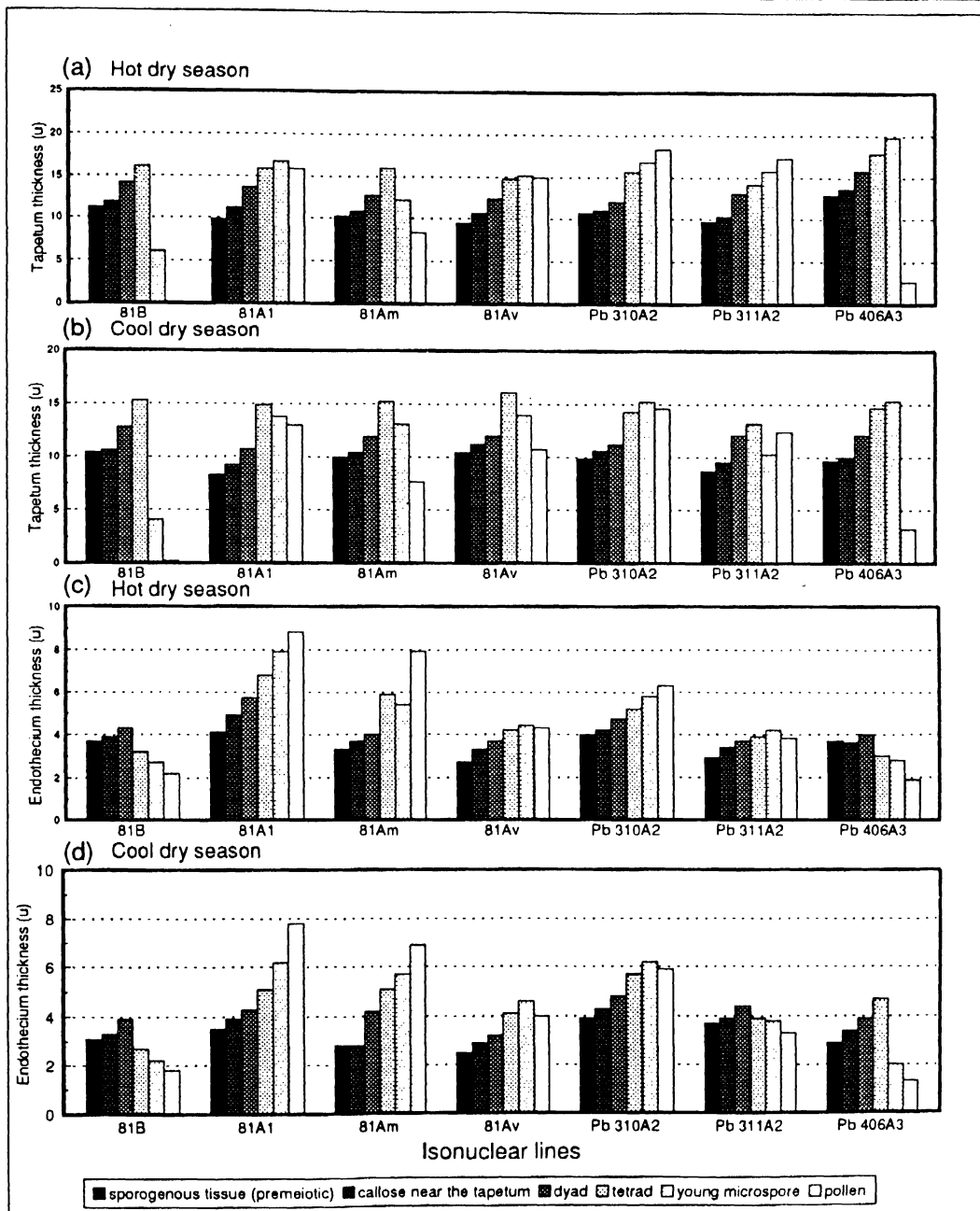


Figure 30. Epidermis and middle layer thickness at different anther developmental stages in pearl millet isonuclear lines

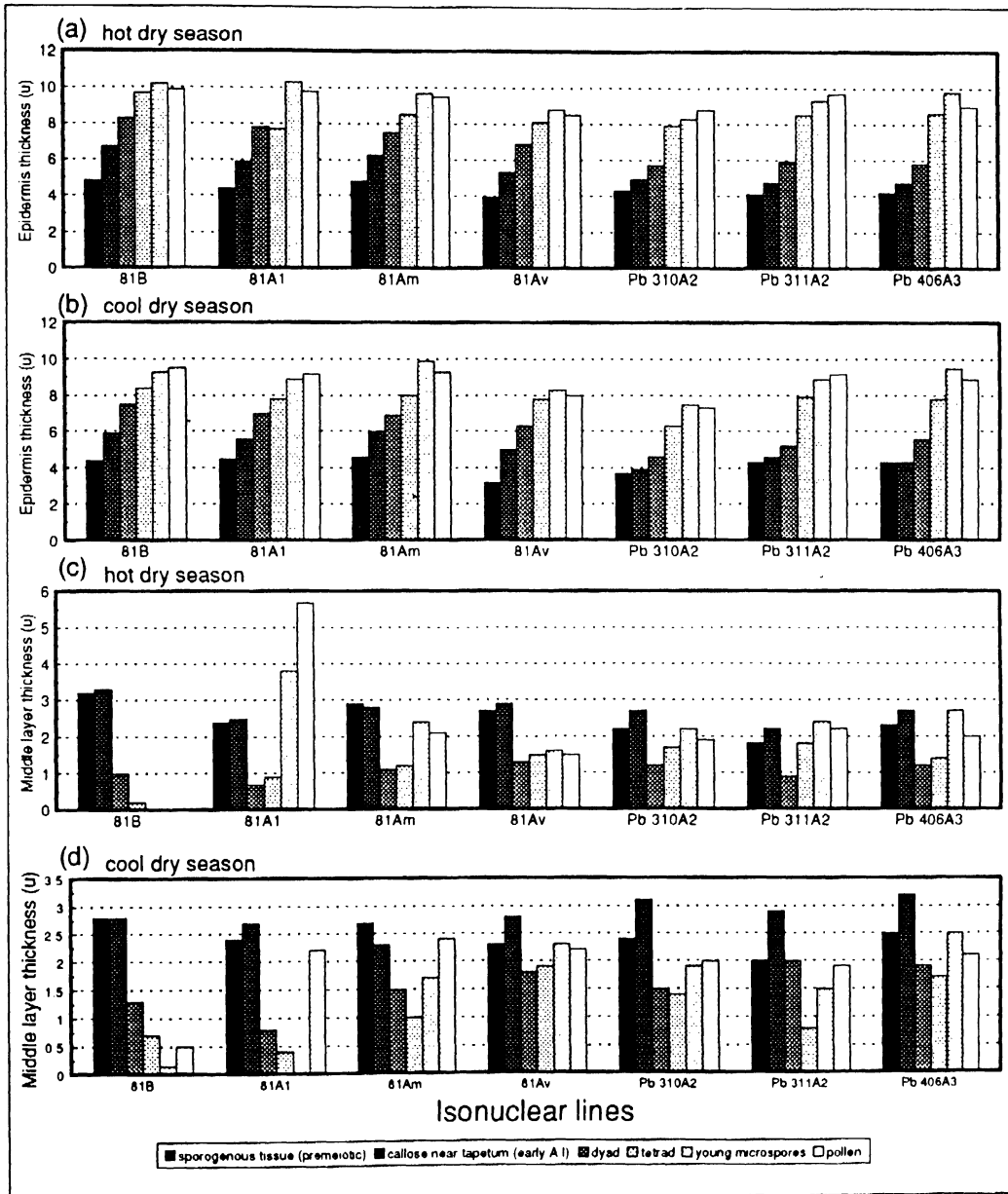
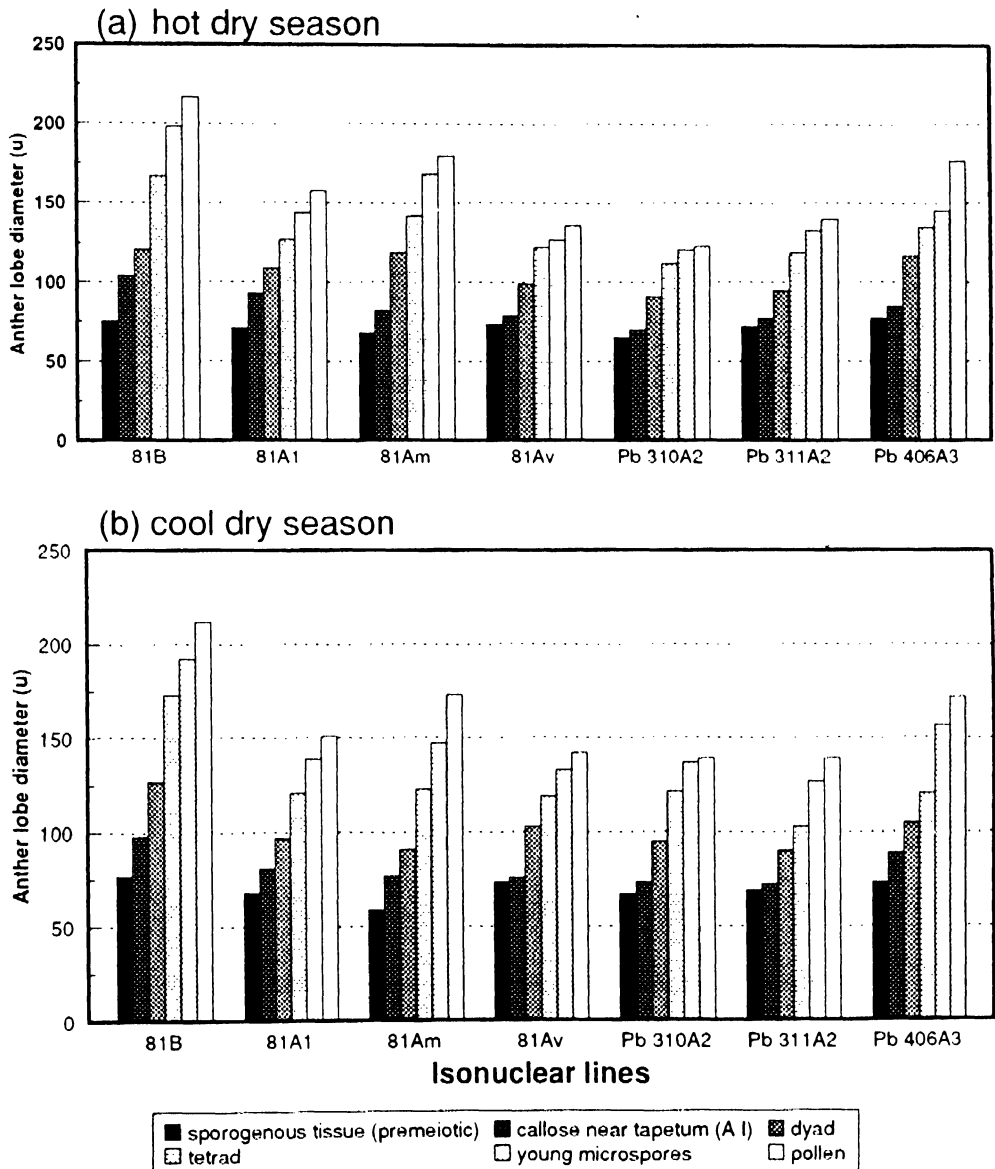


Figure 31. Anther lobe diameter at different anther developmental stages in pearl millet isonuclear lines



categorized as completely fertile (anthers containing only fertile pollen grains), partially fertile (anthers containing mixture of sterile and fertile pollen grains), completely sterile (anthers containing only sterile pollen grains) and empty (anthers without pollen grains).

Mature pollen produced by the fertile plants is well filled with starch grains (Fig. 23Q) and stains light red with acetocarmine (Fig. 34A) or bright red with Alexander's stain (Fig. 34B). On the other hand sterile pollen grains remained yellowish with acetocarmine or stained green (Figs. 34H, 34J, 34K and 34N) with Alexander's stain. We used Alexander's stain as it differentiates well the aborted and the nonaborted pollen grains. Majority of the sterile anthers were completely filled with pollen (Figs. 34C and 34N), whereas, partially filled (Figs. 34L-M) or empty (Fig. 34L) anthers were also observed. Partially fertile anthers of male-sterile and -fertile lines contained mixture of aborted and the nonaborted pollen grains (Figs. 34B and 34H). In some A-lines partially aborted pollen were also observed (Figs. 34E and 34I) which otherwise stained red. These pollen grains appeared to be compressed and contained little cytoplasm. Pollen fertility varied from line to line and season to season. In general it was low in the hot dry season (0.9-19.4%) and relatively high in cool dry season in all isonuclear A-lines (4.3-27.2%).

Critical perusal of Table 25 reveals that little variation exists for pollen fertility among plants within a line and among spikes within a plant in 81A₁, 81A_m, 81A_v and Pb 310A₂; whereas, Pb 311A₂ and Pb 406A₃ showed larger variation in both the seasons. This variation gradually increased among

spikelets within a spike, among florets within a spikelet and among anthers within a floret ranging from 0-100% in all isonuclear A-lines. Although the anthers containing 0-100% fertile pollens were present in all isonuclear A-lines, a large proportion of anthers was completely sterile in 81A_m (93.1-97.7%) and 81A₁ (89.0-97.9%). In 81A_v, the frequency of completely sterile anthers was comparatively less (77-82%) and in Pb 310A₂, Pb 311A₂ and Pb 406A₃ these frequencies further decreased to 26.9-47.4%. The frequencies of partially fertile anthers were $\geq 49\%$ in Pb 310A₂ and Pb 311A₂ in both the seasons (Table 26).

Table 26 further reveals that frequencies of completely fertile anthers were lowest in 81A₁ (0.1% in both the seasons) followed by 81A_v (0.3% in the hot dry season to 1.8% in the cool dry season) and 81A_m (0.8% in the hot dry season to 1.4% in the cool dry season). These frequencies further increased in Pb 310A₂ (2.4% in the hot dry season to 2.6% in the cool dry season), Pb 406A₃ (6.0% in the hot dry season to 6.3% in the cool dry season) and was highest in Pb 311A₂ (6.8% in the cool dry season to 7.5% in the hot dry season).

Narrow range of empty anthers were also observed in A-lines (0.3-2.5%), the lowest frequency being recorded in Pb 311A₂ (0.4-1.0%) and Pb 310A₂ (0.3-1.2%) and highest in 81A_v (1.7-2.5%) and Pb 406A₃ (1.6-2.5%) (Table 26; Fig. 32). In general frequencies of empty anthers were lower in cool dry season than in hot dry season (Table 26; Fig. 32).

Among all the A-lines, 81A_m, 81A₁ and 81A_v had major proportion of their anthers in completely sterile class ranging from 77.1-97.9% of anthers.

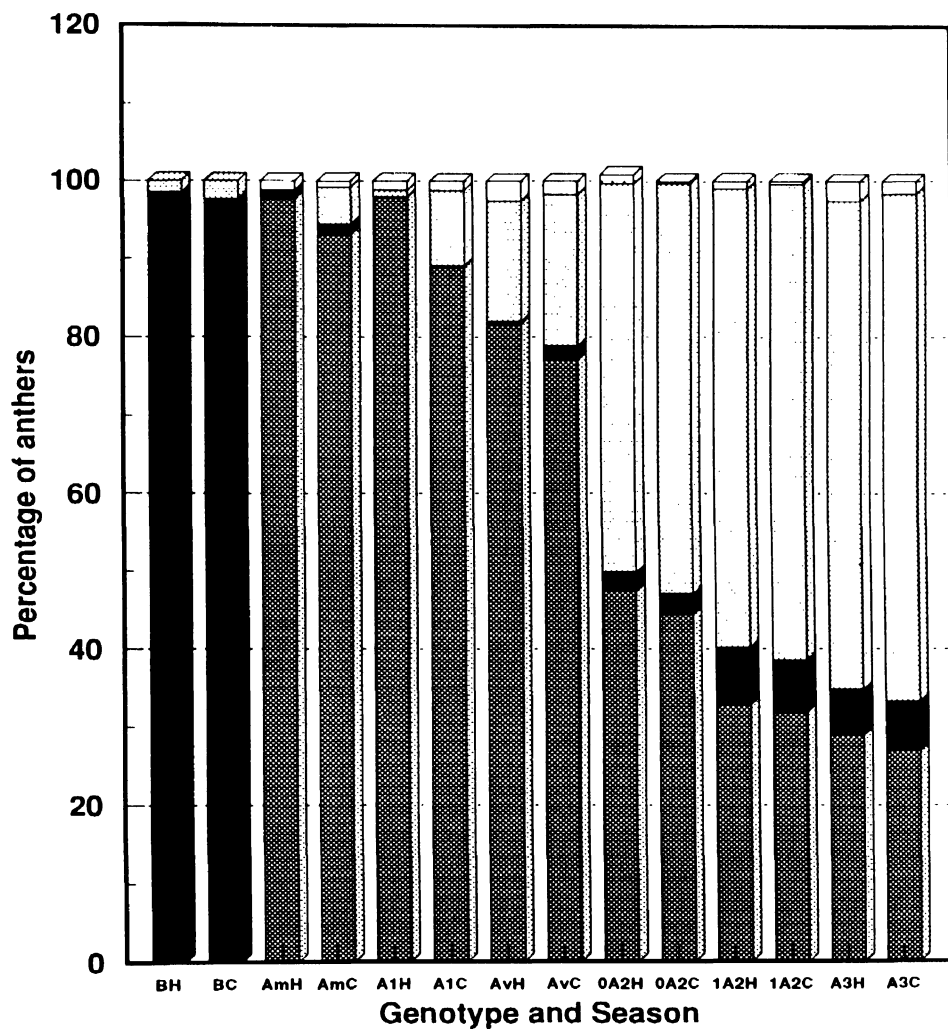
In Pb 310A₂, Pb 311A₂ and Pb 406A₃ the frequency of completely sterile anthers ranged from 26.9-47.4%. The 10.1-20.0% pollen fertility class included 24.0-24.7% of anthers of Pb 310A₂, 21.1-23.1% of anthers of Pb 311A₂ and 19.2-23.6% of anthers of Pb 406A₃. Other lines had very low frequency of anthers (0.0-26%) in this class. Large proportion of anthers (44-53%) fell in 0.1-20% pollen fertility class in Pb 311A₂.

The male-fertile line 81B, had 97.7% of completely fertile anthers in the cool dry season and 98.5% of completely fertile anthers in the hot dry season. Remaining anthers were partially fertile but none of the anther was completely sterile or empty (Table 26 and Fig. 32). Partially fertile anthers were present in 75.1-99.0% pollen fertility class which included 1.5% of anthers in the hot dry season and 2.3% of anthers in the cool dry season (Fig. 33).

Observations on 900 anthers of each isonuclear line in each season revealed that among A-lines, 81A_m was the best with 99.1% pollen sterility in the hot dry season and 95.7% pollen sterility in the cool dry season. Of these, 97.7% of anthers were completely sterile in the hot dry season and 93.1% of anthers in the cool dry season. 81A₁ was the next in order having 98.7% pollen sterility in the hot dry season and 91.8% pollen sterility in the cool dry season including 97.9% of completely sterile anthers in hot dry season and 89% in the cool dry season.

The A₂- and A₃- system A-lines, in addition to having higher frequencies of partially fertile anthers, also had high frequencies of completely fertile anthers.

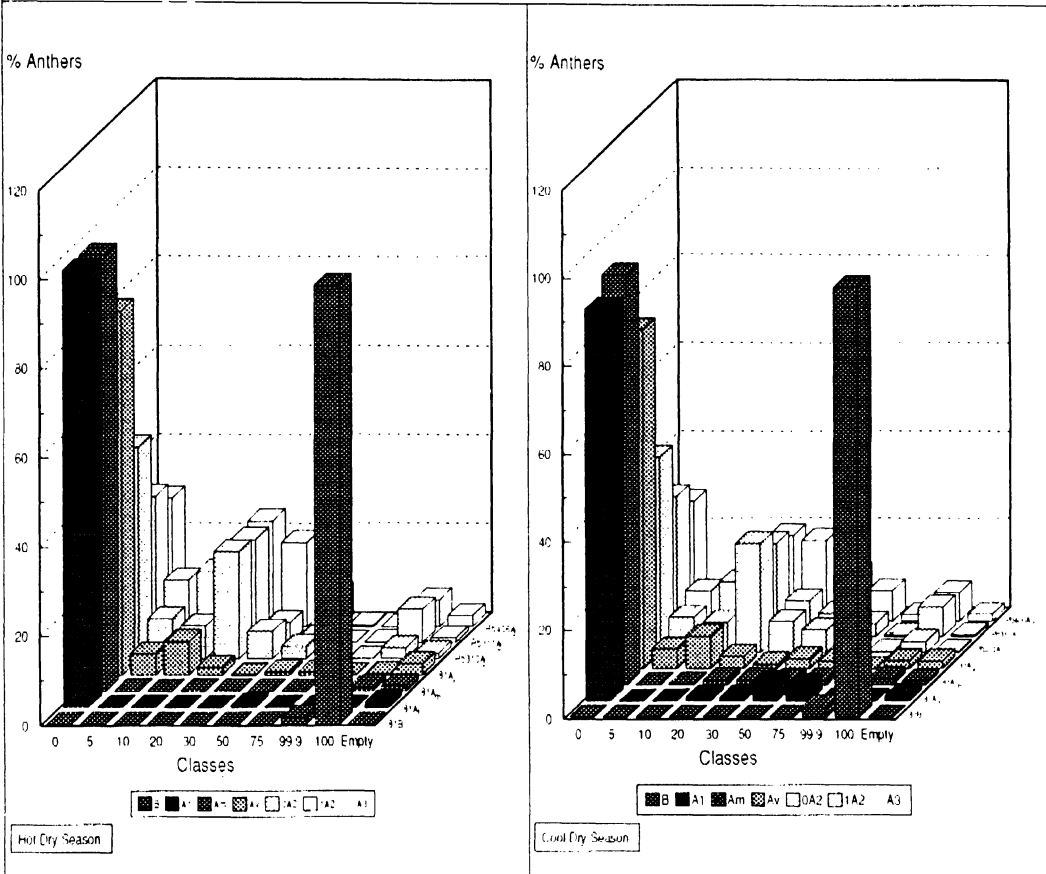
Fig. 32. Frequency distribution of anthers of varying fertility status in pearl millet isonuclear lines



completely sterile anthers
 completely fertile anthers
 partially fertile anthers
 empty anthers

B = 81B; A1 = 81A1, Am = 81Am; Av = 81Av.
 0A2 = Pb 310A2, 1A2 = Pb 311A2, A3 = Pb 406A3
 H = hot dry season, C = cool dry season

Figure 33. Frequency distribution of anthers in percent pollen fertility classes in pearl millet isonuclear lines



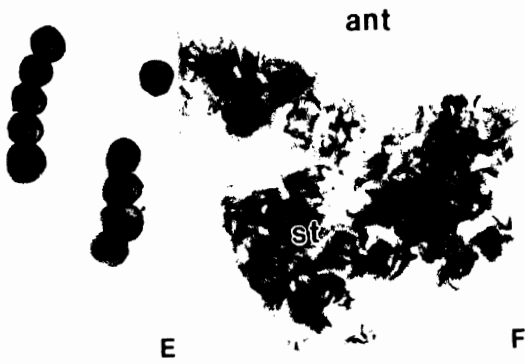
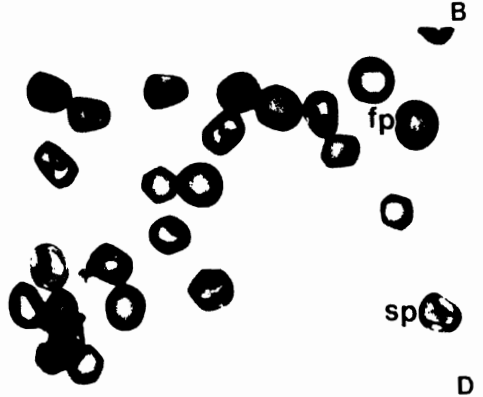
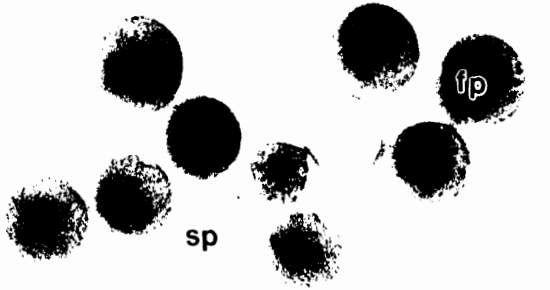
Genotype	Season	Percent of anthers in %fertility classes									
		0.0	0.1-5.0	5.1-10.0	10.1-20.0	20.1-30.0	30.1-50.0	50.1-75.0	75.1-99.0	100	Empty
81A ₁	hot dry season	97.9	0.0	0.0	0.0	0.0	0.7	0.0	0.1	0.1	1.2
	cool dry season	89.0	0.0	0.0	0.9	0.8	4.2	3.4	0.3	0.1	1.2
81B	hot dry season	0.0	0.0	0.0	0.0	0.0	0.0	0.0	1.5	98.5	0.0
	cool dry season	0.0	0.0	0.0	0.0	0.0	0.0	0.0	2.3	97.7	0.0
81A ₂	hot dry season	97.7	0.1	0.0	0.1	0.1	0.0	0.0	0.0	0.8	1.2
	cool dry season	93.1	0.1	0.2	1.1	1.1	1.0	1.1	0.0	1.4	0.8
81A ₃	hot dry season	81.7	4.7	7.4	1.8	0.1	0.7	0.7	0.1	0.3	2.5
	cool dry season	77.1	4.4	7.3	2.7	1.0	2.2	1.7	0.1	1.8	1.7
Pb 310A ₂	hot dry season	47.4	8.9	7.3	24.0	6.1	2.7	0.0	0.0	2.4	1.2
	cool dry season	44.4	8.0	6.9	24.7	7.1	5.1	0.6	0.2	2.5	0.3
Pb 311A ₂	hot dry season	32.7	14.0	16.0	23.1	4.4	1.2	0.0	0.1	7.5	1.0
	cool dry season	31.8	10.4	12.4	21.1	8.2	5.3	3.0	0.4	6.8	0.4
Pb 406A ₃	hot dry season	28.8	5.1	7.5	23.6	18.8	7.3	0.4	0.0	6.0	2.5
	cool dry season	26.9	3.2	5.5	19.2	18.2	10.5	6.9	1.5	6.3	1.5

Figure 34 (A, B, D-J). Staining of aborted and nonaborted pollen grains of male-sterile and -fertile lines of pearl millet.

Figure 34 (C, K-N). Staining of aborted and nonaborted pollen grains inside nondehiscent anthers of male-sterile and -fertile lines of pearl millet.

Note: Alexander's stain was used for determining pollen sterility except for the Fig. 34A where pollen were stained with 2% acetocarmine.

- A. Fertile/nonaborted pollen (fp) of male fertile line 81B. Pollen have been stained by 2% acetocarmine.
- B,H. Aborted (sp) and nonaborted (fp) pollen observed quite infrequently in 81B and with variable frequency in cms lines. (Photographed in Pb 406A₃).
- C, K, N. Aborted (sp) and non aborted (fp) pollen inside the male-sterile (81A₁) and male-fertile (81B) anthers.
- D. Mixture of aborted (sp) and nonaborted (fp) pollen grains (unstained) of cms line Pb 406A₃.
- E. Partially aborted pollen observed in some anthers of 81A_v.
- F. Sticky pollen grains (st) pushed out of the male-sterile anther (ant) of 81A₁.
- G, J. Partial to complete male-sterile pollen of male-sterile anther observed in Pb 310A₂.
- L. Empty (1) and half-filled (2) anthers. Half filled anther has aborted pollen grains, mostly observed in Pb 310A₂, Pb 311A₂ and Pb 406A₃. (Photographed in Pb 406A₃).
- M. Anther (1) containing partially fertile pollen in one lobe (top) and partially fertile to sterile pollen in the other lobe. The other anther (2) has sterile (sticky) pollen grains (green) which usually do not dehisce.



Pollen grains of male-sterile and -fertile lines

contd...



4.3 Experiment No. 3: Isozyme analysis of tall/dwarf near-isogenic pearl millet lines

For each enzyme three kinds of source materials were used (5-day old etiolated seedlings, 18hIS and dry seeds). The results obtained are presented hereunder.

4.3.1 General observations / effect of electrophoretic conditions and source of plant extract on isozyme spectrum

Results obtained using various forms of extracts (sources) and electrophoretic conditions are summarized in Table 9. Four enzymes (ADH, EST, GDH, and SKDH) showed better resolution and separation of bands when extracts from 18hIS were used and run on polyacrylamide gel consisting of stacking gel (4%) and running gel in TG+T (0.25M tris + 0.19M glycine in upper tank and 0.25M tris pH 8.5 in lower tank) buffer. Isozymic forms of MDH and PGI separated well using similar gel and buffer system but with dry seeds extracts. On the other hand, LDH, ME and SOD displayed acceptable resolution when seedling extracts were used to run in tris-glycine pH 8.3 (TG) buffer system. Some enzyme systems (GOT and 6-PGD) gave similar results for all the three extracts and CAT revealed similar results for seedlings and 18hIS. CAT bands were not detectable when dry seeds were used. In some cases, polymerized gels were kept at 4°C for one hour (prechilling treatment) with a view to avoid

Table 9. Effect of source of plant extract and electrophoretic conditions on resolution of isozyme bands.

Enzyme	Source of extract	Electrophoretic conditions						Pre-chilling of gel	No. of bands obtained	Polymorphism
		Gel %		Electric current (m amp)		Electrode buffer				
		Stacking	Running	1 hr	Later					
ADH	Seedlings ¹	A	12	40	60	Tris-glycine, pH 8.3 (PG)	No	1	No	
	† 18 h IS ¹	4	8	20	30	0.25M Tris + 0.19M glycine in upper tank and 0.25M Tris, pH 8.5 in lower tank (TG+T)	Yes	12	Yes	
	Dry seeds	4	8	20	30	TG+T	Yes	?	?	
CAT	† 18 h IS	4	10	20	30	TG+T	No	1	No	
	† Seedlings	A	12	40	60	TG	No	1	No	
	† 18 h IS	A	12	40	60	TG	No	1	No	
	Dry seeds	4	8	40	60	TG+T	Yes	?	?	
EST	Seedlings	A	12	40	60	TG	No	7	Yes	
	Dry seeds	A	12	40	60	TG	Yes	7	Yes	
	† 18 h IS	4	10	20	30	TG+T	Yes	23	Yes	
GDH	Seedlings	A	12	40	60	TG	No	2	No	
	† 18 h IS	A	8	30	40	TG+T	No	4	Yes	
	Dry seeds	A	8	30	40	TG	No	1	No	
GOT	† Seedlings	A	12	40	60	TG	No	4	Yes	
	† Dry seeds	A	12	40	60	TG	No	4	Yes	
	† 18 h IS	A	12	40	60	TG+T	Yes	4	Yes	
LDH	Seedlings	A	12	40	60	TG	No	1 ^f	No	
	Dry seeds	A	12	40	60	TG	No	1 ^f	No	
	18 h IS	A	12	40	60	TG+T	No	1 ^f	No	
MDH	Seedlings	A	12	50	60	TG	No	1 ^f	?	
	18 h IS	A	12	50	60	TG	Yes	1 ^f	?	
	† Dry seeds	4	6	20	30	TG+T	Yes	6	Yes	
ME	† Seedlings	A	12	40	60	TG	No	7	Yes	
	Dry seeds	4	8	40	60	TG	No	?	?	
	18 h IS	4	8	40	60	TG+T	Yes	?	?	
PGI	Seedlings	A	12	40	60	TG	No	1 ^f	Yes	
	18 h IS	A	12	40	60	TG	No	1 ^f	Yes	
	† Dry seeds	4	10	20	30	TG+T	Yes	4	Yes	
6-PGD	† Seedlings	A	12	40	60	TG	No	4	No	
	† 18 h IS	A	12	40	60	TG	No	4	No	
	† Dry seeds	4	10	20	30	TG+T	Yes	4	No	
SKDH	Seedlings	A	12	40	60	TG	No	1 ^f	No	
	† 18 h IS	4	8	20	30	TG+T	Yes	13	Yes	
	Dry seeds	4	6	20	30	TG+T	Yes	13	Yes	
SOD	† Seedlings	A	12	40	60	TG	No	3	Yes	
	18 h IS	A	12	40	60	TG+T	Yes	?	?	
	Dry seeds	A	12	40	60	TG	Yes	?	?	

ADH = Alcohol dehydrogenase; CAT = Catalase; EST = Esterase; GDH = Glutamate dehydrogenase; GOT = Glutamate oxaloacetate transaminase; LDH = Lactate dehydrogenase; MDH = Malate dehydrogenase; ME = Malic enzyme; PGI = Phosphoglucosomerase; 6-PGD = 6-Phosphogluconate dehydrogenase; SKD = Shikimate dehydrogenase; SOD = Superoxide dismutase; 1 = Five days old etiolated seedlings; 2 = Surface sterilised seeds (with 0.1% HgCl₂) were immersed in water for 18 h, ? = indicates poor results. A = stacking gel was not used; 1^f = very faint bands; 1^t = very thick band. † indicates better results.

thermal denaturation of enzymes at the time of sample loading, as otherwise, variation in temperature of the gel and the sample may cause thermal shock to the enzymes present in the sample. Sufficient data could not be generated to conclude whether prechilling of the gel causes any significant impact on resolution of the isozyme bands.

Six (ADH, EST, GDH, MDH, ME and PGI) of the 12 enzymes showed variation within one or more tall/dwarf near-isogenic pairs. Three (GOT, SKDH and SOD) of the remaining six enzymes displayed variation between pairs. CAT, 6-PGD and LDH isozymes patterns were identical for all the lines. All the bands scored for an enzyme using various forms of extracts were considered together to assess the degree of isogenicity within pairs.

4.3.2 Alcohol dehydrogenase [ADH] EC 1.1.1.1.

The isozyme spectrum of ADH is presented in Table 10 its photograph (Fig. 35) and schematic zymogram in Fig. 36. The Rf 0.273 band, obtained from seedling extracts, was present in all pairs (Fig. 36b). However, 12 isozymic forms (bands) were detected (using 18hIS) in all the lines considered together (Fig. 36a). The number of bands varied from 7 in pairs EC1, MC9 and MC10 to 11 in pair EC3. Isolines within pairs EC1 and EC2 and MC9 were identical. Only one band of light intensity (Rf 0.031) showed polymorphism in pair EC2 and two bands (Rfs 0.047, 0.078) of light to very light intensity showed polymorphism in pair MC10. Most polymorphic pairs were EC3 (7/11 bands),

MC6 (4/8 bands) and NC12 (5/9 bands). Of the polymorphic bands, 2 (Rfs 0.047, 0.078) were common in pairs EC3, MC6 and MC10, 1 (Rf 0.148) in pairs EC3, MC6, and NC12, and 1 (Rf 0.101) in pairs MC6 and NC12. Of the two common polymorphic bands in pairs EC3, MC6 and MC10, only 1 (Rf 0.078) showed its consistent presence in tall isolines.

4.3.3 Catalase [CAT] EC 1.11.1.6.

The results of catalase isozymes are presented in Fig. 37. Only one form of CAT (Rf 0.90) obtained from seedlings/18hIS was present in all the pairs. Bands obtained were translucent and disappeared very soon.

4.3.4 Esterase [EST] EC 3.1.1.

Banding pattern of seedlings was similar to those of dry seeds (Figs. 38b, 38c, and 39b). Of the seven bands detected, two EC pairs and two MC pairs were monomorphic with two bands each (Table 11). NC12 was most polymorphic (4/5 bands), followed by MC6 (2/4 bands), and EC3 (1/3 bands).

The zymogram obtained from 18hIS differed considerably from that of seedlings/dry seeds with respect to the numbers and intensity of bands (Figs. 38a and 39a and Table 12). Twenty three bands were detected in all the lines considered together. Two EC pairs (EC2 and EC3) were monomorphic, EC1 and 2 MC pairs (MC9 and MC10) were nearly monomorphic (12-13 out of 13-14 bands). NC12 was highly polymorphic (9/12 bands) as was MC6 (5/12 bands).

Pairs 6 of MC and 12 of NC were most polymorphic, was the common feature of both the zymograms obtained from 18hIS and seedlings/dry seeds.

4.3.5 Glutamate dehydrogenase [GDH] EC 1.4.1.2.

Different zymograms were obtained for all the three sources (Fig. 40). Dry seeds gave only one band (Rf 0.101) and seedlings showed 2 bands (Rfs 0.090, 0.109) in all the pairs (Figs. 41b and 41c). Four bands were detected from 18hIS (Table 13 and Fig. 41a). Isolines within pairs EC1 and EC2, MC9 and MC10, and NC12 were identical. Pair EC3 was most polymorphic (2/3 bands), followed by pair NC12 (1/3 bands).

4.3.6 Glutamate oxaloacetate transaminase [GOT] EC 2.6.1.1

Banding pattern from all the three sources were similar. None of the pairs was polymorphic. Three bands (Rfs 0.120, 0.184, 0.280) were present in all the lines, with an additional band (Rf 0.144) present in both tall dwarf isolines of only NC12 pair (Table 14, Figs. 42a, 43a and 43b).

4.3.7 Lactate dehydrogenase [LDH] EC 1.1.1.27.

Only one faint band (Rf 0.112) that could not be photographed was present in all the tall/dwarf near-isogenic pairs.

4.3.8 Malate dehydrogenase [MDH] EC 1.1.1.37.

In dry seeds, there were six MDH bands. Two of these (Rf 0.464 and 0.574) were present in all the lines. A third band (Rf 0.600) was present in both tall and dwarf lines of 5 pairs and polymorphic in EC2 and EC3. two bands (Rf 0.543 and 0.614) were present in only tall version of EC3 (Table 15, Figs. 42b, 43b).

4.3.9 Malic enzyme [ME] EC 1.1.1.40.

Seven bands were detected using seedling extract (Table 16, Figs. 44a and 45a). Three of these (Rf 0.079, 0.142 and 0.293) were present in all lines and Rf 0.346 in all but EC2. The Rf 0.362 was present in only EC isolines. The two polymorphic bands were Rf 0.401 (MC10) and Rf 0.433 (EC1 and EC2).

4.3.10 6-phosphogluconate dehydrogenase [6-PGD] EC 1.1.1.44.

Four thick bands of 6-PGD activity were resolved in all the three sources and in all near-isogenic lines (Figs. 44b and 45b).

4.3.11 Phosphoglucoisomerase [PGI] EC 5.4.2.2.

Difference in the number of bands was observed when dry seeds and 18hIS were used as the source material for isozyme detection. In seedlings/18hIS, one band Rf 0.240 was present in MC6, and polymorphic in 5 isoline pairs (Table 17, Figs. 46b and 47b). In dry seeds, two bands (Rfs 0.215 and 0.277)

displayed polymorphism in EC3, and monomorphism in all others. Two bands (Rfs 0.246 and 0.300) were present in only tall version of EC3 (Table 18, Figs. 46a and 47a).

4.3.12 Shikimate dehydrogenase [SKDH] EC 1.1.1.25.

SKDH activity was investigated in seedlings, dry seeds and 18 h imbibed seeds, under varying electrophoretic conditions (Table 9). These variations improved the resolution as well as the number of bands with SKDH activity. A very thick band (Rf 0.242) was detected in seedling extract of all the pairs (Figs. 48c and 49b). Whereas, in dry seeds/18hIS 13 bands were detected in all the lines considered together. There was no within-pair polymorphism but substantial variation was observed between the pairs. EC3 and pair NC12 were different from each other as well as from other pairs in having some extra bands (NC12) or substituted bands (EC3).

Three bands (Rfs 0.317, 0.327 and 0.484) were present in all the lines and two bands (Rfs 0.265 and 0.287) in all but EC3 (Table 19). Two bands (Rfs 0.256 and 0.274) were present only in EC pairs. One band (Rf 0.297) was present in EC1 and EC2. Another band (Rf 0.457) was present in these two EC pairs as well as in MC9 and MC10, and NC12. Three bands (Rfs 0.340, 0.366 and 0.437) were present only in NC12.

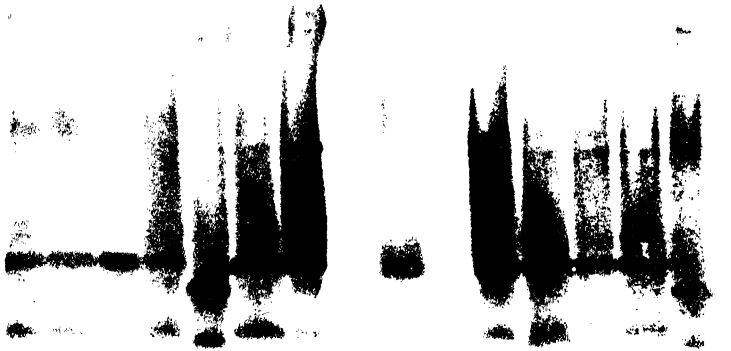
4.3.13 Superoxide dismutase [SOD] EC 1.15.1.1.

Three achromatic/translucent bands of SOD activity were resolved in all the lines considered together (Figs. 50, 51 and Table 20). Two bands (Rfs 0.311 and 0.696) with lowest and highest electrophoretic mobility were quite prominent and present in all the pairs. The band with intermediate mobility (Rf 0.475) was very weak and present in EC1, EC2, MC6 and MC9 only.

ADH

18h

① ① ② ② ③ ③ ④ ④ ⑤ ⑤ ⑥ ⑥ ⑦ ⑦



a

SL

④ ① ① ② ② ③ ③ ④ ④ ⑤ ⑤ ⑥ ⑥ ⑦ ⑦



b

Pair1: tall ① and dwarf ① isolines and so on

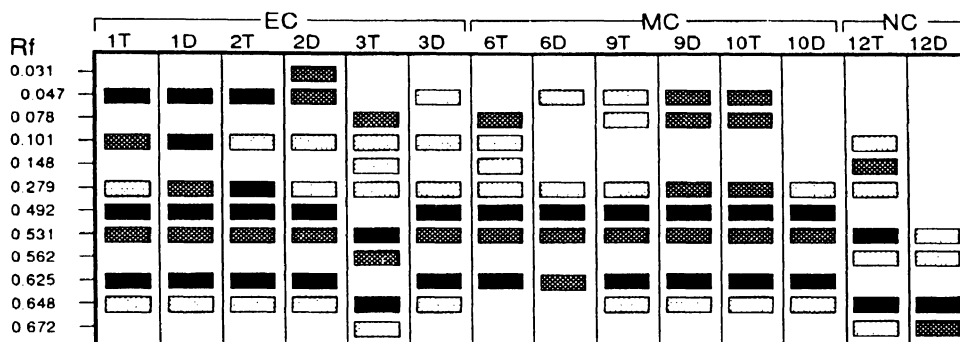
④ = empty well; ④ = extra well

Figure 35. Isozyme spectrum of alcohol dehydrogenase using 18-hour imbibed seeds (18h) and five-day old etiolated seedlings (SL) in tall/dwarf near-isogenic pairs of pearl millet

Lanes from left to right (Figs. 35a and 35b): **Early Composite (EC)**: 1 filled circle = tall isoline of EC1, 1 empty circle = dwarf isoline of pair EC1; 2 filled circle = tall isoline of pair EC2, 2 empty circle = dwarf isoline of pair EC2; 3 filled circle = tall isoline of pair EC3, 3 empty circle = dwarf isoline of pair EC3; **Medium Composite (MC)**: 4 filled circle = tall isoline of pair MC6, 4 empty circle = dwarf isoline of pair MC6; 5 filled circle = tall isoline of pair MC9, 5 empty circle = dwarf isoline of pair MC9; 6 filled circle = tall isoline of pair MC10, 6 empty circle = dwarf isoline of pair MC10; **Nigerian Composite (NC)**: 7 filled circle = tall isoline of pair NC12, 7 empty circle = dwarf isoline of pair NC12.

Figure 36. Schematic zymogram of alcohol dehydrogenase in tall/dwarf near-isogenic lines of pearl millet

(a) Alcohol Dehydrogenase (ADH): 18 h Imbibed seeds



(b) Alcohol Dehydrogenase (ADH): seedlings

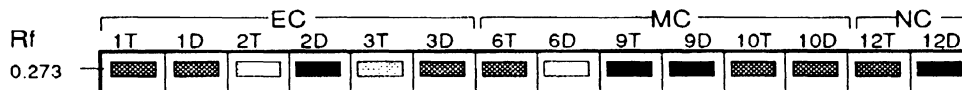
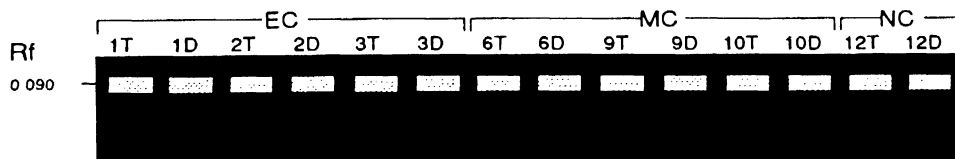


Figure 37. Schematic zymogram of catalase in tall/dwarf near-isogenic lines of pearl millet

Catalase (CAT): Seedlings / 18 h Imbibed seeds



Very dark bands
 Light bands
 Very light bands
 Transparent / translucent bands

EC : Early composite, MC : Medium composite, NC : Nigerian composite

1T & 1D indicates tall and dwarf versions of 1st isogenic pair, 2T & 2D of 2nd pair and so on

Note: Very light bands are usually not detectable in the photographs

Table 10. Banding pattern of Alcohol dehydrogenase (18 h IS) in tall/dwarf near-isogenic pairs of pearl millet.

Rf	Tall/dwarf near-isogenic pairs													
	EC						MC				NC			
	1T	1D	2T	2D	3T	3D	6T	6D	9T	9D	10T	10D	12T	12D
.031	-	-	o	+	-	-	-	-	-	-	-	-	-	-
.047	+	+	+	+	o	+	o	+	+	+	o	-	-	
.078	-	-	-	-	+	o	+	o	+	+	o	-	-	
.101	+	+	+	+	+	+	+	o	-	-	-	-	+	
.148	-	-	-	-	+	o	+	o	-	-	-	-	+	
.279	+	+	+	+	+	+	+	+	+	+	+	+	+	
.492	+	+	+	+	o	+	+	+	+	+	+	+	-	
.531	+	+	+	+	+	+	+	+	+	+	+	+	+	
.562	-	-	-	-	+	o	-	-	-	-	-	-	+	
.625	+	+	+	+	o	+	+	+	+	+	+	+	-	
.648	+	+	+	+	+	+	-	-	+	+	+	+	+	
.672	-	-	-	-	+	o	-	-	-	-	-	-	+	
T	7		8		11		8		7		7		9	
C	7		7		4		4		7		5		4	

Total number of bands: 12

EC = Early Composite; MC = Medium Composite; NC = Nigerian Composite; C = Number of common bands, + indicates uncommon bands within a pair; T = Total number of bands within a pair

Figure 38. Isozyme spectrum of esterase using 18-hour imbibed seeds (18h), five-day old etiolated seedlings (SL) and dry seeds (DS) in tall/dwarf near-isogenic lines of pearl millet

Lanes from right to left (Fig. 36a) and left to right (Figs. 36b and 36c)

Early Composite (EC)

1 filled circle	= 1T i.e. tall isoline of pair EC1
1 empty circle	= 1D i.e. dwarf isoline of pair EC1
2 filled circle	= 2T i.e. tall isoline of pair EC2
2 empty circle	= 2D i.e. dwarf isoline of pair EC2
3 filled circle	= 3T i.e. tall isoline of pair EC3
3 empty circle	= 3D i.e. dwarf isoline of pair EC3

Medium Composite (MC)

4 filled circle	= 6T i.e. tall isoline of pair MC6
4 empty circle	= 6D i.e. dwarf isoline of pair MC6
5 filled circle	= 9T i.e. tall isoline of pair MC9
5 empty circle	= 9D i.e. dwarf isoline of pair MC9
6 filled circle	= 10T i.e. tall isoline of pair MC10
6 empty circle	= 10D i.e. dwarf isoline of pair MC10

Nigerian Composite (NC)

7 filled circle	= 12T i.e. tall isoline of pair NC12
7 empty circle	= 12D i.e. dwarf isoline of pair NC12

EST

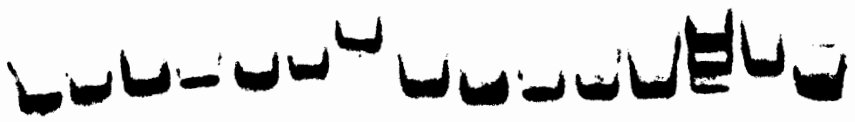
a. 18h

⑦ ⑦ ⑥ ⑥ ⑤ ⑤ ④ ④ ③ ③ ② ② ① ①



b. SL

① ① ② ② ③ ③ ④ ④ ⑤ ⑤ ⑥ ⑥ ⑦ ⑦ e



c. DS

① ① ② ② ③ ③ ④ ④ ⑤ ⑤ ⑥ ⑥ ⑦ ⑦ e

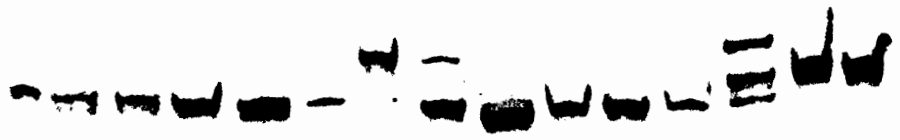
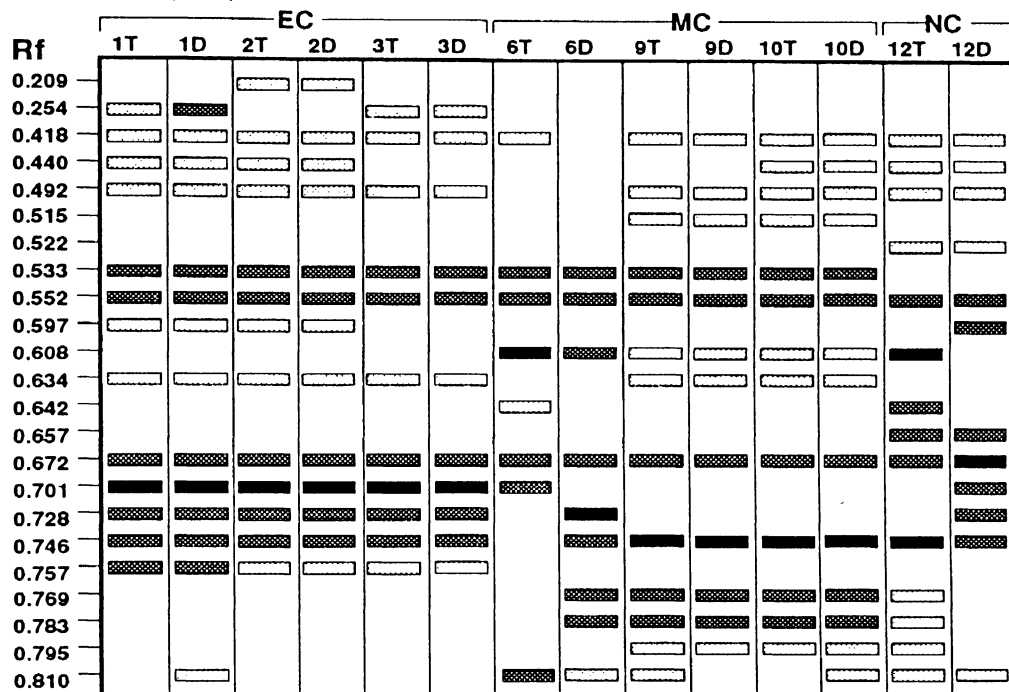
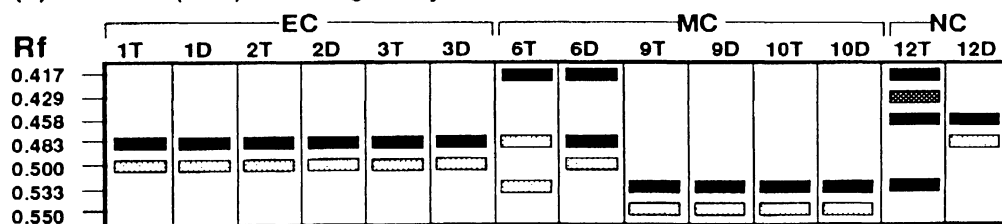


Figure 39. Schematic zymogram of esterase in tall/dwarf near-isogenic lines of pearl millet

(a) Esterase (EST): 18 h imbibed seeds



(b) Esterase (EST): seedlings / dry seeds



Very dark bands Light bands Very light bands

EC : Early composite; MC : Medium composite; NC : Nigerian composite

1T & 1D indicates tall and dwarf versions of 1st isogenic pair, 2T & 2D of 2nd pair and so on

Note: Very light bands are usually not detectable in the photographs

Table 11. Banding pattern of esterase (Seedlings) in tall/dwarf near-isogenic pairs of pearl millet.

Rf	Tall/dwarf near-isogenic pairs													
	EC				MC				NC					
	1T	1D	2T	2D	3T	3D	6T	6D	9T	9D	10T	10D	12T	12D
.417	-	-	-	-	□	⊕	⊕	□	-	-	-	-	⊕	□
.429	-	-	-	-	-	-	-	-	-	-	-	-	⊕	□
.458	-	-	-	-	-	-	-	-	-	-	-	-	+	+
.483	+	+	+	+	+	+	+	+	-	-	-	-	□	⊕
.500	+	+	+	+	+	+	□	⊕	-	-	-	-	-	-
.533	-	-	-	-	-	-	⊕	□	+	+	+	+	⊕	□
.550	-	-	-	-	-	-	-	-	+	+	+	+	-	-
T	2	2	2	3	4	2	5							
C	2	2	2	2	1	2	1							

Total number of bands = 7

EC = Early Composite; MC = Medium Composite; NC = Nigerian Composite; C = Number of common bands, ⊕ indicates uncommon bands within a pair; T = Total number of bands within a pair

Table 12. Esterase (18hIS) banding pattern in tall/dwarf near-isogenic lines of pearl millet.

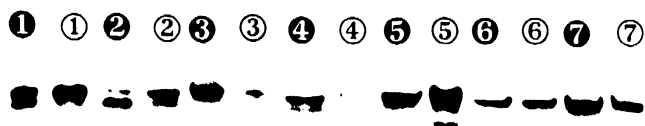
Rf	Tall/dwarf near-isogenic pairs													
	EC						MC						NC	
	1T	1D	2T	2D	3T	3D	6T	6D	9T	9D	10T	10D	12T	12D
.209	-	-	+	+	-	-	-	-	-	-	-	-	-	-
.254	+	+	-	-	+	+	-	-	-	-	-	-	-	-
.418	+	+	+	+	+	+	⊕	⊖	+	+	+	+	+	+
.440	+	+	+	+	-	-	-	-	-	-	+	+	+	+
.492	+	+	+	+	+	+	-	-	+	+	+	+	+	+
.515	-	-	-	-	-	-	-	-	+	+	+	+	-	-
.522	-	-	-	-	-	-	-	-	-	-	-	-	+	+
.533	+	+	+	+	+	+	+	+	+	+	+	+	-	-
.552	+	+	+	+	+	+	+	+	+	+	+	+	+	+
.597	+	+	+	+	-	-	-	-	-	-	-	-	⊖	⊕
.608	-	-	-	-	-	-	+	+	+	+	+	+	⊕	⊖
.634	+	+	+	+	+	+	-	-	+	+	+	+	-	-
.642	-	-	-	-	-	-	⊕	⊖	-	-	-	-	⊕	⊖
.657	-	-	-	-	-	-	-	-	-	-	-	-	+	+
.672	+	+	+	+	+	+	+	+	+	+	+	+	+	+
.701	+	+	+	+	+	+	⊕	⊖	-	-	-	-	⊖	⊕
.728	+	+	+	+	+	+	⊖	⊕	-	-	-	-	⊖	⊕
.746	+	+	+	+	+	+	⊖	⊕	+	+	+	+	+	+
.757	+	+	+	+	+	+	-	-	-	-	-	-	-	-
.769	-	-	-	-	-	-	⊖	⊕	+	+	+	+	⊕	⊖
.783	-	-	-	-	-	-	⊖	⊕	+	+	+	+	⊕	⊖
.795	-	-	-	-	-	-	-	-	+	+	+	+	⊕	⊖
.810	⊖	⊕	-	-	-	-	+	+	⊕	⊖	⊖	⊕	+	+
T	14		13		11		12		13		14		17	
C	13		13		11		5		12		13		9	

Total number of bands = 23

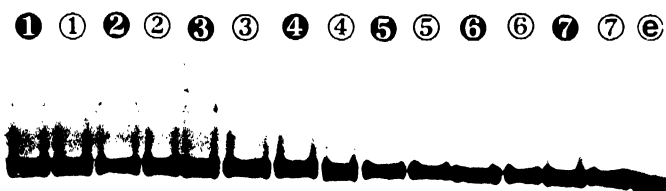
EC = Early Composite; MC = Medium Composite; NC = Nigerian Composite; C = Number of common bands, ⊕ indicates uncommon bands within a pair; T = Total number of bands within a pair

GDH

a. 18h



b. SL



c. DS

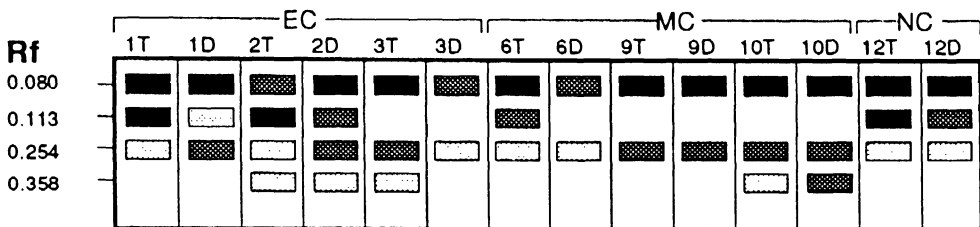


Figure 40. Isozyme spectrum of glutamate dehydrogenase using 18-hour imbibed seeds (18h), five-day old etiolated seedlings (SL) and dry seeds (DS) in tall/dwarf near-isogenic pairs of pearl millet

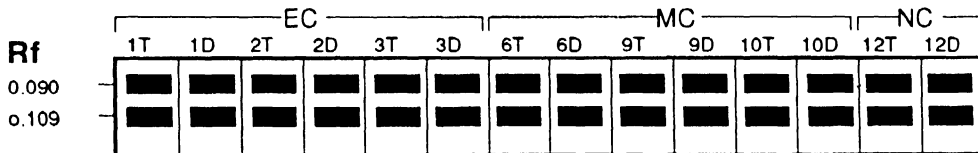
Lanes from left to right (Figs. 40a, 40b and 40c): **Early Composite (EC)**: 1 filled circle = tall isoline of pair EC11, empty circle = dwarf isoline of pair EC1; 2 filled circle = tall isoline of pair EC2, 2 empty circle = dwarf isoline of pair EC2; 3 filled circle = tall isoline of pair EC3, 3 empty circle = dwarf isoline of pair EC3; **Medium Composite (MC)**: 4 filled circle = tall isoline of pair MC6, 4 empty circle = dwarf isoline of pair MC6; 5 filled circle = tall isoline of pair MC9, 5 empty circle = dwarf isoline of pair MC9; 6 filled circle = tall isoline of pair MC10, 6 empty circle = dwarf isoline of pair MC10; **Nigerian Composite (NC)**: 7 filled circle = tall isoline of pair NC12, 7 empty circle = dwarf isoline of pair NC12

Figure 41. Schematic zymogram of glutamate dehydrogenase in tall/dwarf near-isogenic lines of pearl millet

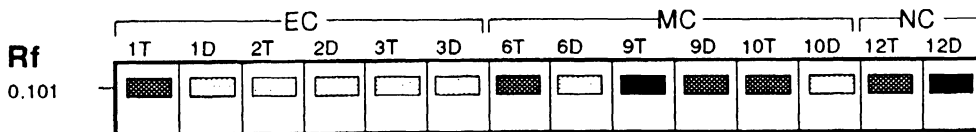
(a) Glutamate dehydrogenase (GDH): 18 h imbibed seeds



(b) Glutamate dehydrogenase (GDH): Seedlings



(c) Glutamate dehydrogenase (GDH): Dry seeds



Very dark bands
 Light bands
 Very light bands

EC : Early composite; MC : Medium composite; NC : Nigerian composite

1T & 1D indicates tall and dwarf versions of 1st isogenic pair, 2T & 2D of 11nd pair and so on

Note: Very light bands are usually not detectable in the photographs

Table 13. Banding pattern of glutamate dehydrogenase (18h IS) in tall/dwarf near-isogenic pairs of pearl millet.

Rf	Tall/dwarf near-isogenic pairs													
	EC				MC								NC	
	1T	1D	2T	2D	3T	3D	6T	6D	9T	9D	10T	10D	12T	12D
.080	+	+	+	+	+	+	+	+	+	+	+	+	+	+
.113	-	-	-	-	-	-	-	-	-	-	+	+	+	-
.254	+	+	+	+	-	+	+	+	+	+	+	+	+	+
.358	-	-	-	-	+	-	-	-	-	-	-	-	-	-
T	2		2		3		2		2		3		3	
C	2		2		1		2		2		3		2	

Total number of bands = 4

EC = Early Composite; MC = Medium Composite; NC = Nigerian Composite; C = Number of common bands, + indicates uncommon bands within a pair; T = Total number of bands within a pair

GOT

DS/18h/SL

① ① ② ② ③ ③ ④ ④ ⑤ ⑤ ⑥ ⑥ ⑦ ⑦ e



a

MDH

DS

① ① ② ② ③ ③ ④ ④ ⑤ ⑤ ⑥ ⑥ ⑦ ⑦ e



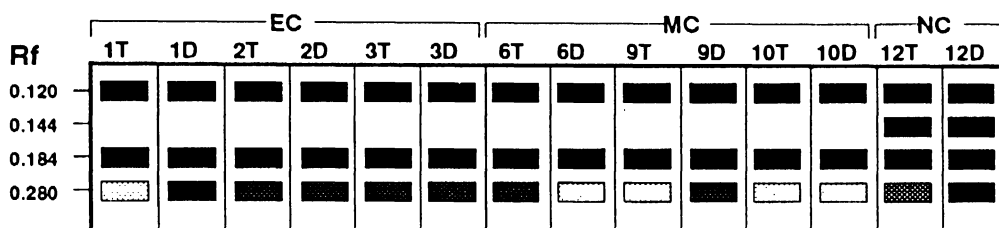
b

Figure 42. Isozyme spectrum of glutamate oxaloacetate transaminase (using 18-hour imbibed seeds (18h), five-day old etiolated seedlings (SL) and dry seeds (DS)) and malate dehydrogenase using DS in tall/dwarf near-isogenic pairs of pearl millet

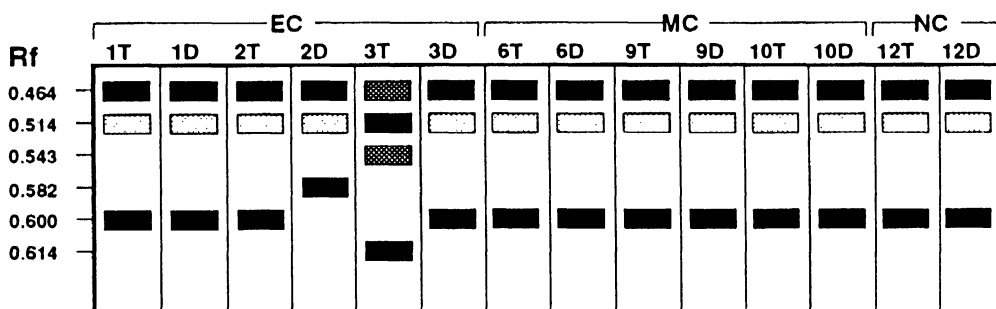
Lanes from left to right (Figs. 42a and 42b): **Early Composite (EC)**: 1 filled circle = tall isoline of pair EC1, 1 empty circle = dwarf isoline of pair EC1; 2 filled circle = tall isoline of pair EC2, 2 empty circle = dwarf isoline of pair EC2; 3 filled circle = tall isoline of pair EC3, 3 empty circle = dwarf isoline of pair EC3; **Medium Composite (MC)**: 4 filled circle = tall isoline of pair MC6, 4 empty circle = dwarf isoline of pair MC6; 5 filled circle = tall isoline of pair MC9, 5 empty circle = dwarf isoline of pair MC9; 6 filled circle = tall isoline of pair MC10, 6 empty circle = dwarf isoline of pair MC10; **Nigerian Composite (NC)**: 7 filled circle = tall isoline of pair NC12, 7 empty circle = dwarf isoline of pair NC12

Figure 43. Schematic zymogram of glutamate oxaloacetate transaminase (a) and malate dehydrogenase (b) in tall/dwarf near-isogenic lines of pearl millet

(a) Glutamate oxaloacetate transaminase (GOT): Seedlings/dry seeds/18h IS



(b) Malate dehydrogenase (MDH): Dry seeds



Very dark bands Black Light bands Stippled Very light bands

EC : Early composite; MC : Medium composite; NC: Nigerian composite
1T & 1D indicates tall and dwarf versions of 1st isogenic pair, 2T & 2D of pair 2 and so on.

Note: Very light bands are usually not detectable in the photographs

Table 14. Banding pattern of glutamate oxaloacetate transaminase (seedling/dry seeds/18h IS) in tall/dwarf near-isogenic pairs of pearl millet.

Rf	Tall/dwarf near-isogenic pairs													
	EC						MC						NC	
	1T	1D	2T	2D	3T	3D	6T	6D	9T	9D	10T	10D	12T	12D
.120	+	+	+	+	+	+	+	+	+	+	+	+	+	+
.144	-	-	-	-	-	-	-	-	-	-	-	-	+	+
.184	+	+	+	+	+	+	+	+	+	+	+	+	+	+
.280	+	+	+	+	+	+	+	+	+	+	+	+	+	+
T	3		3		3		3		3		3		4	
C	3		3		3		3		3		3		4	

Total number of bands = 4

Table 15. Banding pattern of malate dehydrogenase (dry seeds) in tall/dwarf near-isogenic pairs of pearl millet.

Rf	Tall/dwarf near-isogenic pairs													
	EC						MC						NC	
	1T	1D	2T	2D	3T	3D	6T	6D	9T	9D	10T	10D	12T	12D
.464	+	+	+	+	+	+	+	+	+	+	+	+	+	+
.514	+	+	+	+	+	+	+	+	+	+	+	+	+	+
.543	-	-	-	-	+	o	-	-	-	-	-	-	-	-
.582	-	-	o	+	-	-	-	-	-	-	-	-	-	-
.600	+	+	+	o	o	+	+	+	+	+	+	+	+	+
.614	-	-	-	-	+	o	-	-	-	-	-	-	-	-
T	3		4		5		3		3		3		3	
C	3		2		2		3		3		3		3	

Total number of bands = 6.

EC = Early Composite; MC = Medium Composite; NC = Nigerian Composite; C = Number of common bands, + indicates uncommon bands within a pair; T = Total number of bands within a pair

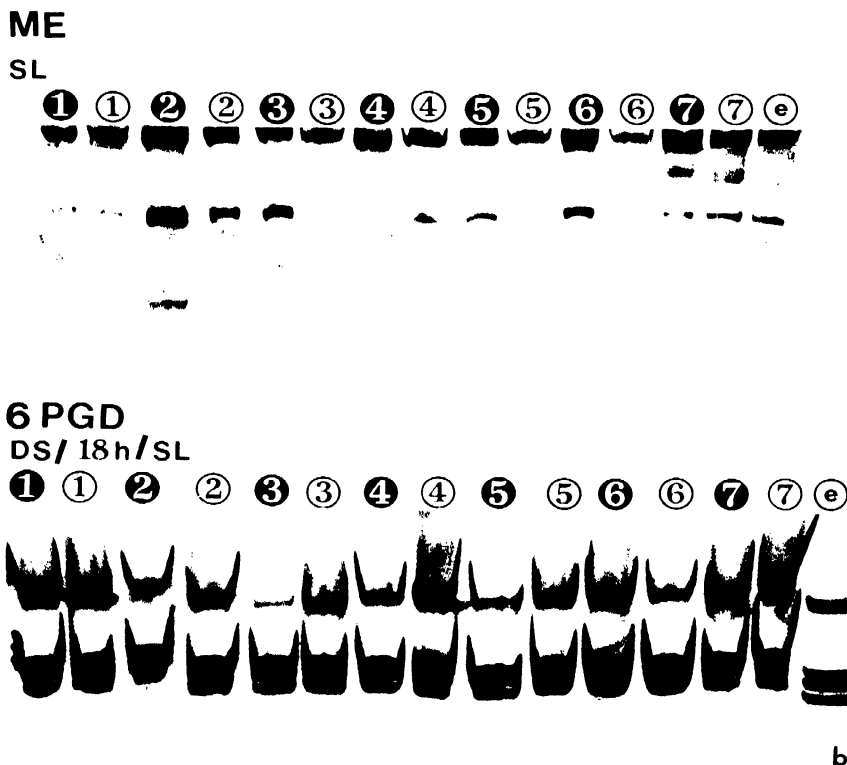
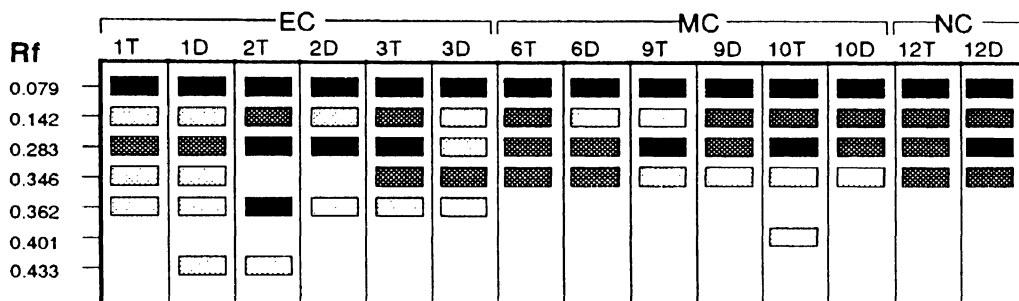


Figure 44. Isozyme spectrum of malic enzyme (using five-day old etiolated seedlings (SL) and 6-phosphoglutarate dehydrogenase using DS, SL and 18hS in tall/dwarf near-isogenic pairs of pearl millet

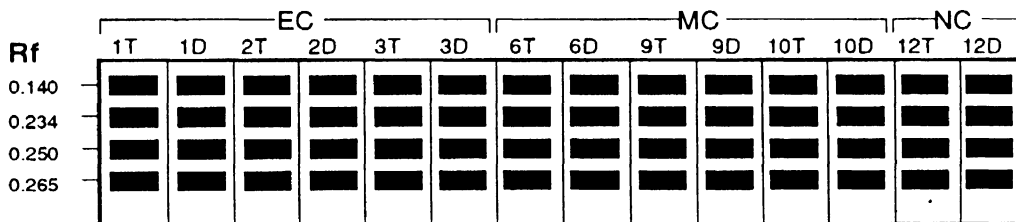
Lanes from left to right (Figs. 44a and 44b) : **Early Composite (EC)**: 1 filled circle = 1T i.e. tall isoline of pair EC1, 1 empty circle = 1D i.e. dwarf isoline of pair EC1; 2 filled circle = 2T i.e. tall isoline of pair EC2, 2 empty circle = 2D i.e. dwarf isoline of pair EC2; 3 filled circle = 3T i.e. tall isoline of pair EC3, 3 empty circle = 3D i.e. dwarf isoline of pair EC3; **Medium Composite (MC)**: 4 filled circle = 6T i.e. tall isoline of pair MC6, 4 empty circle = 6D i.e. dwarf isoline of pair MC6; 5 filled circle = 9T i.e. tall isoline of pair MC9, 5 empty circle = 9D i.e. dwarf isoline of pair MC9; 6 filled circle = 10T i.e. tall isoline of pair MC10, 6 empty circle = 10D i.e. dwarf isoline of pair MC10; **Nigerian Composite (NC)**: 7 filled circle = 12T i.e. tall isoline of pair NC12, 7 empty circle = 12D i.e. dwarf isoline of pair NC12

Figure 45. Schematic zymogram of malic enzyme (a) and 6 phosphogluconate dehydrogenase (b) in tall/dwarf near-isogenic lines of pearl millet

(a) Malic enzyme (ME): Seedlings



(b) 6-Phosphogluconate dehydrogenase (6-PGD): Seedlings/dry seeds/18hIS



Very dark bands Light bands Very light bands

EC : Early composite; MC : Medium composite; NC: Nigerian composite

1T & 1D indicates tall and dwarf versions of 1st isogenic pair, 2T & 2D of 11nd pair and so on

Note: Very light bands are usually not detectable in the photographs

Table 16. Banding pattern of malic enzyme (seedling) in tall/dwarf near-isogenic lines of pearl millet.

Rf	Tall/dwarf near-isogenic pairs													
	EC				MC						NC			
	1T	1D	2T	2D	3T	3D	6T	6D	9T	9D	10T	10D	12T	12D
.079	+	+	+	+	+	+	+	+	+	+	+	+	+	+
.142	+	+	+	+	+	+	+	+	+	+	+	+	+	+
.283	+	+	+	+	+	+	+	+	+	+	+	+	+	+
.346	+	+	-	-	+	+	+	+	+	+	+	+	+	+
.362	+	+	+	+	+	+	-	-	-	-	-	-	-	-
.401	-	-	-	-	-	-	-	-	-	-	+	-	-	-
.433	-	+	+	-	-	-	-	-	-	-	-	-	-	-
T	6		5		5		4		4		5		4	
C	5		4		5		4		4		4		4	

Total number of bands = 7

EC = Early Composite; MC = Medium Composite; NC = Nigerian Composite; C = Number of common bands, + indicates uncommon bands within a pair; T = Total number of bands within a pair

PGI

a. DS

① ① ② ② ③ ③ ④ ④ ⑤ ⑤ ⑥ ⑥ ⑦ ⑦



b. SL / 18h

① ① ② ② ③ ③ ④ ④ ⑤ ⑤ ⑥ ⑥ ⑦ ⑦ ⑧

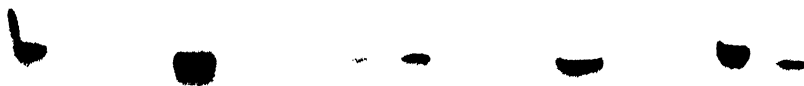
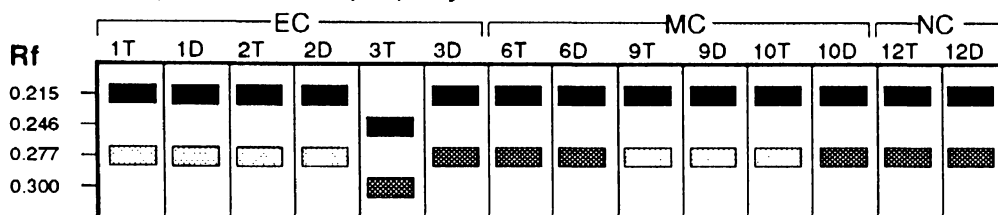


Figure 46. Isozyme spectrum of phosphoglucosomerase using dry seeds (DS), five-day old etiolated seedlings (SL) and 18-hour imbibed seeds (18h) in tall/dwarf near-isogenic pairs of pearl millet

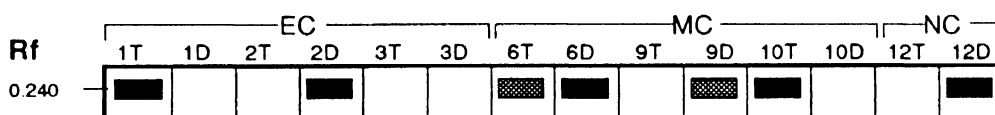
Lanes from left to right (Figs. 46a and 46b): **Early Composite (EC)**: 1 filled circle = tall isoline of pair EC1, 1 empty circle = dwarf isoline of pair EC1; 2 filled circle = tall isoline of pair EC2, 2 empty circle = dwarf isoline of pair EC2; 3 filled circle = tall isoline of pair EC3, 3 empty circle = dwarf isoline of pair EC3; **Medium Composite (MC)**: 4 filled circle = tall isoline of pair MC6, 4 empty circle = dwarf isoline of pair MC6; 5 filled circle = tall isoline of pair MC9, 5 empty circle = dwarf isoline of pair MC9; 6 filled circle = tall isoline of pair MC10, 6 empty circle = dwarf isoline of pair MC10; **Nigerian Composite (NC)**: 7 filled circle = tall isoline of pair NC12, 7 empty circle = dwarf isoline of pair NC12

Figure 47. Schematic zymogram of phosphoglucosomerase in tall/dwarf near isogenic lines of pearl millet

(a) Phosphoglucosomerase (PGI): Dry seeds



(b) Phosphoglucosomerase (PGI): Seedlings / 18h imbibed seeds



Very dark bands
 Light bands
 Very light bands

EC : Early composite; MC : Medium composite; NC: Nigerian composite
 1T & 1D indicates tall and dwarf versions of 1st isogenic pair, 2T & 2D of 2nd pair and so on
 Note: Very light bands are usually not detectable in the photographs

Table 17. Banding pattern of phosphoglucosomerase (seedlings/18h IS) in tall/dwarf near-isogenic pairs of pearl millet.

Rf	Tall/dwarf near-isogenic pairs													
	EC						MC						NC	
	1T	1D	2T	2D	3T	3D	6T	6D	9T	9D	10T	10D	12T	12D
.240	+	o	o	+	-	-	+	+	o	+	+	o	o	+
T	1		1		0		1		1		1		1	
C	0		0		0		1		0		0		0	

Total number of bands = 1

Table 18. Banding pattern of phosphoglucosomerase (dry seeds) in tall/dwarf near-isogenic pairs of pearl millet.

Rf	Tall/dwarf near-isogenic pairs													
	EC						MC						NC	
	1T	1D	2T	2D	3T	3D	6T	6D	9T	9D	10T	10D	12T	12D
.215	+	+	+	+	o	+	+	+	+	+	+	+	+	+
.246	-	-	-	-	+	o	-	-	-	-	-	-	-	-
.277	+	+	+	+	o	+	+	+	+	+	+	+	+	+
.300	-	-	-	-	+	o	-	-	-	-	-	-	-	-
T	2		2		4		2		2		2		2	
C	2		2		0		2		2		2		2	

Total number of bands = 4

EC = Early Composite; MC = Medium Composite; NC = Nigerian Composite; C = Number of common bands, + indicates uncommon bands within a pair; T = Total number of bands within a pair

Figure 48. Isozyme spectrum of shikimate dehydrogenase using dry seeds (DS), five-day old etiolated seedlings (SL) and 18-hour imbibed seeds (18h) in tall/dwarf near-isogenic lines of pearl millet

Lanes from left to right (Figs. 48a, 48b and 48c)

Early Composite (EC)

1 filled circle	= 1T i.e. tall isoline of pair EC1
1 empty circle	= 1D i.e. dwarf isoline of pair EC1
2 filled circle	= 2T i.e. tall isoline of pair EC2
2 empty circle	= 2D i.e. dwarf isoline of pair EC2
3 filled circle	= 3T i.e. tall isoline of pair EC3
3 empty circle	= 3D i.e. dwarf isoline of pair EC3

Medium Composite (MC)

4 filled circle	= 6T i.e. tall isoline of pair MC6
4 empty circle	= 6D i.e. dwarf isoline of pair MC6
5 filled circle	= 9T i.e. tall isoline of pair MC9
5 empty circle	= 9D i.e. dwarf isoline of pair MC9
6 filled circle	= 10T i.e. tall isoline of pair MC10
6 empty circle	= 10D i.e. dwarf isoline of pair MC10

Nigerian Composite (NC)

7 filled circle	= 12T i.e. tall isoline of pair NC12
7 empty circle	= 12D i.e. dwarf isoline of pair NC12

SKDH

a. SKDH DS/18h

*① ① ② ② ③ ③ ④ ④ ⑤ ⑤ ⑥ ⑥ ⑦ ⑦



b. SKDH

① ① ② ② ③ ③ ④ ④ ⑤ ⑤ ⑥ ⑥ ⑦ ⑦



c. SKDH SL

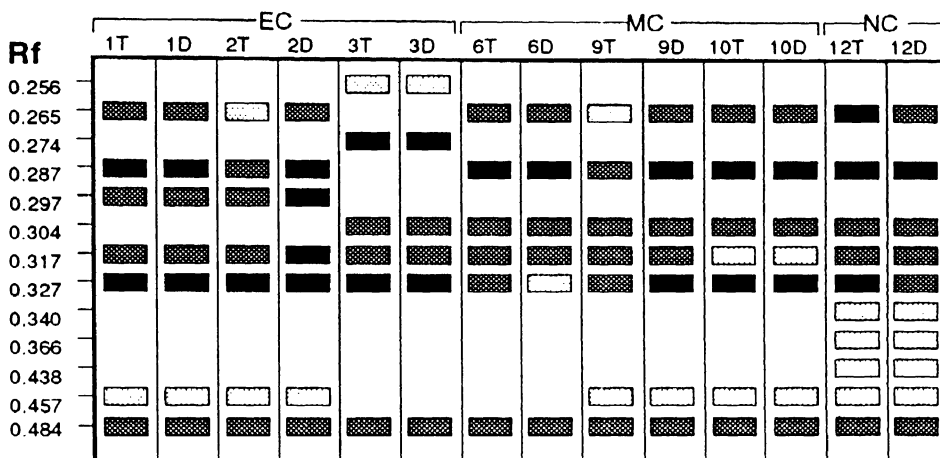
① ① ② ② ③ ③ ④ ④ ⑤ ⑤ ⑥ ⑥ ⑦ ⑦ e



*①- tall and ①- dwarf isolines of first near-isogenic pair...

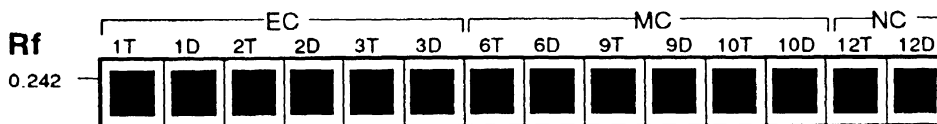
Figure 49. Schematic zymogram of shikimate dehydrogenase in tall/dwarf near isogenic lines of pearl millet

(a) Shikimate Dehydrogenase (SKDH): Dry seeds/18hIS



Note. Zymogram is based upon three gels

(b) Shikimate Dehydrogenase (SKDH): Seedlings



Very dark bands Light bands Very light bands Very thick bands

EC : Early composite; MC : Medium composite; NC : Nigerian composite
 1T & 1D indicates tall and dwarf versions of 1st isogenic pair, 2T & 2D of 11nd

pair and so on ...

Note: Very light bands are usually not detectable in the photographs

Table 19. Banding pattern of shikimate dehydrogenase (18hIS/dry seeds) in tall/dwarf near-isogenic pairs of pearl millet.

Rf	Tall/dwarf near-isogenic pairs													
	EC				MC						NC			
	1T	1D	2T	2D	3T	3D	6T	6D	9T	9D	10T	10D	12T	12D
.256	-	-	-	-	+	+	-	-	-	-	-	-	-	-
.265	+	+	+	+	-	-	+	+	+	+	+	+	+	+
.274	-	-	-	-	+	+	-	-	-	-	-	-	-	-
.287	+	+	+	+	-	-	+	+	+	+	+	+	+	+
.297	+	+	+	+	-	-	-	-	-	-	-	-	-	-
.304	-	-	-	-	+	+	+	+	+	+	+	+	+	+
.317	+	+	+	+	+	+	+	+	+	+	+	+	+	+
.327	+	+	+	+	+	+	+	+	+	+	+	+	+	+
.340	-	-	-	-	-	-	-	-	-	-	-	-	+	+
.366	-	-	-	-	-	-	-	-	-	-	-	-	+	+
.438	-	-	-	-	-	-	-	-	-	-	-	-	+	+
.457	+	+	+	+	-	-	-	-	+	+	+	+	+	+
.484	+	+	+	+	+	+	+	+	+	+	+	+	+	+
T	7		7		6		6		7		7		10	
C	7		7		6		6		7		7		10	

Total number of bands = 13

EC = Early Composite; MC = Medium Composite; NC = Nigerian Composite; T = Total number of bands within a pair; C = Common number of bands within a pair

SOD

SL

① ① ② ② ③ ③ ④ ④ ⑤ ⑤ ⑥ ⑥ ⑦ e ⑦

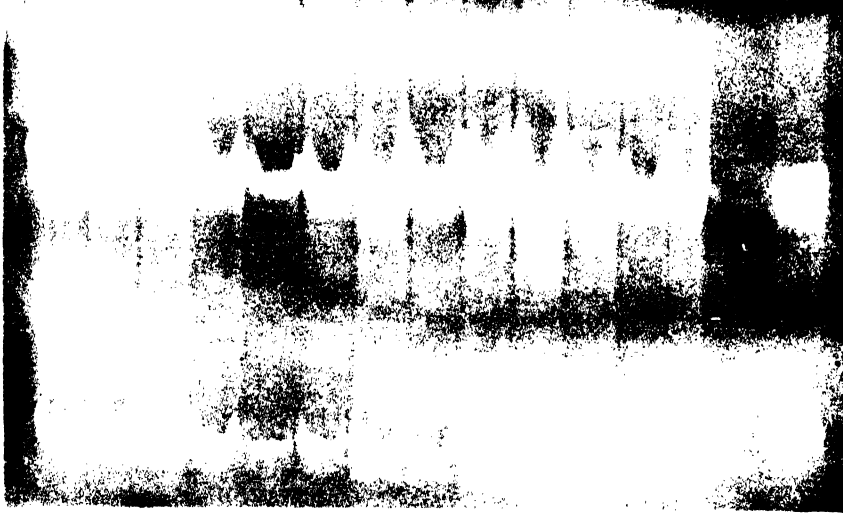
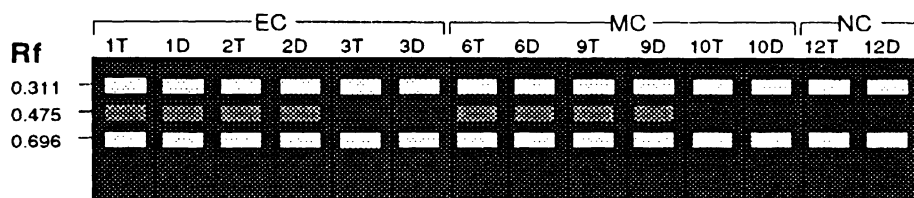


Figure 50. Isozyme spectrum of superoxide dismutase using five-day old etiolated seedlings (SL) in tall/dwarf near-isogenic pairs of pearl millet

Lanes from left to right: **Early Composite (EC)**: 1 filled circle = tall isoline of pair EC1, 1 empty circle = dwarf isoline of pair EC1; 2 filled circle = tall isoline of pair EC2, 2 empty circle = dwarf isoline of pair EC2; 3 filled circle = tall isoline of pair EC3, 3 empty circle = dwarf isoline of pair EC3, **Medium Composite (MC)**: 4 filled circle = tall isoline of pair MC6, 4 empty circle = dwarf isoline of pair MC6; 5 filled circle = tall isoline of pair MC9, 5 empty circle = dwarf isoline of pair MC9; 6 filled circle = tall isoline of pair MC10, 6 empty circle = dwarf isoline of pair MC10; **Nigerian Composite (NC)**: 7 filled circle = tall isoline of pair NC12, 7 empty circle = dwarf isoline of pair NC12

Figure 51. Schematic zymogram of superoxide dismutase in tall/dwarf near-isogenic lines of pearl millet

(a) Superoxide dismutase (SOD): Seedlings



☐ Transparent / translucent bands ▨ Faint bands

EC : Early composite; MC : Medium composite; NC: Nigerian composite
 1T & 1D indicates tall and dwarf versions of 1st isogenic pair, 2T & 2D of 2nd pair and so on

Note: Faint bands are usually not detectable in the photographs

Table 20. Banding pattern of superoxide dismutase (seedlings) in tall/dwarf near-isogenic pairs of pearl millet.

Rf	Tall/dwarf near-isogenic pairs													
	EC				MC				NC					
	1T	1D	2T	2D	3T	3D	6T	6D	9T	9D	10T	10D	12T	12D
.311	+	+	+	+	+	+	+	+	+	+	+	+	+	+
.475	+	+	+	+	-	-	+	+	+	+	-	-	-	-
.696	+	+	+	+	+	+	+	+	+	+	+	+	+	+
T	3		3		2		3		3		2		2	
C	3		3		2		3		3		2		2	

Total number of bands = 3

EC = Early Composite; MC = Medium Composite; NC = Nigerian Composite; T = Total number of bands within a pair; C = Number of common bands within a pair.

V DISCUSSION

5.1 Experiment No. 1: Mitochondrial DNA RFLP analysis of pearl millet CMS lines

The method suggested by Smith *et al.* (1987) yielded mtDNA from pearl millet genotypes suitable for restriction endonuclease digestion. Lack of chloroplast DNA restriction fragment variability among CMS, revertants and fertile normal lines and presence of restriction fragment differences in mtDNA and its possible correlation with plant genotype (Smith *et al.*, 1987) support the significance of mitochondrial genome causing male sterility in pearl millet. This is also in agreement with results from other species (Belliard *et al.*, 1978; Clark *et al.*, 1985; Connett and Hanson, 1990).

Therefore, the present investigation was confined to study mtDNA RFLP pattern in various CMS lines (of known/classified and unknown/unclassified cytoplasmic sources) to explore the possibility of getting new CMS sources.

Analysis of endonuclease restriction fragment patterns has been reported to be a rapid, relatively less expensive (than Southern hybridization) way to characterize male-sterile cytoplasms in pearl millet (Smith and Chowdhury, 1989). In this study individual restriction fragments could not be observed due to presence of continuous smear of digested mtDNA along the entire lane for each genotype as also observed by Sujata *et al.* (1994). Therefore, Southern hybridization using mtDNA specific clones was performed

^{RFL}
to study polymorphism and to classify various CMS sources.

5.1.1 MtDNA RFLP using pearl millet (homologous) clones

Hybridization patterns of *Pst*I-digested mtDNA probed with 4.7 kb or 9.7 kb clone distinguished two major groups, A₁- vs. the non-A₁ group (Figs. 3b and 11). Almost all the CMS lines of the non-A₁ group and 81B produced by *Pst*I-9.7 kb combination were identical except LSGP 36 and LSGP 66 which shared a unique *Pst*I 15.0 kb fragment but absent in other lines (Fig. 11). On the other hand, the non-A₁ group produced by *Pst*I-4.7 kb combination had many subgroups lying close to each other (85% similarity). A₁-group included LSGP 22, EGP 1, EGP 2 and PV 2. All the remaining CMS lines from unknown cytoplasmic sources either formed a separate cluster (e.g., Groups II, III and VI) or grouped with the CMS lines of known sources (e.g., Groups IV and V). MtDNAs digested with the other endonucleases (*Bam*HI and *Hind*III) and probed with various pearl millet clones (4.7 kb, 10.9 kb, and 13.6 kb) displayed two major groups, one having 81A₁ plus 81A_v (A₁A_v group) and rest of CMS lines of known sources in the other group (Figs. 3a, 5, 7 and 9). In all four combinations, 7 CMS lines from unknown cytoplasmic sources (LSGP 6, LSGP 17, LSGP 22, EGP 1, EGP 2, PV 1 and PV 2) were consistently included in A₁A_v group while LSGP 14, LSGP 55 and 81B were in the other cluster. LSGP 66 was completely isolated from the two groups (*Bam*HI-13.6 kb) by the presence of two weakly hybridized but unique bands of low molecular weight

(1.8 kb and 1.2 kb). Other two bands (6.5 kb and 6.0 kb) which had high intensity in all other cytoplasms were faint in LSGP 66 (Fig. 8). Pearl Millet clones, thus distinguished 81A_v, 81A_m, LSGP 55 and LSGP 66, either by the presence or absence of band(s) or by differential mtDNA banding patterns (Tables 21 and 22). None of the homologous probes could discriminate between A₂, A₃ and A_m cytoplasms (Table 23).

5.1.2 MtDNA RFLP using maize (heterologous) clones

Hybridization patterns using maize mtDNA probes revealed further differences among the CMS lines of pearl millet as was also observed by Rajeshwari *et al.* (1994). The maize *atp6* and *coxI* clones in combination with *Bam*HI, and *Pst*I proved to be the most effective in separating CMS lines except A₂ and A₃ sources (Table 23). These cytoplasms were discriminated either by the presence or absence of unique fragment(s) or by their differential banding pattern involving many bands (Tables 21 and 22). Presence of 24.0 kb (*Bam*HI-*atp6* and *Bam*HI-*coxI*), 18.5 kb (*Pst*I-*atp6*) fragments in 81A_v and absence of 4.5 kb (*Pst*I-*atp6*) and 4.7 kb (*Pst*I-*coxI*) in 81A_m distinguished these CMS sources from each other as well as from other CMS sources. In some enzyme-probe combinations, 2-3 unique fragments were responsible to distinguish various CMS sources. For example, the presence of 7.3 kb and 2.4 kb fragments (*Bam*HI-*atp6*), and presence of 7.4 kb and 2.5 kb fragments and absence of 22.4 kb fragment (*Bam*HI-*coxI*) distinguished 81A_m. Our results are

in agreement with the classification of these (known) cytoplasmic sources based on fertility restoration pattern (Rai *et al.*, 1991). Their results showed the distinctness of A_1 , *violaceum* ($81A_v$) and A_m systems but did not find differences between A_2 and A_3 cytoplasm. Besides known CMS sources, three CMS lines from unknown cytoplasmic sources, LSGP 28, LSGP 55 and LSGP 66 were also distinguished by the presence/absence of bands (Table 21) or by differential banding pattern (Table 22), thus indicating their distinctness from the existing sources of cytoplasmic male sterility. In addition, $81A_1$, $81A_v$ and $81B$ could be discriminated by their differential banding patterns using various enzyme-probe combinations.

The homologous pearl millet clones and maize *coxI* are known to distinguish only two groups of cytoplasm i.e. A_1 - versus the non- A_1 group (consisting of all other cytoplasm identified so far and their B-lines), with many probe-enzyme combinations (Sivaramakrishnan *et al.*, 1993; Rajeshwari *et al.*, 1994). Results of the present study showed that out of six enzyme-probe combinations (with homologous probes), only two (*PstI*-4.7 kb and *PstI*-9.7 kb) could distinguish the A_1 -group from the non- A_1 groups. Other four combinations (Table 23) were not able to discriminate between $81A_1$ and $81A_v$. Similarly, *coxI*, the maize clone, when probed either with *Bam*HI- or *PstI*-digested mtDNA blots, distinguished all the existing known cytoplasmic sources of sterility, except A_2 from A_3 .

Maize *atp6* clone is known to distinguish male-sterile cytoplasm into

four major groups: A_1 , A_2 , A_m and A_v (Smith and Chowdhury, 1989; Sivaramakrishnan *et al.*, 1993; Rajeshwari *et al.*, 1994; Sujata *et al.*, 1994). Similar results were also observed in the present investigation using *Bam*HI and *Pst*I endonucleases, whereas, *Hind*III-digested mtDNA hybridized to *atp6* could reveal two groups only, the first group consisting of $81A_1$ and $81A_v$; and the second group had A_2 -lines, Pb 406 A_3 and $81A_m$, thus, relatively less effective to discriminate the CMS sources.

5.1.3 Dendrogram analysis (aggregate)

The dendrogram constructed based on three restriction enzymes and homologous probes revealed three major groups of CMS lines at $F = 0.93$ level of significance (Fig. 53). Three groups included, (1) $81A_1$, (2) $81A_v$, and (3) A_2 , A_3 and A_m lines from known CMS sources. LSGP 66 was the most divergent cytoplasm followed by $81A_v$ and LSGP 55. LSGP 14 closely resembled A_2 - and A_3 -lines; LSGP 6, LSGP 17 and PV 1 were identical and formed a separate group; and LSGP 22, EGP 1, EGP 2 and PV 2 clustered with $81A_1$. Few of the LSGPs (LSGP 28, LSGP 36 and LSGP 43) did not group with any of the existing CMS sources, thus remaining as a separate cluster (Fig. 53).

The classification pattern of aggregate dendrograms (Fig. 60) clearly indicates that clustering pattern from the heterologous probes (with all three enzymes) resembled the grouping pattern obtained from all 12 enzyme-probe combinations. Besides getting similar groups, two of the main groups were

Figure 52. Dendrogram of cytoplasmic male sterile lines of pearl millet based on homologous (4.7 kb, 9.7 kb, 10.9 kb, 13.6 kb) and heterologous (atp6, coxI) clones hybridized to mtDNA digested with three restriction enzymes (BamHI, HindIII, PstI)

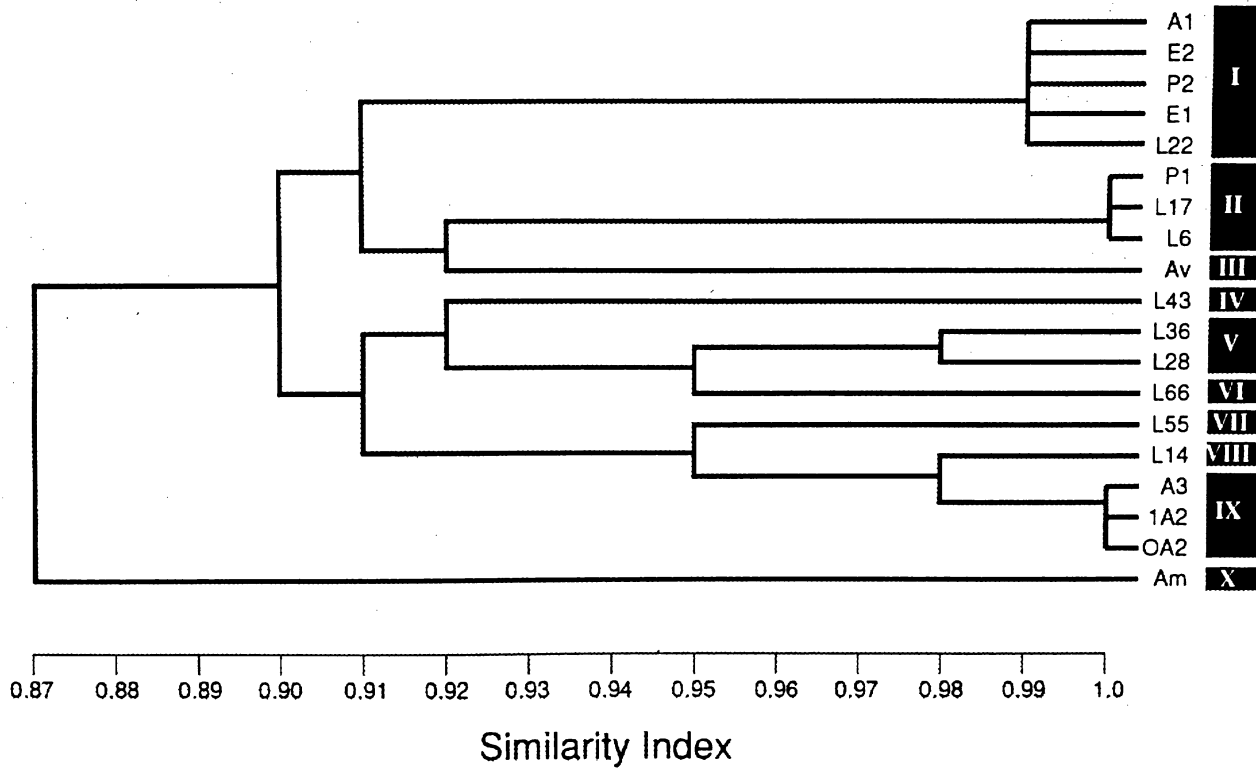


Figure 53. Dendrogram of cytoplasmic male sterile lines of pearl millet based on homologous (4.7 kb, 9.7 kb, 10.9 kb, 13.6 kb) clones hybridized to mtDNA digested with three restriction enzymes (BamHI, HindIII, PstI)

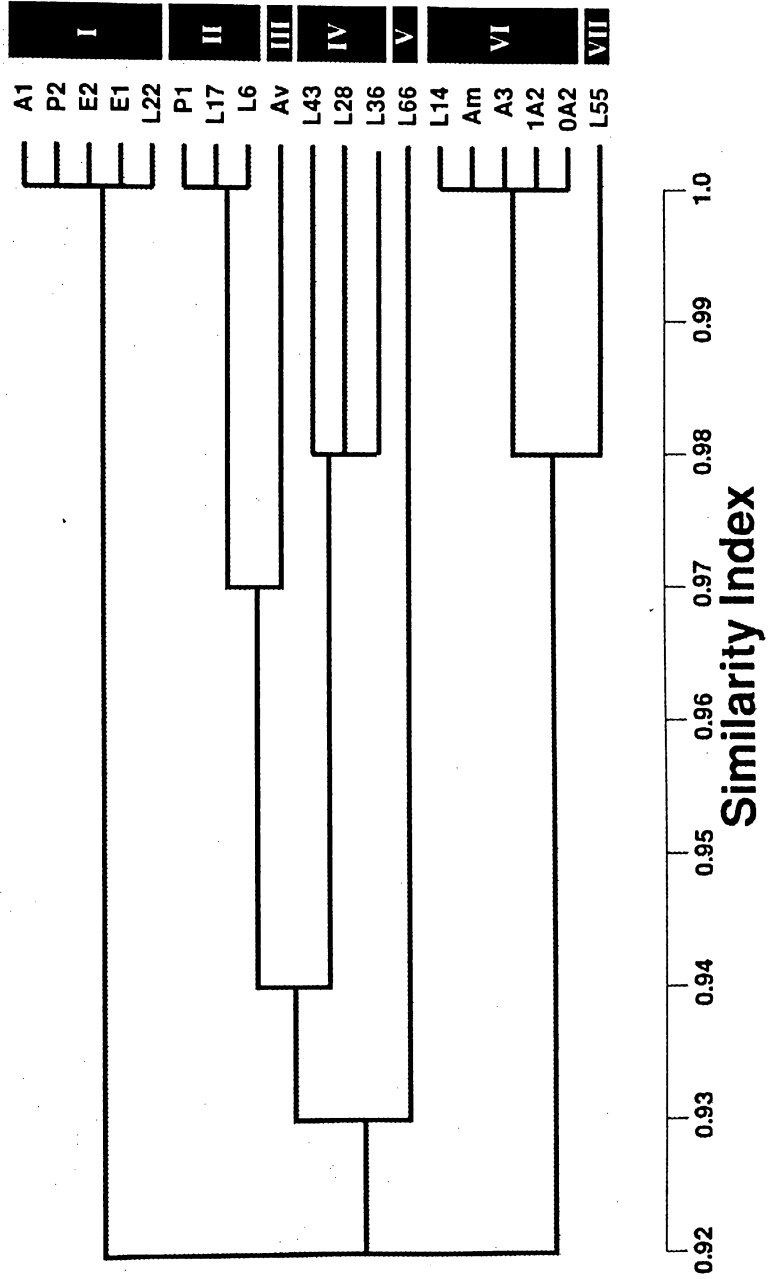


Figure 54. Dendrogram of cytoplasmic male sterile lines of pearl millet based on maize atp6 gene clone hybridized to mtDNA digested with three restriction enzymes (BamHI, HindIII, PstI)

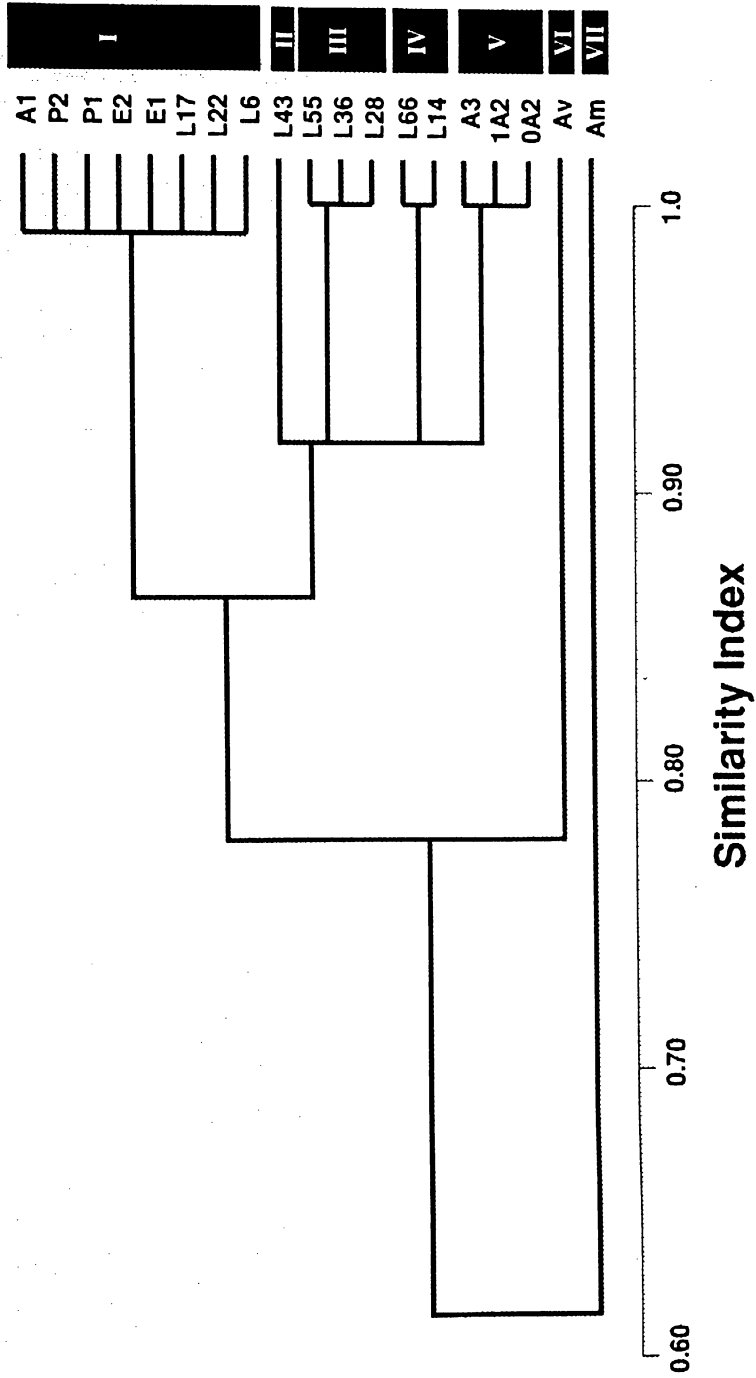


Figure 55. Dendrogram of cytoplasmic male sterile lines of pearl millet based on maize coxI gene clone hybridized to mtDNA digested with three restriction enzymes (BamHI, HindIII, PstI)

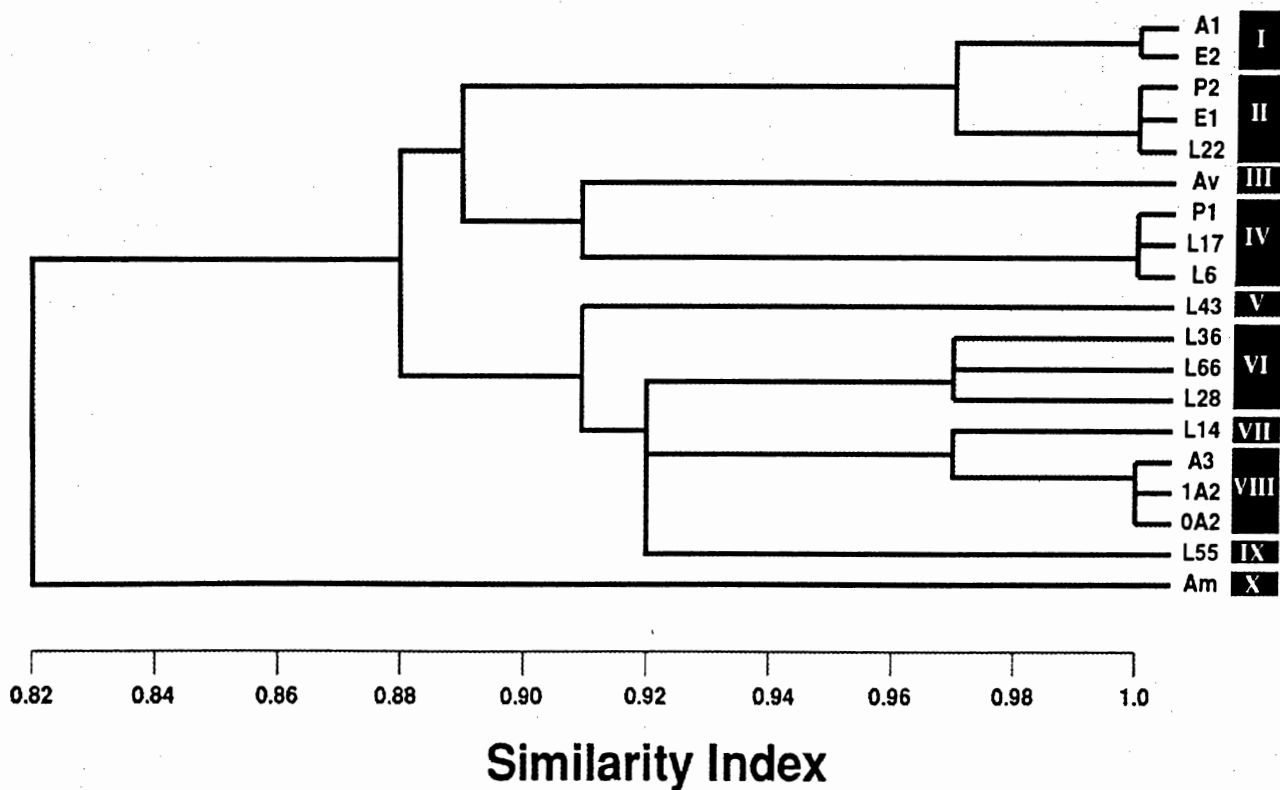
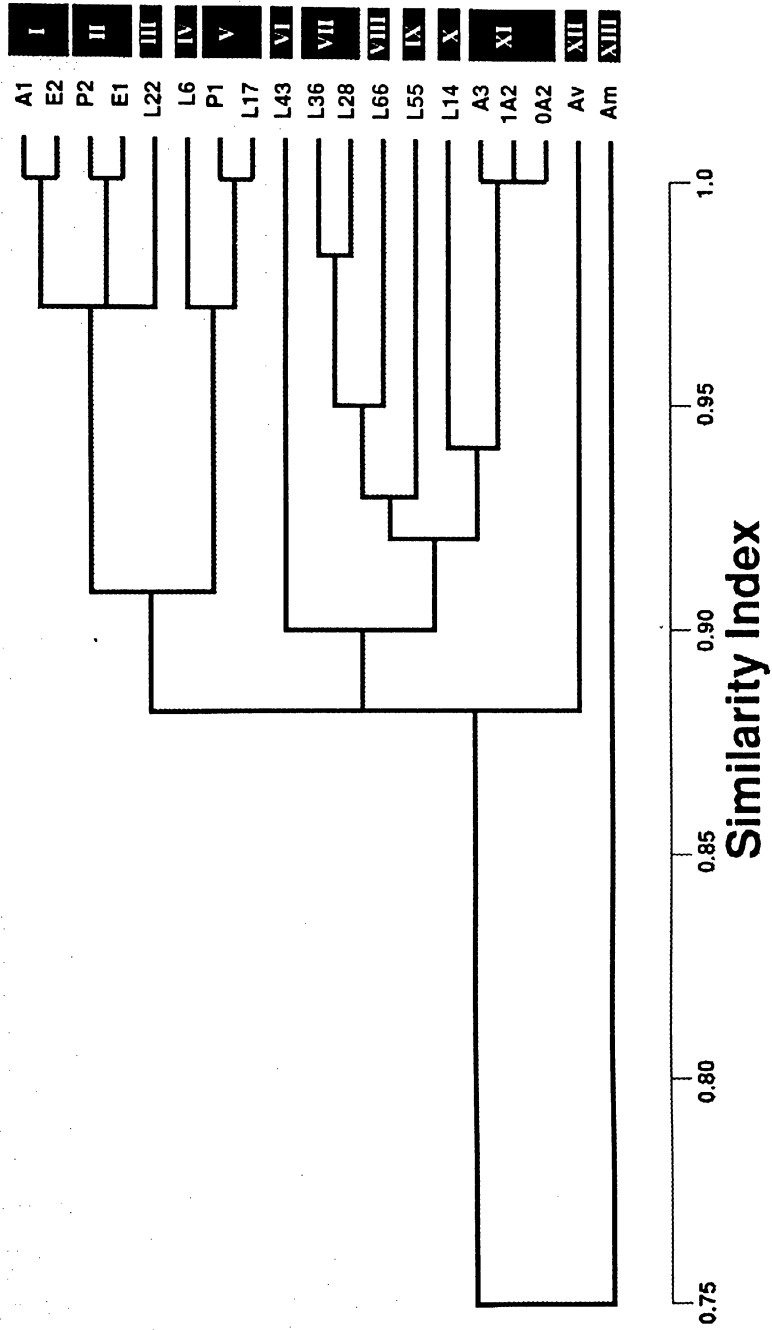


Figure 56. Dendrogram of cytoplasmic male sterile lines of pearl millet based on heterologous (atp6, cox1) clones hybridized to mtDNA digested with three restriction enzymes (BamHI, HindIII, PstI)



further subdivided using heterologous probes. Thus, heterologous probes (*coxI* and *atp6*) alone could suffice the purpose of CMS-sources classification in the present study.

Broadly, two groups are evident, A_m - and the non- A_m group. Six subgroups could be revealed within the non- A_m group at $F = 0.95$, few of which were further subdivided (Fig. 52). Looking at the percent similarity values (Table 24), various dendrograms and Fig. 60 several points emerge:

1. At least seven groups are present in LSGP and two groups each in EGP and PV.
2. Of the LSGP cytoplasms, LSGP 43, LSGP 55 and LSGP 66 were most diverse from each other as well as from $81A_m$, and $81A_v$.
3. LSGP 22, EGP 1, EGP 2 and PV 2 were in A_1 cytoplasmic group and had 99% similarity with $81A_1$.
4. LSGP 6, LSGP 17 and PV 1 were identical ($F = 1.0$). Pb 406 A_3 , Pb 310 A_2 and Pb 311 A_2 also had 100% homology, always clustered together and were closer to LSGP 14; and EGP 1 and PV 2 were also identical ($F = 1.0$).
5. Percent similarity (63%) between $81A_1$ and $81A_m$ indicates that these two CMS lines were the most diverse lines from each other.

Therefore, it is evident that none of the CMS lines from unknown CMS

source(s) completely resembled any of the existing source, however few of the CMS lines of unknown sources had high degree of homology with the one or the other known CMS-sources. For example, EGP 1 and PV 2 had 99% homology with 81A₁; LSGP 22 had 98% homology with 81A₁; LSGP 14 resembled 81A₃ and A₂ CMS lines(98%); and PV 2 was closest to 81A_m with 85% similarity (Table 24).

At the most, six new cytoplasmic groups emerge out of the cluster analysis (Fig. 52). It suggests that each of these possibly contains a unique mitochondrial genome that is different from each other and several others reported earlier (Sivaramakrishnan *et al.*, 1993; Smith and Chowdhury, 1989; Sujata *et al.*, 1994). The uniqueness of these cytoplasm is evident in various Southern blot hybridization patterns with specific enzyme-probe combinations.

The restriction maps (Fig. 1) verified that the four pearl millet fragments contained two sets of repeated sequences, one on the 4.7-, 10.9- and 13.6-kb fragments, the other on the 13.6- and 9.7-kb fragments (Smith and Chowdhury, 1991). Our results completely agreed with this since *Hind*III-4.7 kb hybridization patterns had partial homology with *Hind*III-10.9 kb hybridization patterns (compare Figs. 2 and 4). Similarly, three restriction fragments (6.5-, 6.0-, and 4.9-kb) obtained by *Bam*HI-4.7 kb combination were also identified in *Bam*HI-13.6kb combination (Figs. 6 and 8). These results indicate partial homology between 4.7-, 10.9-, and 13.6-kb fragments. On the other hand, none of the fragments found in *Pst*I-4.7 kb could be detected in

*Pst*I-9.7 kb combination (Figs. 2 and 10), indicating lack of homology between these two pearl millet clones.

Smith and Chowdhury (1991) and Rajeshwari *et al.* (1994) found identical banding patterns with 4.7 kb and *coxI* gene probes. In the present study, *coxI* gene always produced different hybridization pattern as compared to 4.7 kb hybridization patterns. Fragments detected by 4.7 kb were always present in the *coxI* hybridized blots, additionally a few polymorphic bands were also observed with *coxI*. Such results were observed both in mtDNA and tDNA blots. This clearly indicates that pearl millet 4.7 kb fragment contains only a part of *coxI* gene, thus showing partial homology.

In *Bam*HI-4.7 kb combination 6.0 kb fragment was polymorphic (Fig. 6). It is interesting to note that in the absence of this fragment, the intensity of 4.9 kb fragment increases. Similar observations were noticed in *Bam*HI-*coxI* combination.

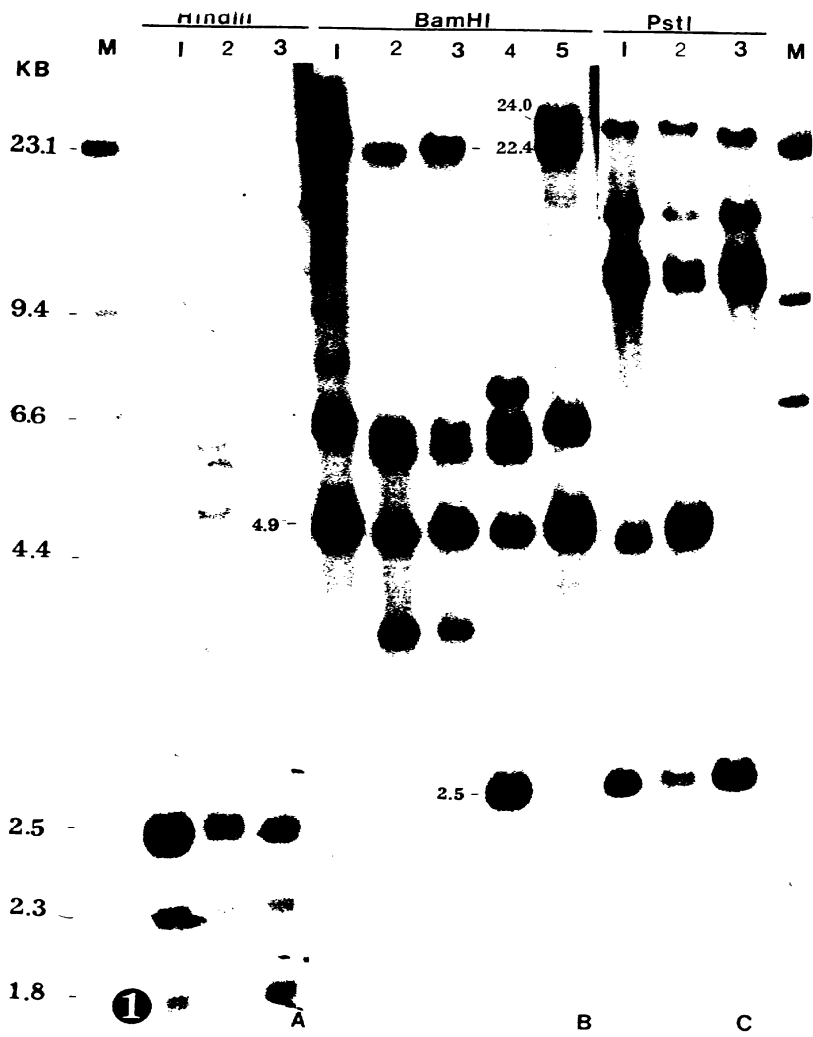
Because of the presence of unique fragment(s), 81A_m, 81A_v and LSGP 66 can be identified using specific enzyme-probe combination (Table 21) or differential fragment pattern may also be used to identify a particular cytoplasm (Table 22).

Open-pollinated and sib seed manifest similar hybridization patterns, thus, either of the two seed lots may be used to conduct mtDNA analysis. Being cost effective and less laborious, OP seed can meet the requirements for mtDNA analysis. However, tDNA and mtDNA southern blots did not give

Figure 58. Southern blot hybridization of the maize *coxI* (1) gene clone to (A) *HindIII*-, (B) *BamHI*-, and (C) *PstI*-digested mtDNA from open pollinated seed of CMS lines; and Southern blot hybridization of the maize *atp6* (2) gene clone to (A) *BamHI*- and (B) *PstI*-digested mtDNA from open pollinated seed of CMS lines

Lane	<i>HindIII-coxI</i>	Lane	<i>BamHI-atp6</i>
1	Pb 310A ₂	1	81A ₁
2	Pb 406A ₃	2	Pb 310A ₂
3	81A _m	3	Pb 406A ₃
		4	81A _m
		5	81A _v
	<i>PstI-coxI</i>		<i>BamHI-atp6</i>
1	Pb 310A ₂	1	81A ₁
2	Pb 406A ₃	2	Pb 310A ₂
3	81A _m	3	Pb 406A ₃
		4	81A _m
		5	81A _v
	<i>PstI-atp6</i>		
1	Pb 310A ₂		
2	Pb 406A ₃		
3	81A _m		

OP Seed ----- **cox1**



----- **atp6**

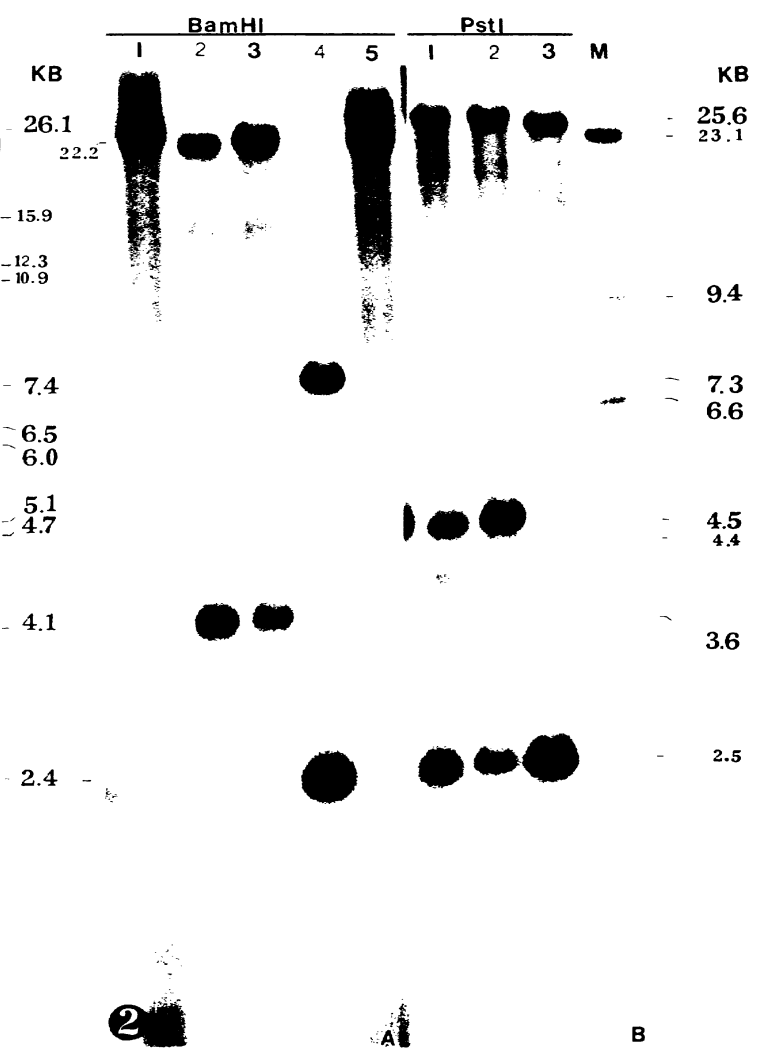


Figure 60. Comparison of grouping pattern of various dendrograms constructed based upon various enzyme-probe combinations

	<div style="display: flex; justify-content: space-around; align-items: center;"> <div style="text-align: center;"> <p>mtDNA digested with three restriction enzymes and hybridized with: ▼</p> </div> <div style="display: flex; justify-content: space-around; width: 100%;"> <div style="text-align: center;">A</div> <div style="text-align: center;">B</div> <div style="text-align: center;">C</div> <div style="text-align: center;">D</div> <div style="text-align: center;">E</div> <div style="text-align: center;">F</div> <div style="text-align: center;">G</div> <div style="text-align: center;">H</div> <div style="text-align: center;">I</div> <div style="text-align: center;">J</div> </div> <div style="text-align: right;"> <p>Number of groups including sub-groups</p> </div> </div>																		
all probes (4.7kb, 9.7kb, 10.9kb, 13.6kb, <i>cox1</i> , and <i>atp6</i>)	A1	E2	P2	E1	L22	L6	P1	L17	AV	L55	L36	L28	L43	L66	L14	A2	A3	Am	10
Homologous (4.7kb, 9.7kb, 10.9kb, and 13.6kb)	A1	E2	P2	E1	L22	L6	P1	L17	AV	L55	L36	L28	L43	L66	L14	A2	A3	Am	7
Heterologous (<i>cox1</i> and <i>atp6</i>)	A1	E2	P2	E1	L22	L6	P1	L17	AV	L55	L36	L28	L43	L66	L14	A2	A3	Am	13
<i>cox1</i>	A1	E2	P2	E1	L22	L6	P1	L17	AV	L55	L36	L28	L66	L43	L14	A2	A3	Am	10
<i>atp6</i>	A1	E2	P2	E1	L22	L6	P1	L17	AV	L55	L36	L28	L43	L66	L14	A2	A3	Am	7

Main group

Sub-group

Table 21. Unique mtDNA fragment(s) of different cytoplasms

Enzyme-probe combination	Cytoplasms with unique band(s)	
	Cytoplasm	Unique fragment(s)
<i>Homologous probes</i>		
<i>Bam</i> HI-13.6kb	LSGP 66	(+1.8kb, +1.2kb)
<i>Heterologous probes</i>		
<i>Bam</i> HI- <i>atp6</i>	81A _m	(+7.3kb, +2.4kb)
	81A _v	(+24kb)
<i>Pst</i> I- <i>atp6</i>	81A _m	(-4.5kb)
	81A _v	(+18.5kb)
<i>Bam</i> HI- <i>cox1</i>	81A _m	(+7.4kb, +2.5k and -22.4kb)
	81A _v	(+24.0kb)
<i>Pst</i> I- <i>cox1</i>	81A _m	(-4.7kb)

+ indicates presence and - indicates absence of fragments that are unique in the indicated cytoplasm

Table 22. Differential mtDNA banding patterns¹ of different cytoplasms

Enzyme-probe combination	Cytoplasms with differential banding pattern
<i>Homologous probes</i>	
<i>Pst</i> I-4.7kb	LSGP 55 81A ₁ LSGP 66 81A _v
<i>Pst</i> I-9.7kb	81A ₁
<i>Heterologous probes</i>	
<i>Bam</i> HI-coxI	81B 81A ₁
<i>Hind</i> III-coxI	81A ₁ 81A _v 81B LSGP 28 LSGP 55
<i>Pst</i> I-coxI	81A ₁ 81A _v 81B LSGP 55 LSGP 66

¹Differential banding pattern means that many bands are involved in identifying the cytoplasm and no unique fragment(s) can characterize it.

Table 23. Effectiveness of various enzyme-probe combinations to distinguish different cms sources in pearl millet

Restriction enzyme-probe combination	Ability to distinguish between cms source pairs										¹ Overall effectiveness
	A ₁ -A ₂	A ₁ -A ₃	A ₁ -A _m	A ₁ -A _v	A ₂ -A ₃	A ₂ -A _m	A ₂ -A _v	A ₃ -A _m	A ₃ -A _v	A _m -A _v	
<i>Homologous probes</i>											
Bam HI-4.7kb	Yes	Yes	Yes	No	No	No	Yes	No	Yes	Yes	ME
Bam HI-13.6kb	Yes	Yes	Yes	No	No	No	Yes	No	Yes	Yes	ME
Hind III-4.7kb	Yes	Yes	Yes	No	No	No	Yes	No	Yes	Yes	ME
Hind III-10.9kb	Yes	Yes	Yes	No	No	No	Yes	No	Yes	Yes	ME
Pst I-4.7kb	Yes	Yes	Yes	Yes	No	No	Yes	No	Yes	Yes	E
Pst I-9.7kb	Yes	Yes	Yes	Yes	No	No	No	No	No	No	LE
<i>Heterologous probes</i>											
Bam HI- atp 6	Yes	Yes	Yes	Yes	No	Yes	Yes	Yes	Yes	Yes	VE
Bam HI- cox I	Yes	Yes	Yes	Yes	No	Yes	Yes	Yes	Yes	Yes	VE
Hind III- atp 6	Yes	Yes	Yes	Yes	No	No	Yes	No	Yes	Yes	E
Hind III- cox I	Yes	Yes	Yes	Yes	No	No	Yes	No	Yes	Yes	E
Pst I- atp 6	Yes	Yes	Yes	Yes	No	Yes	Yes	Yes	Yes	Yes	VE
Pst I- cox I	Yes	Yes	Yes	Yes	No	Yes	Yes	Yes	Yes	Yes	VE

¹ indicates the effectiveness of a particular enzyme-probe combination to differentiate cytoplasms of different sources
 VE = very effective, E = effective, ME = moderately effective and LE = least effective

Table 24. Similarity indices among pearl millet isonuclear cms lines based on mitochondrial DNA RFLP pattern

Isonuclear lines

	A ₁	0A ₂	1A ₂	A ₃	A _m	A _v	L6	L14	L17	L22	L28	L36	L43	L55	L66	E33	E15	P1	P2	
A ₁	1.00	0.71	0.71	0.71	0.63	0.88	0.90	0.73	0.91	0.98	0.79	0.79	0.85	0.74	0.80	0.99	0.99	0.91	0.99	
0A ₂		1.00	1.00	1.00	0.88	0.76	0.77	0.98	0.78	0.71	0.90	0.90	0.85	0.93	0.87	0.72	0.71	0.78	0.72	
1A ₂			1.00	1.00	0.88	0.76	0.77	0.98	0.78	0.71	0.90	0.90	0.85	0.93	0.87	0.72	0.71	0.78	0.72	
A ₃				1.00	0.88	0.76	0.77	0.98	0.78	0.71	0.90	0.90	0.85	0.93	0.87	0.72	0.71	0.78	0.72	
A _m					1.00	0.68	0.68	0.85	0.69	0.63	0.78	0.78	0.72	0.81	0.76	0.64	0.63	0.69	0.64	
A _v						1.00	0.92	0.78	0.93	0.88	0.83	0.83	0.87	0.76	0.80	0.89	0.88	0.93	0.98	
L6							1.00	0.79	1.00	0.92	0.87	0.87	0.91	0.78	0.81	0.91	0.90	1.00	0.91	
L14								1.00	0.80	0.73	0.92	0.92	0.87	0.95	0.89	0.74	0.73	0.80	0.74	
L17									1.00	0.91	0.85	0.85	0.90	0.76	0.82	0.92	0.91	1.00	0.92	
L22										1.00	0.81	0.81	0.85	0.77	0.80	0.99	0.98	0.91	0.99	
L28											1.00	0.98	0.93	0.92	0.93	0.80	0.79	0.85	0.80	
L36												1.00	0.93	0.90	0.95	0.80	0.79	0.85	0.80	
L43													1.00	0.85	0.88	0.83	0.85	0.90	0.83	
L55														1.00	0.85	0.75	0.74	0.76	0.75	
L66															1.00	0.81	0.80	0.85	0.81	
E33																1.00	0.99	0.92	1.00	
E15																	1.00	0.91	0.99	
P1																		1.00	0.92	
P2																				1.00

A₁ = 81A₁, 0A₂ = Pb 310A₂, 1A₂ = Pb 311A₂, A₃ = 81A₃, A_m = 81A_m, A_v = 81A_v, =ICMA88001, L6 = LSGP6, L14 = LSGP14, L17= LSGP17, L22 = LSGP22, L28 = LSGP28, L36 = LSGP36, L43 = LSGP43, L55 = LSGP55, L66 = LSGP66, E33 = EGP 33, E15 = EGP 15, P1 = Popn.var.1, P2 = Popn. var.2

identical patterns in few cases, but did not change the cytoplasmic classification obtained from mtDNA RFLP patterns. Therefore, restricted use of tDNA for cytoplasmic genome analysis is suggested even though the probes are specific to mitochondrial genome. The digested tDNA should be run on a longer gel to get better resolution of the fragments.

Presence of unique bands in 81A_m, and 81A_v in *Bam*HI-*coxI*, *Pst*I-*atp6* and *Bam*HI-*atp6* combinations clearly indicates that rearrangements in *atp6* and *coxI* genes/fragments have resulted in the origin of these cytoplasmic sources. On the other hand, rearrangement in *coxI* region of LSGP 55 and LSGP 66 might have resulted in distinct fragment patterns and fragments of different stoichiometry, thus indicating the possible role of *coxI* in their origin.

5.2 Experiment No. 2: Anther development and microsporogenesis in pearl millet iso-nuclear lines

Flowering represents the end result of many gene-controlled physiological processes, biochemical sequences and morphological events. The principle functions of a flower are: microspore and megaspore formation, pollen release and reception, guide male and female gametophyte development, gametic union and seed formation. All these follow time sequence-programmed gene-controlled functions. Breakdown of any one of these functions occurs due to mutation of the genes controlling them (Kaul and Murty, 1985). One such event causes male sex abolition/abortion and leads to male sterility.

In male sterility, the stamens develop but the sporogenous tissue is either mis- or mal-formed or develop normally, but microsporogenesis is impaired so that either the non-, mis- or mal-formations of pollen or its premature abortion occurs in otherwise normal homomorphic flowers. Hence, the pollen is either completely absent or nonfunctional, or extremely scarce. The abortion of microsporogenous cells may take place before, during or after meiosis. Thus, it predominantly includes premeiotic, meiotic and post-meiotic male-sterile mutants.

During the present study, anther development and microsporogenesis were cytologically compared in pearl millet male-sterile and -fertile isonuclear lines in order to locate the disturbances in microsporogenesis that lead to pollen abortion. In addition, pollen sterility was studied to ascertain the extent of pollen sterility and the stability of lines with respect to male sterility.

5.2.1 Pollen meiosis

Pollen meiosis was regular in all isonuclear A-lines and 81B, except Pb 406A, where a low frequency of PMCs showed anomalous meiosis. In Pb 406A₃ meiotic anomalies were observed from early prophase I till the end of meiosis and even at pollen grain formation. Some of these anomalies like absence of nucleolus, detachment of the chromatin from the nucleolus (Fig. 22A), presence of accessory chromosomes (Fig. 22B) and some univalents (Figs. 22C-E) were detected at early prophase I but could not be seen later suggesting the

degeneration of such PMCs at this stage. These anomalies contribute to pollen sterility was not confirmed as such anomalies were not observed in other male-sterile lines. However, consequences of some of the anomalies observed at anaphase I were seen in advanced meiotic stages with regard to unequal chromosomal disjunction at the late telophase (Figs. 22G-K and 22M-Q), reduced or increased number of chromosomes in the daughter cells at the dyad stage (Fig. 22S) and occurrence of multinucleate pollen grains (Figs. 22V-X). The fertility status of such PMCs could not be ascertained in all A-lines but these might have contributed to the pollen sterility in Pb 406A₃.

Low frequency (0.62%) of syncytes were also observed in Pb 406A₃ (Figs. 22-U) but the cause of their origin was not known. Syncyte formation may result either from (i) the failure of cytokinesis during archesporial mitosis (Smith, 1942; Pantulu and Manga, 1971), (ii) migration of the nucleus from one PMC to the other, as reported in *Triticum* (Kihara and Lilienfeld, 1934) and *Capsicum* (Habib and Chennaveeraiah, 1976) or (iii) fusion of uninucleate PMCs, facilitated by the absence or dissolution of the cell walls surrounding the PMCs. Most of the published cases of syncyte formation belong to the third group. In most of the reported cases of fusion syncyte formation, cell fusion was observed when the nuclear structure hardly imply the onset of meiosis (Mehra and Kalia, 1973) or at pachytene (Rao and Koduru, 1978a). Rao and Koduru (1978a) studied meiosis and microsporogenesis in the male-sterile inbred line IP 482 of *Pennisetum americanum* and assigned male

sterility to plasmodial tapetum, plasmodial PMCs (syncytes), delayed and asynchronous meiotic development, desynapsis and blockage of meiosis. Plasmodial syncytes were also detected in *Pennisetum* by Burton and Powell (1968) in some plants of the mutagen treated population. Pantulu and Manga (1971) reported the formation of plasmodial sporocytes as a result of the homozygous condition of the gene *mu* which suppresses cytokinesis during archesporial mitosis.

Meiotic arrest was also observed in majority of the syncytes of Pb 406A₃ somewhere at prophase I as was also described by Rao and Koduru (1978a) in pearl millet. They reported that in most of the syncytes, a blockage of meiosis occurred either during or after diakinesis, and a wall is formed around the cells leading to the formation of giant pollen grains. These pollen grains were sterile and yielded only a few seeds by selfing. In addition to these anomalies, trilobed anthers (Fig. 26M) were also observed before the onset of meiosis which could not be detected in advance meiotic stages indicating their (anthers) degeneration prior to the onset of meiosis. Anthers with unusual number of locules were also observed in male-sterile rye (*Secale cereale*) by Cebrat and Zadecka (1978). In the male-sterile line Zeelandzkie G3d (ms-HZ), instead of usual three anthers, flowers with four anthers having 2-10 locules were recovered. Initial anther development was similar to that of the fertile plants, but in most of them the sporogenous cells and anther wall layers differentiate abnormally. Such anthers mostly degenerate during early meiosis

(prophase I) and sometimes even before meiotic initiation.

The expression and frequency of all these meiotic anomalies varies from spikelet to spikelet within a spike and floret to floret within a spikelet. In fact, even anthers within a floret exhibit nonsynchronous morphological development (Figs. 26C and 26H) and delayed and highly asynchronous meiosis. In male-sterile plants of inbred IP 482 and Vg 272 of pearl millet, asynchronous meiosis within a floret was observed by Rao and Koduru (1978a).

In different studies on male sterility, it has been shown that sterility may or may not be associated with meiotic irregularities. For instance, some meiotic irregularities were observed in male-sterile *Crotalaria striata* (Kempana, 1960), sweet pepper (Novak, 1971), pearl millet (Rao and Koduru, 1978a). However, no meiotic abnormality were observed in pearl millet male-sterile lines by Balarami Reddy and Reddi (1974) and Sharma (1978). In the present study meiotic anomalies were observed only in Pb 406A₃. All these anomalies, if not the sole cause, must fractionally contribute towards the instability of this line and pollen sterility.

5.2.2 Anther development and microsporogenesis

Most of the cytological studies on male-sterile and male-fertile plants indicated role of tapetal development in pollen fertility. In several cases it has been shown that behavior of the tapetum differs in male-sterile and male-fertile plants. In male-sterile plants the tapetum persists and causes male sterility

Table 26. Frequency distribution of anthers with varying degrees of pollen fertility/sterility in isonuclear lines of pearl millet

Isonuclear lines	Season	Completely sterile anthers (%)	Completely fertile anthers (%)	Partially sterile / fertile anthers (%)	Empty anthers (%)
81B	hot dry	0.0	98.5	1.5	0.0
	cool dry	0.0	97.7	2.3	0.0
81A ₁	hot dry	97.9	0.1	0.8	1.2
	cool dry	89.0	0.1	9.7	1.2
81A _m	hot dry	97.7	0.8	0.3	1.2
	cool dry	93.1	1.4	4.7	0.8
81A _v	hot dry	81.7	0.3	15.5	2.5
	cool dry	77.1	1.8	19.4	1.7
Pb 310A ₂	hot dry	47.4	2.4	49.0	1.2
	cool dry	44.4	2.6	52.7	0.3
Pb 311A ₂	hot dry	32.7	7.5	58.8	1.0
	cool dry	31.8	6.8	61.0	0.4
Pb 406A ₃	hot dry	28.8	6.0	62.7	2.5
	cool dry	26.9	6.3	65.2	1.6

Table 27. Percent pollen fertility within line, within plant, and within spike of pearl millet isonuclear lines in hot dry (HD) and cool dry (CD) seasons of 1993-1994

Plant	Spike	81A ₁		81A _m		81A _v		Pb 310A ₂		Pb 311A ₂		Pb 406A ₃		81B	
		HD	CD	HD	CD	HD	CD	HD	CD	HD	CD	HD	CD	HD	CD
P 1	S1	6.3	9.4	0.4	6.3	1.5	6.3	6.6	7.4	9.8	11.9	9.4	19.8	99.8	99.4
	S2	0.9	8.7	4.7	10.1	2.8	8.1	13.8	13.8	17.6	17.9	12.1	27.1	99.9	99.7
	Average (P1)	3.7	9.0	2.6	8.3	2.1	7.2	9.5	10.0	13.8	15.0	10.7	23.3	99.9	99.6
P 2	S1	0.0	7.4	0.0	8.7	1.4	6.2	11.4	11.4	16.9	21.6	20.5	25.1	99.9	99.8
	S2	0.0	6.9	0.2	7.4	1.2	11.0	5.6	9.2	7.9	7.8	25.0	30.0	99.9	99.8
	Average (P2)	0.0	7.2	0.1	8.1	1.3	8.7	8.4	10.2	12.4	14.9	22.5	27.6	99.9	99.8
P 3	S1	1.1	7.8	2.0	4.9	2.8	5.4	6.1	9.6	17.2	24.8	10.8	22.4	99.8	99.5
	S2	0.0	5.0	0.0	1.0	1.2	4.5	11.4	13.1	8.0	22.1	37.8	43.7	99.8	99.8
	Average (P3)	0.6	6.6	0.9	2.8	2.1	5.0	8.4	11.1	12.9	23.5	25.7	33.9	99.8	99.7
P 4	S1	2.1	9.0	0.0	1.1	4.5	5.6	10.2	15.1	11.6	13.5	20.8	36.6	99.9	99.9
	S2	0.6	10.1	0.0	0.3	2.0	6.4	8.3	11.0	26.3	29.0	28.8	33.6	99.9	99.9
	Average (P4)	1.4	9.5	0.0	0.7	3.4	6.0	9.2	12.9	19.7	22.2	25.2	35.1	99.9	99.9
P 5	S1	0.0	11.0	1.4	2.0	1.2	2.9	13.3	16.0	18.1	19.2	13.1	17.9	100	99.9
	S2	0.9	6.8	0.0	0.5	8.5	8.5	5.9	7.9	9.1	9.1	13.6	17.0	100	100
	Average (P5)	0.5	9.0	0.8	1.3	5.0	5.7	9.2	11.6	13.3	14.0	13.4	17.5	100	99.9
Overall mean (i.e. % fertility within line)		1.3	8.2	0.9	4.3	2.7	6.5	9.0	11.2	14.4	18.0	19.4	27.2	99.9	99.8
% sterility within line		98.7	91.8	99.1	95.7	97.3	93.5	91.0	88.8	85.6	82.0	80.6	72.8	0.1	0.2

HD = hot dry season; CD = cool dry season

(Balarami Reddy and Reddi, 1974; Ohmasa *et al.*, 1976; Lee *et al.*, 1979; Murty 1982). The function of tapetum in relation to pollen fertility has been well defined by various workers. The tapetum is a layer of cells that envelops the sporogenous tissue in developing

Table 28. Stage(s) of tapetum degeneration in isonuclear A-lines of pearl millet

A-line	Stage of tapetum degeneration		
	Premeiotic degeneration	Degeneration during meiosis	Postmeiotic degeneration
81A ₁	-	-	Yes
Pb 310A ₂	-	Yes	Yes
Pb 311A ₂	-	Yes	Yes
Pb 406A ₃	Yes	-	Yes
81A _m	-	-	Yes
81A _v	-	Yes	Yes

angiosperm anthers. There is no direct vascular connection between the parent plant and the sporogenous cells, and all food and other materials must either pass through the tapetum, or be produced there, in order to reach the developing male reproductive cells. It is not surprising, therefore, that the tapetum often has been implicated when failure of microsporogenesis results in male sterility (Painter, 1943; Maheshwari, 1950; Chang, 1954; Overman and Warmke, 1972; Sharma, 1978). Tapetum development differed in many ways in A-lines as compared to 81B, and even within A-lines marked differences in its developmental pattern were noticed during this course of investigation. In 81A₁ and 81A_v tapetum persisted longer and was conspicuous at anther maturity, whereas, in Pb 406A₃ (during postmeiotic microspore degeneration) and A₂-lines it persisted till young microspore stage but abruptly turned into intratapetal syncytem (ITS) and lost its identity. These observations indicated that premeiotic degeneration of tapetum is quite uncommon and occurred only in Pb 406A₃ and postmeiotic tapetal degeneration was quite

habitual phenomenon of A-lines (Table 28). Majority of studies in most of the crops suggested that differences observed in the behavior of tapetum at post meiotic stages were responsible for pollen abortion e.g. in sorghum (Singh and Hadley, 1961; Alam and Sandal, 1967), maize (Chang, 1954; Ohamasa *et al.*, 1976; Lee *et al.*, 1979), carrot (Zenkteler, 1962), flax (Dubey and Singh, 1965), barley (Kaul and Singh, 1966), rapeseed, *Brassica campestris* L. (Hossain, 1989), and pearl millet (Sharma, 1978). In all these cases the tapetal cells persist or get hypertrophied even after the microspore formation. These microspores either die or develop into sterile pollen grains. Hossain (1989) suggested that delayed degeneration of the tapetal cells possibly block the flow of nutrients thus causing the sterility.

In addition to the tapetum, abnormal callose behavior in microsporocytes has been found to be related to cytoplasmic male sterility in sorghum by Damon (1961), Erichsen and Ross (1963) and Warmke and Overman (1972) and in petunia by Frankel *et al.* (1969). Regular callose deposition around PMCs during prophase I is a prerequisite for the initiation and completion of synchronous meiotic division (Eschrich, 1961; Heslop-Harrison, 1964; Frankel and Galun, 1977; Vijayaraghavan and Shukla, 1978). Callose deposition around the tetrads is equally essential for proper and autonomous transformation of the four products (microspores) of meiosis into normal young microspores. For achieving this, the callose covering around each PMC has to be degraded to cause microspore release from the tetrads. The degeneration

is brought about by the enzyme callase i.e. 1,3- β -glucanase (Heslop-Harrison, 1968; Rowley, 1969). The degradation products (d-glucose and its polymers of different lengths) are used in pollen-exine formation and pollen nutrition (Eschrich, 1964; Waterkeyn, 1964; Izhar and Frankel, 1971; Vijayaraghavan and Shukla, 1978). Initially all PMCs in an anther locule are interlinked through conspicuous plasmodesmata. Later on, during Meiosis I, the plasmodesmata are plugged with additional callose deposition. PMC is then almost isolated from the external environment because of the impermeability of callose to high molecular weight substances (Albertini, 1967; Southworth, 1971). Isolation of the sporogenous cell by callose wall is transient and a little after meiosis in PMCs (generally at the tetrad stage), tapetum mediated dissolution of this wall takes place (Eschrich, 1961; Mepham and Lane, 1969). It has been suggested that the callose wall protects the differentiating sporogenous cells from the harmful hormonal and nutritional influence of the surrounding vegetative cells (Godwin, 1968; De Halac and Harte, 1975) and also provides genetic autonomy to the meiocytes (Heslop-Harrison, 1966a,b and 1967). Callose production, accumulation, deposition, formation and timing activity of enzyme callase are all under the control of independently functioning major genes.

In the present study microsporogenesis and anther development were normal in 81B. PMC/microspore/pollen degeneration in A-lines occurred at different stages of anther development. Developing microspores degenerated

at premeiotic stages in about 55% of locules in Pb 406A₃ due to the formation of an intra- tapetal syncytium (ITS). In the other A-lines the majority of anther locules showed microspore degeneration during meiotic stages (Fig. 20): 81A₁ (81-86% at the dyad stage and 14-18% at the tetrad stage), Pb 310A₂ (40-44% at early anaphase I, 40-45% at late anaphase I and 12-14% at early telophase I), Pb 311A₂ (45-50% at early anaphase I, 42-45% at late anaphase I and 8-11% at early telophase I), 81A₁ (98% locules at telophase I), and 81A_m (99% of locules at tetrad stage). The cause of pollen abortion differed from line to line, floret to floret within a spikelet and in some cases even locule to locule within an anther. Each line followed its own anther developmental pattern. Postmeiotic degeneration was recorded in very few locules in each line (2% of locules in Pb 310A₂, 7-10% of locules in Pb 311A₂, 1-2% of locules in 81A₁ and 0.2-0.4% of locules in 81A_m) except in Pb 406A₃ where 40-45% of locules showed postmeiotic degeneration.

Though the anther development was similar in fertile and sterile plants through early meiotic metaphase I (except in Pb 406A₃ where PMCs degeneration occurred before the onset of meiosis in >50% of locules) and callose special wall formation. At this time, however, callose behavior diverges sharply in fertile and sterile anthers in some lines as discussed below.

5.2.3 PMC/Microspore/Pollen abortion

The callose behavior in fertile anthers (of 81B) was similar to the observations

of Warmke and Overman (1972) in male-fertile anthers of sorghum. The central callose mass splits into sectors along the planes of the original microsporocyte walls and comes to form a covering that effectively isolates the microsporocytes and young microspores. This special wall later dissolves to release the microspores from the tetrads (Fig. 23M). These microspores come in contact with tapetum (Fig. 23O) and are nourished to develop into healthy and fertile pollen grains (Figs. 23Q and 23R). The phase specific activity of callase enzyme varies in male-sterile types. In male-fertile lines, callase activity is at a peak at the late tetrad stage (Izhar and Frankel, 1971; Vijayaraghavan and Shukla, 1978). This was cytologically confirmed in 81B, but biochemical analysis was not carried out. In some CMS types no callase activity occurs in anthers and the microspores are not released from the tetrads (Izhar and Frankel, 1971; Vijayaraghavan and Shukla, 1978). However such a situation was not observed in any line during the present investigation. Significant differences between male-sterile and male-fertile sorghum anthers for callase formation and callase activity have been reported (Warmke and Overman, 1972).

In the present investigation callose breakdown was observed just before the dyad stage in 81A₁. Callose becomes fibrous (Fig. 24A) and forms amorphous mass at the center of the locule (Fig. 24D) which later on disappears. Two major differences observed in 81A₁ as compared to 81B were : (1) early callose breakdown, and (2) migration of young microspores towards

the interior of locule. The second condition might have resulted in starvation of young microspores because of loss of close association between the developing microspores and the tapetum. This is one of the most critical stage for pollen development as was observed in 81B. Warmke and Overman (1972) also suggested that most of the sporocytes in sterile anthers fail to come in close association with the tapetum during meiosis. Since sporocytes in fertile anthers lie close to the tapetum, this failure of association in sterile anthers could well contribute to nutritional disturbances. Thus, these two anomalies might have contributed towards pollen sterility in 81A₁. Delayed or precocious callase enzyme activity leading to late or early breakdown of callose disturbs microsporogenesis and leads to male sterility in many crop plants including sorghum (Overman and Warmke, 1972), *Phaseolus* (Pritchard and Hutton, 1972), and *Pisum* (Gottschalk and Kaul, 1974).

The tapetum developmental pattern in 81A₁ differed from 81B after the tetrad stage in terms of vacuolation, growth and persistence. Tapetum of fertile anthers gradually decreased in its thickness (Figs. 29a and 29b), was not vacuolated and stained densely near anther maturity (Fig. 23N) whereas that of 81A₁ remained highly vacuolated thus stained lightly and gradually increased in its thickness (Figs. 29a and 29b) towards pollen maturity and persisted longer.

In 81A₁, callose breakdown in most of the anther locules (81-87%) occurred at the dyad stage (Fig. 28A). Contrary to 81A₁, callose and

microspore degeneration almost occurred simultaneously indicating early callase activity coupled with some other biochemical events which led to the dissolution of the sporocyte walls. In the remaining locules, microspore degeneration occurred not because of the callose breakdown. The tapetum vacuolation and starvation due to loss of contact between developing microsporocytes and tapetum led to sporocytes degeneration (Fig. 28D). In addition, the tapetum thickness continued to increase towards anther maturity and persisted longer than 81B.

Pb 310A₂ and Pb 311A₂ followed four different paths of anther development, each had its own cause of microspore degeneration. It is difficult to pinpoint on single factor that could explain the sole cause of pollen sterility in all the lines. For example, in one of the four paths, cytoplasmic contraction/disruption at anaphase I followed by callose breakdown at the dyad stage might have contributed to the pollen sterility (Figs. 25A and 25B), and in the second path callose breakdown coupled with the tapetal hypertrophy after anaphase I (Fig. 25C) led to pollen abortion. One of the other two paths was exactly similar to 81A₁ (till telophase I in ≈13-15% of locules) in which callose breakdown at late telophase I and might have resulted in pollen abortion. The fourth path which occurred in 1.5-2% of locules, tapetal cytoplasmic mass turned into atypical fibrous mass (Fig. 25F) and pollen abortion occurred at the same time. This could be assigned to the inability of fibrous tapetum to supply nutrition to the developing microspores and starved

them to death. The transport of nutrients through tapetum might not have occurred due to disorganization of normal tapetal cytoplasm.

In Pb 406A₃ and 81A_m, callose breakdown was not involved in pollen abortion because in >55% of locules of Pb 406A₃, PMCs abortion occurred much before the onset of meiosis. This involved various forms of tapetal hypertrophy like enlargement of tapetal cells and intermixing of their cytoplasmic contents (Figs. 26A-C and 26F), vacuolation (almost with no visible cytoplasm) of tapetal cells (Fig. 26D) and disruption of tapetal cells due to imperfect differentiation of related tissues (Fig. 26L). These findings were similar to that of Sun and Ganders (1987) in Hawaiian *Bidens*. They also observed early abnormal vacuolation of tapetal cells during premeiotic period. The vacuolation increases rapidly to produce tapetal cells without cytoplasm and only nuclei are visible. as was also observed in the present study (Fig. 26D). The highly vacuolated tapetal cells press upon the sporogenous cells, ultimately both, the tapetum and sporogenous cells disorganize and disappear. Remaining 45% of locules of Pb 406A₃ exhibited normal anther development as that of 81B till release of the microspores from the tetrads. Thereafter abrupt formation of intratapetal syncytium (ITS) led to microspore degeneration (Figs. 26N-Q). Overman and Warmke (1972) also estimated that as many as 50% of the anthers may be affected by intratapetal syncytium in male-sterile sorghum.

It is generally believed that the tapetal cells play a major role in supplying nutrition to developing microspores by the degenerating tapetal cells

that constitutes the source of nutrients. But it is difficult to explain this phenomenon in respect of 81A_m in which no observable malfunctioning of tapetal cells was noticed i.e. the tapetal cells disintegrated to a greater extent as in 81B, still maintaining the male sterility in 81A_m. It therefore, appears that the persistence of tapetal cells is not necessarily associated with male sterility and, therefore, some abnormality other than the tapetal degeneration also exists in 81A_m leading to male sterility. Similar situation was observed by Balarami Reddy and Reddi (1974) in pearl millet male-sterile line, 628A, Albertsen and Palmer (1979) in soybeans (*Glycine max* (L.) Merr.), Arora and Gupta (1984) in *Crotalaria pallida* Ait., and Lee *et al.* (1980) in corn. However these investigations and similar studies undertaken by earlier researchers (Filion and Christie, 1966; Webster and Singh, 1964; Balarami Reddy and Reddi, 1974) suggested that endothecium also play a major role in pollen fertility, as the male-fertile lines possess very thin endothecium near maturity. No other reason could be assigned for pollen abortion in 81A_m except that it had very thick endothecium (Figs. 29c and 29d) even at anther maturity. Other unknown biochemical events may be involved which lead to degeneration of developing pollen grains in 81A_m.

Differences have also been reported in endothecial development in male-fertile and -sterile strains. It has been shown that thick endothecium gradually becomes attenuated to facilitate dehiscence in male-fertile sorghum (Webster and Singh, 1964), pearl millet (Balarami Reddy and Reddi

1970,1974), and *Cajanus cajan* (Dundas *et al.*, 1981) but in sterile material no such phenomenon was observed. Our results in 81B (fertile), 81A₁ and 81A_m are in agreement with these findings. In these A-lines endothecium thickness increased rapidly as anthers mature which contributed to the nondehiscence of anthers, whereas, in 81A₃ and Pb 311A₂, endothecium thickness declined near maturity. These two lines (81A₃ and Pb 311A₂) had higher pollen fertility than other A-lines in accordance with the findings of Pritchard and Hutton (1972) in *Phaseolus atropurpureus*.

In the present material, stickiness of pollen grains was observed at maturity in all A-lines with very low frequency (Figs. 34F and 34M). Pollen grains tend to adhere together when anthers are pressed to release them. This stickiness of pollen in sterile anther appears to result from the separation of the central callose mass (in which the cell walls are embedded) from the surface of sporocytes, thus leaving them without cellulose or callose walls (Warmke and Overman, 1972).

These studies clearly indicated that anther/pollen development is more irregular in Pb 406A₃. In 81A_m and 81A₁, more than 95% of anther locules followed a definite developmental path leading to pollen abortion. In other A-lines many developmental paths were observed within a line and pollen degeneration occurred at various stages. This leads to instability of male sterility in the A₂ and A₃ systems and better stability of male sterility in the A₁ and A_m systems. Rai (1993) evaluated the effect of five different CMS

sources (A_1 , A_2 , A_3 , A_m , and A_v) on pollen shedder frequency and selfed seed-set in hot dry and rainy seasons and they reported similar findings. They concluded that the A-lines with A_2 and A_3 system, in addition to having more pollen shedders, also had much higher degrees of self seed-set on apparently sterile plants than in $81A_1$, $81A_m$, and ICMA 88001. They further concluded that from the view point of sterility maintenance, the A_1 and A_m CMS systems are better than the A_v , A_2 and A_3 systems, at least in the nuclear background of 81B.

Our findings on pollen fertility/sterility observations indicated that pollen sterility of each A-line was more stable in the hot dry season as frequency of occurrence of fertile pollen was lower than in the cool dry season. Results of Rai (1993) are also in agreement with these findings. They also observed that the frequency of pollen shedders and degree of self seed-set, in general, was higher in the rainy season than in the hot season. These results imply the greater usefulness of the hot dry season for the maintenance of male-sterile lines and the greater usefulness of the cool dry or rainy season for evaluation and purification programs for male sterility maintenance.

The fertility of 81B was quite stable in both the seasons as it neither had completely sterile anthers nor the empty anthers, however partially fertile anthers occupied insignificant proportion of the total anthers examined. The frequency of completely sterile anthers was much higher in $81A_m$, and $81A_1$ than in other A-lines. Other lines ($81A_v$, Pb 310 A_2 , and Pb 406 A_3) also had

higher frequency of completely fertile/partially fertile anthers than 81A_m, and 81A₁. In addition 81A_v and Pb 406A₃ also had higher frequency of empty anthers. All these observations further support that 81A_m was the best followed by 81A₁ among the present material with respect to stability of male sterility.

It may, therefore be concluded that there are several events which determine cytoplasmic male sterility, for example, meiotic anomalies, tapetal hypertrophy, persistence of tapetum, endothecium thickness, anomalies in callose behavior etc. These events differ with respect to specific material and hence it is not possible to generalize the particular event as a cause of male sterility. This was also advocated by Edwardson (1970), Heslop-Harrison (1972), Laser and Larsten (1972), and Arora and Gupta (1984).

5.3 Experiment No. 3: Isozyme analysis of pearl millet tall/dwarf near-isogenic lines

Isolines of tall/dwarf near-isogenic pairs were identical for six of the 12 enzyme systems studied [ADH (SL), CAT (SL, 18 hIS), GDH (SL, DS), GOT (SL, DS, 18 hIS), 6-PGD (SL, DS, 18 hIS) and SKDH (DS, 18 hIS, SL)]. Some of these [ADH (18 hIS) and GDH (18 hIS)] also showed polymorphism within pairs using other sources. Among all the enzymes studied, ADH (18 hIS) and EST (18 hIS) were most effective in determining within and between pairs variation (each enzyme showed within pair variation in five pairs).

The 12 enzyme systems studied displayed their 95 isozymic forms ranging from one for LDH and CAT to 30 in EST (Table 29). Twenty eight of 95 bands were common in all 7 pairs and 24 were present frequently (i.e., in >65% of isolines). Twenty four bands were rare in all the isolines considering all enzymes together (ranging from none for GDH, LDH, 6-PGD and SOD to seven for EST). Three enzyme systems (ADH, EST and SKDH) contributed 60% (57 of 95 bands) of the total bands and about 67% (16 of 24 bands) of the rare bands, thus, indicating their significance in determining the degree of isogenicity of T/D NILs in the present study.

Critical perusal of Table 30 (isozyme spectrum for 12 enzyme systems) reveals that out of seven near-isogenic pairs, three most polymorphic pairs are EC3, MC6, and NC12. Banding pattern of these pairs for enzymes showing polymorphism in either of the pair is given in Table 30. Pairs EC3 and NC12 are equally polymorphic (17 of 25 bands are polymorphic). Two (one each from ADH and EST) of the 35 bands were polymorphic in all the pairs and nine bands showed polymorphism in either two of three pairs. In general, tall isolines are represented by the presence of higher number of bands than their corresponding dwarf isolines. Based upon similarity index values (Table 31) calculated from presence and absence of bands, most isogenic pair was MC9 (SI = 0.98), followed by pairs EC1 (SI = 0.97), and EC2 and MC10 (SI = 0.96). Three most polymorphic pairs had SI = 0.85 (EC3), 0.86 (NC12), and 0.87 (MC6). It clearly shows that isolines of these pairs are still segregating for

Table 29. Distribution of bands with respect to isozyme spectrum in tall/dwarf near-isogenic pairs of pearl millet.

Enzyme*	Number of bands			
	Total	Common in all pairs	Frequent ¹	Rare ²
ADH	13	2	5	4
CAT	1	1	0	0
EST	30	2	10	7
GDH	7	5	0	0
GOT	4	3	0	1
LDH	1	0	0	0
MDH	6	2	1	3
ME	7	3	1	2
PGI	5	0	2	2
6-PGD	4	4	0	0
SKDH	14	4	4	5
SOD	3	2	1	0
Total	95	28	24	24
12				

1 = Band present in more than 65% of lines (i.e., 8 to 13 lines).

2 = Band present in 1 to 3 lines.

* Total number of bands (i.e. number of bands in seedlings + dry seeds + 18h imbibed seeds) excluding those of same Rf value.

many loci.

Dendrogram constructed based on similarity index values reveals MC and NC T/D NILs form three separate groups at 84%, 86% and 85% similarity levels (Fig. 61). EC and MC clusters join to form single cluster at SI = 0.83 and NC pair joins at SI = 0.82. This also indicates that NC pair is the most divergent among the material under study.

Near-isogenic pairs of EC were derived from Indian origin, MC from Indian x African origin and NC from African origin. But our data does not provide any evidence that these groups differ from each other (looking at the mean similarity values within pairs; EC pairs = 0.927, MC pairs = 0.937) as the rate of approaching homozygosity is almost same in EC and MC pairs. But it needs mention that one pair of NC may not be the true representative and moreover, one pair each from EC3 and MC6 were as polymorphic as the NC pair. This implies that these three pairs might have been derived from relatively more heterozygous BC_3F_8 progenies than other pairs. Possibility of any kind of mechanical mixture cannot be ruled out but the phenotypic observations at two locations (CCS Haryana Agricultural University, Hisar and ICRISAT Asia Center, Patancheru) indicated absence of off-types in these pairs. This further strengthens our assumption of existence of more number of segregating loci in these diverse pairs. Dendrogram supports the origin of these T/D NILs as it forms three major clusters, one each of EC, MC and NC pairs (Fig. 61). It further shows that EC pairs are more closer to MC pairs

than NC pair, i.e., NC is the most divergent. This is also in agreement with the parentage of these composites.

Despite the fact that near-isogenic pairs have been subjected to nine cycles of selfings, these pairs still show variations for morphological traits (Appendix I) (Rai and Rao, 1991). Their study showed that these variations were not consistent over the environments. Most of the traits recorded for each pair showed significant differences between tall and dwarf isolines. Looking at the isozyme banding pattern within pairs, four pairs (EC1, EC2, MC9 and MC10) look quite similar (nearly-isogenic) based upon the similarity percentage. However, in field conditions these pairs showed significant differences within pairs for most of the morphological traits recorded. For example, significant differences for head length were observed between isolines of all these pairs, and for head girth in EC1, EC2 and MC9. Isolines of EC1 and EC2 also differed for tillers plant⁻¹ and 100 seed weight, for which NC12 isolines also showed significant differences. EC1 and MC9 isolines recorded differences for days to 50% flowering and also marked differences were observed for grain yield in EC2 and MC9 isolines. This clearly demonstrates that the variations observed at phenotypic level might resulted due to some other segregating loci still prevalent in these pairs which were not detected in the present investigation.

After nine generations of selfing, we expect $\approx 100\%$ homozygosity in any genotype. But the isozymes studied for 12 enzymes indicated that the expected

homozygosity has not been achieved, three pairs even show <88% homozygosity (Table 31). Our observations further suggests that NC12 might had comparably more number of alleles in the heterozygote state than EC1, EC2, MC9 and MC10 pairs as the rate of increase in homozygosity might be slow in NC pair as compared to the above stated EC and MC pairs. There could be following reason(s): (1) mechanical mixture at any stage, (2) preferential union of gametes, and (3) plants selected in advance selfing generation might not be of the desired type (tall or dwarf) which were selfed to get later generations.

Although no definite trend was observed for the presence or absence of all isozyme bands in T/D NILs, (i.e., band present in tall version of EC3 was not always present in the tall version of MC6 and NC12) yet, it needs mention that one ADH band (Rf. 0.148) of very light intensity was present in all the tall isolines of these three pairs and absent in the dwarfs, thus, indicating the possibility of its linkage with d_2 gene. But it could be a matter of chance and its presence might have not been detected in the dwarf isolines due to its low intensity. Two ADH (Rfs. 0.078 and 0.101) and three EST (Rfs. 0.417, 0.533 and 0.642) bands showed their presence in at least two of tall isolines and found absent in their dwarf versions whereas the situation was just reverse for other three isozymes of EST (Rfs. 0.728, 0.769 and 0.783). Thus, analyzing the available data, linkage relationship cannot be established between d_2 dwarfing gene and any of the enzymatic marker. However, Tostain (1985) observed linkage relationship between d_2 dwarfing gene and the loci coding for ADH-A

and SKDH-A. There may be a possibility of breakdown of these linkages due to recombinations during nine generations of selfings in the present material. Moreover the electrophoretic conditions (eg. pH of the electrophoretic buffer) and source material (dry seeds) were different from what we used. It has been shown in their case that pH of the running buffer affects the resolution of ADH bands between the crosses. They could detect only a thick SKDH band whose mobility was reported to be different in different genotypes, instead, we were able to further resolve it into several bands (Figs. 48a-c) under different electrophoretic conditions and using different source materials. Also Tostain could show existence of this linkage in only one cross that too in back cross generation. In present investigation, the consistent presence of an ADH band (Rf. 0.148) in tall isolines of three most polymorphic pairs indicates that there might have existed some linkage between d_2 and *Adh* gene.

It was observed that, more than 50% of the polymorphic bands (in three most polymorphic pairs) had low to very low intensity. This suggests that the major differences within the pairs are due to faint bands. Therefore, based on the present findings, it is suggested that the four nearly-isogenic pairs (EC1, EC2, MC9 and MC10) needs a few more selfings and further testings are required in number of environments to examine the effect of d_2 gene on morphological and yield contributing traits.

Table 30. Isozyme spectrum of twelve enzyme systems in tall/dwarf near-isogenic pairs of pearl millet.

Tall/dwarf near-isogenic pair								Tall/dwarf near-isogenic pair									
Rf	EC			MC			NC	Rf	EC			MC			NC		
	1	2	3	6	9	10	12		1	2	3	6	9	10	12		
(1) 0.256	-	-	+	+	-	-	-	(9) 0.047	+	+	+	+	-	+	+	+	-
0.265	+	+	+	+	-	+	+	0.078	-	-	+	+	-	+	+	+	-
0.274	-	-	-	+	-	-	-	0.101	+	+	+	+	+	-	-	-	-
0.287	+	+	+	-	+	+	+	0.148	-	-	-	+	-	-	-	-	+
0.297	+	+	+	-	-	-	-	0.279	+	+	+	+	+	+	+	+	+
0.304	-	-	-	+	+	+	+	0.492	+	+	+	+	+	+	+	+	-
0.317	+	+	+	+	+	+	+	0.531	+	+	+	+	+	+	+	+	+
0.327	+	+	+	+	+	+	+	0.562	-	-	-	+	-	-	-	-	+
0.340	-	-	-	-	-	-	+	0.625	+	+	+	+	+	+	+	+	-
0.366	-	-	-	-	-	-	+	0.648	+	+	+	+	-	+	+	+	+
0.438	-	-	-	-	-	-	+	0.672	-	-	-	-	-	-	-	-	+
0.457	+	+	+	-	-	+	+	(10) 0.311	+	+	+	+	+	+	+	+	+
0.484	+	+	+	+	+	+	+	0.475	+	+	+	-	+	+	-	-	-
(2) 0.090	+	+	+	+	+	+	+	0.696	+	+	+	+	+	+	+	+	+
0.109	+	+	+	+	+	+	+	(11) 0.101	+	+	+	+	+	+	+	+	+
(3) 0.209	-	+	-	-	-	-	-	(12) 0.120	+	+	+	+	+	+	+	+	+
0.254	+	+	-	+	-	-	-	0.144	-	-	-	-	-	-	-	-	+
0.418	+	+	+	+	+	+	+	0.184	+	+	+	+	+	+	+	+	+
0.440	+	+	+	-	-	-	+	0.280	+	+	+	+	+	+	+	+	+
0.492	+	+	+	+	-	+	+	(13) 0.140	+	+	+	+	+	+	+	+	+
0.515	-	-	-	-	+	+	-	0.234	+	+	+	+	+	+	+	+	+
0.522	-	-	-	-	-	-	+	0.250	+	+	+	+	+	+	+	+	+
0.533	+	+	+	+	+	+	-	0.265	+	+	+	+	+	+	+	+	+
0.552	+	+	+	+	+	+	+	(14) 0.464	+	+	+	+	+	+	+	+	+
0.597	+	+	+	-	-	-	+	0.514	+	+	+	+	+	+	+	+	+
0.608	-	-	-	-	+	+	+	0.543	-	-	+	-	-	-	-	-	+
0.634	+	+	+	+	-	+	+	0.582	-	-	+	-	-	-	-	-	-
0.642	-	-	-	-	+	+	+	0.600	+	+	-	-	+	+	+	+	+
0.657	-	-	-	-	-	-	+	0.614	+	+	-	+	+	+	+	+	+
0.672	+	+	+	+	+	+	+	(15) 0.080	+	+	+	+	+	+	+	+	+
0.701	+	+	+	+	-	-	+	0.113	-	-	-	-	-	-	-	+	+
0.728	+	+	+	+	-	-	+	0.254	+	+	+	+	+	+	+	+	+
0.746	+	+	+	+	-	+	+	0.358	-	-	-	+	-	-	-	-	-
0.757	+	+	+	+	-	-	-	(16) 0.079	+	+	+	+	+	+	+	+	+
0.769	-	-	-	-	+	+	+	0.142	+	+	+	+	+	+	+	+	+
0.783	-	-	-	-	+	+	+	0.283	+	+	+	+	+	+	+	+	+
0.795	-	-	-	-	+	+	+	0.346	+	+	+	+	+	+	+	+	+
0.810	-	+	-	-	+	+	+	0.362	+	+	+	+	-	-	-	-	-
(4) 0.215	+	+	+	+	+	+	+	0.401	-	-	-	-	-	-	+	-	-
0.246	-	-	+	-	-	-	-	0.433	-	+	-	-	-	-	-	-	-
0.277	+	+	+	+	+	+	+	(17) 0.417	-	-	-	+	-	-	-	-	+
0.300	-	-	+	-	-	-	-	0.429	-	-	-	-	-	-	-	-	+
(5) 0.090	+	+	+	+	+	+	+	0.458	-	-	-	-	-	-	-	-	+
(6) 0.242	+	+	+	+	+	+	+	0.483	+	+	+	+	+	-	-	-	+
(7) 0.273	+	+	+	+	+	+	+	0.500	+	+	+	+	+	+	-	-	+
(8) 0.240	+	-	+	-	+	+	+	0.533	-	-	-	-	+	+	+	+	+
(9) 0.031	-	-	+	-	-	-	-	0.550	-	-	-	-	-	+	+	+	-
								(18) 0.112	+	+	+	+	+	+	+	+	+
Total bands present:								60	60	64	59	58	60	68			
No. of common bands:								57	55	47	45	56	55	51			
No. of uncommon bands:								3	5	17	14	2	5	17			

+ - indicates polymorphic bands

(1) = SKDH (18hIS); (2) = GDH (SL); (3) = EST (18hIS); (4) = PGI (DS); (5) = CAT; (6) = SKDH (SL); (7) = ADH (SL); (8) = PGI (SL); (9) = ADH (18hIS); (10) = SOD (SL); (11) = GDH (DS); (12) = GOT; (13) = 6-PGD (SL); (14) = MDH (DS); (15) = GDH (18hIS); (16) = ME (SL); (17) = EST (SL/DS); (18) = LDH

Table 31. Banding pattern of three most polymorphic tall/dwarf near-isogenic pairs of pearl millet

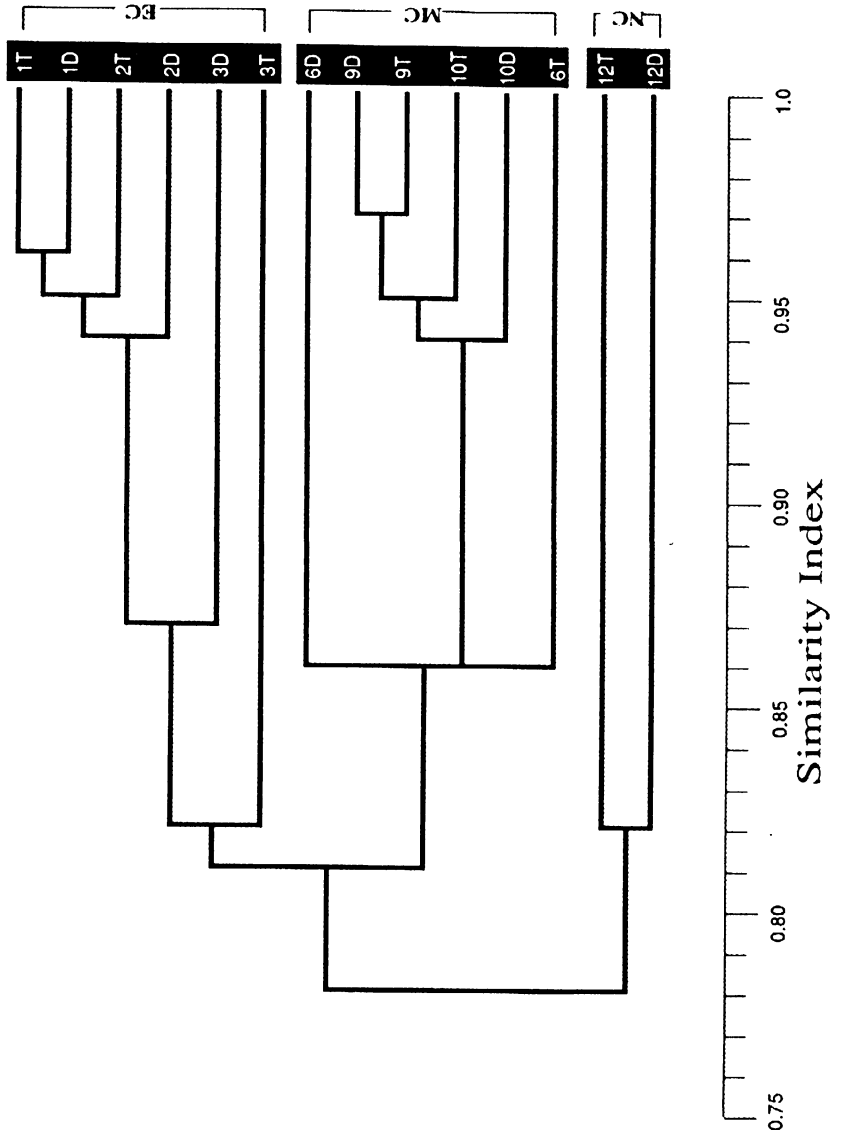
		Tall/dwarf near-isogenic pairs					
Enzyme	Rf	EC3		MC6		NC12	
		Tall	Dwarf	Tall	Dwarf	Tall	Dwarf
ADH (18hIS)	0.047*	o	+	o	+	-	-
	0.078*	+	o	+	o	-	-
	0.101*	+	+	+	o	+	o
	0.148**	+	o	+	o	+	o
	0.279	+	+	+	+	+	-
	0.492	-	+	+	+	-	-
	0.562	+	-	-	-	+	+
	0.625	-	+	+	+	-	-
	0.672	+	-	-	-	+	+
	EST (SL/DS)	0.417**	o	+	+	o	+
	0.429	-	-	-	-	+	-
	0.483	+	+	+	+	-	+
	0.500	+	+	-	+	-	-
	0.533*	-	-	+	o	+	o
EST (18hIS)	0.418	+	+	+	-	+	+
	0.597	-	-	-	-	-	+
	0.608	-	-	+	+	+	-
	0.642*	-	-	+	o	+	o
	0.701*	+	+	+	o	o	+
	0.728*	+	+	o	+	o	+
	0.746	+	+	-	+	+	+
	0.769*	-	-	o	+	+	o
	0.783*	-	-	o	+	+	o
	0.795	-	-	-	-	+	-
GDH (18hIS)	0.113	-	-	-	-	+	-
	0.242	-	+	+	+	+	+
	0.358	+	-	-	-	-	-
MDH (DS)	0.543	+	-	-	-	-	-
	0.600	-	+	+	+	+	+
	0.614	+	-	-	-	-	-
PGI (SL/18hIS)	0.240	-	-	+	+	-	+
PGI (DS)	0.215	-	+	+	+	-	+
	0.246	+	-	-	-	-	-
	0.277	-	+	+	+	+	+
	0.300	+	-	-	-	-	-
Total		17	16	18	16	20	13
	35		25		24		25
No. of polymorphic bands			17		14		17

Table 32. Similarity index values between seven tall/dwarf near-isogenic pairs based upon isozyme spectrum of twelve enzyme systems in pearl millet.

Tall/dwarf near-isogenic pairs													
Early composite				Medium composite					Nigerian composite				
1T	1D	2T	2D	3T	3D	6T	6D	9T	9D	10T	10D	12T	12D
1T	1.00	0.97	0.96	0.77	0.89	0.80	0.84	0.81	0.83	0.91	0.80	0.70	0.79
1D		1.00	0.92	0.76	0.89	0.80	0.83	0.82	0.80	0.79	0.91	0.71	0.79
2T			1.00	0.96	0.87	0.77	0.81	0.80	0.80	0.79	0.79	0.69	0.77
2D				1.00	0.84	0.77	0.80	0.78	0.79	0.78	0.77	0.67	0.76
3T				1.00	0.85	0.70	0.67	0.67	0.67	0.66	0.66	0.65	0.69
3D					1.00	0.80	0.81	0.79	0.79	0.77	0.77	0.69	0.73
6T						1.00	0.87	0.84	0.84	0.80	0.81	0.71	0.75
6D							1.00	0.87	0.87	0.84	0.84	0.73	0.76
9T								1.00	0.98	0.95	0.96	0.79	0.74
9D									1.00	0.97	0.94	0.78	0.74
10T										1.00	0.96	0.80	0.74
10D											1.00	0.83	0.76
12T												1.00	0.86
12D													1.00

1T = tall and 1D = dwarf isolines of pair EC1; 2T = tall and 2D = dwarf isolines of pair EC2 and so on.....

Figure 61. Dendrogram of cluster analysis of the combined three Early Composites (EC), 3 Medium Composites (MC), and 1 Nigerian Composite (NC) tall/dwarf near-isogenic pairs of pearl millet



SUMMARY

Pearl millet [*Pennisetum glaucum* (L.) R.Br.] provides staple food for millions of rural masses in semi-arid regions of Asia and African subcontinents where food supplies depend largely on the vagaries of the rain. The availability of male sterility particularly cytoplasmic-genetic male sterility (CMS) and utilization of d_2 dwarfing genes in the development of semi-dwarf male sterile and restorer lines made possible to develop elite commercial hybrids in pearl millet. The conventional method of classifying CMS lines on fertility restoration patterns is cumbersome and time consuming. Restriction fragment length polymorphism (RFLP) of mitochondrial (mt) DNA provides a rapid and effective method to assess heterogeneity among male-sterile cytoplasms. With this objective, six isonuclear A-lines (81A₁ with Tift 23A₁ cytoplasm, ICMA 88001 (= 81A_v) with *violaceum* cytoplasm, 81A_m (= 81A₄) with *monodii* = *violaceum* cytoplasm, Pb 310A₂ and Pb 311A₂ with A₂ cytoplasm, and Pb 406A₃ with A₃ cytoplasm), nine male-sterile lines from Large-seeded Genepool (LSGP 6, LSGP 14, LSGP 17, LSGP 22, LSGP 28, LSGP 36, LSGP 43, LSGP 43, LSGP 55 and LSGP 66) and two CMS lines each from Early Genepool (EGP 1 and EGP 2) and Population Varieties (PV 1 and PV 2) were characterized for variation in their mitochondrial genomes following Southern blot hybridizations using homologous (pearl millet 13.6 kb, 10.9 kb, 9.7 kb and 4.7 kb clones) and heterologous (maize *atp6* and *coxI* clones) mtDNA probes. Following cluster analysis based on similarity indices for the RFLP banding patterns observed, we identified seven cytoplasmic groups from the LSGP. Of the LSGP cytoplasms, LSGP 43, LSGP 55 and LSGP 66 were most diverse. This clearly indicates that besides serving as a source of diversity for agronomic and adaptation traits, broad-based gene pools can also provide diverse sources of cytoplasmic male sterility.

Microsporogenesis and Anther Development in Pearl Millet Isonuclear Lines was also studied in six isonuclear A-lines (stated above). The 81B was used as a male-fertile control. Observations on meiosis, anther development and microsporogenesis were recorded in cool dry season (CDS) and hot dry season (HDS)

of 1993/94 at ICRISAT Asia Center. Meiosis was regular in all isonuclear A- lines and 81B, except Pb 406A₃ where a low frequency of pollen mother cells (PMCs) showed anomalous meiosis. Microsporogenesis and anther development were normal in 81B. PMC/microspore/pollen degeneration in the six A-lines occurred at different stages of anther development. Developing microspores degenerated at premeiotic stages in about 55% of locules in Pb 406A₃ due to the formation of an intra-tapetal syncytium (ITS). In the other A-lines microspore degeneration occurred during meiotic stages in most anther locules. The cause of pollen abortion differed from line to line, from floret to floret within a spikelet, from anther to anther within a floret, and in some cases even from locule to locule within an anther. Postmeiotic degeneration was recorded in very few locules in each line except in Pb 406A₃ where it occurred in 40-45% of locules. The tapetum attained its maximum thickness at the tetrad stage in most of the isonuclear lines. It was maximum in 81B but reduced drastically and nearly disappeared at anther dehiscence. However in 81A₁ the tapetum was still conspicuous but declined in 81A_m as anthers matured. Further, tapetal cells of 81A_m were not vacuolated and lost their identity at anther maturity. Tapetum thickness continued to increase after the tetrad stage in male-sterile lines having the A₂ and A₃ cytoplasm and the tapetum persisted until anther maturity. The tapetal cells lost their identity because of ITS formation. The endothecium was well developed in all seven isonuclear lines at early stages of anther development. In 81B it attained its maximum thickness at the dyad stage then decreased in thickness as microspores matured, facilitating anther dehiscence. In 81A₁ and 81A_m endothecium thickness increased rapidly as anthers matured. The increase in endothecium thickness might have contributed to the nondehiscence of anthers in these A-lines. In Pb 406A₃ and Pb 311A₂ endothecium thickness declined after the dyad/tetrad stage. Pollen fertility of these two lines was also higher than other A-lines where the endothecium was thicker. Anther epidermis thickness and its growth pattern remained more or less the same in all seven isonuclear lines. The anther middle layer did not follow any consistent developmental pattern in any of the seven isonuclear lines. Anther lobes of 81B were wider than those of its isonuclear A-lines at all growth stages in both the seasons. The developing fertile microspores must exert considerable pressure on anther walls resulting in expansion of the anther lobe and thereby increasing its

diameter. In A-lines the anther lobe was compressed/shrivelled at maturity. These studies clearly indicated that anther/pollen development is more irregular in Pb 406A₃. In 81A_m and 81A₁, more than 95% of anther locules followed a definite developmental path to pollen abortion. In the other A-lines many developmental paths were observed within the line and pollen degeneration occurred at various stages. This could be one of the reasons for greater instability of male sterility in the A₂ and A₃ systems and greater stability of male sterility in the A₁ and A_m systems. Pollen fertility observations were recorded on 5 plants of each line in both seasons. For each plant we used two spikes with 10 spikelets/spike, 3 florets/spikelet and 3 anthers/floret, leading to 180 anthers per plant and 900 anthers per line. Large variation for pollen fertility was observed among spikelets within a spike, among florets within a spikelet, and among anthers within a floret, ranging from 0 - 100% fertility in all the isonuclear A-lines. In general, pollen fertility in all the isonuclear A-lines was low in the hot dry season (0.9-19.4%) and relatively high in cool dry season (4.3-27.2%). A large proportion of anthers were completely sterile in 81A_m (93-98%) and 81A₁ (89-98%). In 81A₂, the frequency of completely sterile anthers was comparatively less (77-82%). In Pb 310A₂, Pb 311A₂ and Pb 406A₃ these frequencies decreased to 27-48%, but partially fertile anthers (mixture of fertile and sterile pollens) were >50% in both seasons. Very low frequencies of empty anthers were also recorded in all A-lines, maximum being observed in 81A₂ and Pb 406A₃ (2-3%). We have also compared seven pairs of tall and dwarf near-isogenic lines from three composites (3 from EC, 3 from MC and 1 from NC) for 12 enzyme systems using polyacrylamide gel electrophoresis. Enzyme systems compared were alcohol dehydrogenase (ADH), catalase (CAT), esterase (EST), glutamate dehydrogenase (GDH), glutamate oxaloacetate transaminase (GOT), lactate dehydrogenase (LDH), malate dehydrogenase (MDH), malic enzyme (ME), phosphoglucoisomerase (PGI), 6-phosphogluconate dehydrogenase (6-PGD), shikimate dehydrogenase (SKD), and superoxide dismutase (SOD). Isolines of tall/dwarf near-isogenic pairs were identical for six of the 12 enzyme systems studied [ADH (SL), CAT (SL, 18 hIS), GDH (SL, DS), GOT (SL, DS, 18 hIS), 6-PGD (SL, DS, 18 hIS) and SKDH (DS, 18 hIS, SL)]. Among all the enzymes studied, ADH (18 hIS) and EST (18 hIS) were most effective in determining within and between pairs variation (each enzyme showed within pair

variation in five pairs). The 12 enzyme systems studied displayed their 95 isozymic forms ranging from one for LDH and CAT to 30 in EST. Twenty eight of 95 bands were common in all 7 pairs and 24 were present frequently (i.e., in >65% of isolines). Twenty four bands were rare in all the isolines considering all enzymes together (ranging from none for GDH, LDH, 6-PGD and SOD to seven for EST). Three enzyme systems (ADH, EST and SKDH) contributed 60% (57 of 95 bands) of the total bands and about 67% (16 of 24 bands) of the rare bands, thus, indicating their significance in determining the degree of isogenicity of T/D NILs in the present study. Isozyme spectrum for 12 enzyme systems revealed that out of seven near-isogenic pairs, three most polymorphic pairs are EC3, MC6, and NC12. Pairs EC3 and NC12 were equally polymorphic (17 of 25 bands are polymorphic). In general, tall isolines are represented by the presence of higher number of bands than their corresponding dwarf isolines. Based upon similarity index (SI) values calculated from presence and absence of bands, most isogenic pair was MC9 (SI = 0.98), followed by pairs EC1 (SI = 0.97), and EC2 and MC10 (SI = 0.96). Three most polymorphic pairs had SI = 0.85 (EC3), 0.86 (NC12), and 0.87 (MC6). It clearly shows that isolines of these pairs are still segregating for many loci. Dendrogram constructed based on similarity index values reveals MC and NC T/D NILs form three separate groups at 84%, 86% and 85% similarity levels. EC and MC clusters join to form single cluster at SI = 0.83 and NC pair joins at SI = 0.82. This also indicates that NC pair is the most divergent among the material under study. Dendrogram supports the origin of these T/D NILs as it forms three major clusters, one each of EC, MC and NC pairs. It further shows that EC pairs are more closer to MC pairs than NC pair, i.e., NC is the most divergent. Therefore, based on the present findings, it is suggested that the four nearly-isogenic pairs (EC1, EC2, MC9 and MC10) needs a few more selfings and further testings are required in number of environments to examine the effect of d_2 gene on morphological and yield contributing traits.

VI LITERATURE CITED

- ✓ Aken'Ova, M.E. (1985). Confirmation of a new source of cytoplasmic-genic male sterility in bullrush millet [*Pennisetum typhoides* (L.) Leeke]. **Euphytica** 34:34-38.
- ✓ Aken'Ova, M.E. and Chheda, H.R. (1981). A new source of cytoplasmic-genic male sterility in pearl millet. **Crop Sci.** 21:984-985.
- ✓ Alam, S. Sandal, P.C. (1967). Cytohistological investigations of pollen abortion in male sterile sudangrass. **Crop Sci.** 7:587-589.
- Albertini, L. (1967). Etude autoradrogaphiques des synthèses de protéines au cours de microsporogenèse chez le *Rhoeo discolor*. **C.R. Acad. Sci. (Paris)** 264D:2773.
- Albertsen, M.C., Palmer, R.G. (1979). A comparative light and electron microscopic study of microsporogenesis in male sterile (ms_1) and male fertile soybeans *Glycine max* (L.) Merr. **Am. J. Bot.** 66:253-265.
- ✓ Alexander, M.P. (1969). Differential staining of aborted and the nonaborted pollen. **Stain Technology** 44(3):117-122.
- Alexander, M.P. (1980). A versatile stain for pollen, fungi, yeast and bacteria. **Stain Technology** 55(1):13-18.
- ✓ Anand Kumar and Andrews, D.J. (1984). Cytoplasmic male sterility in pearl millet [*Pennisetum americanum* (L.) Leeke]-A Review. **Advances in Applied Biology** 10:113-143.
- Anand Kumar, Andrews, D.J., Jain, R.P. and Singh, S.D. (1984). Registration of parental lines. **Crop Sci.** 24:832-833.
- Anand Kumar, Jain, R.P. and Singh, S.D. (1983). Downy mildew reaction of pearl millet lines with and without cytoplasmic male-sterility. **Plant Dis.** 67:663-665.
- ✓ Anonymous (1993). Agricultural statistics at a glance. Directorate of Economics and Statistics, Department of Agriculture and Cooperation, Ministry of Agriculture, Government of India, March 1993. p.19.

- Anonymous (1994). Agricultural statistics at a glance. Directorate of Economics and Statistics, Department of Agriculture and Cooperation, Ministry of Agriculture, Government of India.
- Appa Rao, S., Mangesha, M.H., and Rajagopala Reddy, C. (1986). New sources of dwarfing genes in pearl millet (*Pennisetum americanum*). **Theor. Appl. Genet.** 73:170-174.
- Appadurai, R., Raveendran, T.S. and Nagarajan, C. (1982). A new male-sterility system in pearl millet. *Indian J. Agric. Sci.* 52:832-834.
- Arora, D.K. and Gupta, P.K. (1984). Microsporogenesis in male sterile and male fertile *Crotalaria pallida* Ait. **Cytologia** 49:685-690.
- Avdulov, N.P. (1931). Karyo-systematic investigations in the family Gramineae. **Bull. Appl. Bot. Genet. Plant Breed.**, Suppl. 43 (Russian).
- Bailey-Serres, J., Hanson, D.K., Fox, T.D. and Leaver, C.J. (1986). Mitochondrial genome rearrangement leads to extension and relocation of the cytochrome c oxidase subunit I gene in sorghum. **Cell** 47:567-576.
- Balarami Reddy, and Reddi, M.V. (1970). Studies on the breakdown of male-sterility and other related aspects in certain cytoplasmic male sterile lines of pearl millet (*Pennisetum typhoides* S. and H.). **Andhra Agric. J.** 17:173-180.
- Balarami Reddy, and Reddi, M.V. (1974). Cytohistological studies on certain male-sterile lines of pearl millet (*Pennisetum typhoides* S. and H.). **Cytologia** 39:585-589.
- Banuett-Bourillon, F. (1982a). Linkage of Alcohol Dehydrogenase structural genes in pearl millet (*Pennisetum typhoides*). **Biochem. Genet.** 20:359-367.
- Banuett-Bourillon, F. (1982b). Natural variants of pearl millet (*Pennisetum typhoides*) with altered levels of Set II Alcohol Dehydrogenase activity. **Biochem. Genet.** 20:369-383.
- Banuett-Bourillon, F. and Hague, D.R. (1979). Genetic analysis of alcohol dehydrogenase isozymes in pearl millet (*Pennisetum typhoides*). **Biochem. Genet.** 17:537-551.

Barratt, D.H.P. and Flavell, R.B. (1975). Alterations in mitochondrial associated with cytoplasmic and nuclear genes concerned with male sterility in maize. **Theor. Appl. Genet.** 45:315-321.

✓ Bassett, M.J. and Shuh, D.M. (1982). Cytoplasmic male sterility in common bean. **J. Amer. Soc. Hort. Sci.** 107:791-793.

◦ Bateson, W., Gairdner, A.E. (1921). Male sterility in flax, subject to two types of segregation. **J. Genet.** 11:269-275.

✓ Belliard, G., Pelletier, G., Vedel, F. and Quetier, F. (1978). Morphological characteristics and chloroplast DNA distribution in different cytoplasmic parasexual hybrids of *Nicotiana tabacum*. **Mol. Gen. Genet.** 165:231-237.

Boutry, M. and Briquet, M. (1982). Mitochondrial modification associated with cytoplasmic male sterility in faba beans. **Eur. J. Biochem.** 127:129-135.

Brunken, J., de Wet, J.M.J. and Harlan, J.R. (1977). The morphology and domestication of pearl millet. **Econ. Bot.** 31:163-174.

Burton, G.W. (1958). Cytoplasmic male-sterility in pearl millet [*Pennisetum glaucum* (L.)]. R. Br. **Agron. J.** 50:230-231.

Burton, G.W. (1965). Pearl millet Tift 23A released. **Crop Sci.** 17:633-637.

Burton, G.W. (1969). Registration of pearl millet inbreds Tift 23B, Tift 23A, Tift 23DB and Tift 23DA. **Crop Sci.** 9:397.

Burton, G.W. and Athwal, D.S. (1967). Two additional sources of cytoplasmic male sterility in pearl millet and their relationship to Tift 23A. **Crop Sci.** 7:209-211.

Burton, G.W., and Fortson, J.C. (1966). Inheritance and utilization of five dwarfs in pearl millet (*Pennisetum glaucum*) breeding. **Crop Sci.** 6:69-72.

Burton, G.W., and Powell, J.B. (1968). Pearl millet breeding and cytogenetics. **Adv. Agron.** 20:49-89.

Busri, N. and Chapman, G.P. (1992). Reproductive and isozyme variation in an unstable *Pennisetum* hybrid progeny. In: Desertified grasslands:

their biology and management, pp. 309-313. (**Proceedings: Int. Symp., London, U.K., 27 Feb.-1 Mar. 1991**).

- Cardy, B.J., Stuber, C.W., Wendel, J.F. and Goodman, M.M. (1983). Techniques for starch gel electrophoresis of isozymes from maize (*Zea mays* L.). **Institute of Statistics Mimeograph Series No. 1317**, North Carolina State University, Raleigh, NC.
- Cebrat J. Zadecka A. (1978). Development of anthers in three male sterile lines of rye (*Secale cereale* L.). **Genet. Pol.** **19**:25-31.
- Chahal, S.S., Kumar, R., Sidhu, J.S. and Minocha, J.L. (1986). Peroxidase isozyme pattern in pearl millet lines resistant and susceptible to ergot. **Indian Phytopathology** **39**:65-69.
- Chahal, S.S., Kumar, R., Sidhu, J.S. and Minocha, J.L. (1988). Peroxidase isozyme pattern in pearl millet lines resistant and susceptible to downy mildew. **Plant Breeding** **101**:256-259.
- Chang, T.T. (1954). Pollen sterility in maize. **M.S. Thesis**, Cornell Univ.
- Chowdhury, M.K.U. and Smith, R.L. (1988). Mitochondrial DNA variation in pearl millet and related species. **Theor. Appl. Genet.** **76**(1):25-32.
- Clark, E.M., Izhar, S. and Hanson, M.R. (1985). Independent segregation of the plastid genome and cytoplasmic male sterility in *Petunia somatic* hybrids. **Mol. Gen. Genet.** **199**:440-445.
- Conde, M.F., Pring, D.R., Schertz, K.F. and Ross, W.M. (1982). Correlation of mitochondrial DNA restriction endonuclease patterns with sterility expression in six male-sterile sorghum cytoplasms. **Crop Sci.** **22**:536-539.
- Connett, M.B. and Hanson, M.R. (1990). Differential mitochondrial electron transport through the cyanide-sensitive and cyanide-insensitive pathways in isonuclear lines of cytoplasmic male sterile, male fertile, and restored *Petunia*. **Plant Physiol.** **93**:1634-1640.
- Dallaporta, S.L., Wood, J. and Hicks, J.B. (1983). A plant miniprep: version II. **Plant Mol. Biol. Rep.** **4**:19-21.
- Damon, E.G. (1961). Studies on the occurrence of multiploid sporocytes in three varieties of cytoplasmic male-sterile and the normal fertile variety,

Resistant Wheatland sorghum. **Phyton** 17:193-203.

- De Halac, I.N., and Harte, C. (1975). Female gametophyte competence in relation to polarization phenomena during megagametogenesis and development of the embryo sac in the genus *Oenothera*. In "**Gamete Competition in Plants and Animals**" (Ed. D.L. Mulcahy), pp. 43-56, North Holland Publishing Co., Amsterdam.
- Dewey, R.E., Levings, C.S. III. and Timothy, D.H. (1986). Novel recombinations in the maize mitochondrial genome produce a unique transcriptional unit in the Texas male-sterile cytoplasm. **Cell** 44:439-449.
- Dewey, R.E., Levings, C.S. III. and Timothy, D.H. (1985). Nucleotide sequence of ATPase subunit 6 gene of maize mitochondria. **Plant Physiol.** 79:914-919.
- Dewey, R.E., Levings, C.S. III. and Timothy, D.H. (1987). A mitochondrial protein associated with cytoplasmic male sterility in the T cytoplasm of maize. **Proc. Natl. Acad. Sci. USA** 84:5374-5378.
- Dewey, R.E., Siedow, J.N., Timothy, D.H. and Levings, C.S. III. (1988). A 13-kilodalton maize mitochondrial protein in *E. coli* confers sensitivity to *Bipolaris maydis* toxin. **Science** 239: 293-295.
- Dhesi, J.S., Gill, B.S., and Sharma, H.L. (1973). Cytological studies of desynaptic stock in pearl millet [*Pennisetum typhoides* (Burm.) S&H]. **Cytologia** 38(2):311-316.
- Dubey, D.K., and Singh, S.P. (1965). Mechanism of pollen abortion in three male sterile lines of flax. **Crop Sci.** 5:121-124.
- Duke, S.O., Vaughn, K.C. and Meeusen, R.L. (1984). Mitochondrial involvement in the mode of action of Acifluorfen. **Pesticide Biochem.** 21:368-376.
- ✓ Dundas, I.S., Saxena, K.B., and Byth, D.E. (1981). Microsporogenesis and anther wall development in male-sterile and fertile lines of pigeonpea [*Cajanus cajan* (L.) Millsp.]. **Euphytica** 30(2):431-435.
- ✓ Dundas, I.S., Saxena, K.B., and Byth, D.E. (1982). Pollen mother cell and anther wall development in a photoperiod-insensitive male-sterile mutant of pigeon pea [*Cajanus cajan* (L.) Millsp.]. **Euphytica**

31(2):371-375.

- ✓ Durbin, R.D. and Uchytel, T.F. (1977). Cytoplasmic inheritance of chloroplast coupling factor 1 sub-units. **Biochem. Genet.** 15:1143-1146.
- ✓ Durick, D.N. (1965). Cytoplasmic pollen sterility in corn. **Adv. Genet.** 13:1-52.
- Edwardson, J.R. (1970). Cytoplasmic male sterility. **Bot. Rev.** 36:341-420.
- Erichsen, A.W., and Ross, T.G. (1963). Irregularities at microsporogenesis in colchicine-induced male-sterile mutants of *Sorghum vulgare* Pers. **Crop Sci.** 3:481-483.
- Erickson, L.R., Grant, I. and Beaversdorf, W.D. (1986). Cytoplasmic male sterility in rapeseed (*Brassica napus* L.). 1. Restriction patterns of chloroplast and mitochondrial DNA. **Theor. Appl. Genet.** 72:145-150.
- Eschrich, W. (1961). Untersuchungen über den Ab-und Aufbau der Callose. **Z. Bot.** 49:153-218.
- Eschrich, W. (1964). Die callosesynthese bei Pollenmutterzellen von *Cucurbita ficifolia*. In **Pollen Physiology and Fertilization**, H.F. Linskens, Ed., North Holland Publ. Co., Amsterdam. pp. 48-51.
- Feinberg, A.P. and Vogelstein, B. (1983). A technique for radiolabeling DNA restriction endonuclease fragments to high specific activity. **Anal. Biochem.** 137:266-267.
- Filion, W.G., and Christie, B.R. (1966). The mechanism of male sterility in a clone of orchard grass (*Dactylis glomerata* L.). **Crop Sci.** 6:345-347.
- Frankel, R., and Galun, E. (1977). **Pollination mechanisms, reproduction and plant breeding**. Springer, Berlin, Beidelberg, New York, pp. 281.
- Frankel, R., Izahar, S., and Nitsan, J. (1969). Timing of callase activity and cytoplasmic male sterility in Petunia. **Biochem. Genet.** 3:451-455.
- Ghosh, B. and Chaudhuri, M.H.H. (1984). Ribonucleic acid breakdown and loss of protein synthetic capacity with loss of viability of rice embryos (*Oryza sativa*). **Seed Sci. Technol.** 12:669-677.
- Gill, K.S., Virk, D.S., Singh, N.B., and Srivastava, M. (1986). Pb 405A - a new

- male-sterile line of bajra in A_3 source of sterility. **Seeds and Farms** 12:29-32.
- Godwin, H. (1968). The origin of exine. **New Phytologist** 67:667-676.
- Gottschalk, W., and Kaul, M.L.H. (1974). The genetic control of microsporogenesis in higher plants. **Nucleus (Calcutta)** 17:133-166.
- Gracen, V.E., Grogan, C.O. and Forster, M.J. (1972). Permeability changes induced by *Helminthosporium maydis*, race T, toxin. **Canad. J. of Botany** 50:2167-2170.
- Gracen, V.E., and Grogan, C.O. (1974). Diversity and suitability for hybrid production of different sources of cytoplasmic male sterility in maize. **Agron. J.** 66:654-657.
- Gupta, D.N., Roy, M.K., Mehta, S.L., Singhal, G.L. and Murty, B.R. (1980). Peroxidase and esterase isozymes in downy mildew susceptible and resistant cultivars of pearl millet, *In: Trends in Genetical Research on Pennisetums*. eds. V.P. Gupta and J.L. Minocha, Punjab Agric. Univ., Ludhiana, India, pp. 173-178.
- Gupta, V.P., Ranbir Bhowra and Dhiman, K.R. (1980). Variation in enzyme pattern in relation to protogyny in pearl millet. *In: Trends in Genetical Research on Pennisetums*, V.P. Gupta and J.L. Minocha, eds. Punjab Agric. Univ., Ludhiana, pp. 179-188.
- Habib, A.F., and Chennaveeraiah, M.S. (1976). Cytomixis in *Capsicum annum* L. **J. Cytol. Genet.** 11:51-55.
- Hanna, W.W. (1987). A new stable cytoplasm in pearl millet. *In Agronomy Abstracts*. American Society of Agronomy, Inc., Madison, Wisconsin. p. 64.
- Hanna, W.W. (1989). Characteristics and stability of a new cytoplasmic-nuclear male-sterile source in pearl millet, **Crop Sci.** 29:1457-1459.
- Hanna, W.W. and Dujardin, M. (1982). Apomictic interspecific hybrids between pearl millet and *Pennisetum orientale* L.C. Rich. **Crop Sci.** 22:857-859.
- Hanson, M.R., Boeshore, M.L., McClean, P.E., O'Connell, M.A. and Nivison, H.T. (1986). The isolation of mitochondria and mitochondrial DNA.

Methods in Enzymology 118:437-453

- Hanson, M.R. and Conde, M.F. (1985). Functioning and variation of cytoplasmic genomes: lessons from cytoplasmic-nuclear interactions conferring male sterility in plants. **Int. Rev. Cytol.** **94**:213-267.
- Hanson, M.R., Pruitt, K.D. and Nivison, H.T. (1989). Male sterility loci in plant mitochondrial genomes. *Oxford Surv. Plant Mol. Cell. Biol.* **6**:61-85.
- Harlan, J.R. (1971). Agricultural origins: centers and the non-centers. **Science** **174**:468-474.
- Hash, C.T. (1991). ICRISAT pearl millet breeding and the potential use of RFLPs. pp. 28-29 in Report of Meeting, Rockefeller Foundation Conference: **The Establishment of a Sorghum and Millet RFLP Network to Support Breeding in Developing Countries** (USA), 6-10 May, 1991, N.Y., USA.
- Herrman, R.B. (1970). Multiple amounts of DNA related to the size of chloroplasts. I. An autoradiographic study. **Planta (Berl)** **90**:80-96.
- Heslop-Harrison, J. (1964). Cell walls, cell membranes and protoplasmic connections during meiosis and pollen development. *In* **Pollen Physiology and Fertilization**. H.F. Linskens, Ed., North Holland Publ. Co., Amsterada, pp. 39-47.
- Heslop-Harrison, J. (1966a). Cytoplasmic connections between angiosperm meiocytes. **Ann. Bot.** **30**:221-230.
- Heslop-Harrison, J. (1966b). Cytoplasmic continuities during spore formation in flowering plants. **Endeavor.** **25**:65-72.
- Heslop-Harrison, J. (1968). Synchronous pollen mitosis and formation of the generative cell in massulate orchids. **J. Cell Sci.** **3**:457-466.
- Heslop-Harrison, J. (1972). Sexuality of Angiosperms. **Physiology of development: From Seeds to Sexuality in Plant Physiology** (F.C. Steward, ed.), Vol. VIC:133-289. Academic Press, New York.
- Heslop-Harrison, J., and MacKenzie, A. (1967). Autoradiography of soluble (^{14}C) - thymidine derivatives during meiosis and microsporogenesis in *Lilium* anthers. **J. Cell. Sci.** **2**:387-400.

- Hooker, A.L. (1972). Southern leaf blight of corn - Present status and future prospects. **J. Evir. Qual.** 1:244-249.
- Hooker, A.L., Smith, D.R., Lim, S.M. and Beckett, J.B. (1970a). Reaction of corn seedlings with male sterile cytoplasm to *Helminthosporium maydis*. **Plant Disease Reporter** 54:708-712.
- Hooker, A.L., Smith, D.R., Lim, S.M. and Musson, M.D. (1970b). Physiological races of *Helmonthosporium maydis* and disease resistance. **Plant Disease Reporter** 54:1109-1110.
- Hossain-Salma (1989). Anatomical studies of sterile anthers in male sterile lines of rapeseed (*Brassica campestris* L.). **Proceedings of the 6th National Botanical Society, Chittagong** (Bangladesh), BBS. p. 17.
- Humaydan, H.S. and Scott, E.W. (1977). Methomyl insecticide selective phytotoxicity on sweet corn hybrids and inbreds having the Texas male sterile cytoplasm. **Hort. Science** 12:312-313.
- Hunter, R.L. and Markert, C.L. (1957). Histochemical demonstration of enzymes separated by zone electrophoresis in starch gels. **Science** 125:1294-1295.
- Hussain, S.N., S aideswara Rao, Y., Manga, V. and Subba Rao, M.V. (1990). Chaemotaxonomic studies on the genus *Pennisetum* L. Rich. by isozyme analysis. Beitr, **Biol. pflanzen.** 65:211-222.
- ICRISAT (1985). Pearl Millet male-sterile line ICMA 1 and its maintainer line ICMB 1. Plant material descriptor No. 4, International Crops Research Institute for the Semi-arid Tropics, Patancheru, India.
- Isaac, P.G., Jones, V.P. and Leaver, C.J. (1985). The maize cytochrome c oxidase subunit I gene: sequence, expression, and rearrangement in cytoplasmic male-sterile plants. **EMBO J.** 4:1617-1623.
- Izhar, S. and Frankel, R. (1971). Mechanism of male-sterility in *Petunia*: The relationship between pH, callase activity in the anthers, and the breakdown of microsporogenesis. **Theor. Appl. Genet.** 41:104-108.
- Jauhar, P.P. (1969). Partial desynapsis in pearl millet (*Pennisetum typhoides* Stapf & Hubb.). **Naturwissenschaften** 56:571-572.
- Kadam, B.S., Patel, S.M., Kulkarni, R.K. (1940). Consequences of inbreeding

- in bajri. **J. Hered.** **31**:201-207.
- Kadowaki, K., Suzuki, T. and Kazama, S. (1990). A chimaeric gene containing the 5' portion of *atp6* is associated with cytoplasmic male-sterility of rice. **Mol. Gen. Genet.** **224**:10-16.
- Kajjari, N.B., and Patil, N.B. (1956). A male sterile bajri. **Indian J. Genet Plant Breed.** **16**:46.
- Kaul, C.L., and Singh, S.P. (1966). Studies in male-sterile barley II. Pollen abortion. **Crop Sci.** **6**:539-541.
- Kaul, M.L.H. and Murty, T.G.K. (1985). Mutant genes affecting higher plant meiosis. **Theor. Appl. Genet.** **70**:449-466.
- Kaushal, P. and Sidhu, J.S. (1993). Chaemotaxonomic studies in *Pennisetum* species. **Crop Imp.** **20**(1):78-80.
- Kemble, R.J., Gunn, R.E. and Flavell, R.B. (1980). Classification of normal and male-sterile cytoplasm in maize. II. Electrophoretic analysis of DNA species in mitochondria. **Genetics** **95**:451-458.
- Kempana, C. (1960). Cytology of male sterile *Crotalaria striata*. **Curr. Sci.** **27**:181.
- Khairwal, I.S., Chandgi Ram and Chhabra, A.K. (1990). **Pearl millet: Seed production and technology**. Manohar Publications, New Delhi, India. pp. 208.
- Khairwal, I.S, Singh, S., and Prakash, O. (1986). Smut reactions of pearl millet lines and hybrids with and without cytoplasmic male sterility. **Proc. Indian Nat. Sci. Acad.** **B52**: 751-754.
- Khairwal, I.S., Tomar, R.P.S. and Raj, L. (1992). Effect of *d₂* dwarfing gene on seed and seedling characters in pearl millet. **Crop Improvement** **19**: 53-55.
- Kihara, H., and Lilienfeld, F. (1934). Kernein wanderung und Building Syndiploider pollen mutterzellen bei dem F₁ bastard *Triticum aegilopoides* x *Aegilops squarrosa*. **Jap. J. Genet.** **10**:1-28.
- Kirk, J.T.O. (1971). Chloroplast structure and biosynthesis. **Annu. Rev. Biochem.** **40**:161-196.

- Krishnaswamy, N. (1962). "Bajra, *Pennisetum typhoides* S. & H." **Indian Council Agric. Res.**, New Delhi.
- Krishnaswamy, N., and Ayyangar, G.N.R. (1941). Chromosomal alterations induced by x-rays in bajri (*Pennisetum typhoides* S. and H.). **J. Indian Bot. Soc.** **20**:111-117.
- Krishnaswamy, N., and Ayyangar, G.N.R. (1942). Certain abnormalities in millets induced by x-rays. **Proc. Indian Acad. Sci. B.** **16**:1-9.
- Krishnaswamy, N., and Raman, V.S. (1953). Cytogenetical studies in the interspecific hybrid of *Pennisetum typhoides* Stapf and Hubbard and *P. purpureum* Schumach. pp. 43-71. In **Proc. 1st Sci. Workers Conf., Agric. Coll. Res. Inst.**, Coimbatore, Supdt. Govt. Press, Madras (India).
- Krishnaswamy, N., Raman, V.S., and Menon, P.M. (1949). Abnormal meiosis in *Pennisetum typhoides*. I. Desynapsis. **Proc. Indian Acad. Sci.** **30**:195-206.
- Kumar, R., Chahal, S.S., Sidhu, J.S. and Minocha, J.L. (1987). Peroxidase isozyme studies in pearl millet related to downy mildew resistance. **Plant Disease Research** **2**:113-115.
- Ladizinsky, G. and Hymowitz, T. (1979). Seed protein electrophoresis in taxonomic and evolutionary studies. **Theor. Appl. Genet.** **54**:145-151.
- Lagudah, S.S. and Hanna, W.W. (1989). Species relationships in the *Pennisetum* gene pool. Enzyme Polymorphism. **Theor. Appl. Genet.** **78**:801-808.
- Lambert, C. (1983). IRAT work on millet improvement. **Agronomie Tropicale** **38**:78-88.
- Lasar, K.D., and Larsten, N.R. (1972). Anatomy and cytology of microsporogenesis in cytoplasmic male sterile angiosperm. **Bot. Rev.** **38**:425-454.
- Lavergne, D., Bouraima, S., Tostian, S. and Champigny, M.L. (1986). Thermal sensitivity of NAD-malate dehydrogenase isoforms from various *Pennisetum* ecotypes. **Pl. Sci.** **45**:87-94.
- Leaver, C.J., Hack, E. and Forde, B.G. (1983). Protein synthesis by isolated plant mitochondria **Methods in Enzymology** **97**:476-484.

- ✓ Lee, S.L.J., Earle, E.D., and Gracen, V.E. (1980). The cytology of pollen abortion in S-cytoplasmic male-sterile corn anthers. **Amer. J. Bot.** **67**:237-245.
- ✓ Lee, S.L.J., Gracen, V.E., and Earle, E.D. (1979). The cytology of pollen abortion in C-cytoplasmic male sterile corn anthers. **Amer. J. Bot.** **66**:656-667.
- , Levings, C.S. III. (1990). The Texas cytoplasm of maize: cytoplasmic male sterility and disease susceptibility. **Science** **250**:942-947.
- ✓ Levings, C.S. III. and Pring, D.R. (1976). Restriction endonuclease analysis of mitochondrial DNA from normal and Texas cytoplasmic male-sterile maize. **Science** **193**:158-160.
- Liu, C.J., Witcombe, J.R., Pittaway, T.S., Nash, M., Hash, C.T., Busso, C.S. and Gale, M.D. (1992). Progress in the construction of a RFLP-based genetic maps for pearl millet (*Pennisetum americanum*). pp. 37 **In Plant Genome 1: Official Program Abstracts, International Conference on the Plant Genome**, San Diego, California, USA, 9-11 Nov 1992. New York, USA.
- Liu, C.J., Witcombe, J.R., Pittaway, T.S., Nash, M., Hash, C.T., Busso, C.S. and Gale, M.D. (1994). An RFLP-based genetic map of pearl millet (*Pennisetum glaucum*). **Theor. Appl. Genet.** **89**:481-487.
- Lobana, K.S., and Gill, B.S. (1973). Pachytene chromosomes of *Pennisetum typhoides*. **Cytologia** **38**:713-717.
- Maheshwari, P. (1950). **An Introduction to Embryology of Angiosperms**. McGraw-Hill, New York.
- , Makaroff, C.A., Apel, I.J. and Palmer, J.D. (1989). The *atp6* coding region has been disrupted and a novel reading frame generated in the mitochondrial genome of cytoplasmic male-sterile radish. **J. Biol. Chem.** **264**:11706-11713.
- Mangat, B.K. and Virk, D.S. (1992). Diversification of male sterile lines in pearl millet. **In: Scientific Programme and Abstracts (p. 48) of Siler Jubilee Symp. on Crop Breeding in India: Current Status and Future Strategy**, G.B. Pant University of Agriculture, Pantnagar,

U.P., India.

- Maniatis, T., Fritsch, E.F. and Sambrook, J. (1982). Molecular cloning. A Laboratory Manual. Cold Spring Harbor Press, Cold Spring Harbor, N.Y., USA.
- Marchais, L. (1994). Wild pearl millet population (*Pennisetum glaucum*, Poaceae) integrity in agricultural Sahelian areas. An example from Keita (Niger). **Plant Systematics and Evolution** 189(3/4):233-245.
- Marchais, L. and Pernes, J. (1985). Genetic divergence between wild and cultivated pearl millets (*Pennisetum typhoides*). I. Male sterility. **Z. Pflanzenzuecht** 95:103-112.
- Markert, C.L. and Moller, F. (1959). Multiple forms of enzymes: tissue ontogenetic, and species specific patterns. **Proc. Natl. Acad. Sci.** 45:753-763.
- Mehra, P.N., and Kalia, V. (1973). Accessory chromosomes and multinucleate pollen mother cells in *Saccharum benghalense*. **Rets. Complex. Nucleus** 16:75-78.
- Menon, P.M. (1959). Occurrence of cytoplasmic male sterility in pearl millet (*Pennisetum typhoides* S. and H.). **Curr. Sci.** 28:165-167.
- Mephram, R.H., and Lane, G.R. (1969). Formation and development of tapetal periplasmodium in *Tradescantia bracteata*. **Protoplasma** 68:175-192.
- Minocha, J.L. and Singh, A. (1971). A meiotic study of a hybrid between *Pennisetum typhoides* and *P. purpureum*. **Sci. Cult.** 37:198-199.
- Minocha, J.L., Gills, B.S., and Singh, Sadhu (1968). Desynapsis in pearl millet. **J. Res. Punjab. Agric. Univ.** 5(2, Suppl.):32-36.
- Murty, U.R. (1982). Milo and the non-milo cytoplasm in sorghum: Review of literature and notes on microsporogenesis. National Fellow Project on Sorghum and Groundnut, IARI-Regional Station, Hyderabad. **Tech. Bull. No. 3.**
- Nei, M. (1987). **Molecular evolutionary genetics.** Columbia University Press, New York, USA.
- Novak, F. (1971). Cytoplasmic male sterility in sweet pepper (*Capsicum*

- annuum* L.). II. Tapetal development in male sterile anthers. **Z. Pflanzenzüchtg** **65**:221-232.
- O. Malley, D., Wheeler, N.C. and Guries, R.P. (1980). **A manual for starch gel electrophoresis**. Staff paper series #11. University of Wisconsin-Madison, Madison, WI.
- Ohamasa, M., Watanabe, Y., and Murata, N. (1976). A biochemical study of cytoplasmic male sterility of corn: Alteration of cytochrome oxidase and malate dehydrogenase activities during pollen development. **Jap. J. Breed.** **26**:40-50.
- Östergren, G. and Heneen, K. (1962). A squash technique for chromosome morphological studies. **Hereditas** **48**:332-341.
- Overman, M.A., and Warmke, H.E. (1972). Cytoplasmic male sterility in *Sorghum*. II. Tapetal behaviour in fertile and sterile anthers. **J. Hered.** **63**:227-234.
- Ozias-Akins, P. (1991). Apomixis in *Pennisetum* and the application of molecular techniques to facilitate introgression of the trait in to pearl millet. pp 37-38 **In Report of Meeting, Rockefeller Foundation Conference: The Establishment of a Sorghum and Millet RFLP Network to Support Breeding in Developing Countries, USA, 6-10 May 1991. New York, USA.**
- Ozias-Akins, P., Lubbers, E.L., Hanna, W.W. and McNay, J.W. (1993). Transmission of the apomictic mode of reproduction in *Pennisetum*: Co-inheritance of the trait and molecular markers. **Theor. Appl. Genet.** **85**:632-638.
- Ozias-Akins, P., Tabaeizadeh, Z., Pring, D.R. and Vasil, I.K. (1988). Preferential amplification of mitochondrial DNA fragments in somatic hybrids of the Gramineae. **Curr. Genet.** **13**(3):241-245.
- Painter, T.S. (1943). Cell growth and nucleic acids in pollen of *Rheo discolor*. **Bot. Gaz.** **105**:58-68.
- Pantulu, J.V. (1958). A case of chromosomal interchange in pearl millet. **Curr. Sci.** **27**:497-498.
- Pantulu, J.V., and Manga, V. (1971). Monofactorial 'multiploid sporocytes' condition induced by EMS in pearl millet. **Genetica** **42**:214-218.

- Patil, B.D. and Singh, A. (1964). An interspecific cross in the genus *Pennisetum* involving two basic numbers. **Curr. Sci.** 33:255.
- Patil, B.D., and Vohra, S.K. (1962). Desynapsis in *Pennisetum typhoides* Stapf and Hubb. **Curr. Sci.** 31:345-346.
- Porteres, R. (1962). Bereaux agricoles primaires sur le continent africain. **J. Afr. Hist.** 3:195-210.
- Powling, A. (1982). Restriction endonuclease analysis of mitochondrial DNA from sugarbeet with normal and male-sterile cytoplasms. **Heredity** 49:117-120.
- Pring, D.R., Conde, M.F. and Schertz, K.F. (1982). Organelle genome diversity in sorghum: male-sterile cytoplasms. **Crop Sci.** 22:414-421.
- Pring, D.R. and Levings, C.S. III (1978). Heterogeneity of maize cytoplasmic genomes among male-sterile cytoplasms. **Genetics** 89:121-136.
- Pring, D.R., Levings, C.S. and Conde, M.F. (1979). The organelle genomes of cytoplasmic male sterile maize and sorghum. *In: Proc. 4th John Innes Symp.* pp 111-120.
- Pring, D.R. and Lonsdale, D.M. (1985). Molecular biology of higher plant mitochondrial DNA. **Int. Rev. Cytol.** 97:1-46.
- Pritchard, A.J., and Hutton, E.M. (1972). Anther and pollen development in male-sterile *Phaseolus atropurpureus*. **J. Hered.** 63:280-282.
- Purseglove, J.W. (1976). Millets-Eleusine Coracana, *Pennisetum americanum* (Gramineae). *In: Evolution of Crop Plants*, N.W. Simmonds, ed., New York, pp. 91-93.
- Quetier, F. and Vedel, F. (1977). Heterogeneous population of mitochondrial DNA molecules in higher plants. **Nature** 168:365-368.
- Rai, K.N. (1990). Development of high-yielding dwarf composites of pearl millet. **Crop Improvement** 17:96-103.
- Rai, K.N. (1993). Selfed seed-set in male-sterile lines of pearl millet. **Annual Report Cereals Program**, ICRISAT (1993), pp.84-87.
- Rai, K.N. and Hanna, W.W. (1990). Morphological characteristics of tall and

dwarf pearl millet isolines. **Crop Sci.** 30:889-892.

Rai, K.N. and Hash, C.T. (1990). Fertility restoration in male sterile x maintainer hybrids of pearl millet. **Crop Sci.** 30:889-892.

Rai, K.N. and Hash, C.T. (1993). A new source of cytoplasmic-nuclear male sterility in pearl millet. **Cereals Program, ICRISAT. Annual Report (1992)**. Cereals Program, International Crops Research Institute for the Semi-Arid Tropics, Patancheru, India.

Rai, K.N. and Rao, A.S. (1991). Effect of d_2 dwarfing gene on grain yield and yield components in pearl millet near-isogenic lines. **Euphytica** 52:25-31.

Rai, K.N., Virk, D.S. and Harinarayana, G. (1991). Fertility restoration patterns of near-isonuclear hybrids. **Cereals Program Annual Report, ICRISAT**. pp. 79-80.

Rajeshwari, R., Sivaramakrishnan, S., Smith, R.L. and Subrahmanyam, N.C. (1994). RFLP analysis of mitochondrial DNA from cytoplasmic male-sterile lines of pearl millet. **Theor. Appl. Genet.** 88:441-448.

Raman, V.S. (1965). Progress of cytogenetic research in Madras state. In: **Advances in Agricultural Sciences and their Applications**, ed. S. Krishnamurthi, Agric. Coll. Res. Inst., Coimbatore, India. pp 122-143.

Ramanan, R. (1992). **Mitochondrial DNA polymorphisms in cytoplasmic male-sterile and maintainer lines, related species and interspecific hybrids of pearl millet (*Pennisetum glaucum* (L.) R. Br.)**. Ph.D. Thesis, University of Hyderabad, Hyderabad, Andhra Pradesh, India.

Rangaswamy, K. (1935). On the cytology of *Pennisetum typhoideum* Rich. **J. Indian Bot. Soc.** 14:125-131.

Rao, M.K., and Koduru, P.R.K. (1978a). Cytogenetics of a factor for syncyte formation and male sterility in *Pennisetum americanum*. **Theor. Appl. Genet.** 53:1-7.

Rao, M.K., and Koduru, P.R.K. (1978b). Inheritance of genetic male-sterility in *Pennisetum americanum* (L.) Leeke. **Euphytica** 27:777-783.

Rao, M.V.S., Sujatha, D.M., Rao, Y.S. and Manga, V. (1988). Chaemotaxonomic characters in twelve species of the genus *Pennisetum*

- (Poaceae). *In: Proceedings of the Indian Academy of Sciences, Plant Sciences* **98(2)**:111-120.
- Rao, N.G.P., Tripathi, D.P. and Rana, B.S. (1984). Genetic analysis of cytoplasmic systems in sorghum. *Indian J. Genet.* **44**:480-496.
- Rau, N.S. (1929). On the chromosome numbers of some cultivated plants of South India. *J. Indian Bot. Soc.* **8**:126-128.
- Rhoades, M.M. (1931). Cytoplasmic inheritance of male-sterility in *Zea mays*. *Science* **73**:340-341.
- Rhoades, M.M. (1933). The inheritance of male-sterility in *Zea mays*. *J. Genet.* **27**:71-93.
- Rhoades, M.M. (1950). Gene induced mutation of a heritable cytoplasmic factor producing male sterility in maize. *Proc. Natl. Acad. Sci. (USA)* **36**:634-635.
- Roberts, E.E., Payne, P.I., and Osborne, D.J. (1973). Protein synthesis and the viability of rye grains. *Biochem. J.* **131**:275-280.
- Rowley, J.R. (1969). The fine structure of the pollen wall in the Commelinaceae. *Grana Palynol.* **2**:3-31.
- Saideswara Rao, Y., Sujatha, D.M., Manga, V. and Subba Rao, M.V. (1986). Esterase variability in five species of the genus *Pennisetum* L. Rich (Gramineae). *Geobios* **13**:108-111.
- Sandmeier, M. (1993). Selfing rates of pearl millet (*Pennisetum typhoides* Stapf and Hubb.) under natural conditions. *Theor. Appl. Genet.* **86(4)**:513-517.
- Sandmeier, M., Beninga, M. and Pernes, J. (1981). Genetic analysis of the relationships between spontaneous and cultivated forms of pearl millet. III. Inheritance of esterases and anodic peroxidase isozymes. *Agronomie* **1**:487-494.
- Sarr, A., Sandmeier, M. and Pernes, J. (1988). Gametophytic competition in pearl millet, *Pennisetum typhoides* (Stapf et Hubb.). *Genome* **30(6)**:924-929.
- Satiya, D.R., Thukral, S.K. and Gupta, V.P. (1983). Role of polyphenoloxidase

- in imparting resistance to downy mildew in pearl millet. **MILWAI Newsletter** 2:5-6.
- Schertz, K.F. and Ritchey, J.M. (1978). Cytoplasmic-genic male-sterility systems in sorghum. **Crop Sci.** 18:890-893.
- Seevers, P.M., Daly, J.N. and Catedral, F.F. (1971). The role of peroxidase isozymes in resistance to wheat stem rust disease. **Plant Physiol.** 48:353-360.
- Sharma, Y.P. (1978). Investigation into the cause of male sterility in pearl millet. (*Pennisetum glaucum* Linn.). R. Br. **Bangladesh J. Bot.** 7(2):6-9.
- Shekhawat, N.S., Purohit, S.D. and Arya, H.C. (1984). Changes in isozymes of peroxidase in green-ear of pearl millet. **Curr. Sci.** 53(21):1157-1158.
- Shekhawat, N.S. and Arya, H.C. (1979). Biochemical changes in green-ear of pearl millet caused by *Sclerospora graminicola* (Sacc.) Schroet. **Indian J. Exp. Biol.** 17:228-230.
- Shenoy, V.B. and Vasil, I.K. (1992). Biochemical and molecular analysis of plants derived from embryogenic tissue cultures of napier grass (*Pennisetum purpureum* K. Schum). **Theor. Appl. Genet.** 83(8):947-955.
- Sheorain, V.S. and Wagle, D.S. (1981). Beta amylase isoenzymes of bajra (*Pennisetum typhoides*) and barley (*Hordeum vulgare*) during germination. **Ind. J. Agric. Res.** 15:63-66.
- Singh, S.P., and Hadley, H.H. (1961). Pollen abortion in cytoplasmic male sterile sorghum. **Crop Sci.** 1:430-432.
- Singh, S.P., and Sharma, Y.P. (1963). Preliminary observations on the breeding of *Pennisetum* at BR College Bichpuri Agra. **Sorghum Newslett.** 6:26-28.
- Sivaramakrishnan, S., Rajeshwari, R., Subrahmanyam, N.C., Smith, R.L., Sujata, V. and Rai, K.N. (1993). Molecular characterization of cytoplasmic male sterile line of pearl millet. **Cereals Program, ICRISAT. Annual Report (1992)**. Cereals Program, International Crops Research Institute for the Semi-Arid Tropics, Patancheru, India.

pp. 83-85.

- Smith, L. (1942). Cytogenetics of a factor for multiploid sporocytes in barley. **Amer. J. bot.** **29**:451-456.
- Smith, R.L. and Chowdhury, M.K.U. (1989). Mitochondrial DNA polymorphism in male-sterile and fertile cytoplasm of pearl millet. **Crop Sci.** **29**(3):809-814.
- Smith, R.L. and Chowdhury, M.K.U. (1991). Characterization of pearl millet mitochondrial DNA fragments rearranged by reversion from cytoplasmic male-sterility to fertility. **Theor. Appl. Genet.** **81**:793-799.
- Smith, R.L., Chowdhury, M.K.U. and Pring, D.R. (1987). Mitochondrial DNA rearrangements in *Pennisetum* associated with reversion from cytoplasmic male sterility to fertility. **Plant Mol. Biol.** **9**:277-286.
- Soltis, D.E., Haufler, C.H., Darrow, D.C. and Gastony, G.J. (1983). Starch gel electrophoresis of ferns: A compilation of grinding buffers, gel and electrode buffers, and staining schedules. **Amer. Fern. J.**, **73**(1):9-27.
- Southworth, D. (1971). Incorporation of radioactive precursors into developing pollen walls. In **Pollen: Development and Physiology**. J. Heslop-Harrison, Ed., Butterworths, London. pp. 115-120.
- Spurr, A.R. (1969). A low viscosity epoxy resin embedding medium for electronmicroscopy. **J. Ultrastruct Res.** **26**:31.
- Srivastava, H.K. (1981). Intergenomic interaction, heterosis and improvement of crop yield. **Adv. Agron.** **34**:117-195.
- Stamper, S.E., Dewey, R.E., Bland, M.M. and Levings, C.S. (1987). Characterization of the gene *urf13-T* and an unidentified reading frame, *orf25* in maize and tobacco mitochondria. **Curr. Genet.** **12**:457-463.
- Subba Rao, M.V., Saideswara Rao, Y. and Manga, V. (1989). Genetics of five seed esterase isozymes in pearl millet. **Plant Breeding** **102**:133-139.
- Subba Rao, M.V., Sujatha, D.M., Saideswara Rao, Y. and Manga, V. (1988). Chaemotaxonomic characters in twelve species of the genus *Pennisetum* (Poaceae). **Proc. Ind. Acad. Sci.** **98**:111-120.
- Sujata, V., Sivaramakrishnan, S., Rai, K.N. and Seetha, K. (1994). A new

- source of cytoplasmic male sterility in pearl millet: RFLP analysis of mitochondrial DNA. **Genome** **37(3)**:482-486.
- Sujatha, D.M. (1984). **Studies on some biosystematic aspects of twelve species of the genus *Pennisetum* L. Rich. (Poaceae)**. Ph.D. Thesis, Andhra University, Visakhapatnam, A.P., India.
- Sun, M., and Ganders, F.R. (1987). Microsporogenesis in male-sterile and hermaphroditic plants of nine Gynodioecious taxa of Hawaiian *Bidens* (Asteraceae). **Amer. J. Bot.** **74(2)**:209-217.
- Thakare, R.B. and Murty, B.R. (1972). Effect of dwarfing genes on combining ability in pearl millet (*Pennisetum typhoides* (Burm f.) Stapf and CE Hubb). **Indian J. Agric. Sci.** **42**: 392-397.
- Thakur, R.P, Rao, V.P. and King, S.B. (1989). Ergot susceptibility in relation to cytoplasmic male sterility in pearl millet. **Plant Diseases** **73**:676-678.
- Thakur, S.R. and Murty, B.R. (1993). Esterase isozyme patterns in three isonuclear cytoplasmic male sterile lines of pearl millet. **Crop Improvement** **20(1)**:81-87.
- Thukral, S.K., Satija, D.R. and Gupta, V.P. (1983). Isozyme patterns in relation to downy mildew resistance in pearl millet. *In: Abstracts of contributed papers, V2:p 738, 15th Int. Cong. of Genet.*, 12-21 Dec. 1983, New Delhi, India.
- Tostain, S. (1985). Mise en evidence d'une liaison genetique entre un gene de nanisme et des marqueurs enzymatique chez le mil penicillaire (*Pennisetum glaucum* L.). **Can. J. Genet. Cytol.** **27**:751-758.
- Tostain, S. (1992). Enzyme diversity in pearl millet (*Pennisetum glaucum* L.). 3. Wild millet. **Theor. Appl. Genet.** **83(6-7)**:733-742.
- Tostain, S. and Marchais, L. (1989). Enzyme diversity in pearl millet (*Pennisetum glaucum*). 2. Africa and India. **Theor. Appl. Genet.** **77**:634-640.
- Tostain, S. and Riandey, M.F. (1984). Polymorphisme et determinisme genetique des enzymes de mil (*Pennisetum glaucum* L.): Etude des alcohol dehydrogenases, catalases, endopeptides et esterases. **Agron. Trop.** **39**:335-345.

- Tostain, S. and Riandey, M.F. (1985). Polymorphisme et déterminisme génétique des enzymes du mil pencillaire (*Pennisetum glaucum*). Etude des malades dehydrogenases. **Agronomie** 5:227-238.
- Tostain, S. Riandey, M.F. and Marchais, L. (1987). Enzyme diversity in pearl millet (*Pennisetum glaucum*). I. West Africa. **Theor. Appl. Genet.** 74:188-193.
- Trigui, N., Sandmeier, M., Salanoubat, M. and Pernes, J. (1986). Utilisation des données enzymatiques et morphologiques pour l'étude des populations et de la domestication des plantes. I. Séparation et identification génétique d'isozymes chez le mil (*Pennisetum typhoides* Burm. Stapf et Hubb.) **Agronomie** 6(9):779-788.
- Turner, M.T. and Martinson, C.A. (1972). Susceptibility of cron lines to *Helminthosporium maaydis* toxin. **Plant Disease Reporter** 56:29-32.
- Tyagi, B.R. (1975). Karyomorphology of somatic chromosomes in pearl millet. **Proc. Indian Natl. Sci. Acad. B**, 41:462-465.
- Ullstrop, A.J. (1972). The impacts of the southern corn leaf blight epidemics of 1970-1971. **Ann. Rev. Phytopathology** 10:37-50.
- Varier, A. and Cooke, R.J. (1992). Discrimination between cultivars and lines of pearl millet by isoelectric focussing. **Seed Sci. and Tech.** 20(3):711-713.
- Varier, A. and Dadlani, M. (1992). Effect of ageing on profiles of soluble protein of cotton and esterase isoenzymes of pearl millet seeds. **Ind. J. Pl. Physiol.** 35(2):145-151.
- Varier, A., Vashisht, V. and Agrawal, P.K. (1992). Identification of pearl millet cultivars using PAGE of soluble proteins and isoenzymes of seed. *In Proc. International Conference on Seed Science and Technology*, New Delhi 1990.
- Venkateswarlu, J., and Pantulu, J.V. (1968). Morphology of pachytene chromosomes in pearl millet. **J. Hered.** 59:69-70.
- Vijayaraghavan, M.R., and Shukla, A.K. (1978). Role of callose during microsporogenesis. **J. Cytol. Genet.** 13:129-131.

- Virk, D.S., and Brar, J.S. (1993). Assessment of cytoplasmic differences of near-isonuclear male-sterile lines in pearl millet. **Theor. Appl. Genet.** **87**:106-112.
- Virk, D.S., Brar, J.S. and Mangat, B.K. (1993). Cytoplasmic differentiation using near-isonuclear polycytoplasmic male sterile lines in pearl millet. **Euthytica** **67**(1-2):127-134.
- Virk, D.S., and Mangat, B.K. (1987). Substitution of CMS 81B genome into A₂ cytoplasm. **Millet News Lett.** **6**:6.
- Virk, D.S., and Mangat, B.K. (1988). Substitution of 81B genome into A₃ cytoplasm. **Millet News Lett.** **7**:3.
- Virk, D.S., and Mangat, B.K. (1989). Alloplasmic lines of L67A in pearl millet. **Millet News Lett.** **8**:3.
- Virk, D.S., Mangat, B.K., and Gill, K.S. (1990a). Pb 310A₂ and Pb 406A₃, isonuclear male sterile lines of pearl millet. **J. Res. Punjab Agric. Univ., Ludhiana.** **27**:359
- Virk, D.S., Mangat, B.K., and Gill, K.S. (1990b). Pb 407A₃ and Pb 408A₃, male-sterile lines of pearl millet. **J. Res. Punjab Agric. Univ., Ludhiana** **27**:548.
- Virk, D.S., Mangat, B.K., and Gill, K.S. (1990c). Pb 501A_(g) and Pb 601A_(v), male-sterile lines of pearl millet in diverse cytoplasm. **J. Res. Punjab Agric. Univ., Ludhiana** **27**:549.
- Virk, D.S., Mangat, B.K., Singh, N.B. and Gill, K.S. (1989). Pb 208A₁ and Pb 305A₂ male sterile lines of pearl millet. **Journal of Res. (PAU)** **26**:732.
- Virmani, S.S., and Gill, B.S. (1972). Somatic chromosomes of *Pennisetum typhoides* (Burm.) S.& H. **Cytologia** **37**:257-260.
- Ward, B.I., Anderson, R.S. and Bendich, A.J. (1981). The mitochondrial genome is large and variable in a family of plants (*Cucurbitaceae*). **Cell** **25**:793-803.
- Warmke, H.E., Overmann, M.A. (1972). Cytoplasmic male sterility in *Sorghum*. I. Callose behaviour in fertile and sterile anthers. **J. Hered.** **63**:103-108.

- Waterkeyn, L. (1964). Callose microsporocytaire et callose pollinique. *In*: Linskens, H.F. (ed.) **Pollen Physiology and Fertilization**, North Holland, Amsterdam. pp. 52-58.
- Webster, O.J., and Singh, S.P. (1964). Breeding behaviour and histological structure of a the non-dehiscent anther character in *Sorghum vulgare* Pers. **Crop Sci.** 4:656-658.
- Wendel, J.F. (1980). Enzyme extraction from a tannin-rich plant. **Isozyme Bull.** 13:116.
- Wendel, J.F. and Weeden, N.F. (1989). Visualization and interpretation of plant isozymes. *In*: D.E. Soltis and P.S. Soltis (eds.). **Isozymes in Plant Biology**. pp. 5-45. Discorides Press, Portland, Oregon, USA.
- Wise, R.P., Fliss, A.E., Pring, D.R. and Gengenbach, B.G. (1987). Urf 13-T of T cytoplasm maize mitochondria encodes a 13 KD polypeptide. **Plant Mol. Biol.** 9:121-126.
- Young, E.G. and Hanson, M. (1987). A fused mitochondrial gene associated with cytoplasmic male sterility is developmentally regulated. **Cell** 50:41-49.
- Zenkter, M. (1962). Microsporogenesis and tapetal development in normal and male sterile carrots (*Daucus carota*). **Amer. J. Bot.** 49:341-348.

APPENDIX

Appendix I. Mean performance of tall and dwarf near-isogenic lines for plant height, time to 50% flowering, grain yield and its components over four environments.

Character	Near-isogenic pair												Mean		
	Early Composite				Medium Composite				Nigerian Composite						
	Tall 1T	Dwarf 1D	Tall 2T	Dwarf 2D	Tall 3T	Dwarf 3D	Tall 6T	Dwarf 6D	Tall 9T	Dwarf 9D	Tall 10T	Dwarf 10D		Tall 12T	Dwarf 12D
Plant height (cm)	173	110**	126	80*	138	73**	174	95**	151	87**	150	83**	190	90**	157.4/88.3
Time to 50% flowering	53	55**	53	51	51	53**	55	52**	59	61*	64	63	59	63**	56.3/56.8
Grain yield (kg ha ⁻¹)	1520	1470	1610	1300**	1390	1150*	1850	1840	2250	1870**	1910	1390**	1670	1090**	1742.8/1444.3
Head length (cm)	24.0	22.5**	15.0	17.0**	18.3	18.4	17.9	21.2**	17.9	16.6**	16.3	19.0**	22.9	20.7*	18.9/19.3
Head girth (mm)	22.4	18.8**	19.4	18.0**	17.1	17.3	22.6	22.2	24.2	22.0**	22.2	21.4	21.5	16.8**	21.3/19.5
Tillers plant ⁻¹	1.5	1.3**	1.9	2.3*	1.7	1.6	1.4	1.5	1.7	1.7	1.7	1.6	1.3	1.6*	1.60/1.66
100 seed weight (g)	7.9	7.6*	5.8	6.2*	6.8	6.3**	6.8	8.4**	7.1	6.8	7.1	7.5*	8.5	7.2**	7.14/7.14
Similarity(%) based on isozyme spectrum (present observations)	97.0%		96.0%		85.0%		87.0%		98.0%		96.0%		86.0%		

* = significant at 5% and ** = significant at 10% probability levels

Source: Rai and Rao (1991)

Appendix II

Preparation of buffers and other chemicals for mtDNA analysis

0.5M EDTA pH 8.0 (500ml)

0.5M Tris-Cl pH8.0	150ml	0.15M
0.5M EDTA (pH 8.0)	8ml	0.008M
NaCl	2.92g	0.1M
SDS(kept at 65°C)	7.5g	1.5%

93.05g EDTA + 300ml sterile dH₂O in 1000ml beaker + little sodium hydroxide ⇒ stir while heating ⇒ add little amount of sodium hydroxide in between - it takes time to dissolve ⇒ continue till it gets dissolved and turns transparent ⇒ **adjust the pH to 8.0 with sodium hydroxide** ⇒ make the volume 500ml with SDW.

STORE AT ROOM TEMPERATURE

DNase (2mg/ml)

8mg DNase + 4ml SDW ⇒ shake gently and divide into 4 aliquots of 1ml each to get 2mg/ml conc. ⇒ store at -20°C.

Saline wash buffer

Constituent	g/l	Final conc.
NaCl	58.44g	1M
0.5M Tris-Cl pH8.0	100ml	50mM
0.5M EDTA (pH 8.0)	40ml	20mM

STORE IN COOL

Proteinase K (2mg/ml)

20mg proteinase K + 10ml SDW ⇒ shake gently and divide into 10 aliquotes of 1 ml each to get conc. of 2mg/ml ⇒ store at -20°C.

Shelf buffer

Constituent	g/500ml	Final conc.
Sucrose	102.69g	0.6M
0.5M Tris-Cl pH7.5	10ml	10mM
0.5M EDTA (pH 8.0)	20ml	20mM

STORE IN COOL

Saline A Extraction buffer pH8.0

Constituent	g/l	Final conc.
NaCl	58.4	1M
0.5M Tris-Cl pH8.0	100ml	0.05M
0.5M EDTA (pH 8.0)	10ml	0.005M
BSA (to be added fresh)	1g	0.1mg/ml

NN-Buffer

Constituent	100 ml ⁻¹	Final conc.
0.5M Tris-Cl pH 8.0	10 ml	50mM
0.5M EDTA pH 8.0	4 ml	20 mM

STORE IN COOL

STORE IN COOL

Buffer G pH 7.5

Constituent	g/l	Final conc.
0.5M Tris-Cl pH7.5	100ml	0.05M
NaCl	8.77g	0.15M

70% Ethanol

Constituent	ml/litre	Final conc.
Absolute Ethanol	700 ml	70%

STORE IN COOL

2x Extraction buffer pH 8.0

Constituent	g/500ml	Final conc.
-------------	---------	-------------

SDW 300 ml

0.5M Tris-Cl pH 8.0

Constituent	g/lite
Trizma base	60.507

Adjust pH with 6N HCl to 8.0

0.5M Tris-Cl pH 7.5

Constituent	g / liter
Trizma base	60.507

Adjust pH with 6N HCl to 7.5

5M Potassium acetate

Constituent	100 ml ¹
Potassium acetate	49.07 g

pH not adjusted

T₅₀E₁₀ Buffer

Constituent	100 ml ¹
0.5M Tris-Cl pH8.0	10 ml
0.5M EDTA pH 8.0	2.0 ml

₁₀E₁ Buffer

Constituent	liter ¹
0.5M Tris-Cl pH 8.0	20 ml
0.5M EDTA pH 8.0	2.0 ml

Denaturing solution

Constituent	liter ¹
1.5M NaCl	87.66 g
0.5M NaOH	20.00 g

Neutralizing Buffer

Constituent	liter ¹
1.5M NaCl	87.66 g
1M Tris	121.1 g

Adjust pH to 8.0

Chloroform (24:1)

Constituent	100ml ¹
Isoamyl alcohol	4.0 ml
Chloroform	96.0 ml

0.25N HCl

Constituent	liter ¹
Conc. HCl (11.6N)	21.6 ml
SDW	78.4 ml

7.5M Ammonium acetate

Constituent	100 ml ¹
Ammonium acetate	57.75 g

10x TBE Buffer

Constituent	liter ¹
Trizma base	108.0 g
Boric acid	55.0 g
0.5M EDTA	40 ml

Adjust pH 8.4 With 6N HCl

20x SSC

Constituent	2 liter ¹
3M NaCl	350.64 g
0.3M Na ₃ citrate	176.46 g

Prehybridization solution / 7% SDS Phosphate solution

Constituent	500 ml ¹
Disodium hydrogen phosphate (Na ₂ HPO ₄)	35.5 g
BSA	5 g
SDS	35 g

Adjust pH with H₃PO₄ (Phosphoric acid)

³²P Blots Wash Solution

Constituent	liter ¹
-------------	--------------------

20x SSC	150ml
10% SDS	10 ml

10x TBE

Constituent	liter ⁻¹
Tris base	108 g
Boric acid	55 g
0.5M EDTA pH8	40 ml
<i>pH automatically comes to 8.4 if weighed exactly (otherwise adjust pH by adding 6N HCl)</i>	

Probe stripping solution I

Constituent	250 ml ⁻¹
NaOH	4.0 g
10% SDS	10 ml

Probe stripping solution II

Constituent	250 ml ⁻¹
20x SSC	2.5 ml
10% SDS	2.5 ml
Tris-Cl pH 7.5	100 ml

Developer

Constituent	liter ⁻¹
SDW	1000 ml(52°)
D-19	157 g..add
	slowly

Stop bath (3% of HAC)

Constituent	liter ⁻¹
HAC (Acetic acid)	30 ml

Rapid Fixer

Constituent	liter ⁻¹
Solution A	250 ml
SDW	750 ml
Solution B	28 ml...add
	slowly at room temperature

Loading buffer

Constituent	10 ml ⁻¹
Sucrose	4 g
Bromophenol blue	25 mg
0.5M EDTA pH 8	400 ul

Appendix III

Southern Transfer by Vacuum Blotting

1. Nylon membrane was pre-wetted by dipping in 3x SSC for 2 min.
2. Porous support screen (teflon screen) was soaked in SDW and placed on the inner rim of the base unit with the shiny side up.
3. Placed the plastic mask with the window on the support screen.
4. Positioned the pretreated transfer membrane under the mask so that it covered the window in the plastic mask completely. Air bubbles trapped in between the membrane and the porous support screen were removed.
5. Starting with one of the gel edges, gradually slide the gel from the support plate onto the membrane to fill the window. Trapping of air bubbles between the gel and the membrane was avoided.
6. Fitted the top frame and tighten the four clamps, switched on the vacuum pump to immobilize the gel. Immediately after switching on the pump, poured on "depurination solution" (0.25 N HCl) onto the center of the gel. Left for 20 min, and ensured that the gel remains covered with solution during the treatment. During the depurination step, stabilize the vacuum at ≈ 50 mbar. After the first treatment was over, tilted the blotting unit, removed residual liquid by pipette. Poured on SDW onto the gel and removed it (SDW) by pipetting after tilting the apparatus.
7. Poured on "denaturation solution" (500 mM NaOH and 150 mM NaCl) enough to cover the gel surface. Ensured that the gel remains covered with solution during the treatment. Left for 20 min and then remove completely and washed the gel with SDW as before.
8. Similarly, poured on "neutralizing solution" (1 M Tris-HCl, pH 8.0, and 1.5 M NaCl) as before. Left for 20 min and then removed completely and washed the gel as before.
9. Poured on "transfer solution" (20x SSC; 1x SSC = 150 mM NaCl and 15 mM sodium citrate, pH 7.5) to cover the gel, left for 60 min. Ensured that the gel remains immersed during this time. Removed the transfer solution as before. With the vacuum still on, lifted up a corner of the gel and peeled it off, leaving the membrane in place. Switched off the vacuum. Removed the membrane, washed in 3x SSC, blotted it between filter papers, performed UV cross-linking using UV Cross Linker (UV Stratalinker 1800) and stored at 4°C after putting in Saran wrap till further use.

Appendix IV

Purification of DNA inserts from plasmid DNA (Maniatis *et al.* , 1982):

According to this procedure the gene inserts of the clones were cleaved from their vectors using the appropriate restriction endonuclease(s) and fractionated by electrophoresis on a minigel of 0.8% agarose in TBE buffer containing ethidium bromide (0.5 µg/ml). The electrophoresis was carried out with TBE buffer for 3 h at 6 v/cm. The gels were observed on a UV-transilluminator and the desired fragment was transferred on to NA 45 membrane (Schleicher and Schull, Inc., Keene, NH) by placing the membrane in a slit just behind the band of interest and allowing the electrophoresis to resume for further 30 min. The DNA was eluted from the membrane by addition of sufficient high salt buffer (1 M NaCl, 0.1 mM EDTA, 20 mM Tris-HCl, pH 8.0) to cover the membrane followed by incubation at 65°C for 45 min. Ethidium bromide was removed by extraction with TE saturated n-butanol and DNA was precipitated with 0.5 vol of isopropanol at -80°C for 30 min and pelleted in a Sorvall microfuge at 10,000 rpm for 10 min. The pellet was washed in 70% ethanol, dried under vacuum and dissolved in T₁₀E₁.

Appendix V

Protocol for total DNA isolation: Dellaporta et al. (1983)

Miniprep procedure

1. Weigh 5 g of 5-day old etiolated seedlings, quick freeze in liquid nitrogen and grind to a fine powder in a prechilled mortar and pestle. Transfer powder with liquid nitrogen into a 30 ml Oak Ridge tube.
Note: Avoid thawing of tissue once frozen until buffer is added, and do not cap the tubes while nitrogen is evaporating.
2. Add 20 ml of preheated (65°C) Extraction Buffer (Dellaporta Buffer), mix gently to avoid shearing of DNA
Dellaporta Buffer: 100 mM Tris-HCl pH 8.0, 50 mM EDTA pH 8.0, 100 mM NaCl, 2% of 10% SDS.
3. Add 100 µl of 10 mg/ml proteinase K (final concentration of 0.05 mg/ml), mix gently and incubate at 65°C in hot water bath for 1 h with occasional gentle inversion to mix tube contents.
4. Add 10 ml phenol + 10 ml chloroform (24 chloroform:1 isoamyl alcohol) in each tube, mix gently by inversion to form an emulsion. Make sure that the samples are completely mixed.
5. Centrifuge at 2000 rpm for 20 min in bench-top centrifuge to separate phases, take supernatant and pour into fresh tubes. The phenol/chloroform extraction may be repeated.
6. Add equal volume (20 ml) of chloroform in each tube, mix gently and centrifuge at 2000 rpm for 5-10 min, and transfer the supernatant to the fresh tubes.
7. To the supernatant, add 0.6 volume (15 ml) of isopropanol and mix by inversion. DNA precipitate appears at interphase. Spool out the precipitate with a glass hook, and rinse in an excess of 70% ethanol. Place precipitate into a 1.5 ml polypropylene centrifuge tube, rinse 2-3 times with 70% ethanol and air dry/vacuum dry briefly (avoid over drying).
8. Dissolve the pellet in 700 µl of T₅₀E₁₀. Warming (50°C) helps, but keep for long at 4°C.
9. Add 7 µl RNase (final concentration of 50 µg/ml) incubate at 37°C for 1 h.
10. Add 350 µl phenol + 350 µl chloroform, mix gently by inversion and centrifuge at 12000 rpm for 5 min. Save supernatant, and repeat phenol/chloroform extraction.
11. To the supernatant, add equal volume (700 µl) chloroform, mix gently by inversion and centrifuge at 12000 rpm for 5 min. Repeat chloroform extraction if interphase is excessive.
12. Add equal volume of chilled isopropanol, mix by inversion. DNA precipitate appears. Spool out DNA on glass hook, rinse in 70% ethanol, place in a sterile 2 ml screw cap tube and drain excess 70% ethanol after quick centrifugation. Air dry O/N or vacuum dry briefly.
13. Add 0.5 to 1.5 ml of T₁₀E₁ (depending upon the size of DNA pellet), and allow DNA to dissolve.
14. Samples are stored at 4°C for use.

Appendix VI

Grinding/extraction buffer recipe for Isozyme electrophoresis (Modified from Wendel 1980)

Ascorbic acid	5 mM (88 mg)
Sodium phosphate, di basic (unhydrous)	42.3 mM (600 mg)
Sucrose	0.21 M (7.2 g)
EDTA - disodium salt	1.55 mM (52 mg)
PVP-40	5% w/v (5 g)
2-Mercaptoethanol	0.014 M (100 ul)

Adjust to pH 7.5 with NaOH, add dH₂O to 100 ml.

Stored at 4°C in a dark bottle for and used within two weeks.

Appendix VII

Buffers used for electrophoresis

- 1. Tris-glycine buffer, pH 8.3 (3L)**

Tris	9.08 g
Glycine	43.24 g
dH ₂ O	3 litre
 - 2. TG + T**

Upper tank buffer : 0.25M Tris + 0.19 M glycine
Lower tank buffer : 0.25M Tris, pH 8.5.
-

Reagents for polyacrylamide gel electrophoresis

Stock Reagent Preparation

- 1. Acrylamide/Bis (30% T, 2.67% C)**

Acrylamide	146.0 g
N,N'-methylene-bis acrylamide	4.0 g

- 2. 1.5 M Tris-HCl, pH 8.8**

54.45 g tris base
60 ml distilled water
Adjust to pH 8.8 with 10 N HCl. Distilled water to 3000 ml. Store at 4°C.

- 3. 0.5 M Tris-HCl, pH 6.8**

6 g Tris base
60 ml distilled water
Adjust to pH 6.8 with 10 N HCl. Distilled water to 100 ml. Store at 4°C.

- 4. 10% ammonium persulfate (w/v)**

Dissolve 100 mg ammonium persulfate in 1 ml distilled water.

- 5. 5x electrode (running) buffer**

(1x = 25 mM Tris, 192 mM glycine, 0.1% SDS, pH 8.3)

Tris base	45.0 g
Glycine	216.0 g

Appendix VIII Staining Recipes

Alcohol dehydrogenase (ADH) EC 1.1.1.1. Anodal (Cardy *et al.* 1983)

0.1M Tris-HCl (pH 8.0)	100 ml
NAD	20 mg
MTT	20 mg
PMS	4 mg
Ethanol 95%	2 ml

Mixed the above chemicals and incubated for 1 h at 37°C in dark. Rinse and fix in alcohol.

Catalase (CAT) EC 1.11.1.6. Anodal (Cardy *et al.* 1983)

Hydrogen peroxide, 0.01% (fresh)	50 ml
H ₂ O	50 ml
Ferric chloride	500 mg
Pottasium ferricyanide	500 mg

Pour H₂O₂ on gel slice and leave for 5 min. Meanwhile, mix remaining ingredients. Pour off peroxide and add stain solution. Agitate the gel gently until bands are developed. Bands appear as achromatic zones on dark green background. Rinse and fix.

Note: *Bands disappeared very soon and whole of the gel turned dark bluish green.*

Esterase (EST) EC 3.1.1. Anodal & Cathodal (Gaur 1990)

Method I

0.1M sodium phosphate buffer (pH 7.2)	100 ml
α - naphthyl acetate	20 mg (dissolve in 2 ml acetone)
Fast blue RR salt	50 mg

Add fast blue salt to the phosphate buffer and stir till fully dissolved. Just before staining add α - naphthyl acetate to the buffer, mix and pour it on the top of the gel. Incubate for 30-40 min in dark at 37°C. Wash and fix the gels when the bands are clearly visible.

Method II

0.1M potassium phosphate buffer (pH 6.0)	100 ml (adjust pH with NaOH)
Fast blue RR salt	80 mg
α - naphthyl acetate	200 mg (in 10 ml acetone)

Procedure for staining is same except for the time of incubation. Bands fully appear within 15 min of incubation at 37°C.

Glutamate dehydrogenase (GDH) EC 1.4.1.2. Anodal (Cardy *et al.* 1983)**Method I**

0.1M Tris-HCl (pH 8.5)	100 ml
L-Glutamic acid	300 mg
NAD	40 mg
NBT/MTT	30 mg
PMS	10 mg
CaCl ₂	100 mg

Mix ingredients and pour over the gel. Incubate until blue bands appear. Rinse and store in water (when NBT used).

Method II

All ingredients same except that CaCl₂ is not included.

Glutamate oxaloacetate transaminase (GOT) EC 2.6.1.1. Anodal (Cardy *et al.* 1983)

AAT substrate solution*	50 ml
H ₂ O	50 ml
Fast blue BB salt	100 mg

*** AAT substrate solution (pH 7.4 with NaOH):**

H ₂ O	800 ml
α - ketoglutaric acid	292 mg
L - aspartic acid	1.07 g
PVP-40	4.00 g
EDTA, Na ₂ salt	400 mg
Sodium phosphate, dibasic	11.36 g

Add fast BB to substrate solution and incubate at room temperature in the dark until blue bands appear. Rinse and fix.

Lactate dehydrogenase (LDH) EC 1.1.1.27. Anodal (Wendel and Weeden 1989)

0.05M Tris HCl (pH 8.0)	100 ml
NAD	20 mg
Lactic acid, lithum salt	200 mg
MTT/NBT	20 mg
PMS	4 mg

Combine all the ingredients and pour over the gel. Incubate until blue bands appear. Rinse and fix.

Malate dehydrogenase (MDH) EC 1.1.1.37. Anodal (Cardy *et al.* 1983)

0.1M Tris HCl (pH 9.1)	100 ml
Neutral malic acid	200 mg
NAD	40 mg
NBT	20 mg
PMS	2 mg

DI-malic acid was added as a neutralized (with NaOH) aqueous solution. Ingredients were combined and poured over the gel. Incubated until blue bands appeared. Rinsed and stored in water.

Malic enzyme (ME) EC 1.1.1.40. Anodal (Soltis *et al.* 1983)

0.1M Tris HCl (pH 8.6)	100 ml
L-malic acid	280 mg
NADP	20 mg
NBT	30 mg
PMS	5 mg
1M MgCl ₂	0.1 ml

Mix the above chemicals and pour over the gel. Incubate in dark at room temperature until blue bands appear (may

take 15 h).

Phosphoglucosomerase (PGI) or Glucose-6-phosphate isomerase EC 5.4.2.2.
(formerly EC 2.7.5.1.) Cathodal & Anodal (O. Malley *et al.* 1980)

0.1M Tris - HCl (pH 7.5)	100 ml
Fructose-6-phosphate	15 mg
NADP	7 mg
MTT	15 mg
Glucose-6-phosphate dehydrogenase	20 units
1M MgCl ₂	1.0 ml

Combine all the ingredients and pour over the gel. Incubate until blue bands develop at 32°C. Rinse and fix the gel.

6-phosphogluconate dehydrogenase (6-PGD) EC 1.1.1.44. Anodal (Modified O. Malley *et al.* 1980)

0.05M Tris-HCl (pH 7.5)	100 ml
6-phosphogluconate (in 1 ml H ₂ O)	40 mg
NADP	10 mg
MgCl ₂	100 mg
MTT	10 mg
PMS	2 mg

Combine all the ingredients and pour over the gel. Incubate at 37°C until blue bands appear. Rinse and fix.

Shikimate dehydrogenase (SKDH) EC 1.1.1.25. Anodal (Soltis *et al.* 1983)

0.1M Tris-HCl (pH 8.5)	100 ml
Shikimic acid	100 mg
NADP	20 mg
MTT	20 mg
PMS	4 mg

Combine all the ingredients and incubate the gel at 37°C for 1 h and keep at room temperature overnight in the dark. Rinse and fix.

Superoxide dismutase (SOD) EC 1.15.1.1. Anodal (Wendel and Weeden 1989)

0.05M Tris-HCl (pH 8.2)	100 ml
Riboflavin	2 mg
EDTA	1 mg
NBT	10 mg

Combine ingredients and pour over the gel. Incubate for 30 min in dark at 37°C. Remove from incubator and illuminate on a light box. Zones of SOD activity are revealed as achromatic regions on a dark blue background. Rinse with water and fix.

MOLECULAR CHARACTERIZATION OF CYTOPLASMIC-NUCLEAR MALE STERILITY (CMS) SOURCES AND TALL/DWARF NEAR-ISOGENIC LINES IN PEARL MILLET

By

Ashok Kumar Chhabra (91A57D)

Major Advisor:

Dr. I.S. Khairwal

Associate Professor, Department of Plant Breeding
CCS, Haryana Agricultural University, Hisar 125 004, Haryana, India.

ABSTRACT

The conventional method of classifying CMS lines on fertility restoration patterns is cumbersome and time consuming. Restriction fragment length polymorphism (RFLP) of mitochondrial (mt) DNA provides a rapid and effective method to assess heterogeneity among male-sterile cytoplasm. With this objective, six isonuclear A-lines (81A₁ with Tift 23A₁ cytoplasm, ICMA 88001 (= 81A₁) with *violaceum* cytoplasm, 81A₇ (= 81A₁) with *monodii* = *violaceum* cytoplasm, Pb 310A₂ and Pb 311A₂ with A₂ cytoplasm, and Pb 406A₃ with A₃ cytoplasm), nine male-sterile lines from Large-seeded Genepool (LSGP 6, LSGP 14, LSGP 17, LSGP 22, LSGP 28, LSGP 36, LSGP 43, LSGP 55 and LSGP 66) and two CMS lines each from Early Genepool (EGP 1 and EGP 2) and Population Varieties (PV 1 and PV 2) were characterized for variation in their mitochondrial genomes following Southern blot hybridizations using homologous (pearl millet 13.6 kb, 10.9 kb, 9.7 kb and 4.7 kb clones) and heterologous (maize *atp6* and *cox1* clones) mtDNA probes. Based on RFLP banding pattern we identified seven cytoplasmic groups from the LSGP. Of the LSGP cytoplasm, LSGP 43, LSGP 55 and LSGP 66 were most diverse.

Microsporogenesis and Anther Development in Pearl Millet Isonuclear Lines was also studied in six isonuclear A-lines (stated above).² The 81B was used as a male-fertile control. Meiosis was regular in all isonuclear A- lines and 81B, except Pb 406A₃ where a low frequency of pollen mother cells (PMCs) showed anomalous meiosis. Microsporogenesis and anther development were normal in 81B. PMC/microspore/pollen degeneration in the six A-lines occurred at different stages of anther development. The cause of pollen abortion differed from line to line, from floret to floret within a spikelet, from anther to anther within a floret, and in some cases even from locule to locule within an anther. Meiotic and postmeiotic degeneration of pollen grains was commonly observed phenomenon in CMS lines. In the other A-lines many developmental paths were observed within the line and pollen degeneration occurred at various stages. Large variation for pollen fertility was observed among spikelets within a spike, among florets within a spikelet, and among anthers within a floret, ranging from 0 - 100% fertility in all the isonuclear A-lines. Very low frequencies of empty anthers were also recorded in all A-lines, maximum being observed in 81A₁ and Pb 406A₃ (2-3%).

We have also compared seven pairs of tall and dwarf near-isogenic lines from three composites (3 from EC, 3 from MC and 1 from NC) for 12 enzyme systems using polyacrylamide gel electrophoresis. Enzyme systems compared were alcohol dehydrogenase (ADH), catalase (CAT), esterase (EST), glutamate dehydrogenase (GDH), glutamate oxaloacetate transaminase (GOT), lactate dehydrogenase (LDH), malate dehydrogenase (MDH), malic enzyme (ME), phosphoglucosomerase (PGI), 6-phosphogluconate dehydrogenase (6-PGD), shikimate dehydrogenase (SKD), and superoxide dismutase (SOD). Isolines of tall/dwarf near-isogenic pairs were identical for six of the 12 enzyme systems studied. Among all the enzymes studied, ADH (18 h imbibed seed) and EST (18 h imbibed seed) were most effective in determining within and between pairs variation. Isozyme spectrum for 12 enzyme systems revealed that out of seven near-isogenic pairs, three most polymorphic pairs are EC3, MC6, and NC12. Pairs EC3 and NC12 were equally polymorphic. In general, tall isolines are represented by the presence of higher number of bands than their corresponding dwarf isolines. Based upon similarity index (SI) values calculated from presence and absence of bands, most isogenic pair was MC9 (SI = 0.98), followed by pairs EC1 (SI = 0.97), and EC2 and MC10 (SI = 0.96). Three most polymorphic pairs had SI = 0.85 (EC3), 0.86 (NC12), and 0.87 (MC6). It clearly shows that isolines of these pairs are still segregating for many loci.